STUDIES OF DJ-1, PARKIN, AND ALPHA-SYNUCLEIN GIVE INSIGHTS INTO PLAUSIBLE MECHANISMS FOR PARKINSON'S DISEASE PATHOGENESIS

Chenere P. Ramsey

A DISSERTATION

in

Neuroscience

Presented to the Faculties of the University of Pennsylvania

in Partial Fulfillment of the Requirements for the

Degree of Doctor of Philosophy

2010

_____

Supervisor of Dissertation: Benoit I. Giasson, Ph.D., Assistant Professor, Dept. of Pharmacology

_____

Graduate Group Chairperson: Rita Balice-Gordon, Ph.D., Professor, Dept. of Neuroscience

Dissertation Committee

Harry Ischiropoulos, Ph.D., Research Professor of Pediatrics and Pharmacology

Kelly Jordan-Sciutto, Ph.D., Assoc. Professor, Dept of Pathology School of Dental Medicine

Virginia M. Y. Lee, Ph.D., M.B.A., Professor of Pathology and Lab Medicine

David R. Lynch, M.D., Ph.D., Assoc. Professor of Neurology and Pediatrics

DEDICATION

This dissertation is dedicated to Jesus Christ for getting me through this graduate school experience. He gave me great ideas and afforded me the strength to return to the lab each day. I also dedicate this work to my parents, Drs. Roscoe and Patricia Ramsey. Without you two, I would not be here.

"And we know that all things work together for good to them that love God, to them who are the called according to His purpose" (Romans 8:28, KJV).

"…Even hope may seem but futile, when with troubles you're beset, but remember you are facing just what other men have met. You may fail, but fall still fighting: don't give up, whate'er you do; eyes front, head high to the finish. See it through" (*See it Through* by Edgar A. Guest).

ACKNOWLEDGMENTS

I am very thankful for each and every experience that I have had during my tenure as a graduate student at the University of Pennsylvania. Though the road has been rough, I would like to offer a special thanks to my advisor, Benoit for pushing me and for helping to shape me into the stronger person and scientist that I am today. In addition to a great deal of scientific expertise, my experiences in Benoit's lab taught me great lessons about the power of the will. These are lessons that may not have been learned elsewhere so Benoit, thank you. I thank Kelly for all of her advice and moral support and for being the role model that I needed when she didn't even know I was watching. I thank Harry for being such a precious gem, having a brilliant mind but yet with a soft heart towards students. I thank Virginia for the role she plays as director of the Center for Neurodegenerative Disease Research (CNDR). During my time here, many resources were made available to me from the CNDR, and I am grateful for that. I thank Dave for serving as chair of my thesis committee and for having the foresight to steer me in the direction that lead to the successful end of this long journey. I would also like to thank all of the individuals who played major roles in assisting me with experiments and/or data collection through-out the years, LaTasha Boateng, Elpida Tsika , Cagla Akay, Camella Wilson, and Kristel Emmer. Additionally, heartfelt thanks go to the members of the Giasson lab for creating a safe and cooperative work environment. Jason Covy, Kristel Emmer, and Elisa Waxman. Thank you. I also would not have made it through this experience without the moral support I gained from members of the Ernest E. Just Biomedical Society, Black Graduate and Professional Student Assembly, Fontaine Society, Voices of Sharon, and Sharon Baptist Church Mass Choir.

Thank you all sincerely. You are all greatly appreciated.

ABSTRACT

STUDIES OF DJ-1, PARKIN, AND ALPHA-SYNUCLEIN GIVE INSIGHTS INTO PLAUSIBLE MECHANISMS FOR PARKINSON'S DISEASE PATHOGENESIS

Chenere P. Ramsey

Advisor: Benoit I. Giasson, Ph.D.

Parkinson's disease (PD) is an insidious neurodegenerative disorder characterized by a range of motor symptoms which develop predominantly as a consequence of striatal dopamine depletion. The majority of PD cases are idiopathic; however, discoveries of genetic mutations linked to familial forms of PD, including mutations in the genes encoding DJ-1, parkin, and α-synuclein (α-syn), have provided insights into sporadic PD pathogenesis.

Mutations in the gene encoding DJ-1 cause autosomal recessive early-onset PD (AREP). Though the physiological role for DJ-1 is not fully elucidated, it is thought that DJ-1 mutations contribute to disease as a consequence of a loss-of-function. Herein, we show that wild-type (WT) DJ-1 is a relatively stable and soluble homodimer that has diffuse cellular distribution and that can protect mammalian cells against a variety of noxious insults. Pathogenic mutant DJ-1 proteins, L10P, P158DEL, E163K, and L166P display diverse altered biochemical properties. Thus, it is concluded that alterations to distinct DJ-1 residues may specifically affect individual protein functions and may also implicate DJ-1 in a variety of biochemical pathways.

When expressed in mice, human pathogenic mutant A53T α-syn can aggregate and result in fatal motor impairments. It was hypothesized that DJ-1 may act to modulate this effect. Herein, DJ-1 null transgenic animals are generated and assessed for viability against toxic A53T α-syn. However, in double transgenic DJ-1 null mice expressing human pathogenic A53T α-syn, the consequences of DJ-1 deficiency are not apparent and thus it is concluded that DJ-1 may not directly modulate α-syn nor mitigate the deleterious effects of α-syn aggregation *in vivo*.

Parkin mutations cause AREP which is thought to develop secondary to a loss in parkin function. We discover a novel endogenous parkin mutation in C3H mice, E398Q which impairs the function of parkin in a similar manner to that of pathogenic missense parkin mutations. It is therefore concluded that C3H mice may serve as suitable models for future studies to assess the effects of parkin loss-of-function in vivo.

TABLE OF CONTENTS

LIST OF TABLES

Chapter One

Chapter Three

Chapter Five

LIST OF ILLUSTRATIONS

CHAPTER ONE

CHAPTER TWO

CHAPTER THREE

CHAPTER FOUR

CHAPTER FIVE

CHAPTER ONE

Introduction

1.1 "La maladie Parkinson"

Dr. James Parkinson (1755-1824) was a surgeon who lived and worked in the southern part of London, England. Throughout his career, he wrote copiously on many topics related to medicine and politics. He is most well-known for his work, *An Essay on the Shaking Palsy*, which was written in 1817. In his essay, James Parkinson described a motor condition which was coined some years later as "La maladie Parkinson" (39). Parkinson's account was based on conclusions drawn from only six patients (344). He summarized the condition as, "Involuntary tremulous motion, with lessened muscular power…with a propensity to bend the trunk forward, and to pass from a walking to a running pace: the senses and intellect being uninjured"(344). According to Parkinson, these symptoms, which progressively worsened over time, eventually debilitated the affected individuals to the point of complete dependence on external care givers (344). The classical symptoms described by Parkinson are common to the insidious disorder that is known today as Parkinson's disease (PD).

1.2 PD: a neurodegenerative movement disorder

PD is the leading cause of parkinsonism. Parkinsonism is the term used to describe a group of symptoms that include tremor, slowness of movement (bradykinesia), rigidity, and postural instability. PD is one of several neurological disorders that produce similar symptoms (399;465). PD results from progressive degeneration of selective and heterogeneous neuronal populations (**Figure 1-1)** (234). Among the neuronal populations affected are the dopaminergic neurons (also known as the A9 group) of the substantia nigra pars compacta (SNpc). Although PD is not limited to the SNpc, degeneration of

Figure 1-1

A schematic showing the sites of neurodegeneration and neurochemical pathways that are involved in PD.

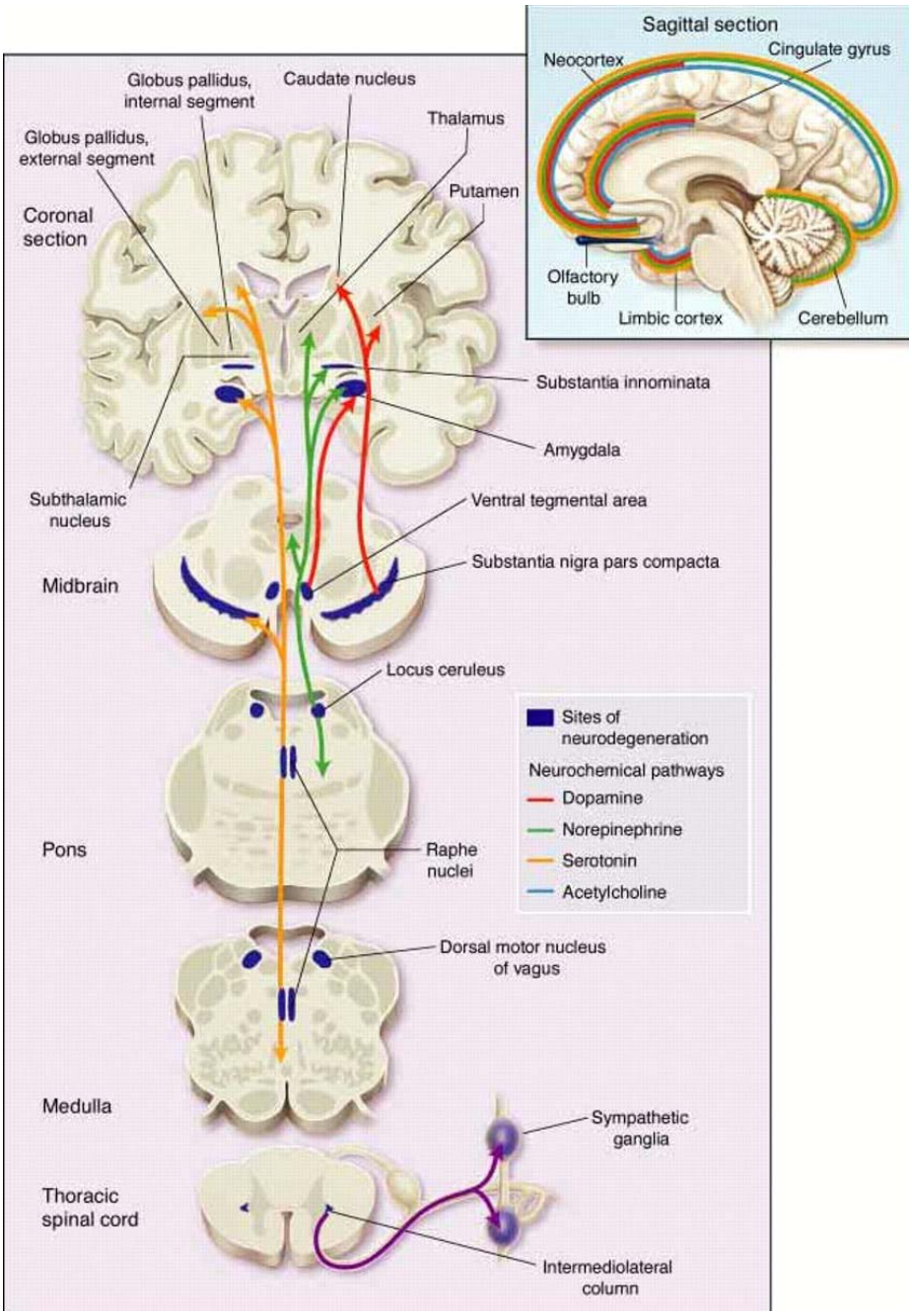

The sites of neurodegeneration are marked in dark blue. The colored arrows show the neurochemical pathways that are affected by the disease. Red arrows depict DA pathways, green arrows depict norepinephrine pathways, yellow arrows depict serotonin pathways, and turquoise or purple arrows depict acetylcholine pathways. The same color scheme is also used in the inset which shows the destinations of the various neurochemical pathways from a saggital section view.

Figure is from Lang and Lozano, New Eng J Med, 1998 (234).

the nigra plays a major role in the pathobiology of the disease (112).

1.3 The direct/indirect pathways of motor control

Dopaminergic neurons of the SNpc release dopamine (DA) into the striatum via the nigrostriatal pathway (**Figure 1-2A and B**). The striatum is largely composed of medium spiny neurons (MSNs). Striatal MSNs generally express either D1 DA receptors (striasome neurons) or D2 DA receptors (matriasome neurons) and can thereby be regulated in parallel with respect to the type of receptor that they express. Striasome MSNs are activated by DA while matriasome MSNs are inhibited by DA. Activation of striasome neurons facilitates movement in a pathway known as the direct pathway (**Figure 1-2C**)(92). Conversely, in the absence of DA, matriasome neurons are activated and this acts to inhibit movement in a pathway known as the indirect pathway. These processes require tight regulation and together, they play a role in fine-tuning motor control (92;195).

1.4 Parkinsonism: the effects of depleted striatal DA content

In PD, as nigral neurons degenerate, striatal DA levels significantly depreciate and this results in deactivation of the direct pathway while it simultaneously enhances the indirect pathway. The deregulation of these two pathways leads to the onset of motor impairments. PD is diagnosed if bradykinesia and at least one of the other cardinal parkinsonism symptoms presents (377). It is thought that motor impairments first develop when eighty percent of nigral neurons have already degenerated (234).

Figure 1-2

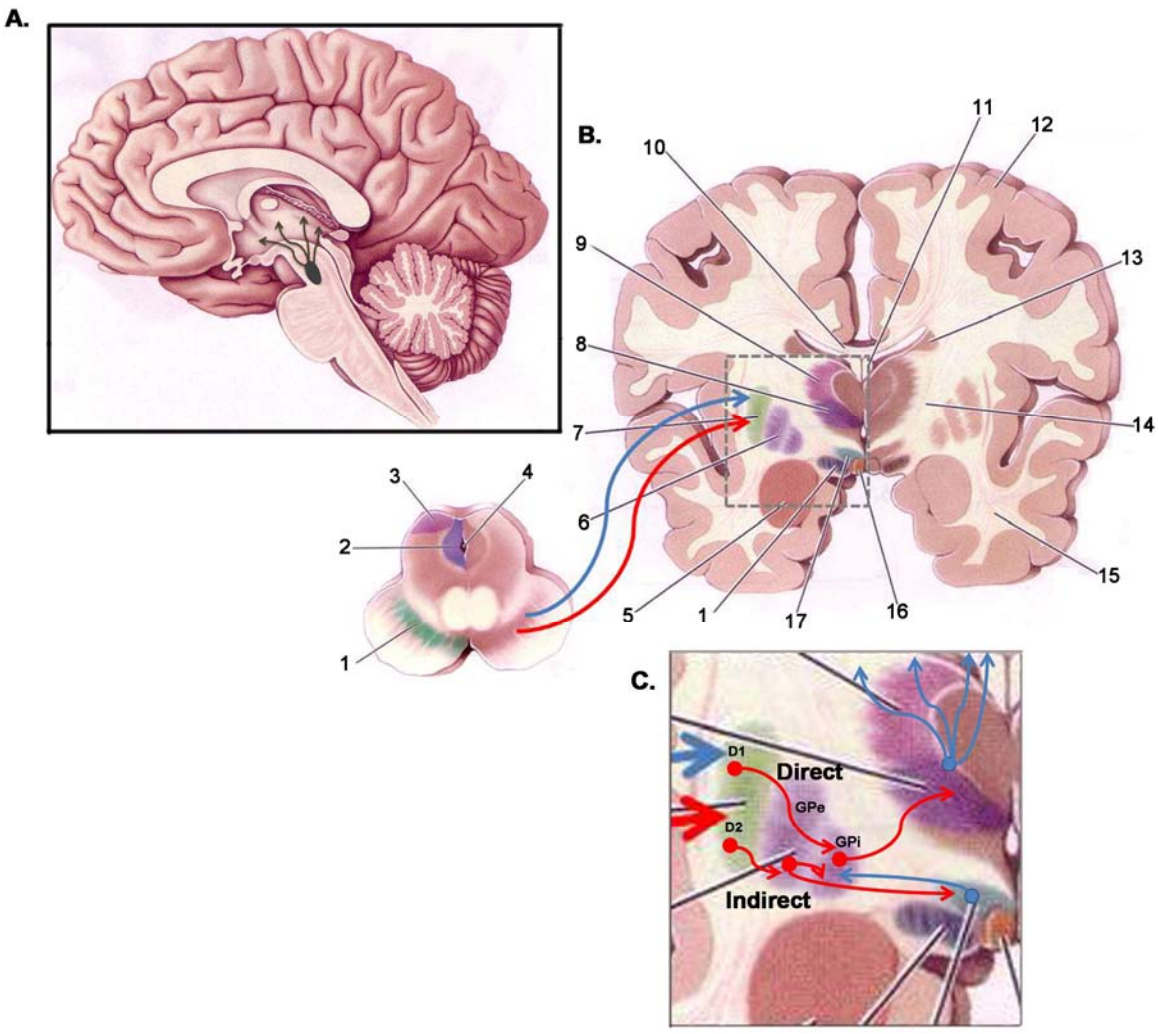

Nigrostriatal signaling pathways involved in movement.

Part **A** shows a saggital illustration of the human brain. The grey area highlights the substantia nigra and the arrows depict nigral dopaminergic projections into the striatum. Part **B** shows the nigrostriatal pathway illustrated in coronal sections. Dopaminergic neurons in the substantia nigra pars compacta ("1") release DA into the striatum which is composed of the caudate nucleus ("13") and putamen ("7"). Part **C** is a magnification of the box drawn in **B**. Part **C** shows the direct and indirect pathways of DA neurotransmission. Inhibitory projections are depicted in red and excitatory projections are depicted in blue. DA excites striatal MSNs which express D1 DA receptors and simultaneously inhibits striatal MSNs which express D2 DA receptors. This affects subsequent basal ganglia signaling which is also illustrated in **C**.

Legend: 1-substantia nigra, 2-periaqueductal grey matter, 3-inferior colliculus, 4-cerebral aqueduct, 5-amygdala, 6-globus pallidus (Gpe-globus pallidus externus, Gpi-globus pallidus internus), 7-putamen, 8-ventral posterior thalamic nucleus, 9-ventral lateral thalamic nucleus, 10-corpus callosum, 11-fornix, 12-cerebral cortex, 13-caudate nucleus, 14-internal capsule, 15-cortical white matter, 16-mammillary body, 17-subthalamic nucleus

Figure 1-2 was generated using illustrations from Bear et al., An Illustrated Guide to Human Neuroanatomy, 2007 (30).

1.5 PD prevalence, risks, and causes

The worldwide prevalence of PD is difficult to ascertain (58). In the United States, PD is estimated to affect 1-2 percent of the population of age 65 years or older (465). It is thought that 40,000 new cases of PD are diagnosed annually (465). Though the disease has existed for hundreds of years, the cause for PD is still largely a mystery. In fact, the only proven risk factor for idiopathic PD is old age (58;465). PD is rare in individuals before the age of 50 but the risk increases greatly among the elderly(58).

A number of other risk factors for sporadic PD have also been proposed including gender, ethnicity, family history, exposure to various chemicals or infectious agents, head trauma, and even diet. However, many of these factors are controversial and have shown to be inconsistent between studies. It is thought that PD is a multifactorial disease and thus identifying a single cause has proven to be difficult (58;128).

1.6 PD treatments: L-DOPA is effective but also has limitations

There are no available methods to stop the progression of neurodegeneration in PD; however, there are several pharmacologic treatments which act to temporarily abate disease symptoms (**Table 1-1)**. Each PD patient can respond differently to treatments and thus, medication selection and dosage is made on an individual basis and may change over the course of a patient's disease progression (105). L-dihydroxyphenylalanine (L-DOPA) is one of the most effective symptomatic medications for PD (25). In 1961, small doses of L-DOPA (also known as levodopa) were first administered to PD patients as a means to transiently reverse motor impairments (105). Levodopa acts to supplement DA

that has been lost due to nigral degeneration. Unlike DA, levodopa can cross the blood brain barrier. Subsequently, it can be converted into DA by aromatic L-amino acid decarboxylase, an enzyme that is abundantly expressed in dopaminergic neurons (**Figure 1-3)**. PD patients typically respond well to levodopa treatments initially. Responsiveness to levodopa is often used as an indicator to distinguish PD from other types of parkinsonism. However, while PD patients respond well to levodopa during early treatments, for reasons that are poorly understood, the drug eventually loses its effectiveness after roughly 5 years of use. It also has a number of negative side effects (24;92;105).

Table 1-1 (25;105;235)

Treatment	**Mode of Action**	**Examples**	**Side Effects**
monamine oxidase (MAO)-B inhibitors	Decreases endogenous dopamine (DA) catabolism	selegiline; rasagiline	effects resulting from interactions with other medications
DA receptor agonists	Acts directly on DA receptors to mimic DA activity	apomorphine, bromocriptine, pergolide, ropinirole, pramipexole	nausea, vomiting, psychosis , dyskinesias
DA precursors	Converted to DA in the CNS as a form of DA replacement (often administered in combination with inhibitors of peripheral degradation enzymes)	levodopa/carbidopa, levodopa/benserazide, levodopa/entacapone, levodopa/tolcapone	dyskinesias, nausea, wearing-off effect
Anticholinergics	Restrict the action of acetylcholine, blocking nerve impulses at the level of the muscle	benztropine, biperiden, diphenhydramine, ethopropazine, orphenadrine, procyclidine, trihexyphenidyl	dry mouth, confusion, memory loss, nausea, blurred vision, constipation, urinary retention
Antiglutamatergics	blocks NMDA receptor (not completely clear why this reduces parkinsonism)	Amantadine	Confusion, insomnia, hallucinations, leg swelling

Figure 1-3 Pathways of DA synthesis and catabolism.

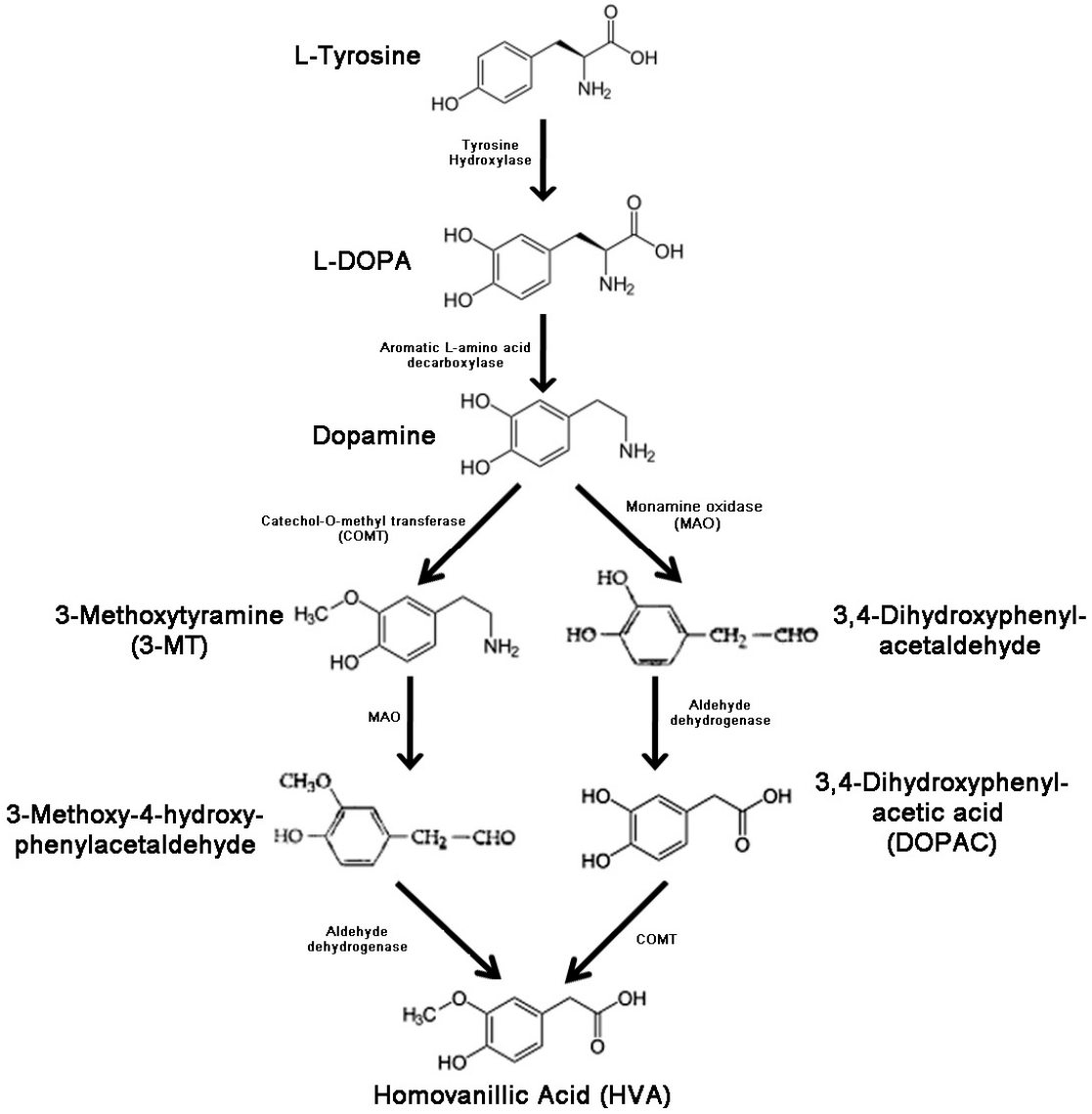

1.7 Hypotheses for PD pathogenesis

With the increasing age of the population in advanced countries, the risk for PD will continue to rise. It is therefore of great interest to improve treatments and to determine better modes of disease prevention. Gaining insights into disease pathogenesis

will be crucial in this effort. PD may develop as a consequence of dysfunctions in various biochemical pathways (82;88;109;234;365). Hypotheses related to the effects of proteasome, oxidative, and mitochondrial impairments on PD pathogenesis will be briefly discussed below.

1.8 The ubiquitin-proteasome system

It is thought that PD may be caused by impairments in the ubiquitin-proteasome system (UPS) (31;79;323). In order for protein substrates to be degraded in the UPS pathway, a series of tightly controlled events must occur (73;159;160). First, ubiquitin-activating enzymes (E1 enzymes) modify ubiquitin protein molecules in a two-step reaction which requires ATP. Once ubiquitin molecules have been activated by E1 enzymes, they are transferred to E2 ubiquitin-conjugating enzymes (E2 enzymes), forming E2 enzyme-ubiquitin complexes. Next, E3 ubiquitin-protein ligases (E3 ligases) act to facilitate covalent ligation of ubiquitin to protein substrates.

Different types of E3 ligases may facilitate protein-ubiquitin ligation by distinct mechanisms (160). Many E3 ligases can bind to protein substrates and corresponding E2 enzymes simultaneously to form protein substrate-E3 ligase-E2 enzyme-ubiquitin complexes. These complexes allow for the direct transfer of ubiquitin from E2 enzymes onto specific lysine residues of respective protein substrates. Once a substrate protein is ubiquitinated, E1, E2, and E3 enzymes can promote subsequent polyubiquitination of the substrate by covalent linkage of ubiquitin molecules onto residue Lys 48 of the previously conjugated ubiquitin molecule. The addition of a chain of at least four Lys-48-

linked ubiquitin molecules onto a substrate protein marks the substrate for degradation by the 26S proteasome (73;159;160).

The 26S proteasome is a complex consisting of a large protease (the 20S proteasome) and several regulatory subunits (19S/PA 700, PA 200, PA28) (3;323;369). It is arranged into a hollow symmetrical dumbbell-like structure with the catalytic 20S subunit at the central core and regulatory subunits on either end (3;73;369). The 20S catalytic core possesses chymotrypsin-like, trypsin-like, and peptidylglutamyl-peptide hydrolase (PGPH)-like protease activities which act to break down substrate proteins into small 2-25 amino acid peptide fragments. Such peptides can be further hydrolyzed into individual amino acids which can be used to make new proteins (3;246;323).

It is important to note that when clearing proteins via the UPS pathway, each E2 enzyme only binds to a subset of E3 ligases and each E3 ligase only binds to a specific number of protein substrates. While there is likely some redundancy in this system, the failure of an E3 ligase to bind its substrates or to interact with corresponding E2 enzymes could result in substrate accumulation and subsequent protein aggregation. It is hypothesized that aggregated proteins can resist proteasomal degradation and that they may even clog and inactivate 20S catalytic subunits (323 and references therein). When misfolded proteins are not cleared, they can accumulate or aggregate, resulting in the formation of proteinaceous inclusions.

1.9 Lewy bodies in PD and proteasome dysfunction

In 1910, Fritz Heinrich Lewy, a German born neurologist and histopathology specialist, presented a paper, *To the Pathological Anatomy of the Paralysis Agitans*, at the Seventh Annual Meeting of the Society of German Neurologists. During his presentation, Lewy described his discovery of intracellular "balls" that were detected in PD basal ganglia tissues during post mortem analyses. These "balls" were noted to be proteinaceous, eosinophilic and variable in size (382). In 1918, the term, "corpe de Lewy" or "Lewy bodies", was first used to describe these pathologies (166;382). Today it is known that Lewy bodies (LBs) are the common neuropathological hallmark of PD (396).

LBs are intraneuronal, cytoplamsic inclusions that typically only affect specific neuronal populations in PD brains. The classical LB is spherical in shape with a dense granular core and fibrillar halo (219;396)(**Figure 1-4**). The preponderance of LBs in PD brains significantly links these pathologies to nerve cell degeneration. However, it is not fully understood what molecular events lead to LB formation (112). It is known that LBs are composed of deposits of aggregated proteins that are often ubiquitinated (356), and it is possible that these proteins may accumulate and associate into LBs as a consequence of proteasome impairments in PD. To support this idea, enzymatic analyses reveal that PD substantia nigra tissues demonstrate reduced proteasome activities (287;290). Additionally, decreased levels of regulatory subunits of the 26S proteasome have been observed in PD (287;288). These findings may link proteasome impairments to PD pathogenesis; however it is still unknown whether such changes may be causal of disease.

Figure 1-4

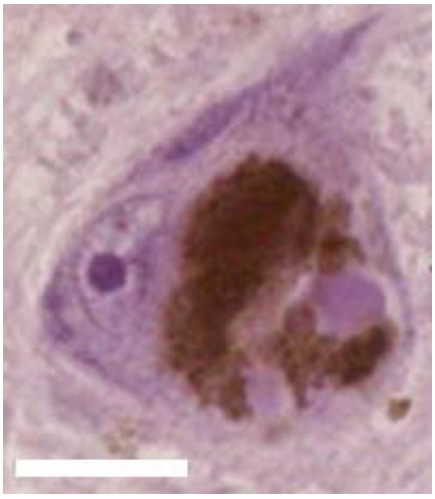

Lewy Body. The image shows multiple LBs in the same neuron of the SNpc stained with hematoxylin-eosin. Scale bar is 25µm.

Figure modified from Kovari et al., Brain Res Bull 2009 (219).

1.10 Proteasome Inhibitors

Studies to understand the effects of proteasome dysfunction in rodent and cell culture models of PD often utilize proteasome inhibitors such as carbobenzoyl-leu-leu-leucinal (MG-132), lactacystin, and epoxomicin. MG-132 is a synthetic cell-permeable peptide-aldehyde that can reversibly bind and inhibit chymotrypsin-like activities of the 20S proteasome (436;437). MG-132 is also known to inhibit calcium-modulated cysteine proteases (calpains) to a lesser degree (437). Lactacystin is a naturally occurring compound that was isolated from Actinomycetes in 1991 (326). It covalently binds to 20S proteasome subunits and acts to inhibit chymotrypsin-like and trypsin-like activities in an irreversible manner while inhibiting PDPH-like activities in a reversible manner (108). In aqueous solution, lactacystin is converted by hydrolysis into its active form, *clasto*-lactacystin-β-lactone (Omuralide) (97). Omuralide specifically inhibits the proteasome although it has also been shown to inhibit capthepsin A to a lesser degree

(246). Since both MG-132 and omuralide can inhibit proteases in addition to the 20S proteasome, when using these agents to study proteasome function, it is best to show similar effects with other proteasome inhibitors (246). One such inhibitor, epoxomicin, was originally isolated from an Actinomycetes strain in 1992 (149). Epoxomicin was later discovered to be a provocative, irreversible and selective inhibitor of all 3 protease activities of the 20S proteasome (293). Importantly, epoxomicin does not act to inhibit other known cellular proteases, making it a suitable agent in proteasome studies (293).

1.11 Proteasome inhibitors are used to induce parkinsonism in rodent models.

There is evidence to suggest a strong link between the UPS and nigral neuronal health. For instance, it has been shown that intranigral injections of lactacystin into rats causes protein inclusion formation, nigral and extranigral lesions as well as parkinsonian-like behavioral impairments (289;451;300;318). Epoxomicin has similar effects on rats, even when introduced systemically (292). Similarly, mice display nigral specific degeneration following MG-132 exposure (415). MG-132 is also selectively toxic to primary dopaminergic neurons in culture (415). It is not clear why proteasome inhibitors are particularly toxic to nigral neurons. Determining the answer to this question will give insights into the role of proteasome impairments in the etiology of PD.

1.12 Reactive oxygen species and oxidative stress

Oxidative stress is a term used herein to describe cellular damage which results from reactive oxygen species (ROS). The term ROS can be used to describe any strong electrophile which is composed in part by oxygen (15). In animal cells, while there are

various sources of ROS, ROS can be generated by mitochondria during the process of aerobic respiration (101;221;408). During respiration, in order to efficiently generate energy in the form of ATP, electrochemical proton gradients must be established across inner mitochondrial membranes (6). To generate these gradients, electrons are transferred from an initial electron donor to electron acceptors in various mitochondrial enzyme complexes which are together referred to as the electron transport chain (ETC). The transfer of electrons along the ETC begins at mitochondrial complex I (or alternatively at complex II) and proceeds in series until it terminates at mitochondrial complex IV. Complex IV then catalyzes a series of reactions which transfers reactive ETC electrons to O_2 and this eventually results in the formation of water. Prior to reaching complex IV, however, electrons can leak prematurely during each successive transfer along the ETC. The monoelectronic transfer of one of these leaked electrons to an O_2 molecule forms superoxide ($^{\cdot-}O_2$).

Superoxide can be generated by mitochondria as well as other enzymes and can serve as a progenitor for other ROS (408;435). For example, mitochondrial superoxide dismutase dismutates $^{\cdot-}O_2$ to hydrogen peroxide (H_2O_2), which is another ROS. H_2O_2 can readily diffuse across mitochondrial membranes and out into the cell where it can affect various cellular processes (64;221). Alternatively, in the presence of iron (Fe^{2+}), H_2O_2 can be converted into highly reactive hydroxyl ($^{\cdot}OH$) radicals which are thought to be very damaging (221;78). In addition to H_2O_2 and $^{\cdot}OH$ radicals, $^{\cdot-}O_2$ is also a progenitor for another extremely reactive species, peroxynitrite ($ONOO^-$), which is formed by the reaction of $^{\cdot-}O_2$ with nitric oxide (NO^-) (183;221). $ONOO^-$ can lead to the generation of

additional reactive radicals including ˙OH radicals, nitrogen dioxide ($^{\cdot}NO_2$), and carbonate ($CO_3^{\cdot-}$) (417).

1.13 Oxidative stress and peroxiredoxins

If left unchecked, ROS can indiscriminately attack cellular proteins, lipids, and nucleic acids resulting in variable degrees of oxidative damage (9;64;215;435). To protect against this, healthy cells utilize a variety of regulatory enzymes that act to inhibit undesirable redox reactions (9;408). However, such compensatory enzymes can become overwhelmed when oxidants are overabundant, and the consequences of this can be fatal (215;221). For example, the family of antioxidant peroxidase enzymes, peroxiredoxins (Prxs), acts to decompose H_2O_2 and other intracellular peroxides by reducing them to less reactive forms (147). In mammals, the Prx enzyme family is composed of six different isoforms which confers tissue and subcellular expression specificities to each of its members (193;222). It is known that Prxs utilize conserved cysteine residues that donate electrons to peroxide substrates, resulting in the formation of Prx cysteine sulfenic acid (147;472). Ideally, following oxidation to sulfenic acid forms, Prxs can be subsequently reduced either by neighboring Prx molecules or by other electron donors (147;472).This serves to recharge Prx enzymes for future reactions. However, when peroxide levels are overwhelming, oxidation of Prxs to cyteine sulfinic or sulfonic acid forms can occur and these modifications have been shown to disrupt future Prx enzyme activities (147;472).

1.14 Oxidative stress in PD

In a study to assess for expression of Prx isoforms in neurodegenerative diseases, a specific increase of PrxVI was detected in frontal cortex regions in PD brains as compared to normal, Down's syndrome, or Alzheimer's disease brains (222). Interestingly, this increase was not detected for other Prx isoforms, suggesting a specific role for PrxVI in PD (222). Confirming this idea, Power et al. reported increased levels of PrxVI in PD brain homogenates in comparison to homogenates from normal brains (360). Histological analyses also revealed that PD brains exhibited increased PrxVI staining as compared to controls (360). These findings could be correlated to an overabundance of oxidation in PD.

Several common pathological markers for oxidative stress are known to be associated with PD including DNA and protein oxidation, lipid peroxidation and alterations in antioxidant levels (9;215;278). For instance, depleted levels of the antioxidant glutathione (GSH) can often correlate with severe nigral degeneration in PD (9;278). GSH is a tripeptide that is used as a souce of reducing equivalents in cells (278). Interestingly, GSH serves to reactivate PrxVI following its conversion to cysteine sulfenic acid forms (272). However, when GSH levels are depleted, it is possible that PrxVI could become inactivated by excessive oxidation and it is not known whether this could result in subsequent aggregation of the inactivated PrxVI enzyme. It is interesting to note that PrxVI co-localized to nigral Lewy inclusions in PD brains (360). This is one of many findings that may implicate a role for oxidative stress in LB formation.

1.15 Oxidation in dopaminergic neurons

It is thought that dopaminergic neurons may be particularly vulnerable to oxidative stress since oxidation is inherent in these cells even in healthy individuals. It is known that DA can spontaneously oxidize to form electrophilic quinones, which can lead to oxidative damage of proteins (140;267). DA itself can be metabolized by MAO to form H_2O_2 (64). Additionally, the DA metabolite, 3,4-dihydroxyphenylacetic acid (DOPAC) can also be converted to quinones which generate ROS (64).Thus, without proper regulation, DA itself could promote oxidative stress which could result in dopaminergic neuron toxicity. However, the heterogeneous pattern of dopaminergic neurodegeneration in PD is confounding since dopaminergic neurons in extranigral brain regions are less affected in disease (94;162).

1.16 Oxidative stress in PD models

Experimental paradigms designed to better understand the role for oxidative stress on nigral neurodegeneration often utilize oxidizing agents such as paraquat, 6-hydroxydopamine or H_2O_2. Reduction-oxidation cycling of paraquat leads to the formation of $^{\cdot-}O_2$ radicals (362;48;36). Paraquat can also oxidize Fe^{3+} to Fe^{2+} which can then subsequently react with H_2O_2 to form $^{\cdot}OH$ radicals (362). Paraquat also acts to increase nitric oxide levels, eventually leading to the formation of reactive $ONOO^-$ (89;330). Traditionally, paraquat has been used as an herbicide since it efficiently disrupts photosynthesis by scavenging electrons (414). Of interest to PD studies, paraquat exposure in rodents results in nigrostriatal dopamine neuron degeneration and this can result in parkinsonian motor impairments (49;231;286;331;430). However, it is not fully understood why nigrostriatal neurons are particularly vulnerable to paraquat insult (36).

The oxidizing agent, 6-hydroxydopamine (6-OHDA), can act to generate $^{\cdot}O_2^-$, H_2O_2, or $^{\cdot}OH$ radicals (78). Due to its close structural similarity to the catecholamines DA and norepinephrine, 6-OHDA is selectively taken up into catecholaminergic neurons where it can exert its deleterious effects (397). For instance, when 6-OHDA is infused into striatal or nigral tissues in various animal models, it results in dopaminergic neurodegeneration and behavioral impairments that resemble those observed in PD. Thus 6-OHDA is a tool that is widely used to model PD; however, it is somewhat limited since proteinaceous Lewy-like inclusions are not formed as a consequence of its use (397).

Yet an additional oxidizing agent, H_2O_2, can be used to induce oxidative stress in vitro and in PD cell culture studies. For example, in a recent study by Zhou and Lim, H_2O_2 treatment of mouse mesencephalic MN9D dopaminergic cells acted to inhibit proteasome activity. It also sensitized these cells to MG-132 and resulted in cell toxicity (495).

These findings suggest that oxidative stress may be a causal stimulus for degeneration in PD. Thus, it will be beneficial to determine what specific factors can act to mitigate oxidative insults that may occur with respect to the disease.

1.17 MPTP parkinsonism syndrome and mitochondrial dysfunction in PD

In a report in 1979, Davis et al. described a 23 year old male who presented with acute parkinsonism following self-administration of home-made 4-propyloxy-4-phenyl-*N*-methylpiperidine (MPPP). MPPP is an opiate which has similar effects as the

analgesic, Demerol (meperidine). While synthesizing MPPP, the patient also accidentally generated a toxic byproduct, N-methyl-4-phenyl-1,2,3,6-tetrahydropyridine (MPTP), which contaminated his illegal drug preparations. Following self administration of this preparation, the patient developed, "a state of muteness, severe rigidity, weakness, tremor, flat facial expression, and altered sensorium" (87). In a later report, Langston et al. described four heroin addicts who also developed severe parkinsonism subsequent to only one week of illegal MPPP/MPTP contaminated drug use (237). Other similar reports later followed (20;236;473). The agent responsible for the onset of disease symptoms was concluded to be the MPTP contaminant (237).

Interestingly, the MPTP-induced parkinsonism syndrome was remarkably similar to that of idiopathic PD. Further, post mortem histological analyses of four affected patients revealed dramatic degeneration of nerve cells within SNpc as well as associated gliosis and microglial activation (87;237;239). However, distinct from sporadic PD, no MPTP-induced neuronal effects were detected in other brain regions such as locus coeruleus, basal ganglia, hypothalamus, thalamus, cortex, cerebellum, or nucleus basalis of Meynert. Further, traditional Lewy bodies were not apparent (239).

Following these reports, aggressive studies were conducted to understand the mechanism by which MPTP induced cell toxicity. It was discovered that MPTP can rapidly diffuse across lipid bilayer membranes into the brain where it can be metabolized by the MAO type B (MAO-B) enzyme to form 1-methyl-4-phenylpyridnium (MPP^+). This reaction is thought to occur in glia since appreciable levels of MAO-B enzyme localize particularly to glial cells and serotonergic neurons in the brain (466;467). The

MPP^+ metabolite is the chemically active form of MPTP, but since it is not as lipophilic as the MPTP parent compound, to enter cells quickly, the MPP^+ metabolite requires active transport. Incidentally, MPP^+ is a substrate for the dopamine transporter (DAT) and can thereby selectively enter dopaminergic neurons. Once inside the cell, MPP^+ accumulates in mitochondria where it can bind at two distinct sites in mitochondrial complex I and thus disrupt complex I catalytic activity (363). Inhibition of complex I can cause cellular dysfunction by the production of ROS (363;365;398). Discoveries of the inhibition of mitochondrial complex I by MPTP/MPP^+ and its specific effects on dopaminergic neurons in humans provided the first line of evidence for the role of mitochondrial impairments in PD pathogenesis.

1.18 Mitochondrial impairments in sporadic PD

Shortly thereafter, it was discovered that PD patients exhibited reduced activity in mitochondrial complex I when compared to normal individuals (273;380) and that this deficiency was specifically observed in the substantia nigra brain region (273;381). In comparison to controls, some PD patients were also deficient in mitochondrial complex I subunits in striatal tissues (302). It was also reported that PD patients demonstrated reduced activities of mitochondrial complexes I, II, and IV in skeletal muscle (40), although this finding has not been supported by other studies (10;273). Additionally, reduced activity in mitochondrial complex I can be detected in platelets of PD patients (145;223;223), although this idea may also be controversial (273). Taken together, these

findings suggest that mitochondrial dysfunction is the link that connects MPTP-induced parkinsonism to sporadic PD.

1.19 MPTP and parkinsonism animal models

Interestingly, the effects of MPTP on animal models also resemble features that are common to idiopathic PD. When administered to nonhuman primates or mice, MPTP/MPP^+ selectively and irreversibly damages dopaminergic neurons of the SNpc and markedly reduces striatal dopamine content (48;50;111;238). Additionally, protein inclusion formation can result from chronic MPTP exposure in mouse models of PD, though these inclusions are not necessarily reminiscent of LBs (111;192;295). Exposure to MPTP can also lead to protein aggregation in primates (113;114;220).

In addition, MPTP can be a valuable tool for in vitro studies. For example, Pavlovic et al. show that although mouse Neuro-2A (N2A) neuroblastoma cells do not express the plasma membrane DAT, MPP^+ is able to enter these cells by passive diffusion, albeit relatively slowly (346). Following N2A cell entry, MPP^+ can decrease mitochondrial membrane potential, increase ROS, activate caspases, and induce apoptosis (346). Thus MPTP is widely used in studies to model mitochondrial dysfunction.

1.20 Rotenone models of PD

Another commonly used mitochondrial inhibitor is rotenone. For centuries prior to 1924, rotenone had been harvested from indigenous plants in South American countries and was used by natives as a fish poison (225). Rotenone was later discovered

to act as a potent insecticide and became widely used in the United States for this purpose (225). Investigations into the physiological mechanism of the rotenone toxin determined that it can tightly bind to mitochondrial complex I and thereby block electron transfer along the ETC (168;258;259;322). Rotenone is lipophilic and thus it can ubiquitously and indiscriminately enter brain cells to exert its inhibitory effects on mitochondria (240).

Rotenone is actually proven to be a more potent complex I inhibitor than MPP^+ (363) and thus it is often used to induce mitochondrial stress in various experimental paradigms. Interestingly, while chronic systemic rotenone exposure in rats depletes complex I enzyme levels throughout the entire brain, this can result in specific degeneration in nigrostriatal tissues as well as intracellular inclusion formation and associated parkinsonian behavioral traits (38;54;390). While rotenone may preferentially affect nigral dopaminergic neurons for degeneration, other studies have shown that neuronal loss can also be detected in rat locus coeruleus, cerebellum and mildly in frontal cortex tissues (165). It is thought that the particular toxicity of rotenone on nigrostriatal dopaminergic neurons may be due to the increased levels of oxidative stress that arise secondary to mitochondrial complex I inhibition (429). Supporting this idea, a recent study by Pan-Montojo et al. showed that chronic intragastric rotenone administration in mice resulted in decreased motor activity and intracellular protein inclusion formation in spinal cord, brainstem, and substantia nigra (336). It also resulted in nigral dopaminergic neurodegeneration. This was likely due to secondary effects of rotenone exposure in these animals since rotenone was not detected in systemic blood or in the central nervous system (336). Other studies also confirm that rotenone has a toxic effect on mouse nigrostriatal tissues following chronic oral administration (179;180). Together, these

findings suggest that nigral dopaminergic neurons are vulnerable to mitochondrial complex I inhibitors and this may further implicate a role for mitochondrial dysfunction in PD pathogenesis. Nevertheless, more work must be done to determine what factors may act to modulate this.

1.21 Genetic causes of PD

Discoveries of inherited forms of PD have increased awareness about physiological mechanisms that may be implicated in the etiology of the disease. To date, at least 14 chromosomal loci and 9 genes have been identified which cause monogenic forms of PD (**Table 1-2**) (152;250). Although familial forms of the disease only comprise ~ 5% of all PD cases, studies of the gene products encoded by PD-linked genes have given insights into the factors that may be relevant to understanding sporadic PD (152;250). The roles of the PD-linked genes *PARK1/4 (SNCA*), *PARK*2 (*parkin*), and *PARK6 (DJ-1)* will be the subject of the following sections.

Table 1-2

Locus	Chromosome	Year of discovery	Gene	Inheritance
PARK1/PARK4	4q21-q23	1997 (357)	*SNCA*/α-synuclein	Dominant
PARK2	6q25.2-27	1997 (284)	parkin (208)	Recessive
PARK3	2p13	1998 (125)	Unidentified	Dominant
PARK5	4p13	1998(249)	UCHL1	Dominant
PARK6	1p36.12	2001 (442)	PINK1 (441)	Recessive
PARK7	1p36	2001(446)	DJ-1 (47)	Recessive
PARK8	12q12	2002 (118)	LRRK2 (333;497)	Dominant
PARK9	1p36	2005 (468)	ATP13A2 (364)	Recessive
PARK10	1p	2002 (161)	Unidentified	Unknown
PARK11	2p37.1	2008 (241)	GIGYF2	Unknown
PARK12	Xq21-q25	2002 (337)	Unidentified	X-linked
PARK13	2p13.1	2005 (412)	Omi/HtrA	Dominant
PARK14	22q13.1	2009 (332)	PLA2G6	Recessive
PARK15	22q11.2	2009 (96)	FBXO7	Recessive

1.22 *PARK*1/4 (*SNCA*)/α-syn

In 1990, Golbe and colleagues released reports about an endemic of PD within a large family from Contursi village in southern Italy (134). The affected individuals developed early-onset disease at ~47 years of age and had relatively rapid courses of less than 10 years from disease onset to death. At the time of the report, it was concluded that a single gene was causal of this form of PD, though no putative gene candidates had yet been identified (134). Years later, a genome wide scan in the affected Italian family identified loci at chromosome 4q21-q23 that linked to the disease phenotype (357). *SNCA* or alternatively *PARK1/4* was among many genes that mapped to this particular chromosomal region. Further sequence analysis of the *SNCA* gene in the Contursi kindred revealed a single nucleotide (G209A) missense mutation which resulted in the A53T α-synuclein (α-syn) amino acid substitution (357). The pathogenic A53T α-syn mutation showed an autosomal dominant pattern of inheritance and this finding provided the first solid evidence for a monogenic cause of PD.

α-syn immediately became a hot topic of discussion in the field of PD research. Human α-syn had been previously cloned in 1993 by Ueda and colleagues as an "unrecognized component of amyloid in Alzheimer disease" (438). In the initial report by Ueda and colleagues, α-syn was detected in diffuse, primitive and mature amyloid plaques but was absent in neurofilbrillay tangles. Thus it was called non-Aβ component of AD amyloid (NACP) (438). The identified NACP species was later coined "α-synuclein" by Jakes and colleagues (188) based on its close sequence homology to previously described synuclein proteins (277).

α-Syn is a small protein of 140 amino acid residues which is predominantly expressed in the brain and which localizes to presynaptic nerve terminals (187;188;277). It is largely a hydrophilic protein with the exception of a central hydrophobic core which is designated as the "NAC" region (187). The amino terminus of α-syn contains repeat motifs consisting of the residues, K-T-K-E-G-V (277), and the carboxyl terminus is acidic due to prevalent Glu residues (187).

In the same year following the report of the Contursi kindred, it was discovered that α-syn protein localized to LBs in idiopathic PD brains (405). Full-length, partially truncated and insoluble forms of α-syn were detected in these pathologies and it was eventually concluded that, "α-syn is the building block of LBs" (18;119;182;396). These findings were the first to implicate a fundamental role for α-syn in the etiology of both inherited and sporadic forms of PD.

To date, several mutations in the *SNCA* gene are known to cause autosomal dominant PD. In addition to the initial report of the Italian Contursi kindred (357), the A53T α-syn mutation has been identified in many PD patients of European descent (17;276;338;406). In addition, a missense mutation resulting in the A30P amino acid substitution in α-syn was shown to be causal of PD in a German family (224). In a Spanish kindred, severe parkinsonism phenotypes are also associated with another α-syn amino acid substitution, E46K (488). Furthermore, short chromosomal duplications and triplications that include the *SNCA* gene are associated with clinical phenotypes that resemble idiopathic PD (61;107;176;400). Taken together, these findings implicate α-syn protein as an important player in parkinsonism-associated diseases.

Although the physiological role for α-syn has yet to be identified, years of extensive analyses point towards several putative functions. Some studies suggest that α-syn may normally behave in a protective capacity (76;368). For example, α-syn may act to regulate synaptic vesicle integrity since it can co-localize with the vesicle membrane protein, synaptophysin (187), and is also known to be in close proximity or in association with synaptic vesicles (187;277). α-Syn also exhibits chaperone-like activity (5;205;206;343;403) and may even act as an auxiliary molecular chaperone for synaptic vesicle proteins (59). Additionally, α-syn may act to protect against dopamine induced oxidative stress. For instance, α-syn may down-regulate dopamine synthesis by modulating the tyrosine hydroxylase (TH) or aromatic L-amino acid decarboxylase enzymes (7;348;351;427;70).

Though α-syn may exhibit protective features under certain experimental conditions, it is thought that α-syn mutations contribute to PD by a gain-of-function. For instance, studies suggest that α-syn may induce and/or enhance oxidative stress which acts to promote cell toxicity (27;95;169;191;197;339;340;413). It is also known that α-syn can polymerize into filaments and aggregate into amyloidogenic inclusions, and that this ability is enhanced by A53T and E46K mutations (464). Further, α-syn inclusion formation may be lethal in vivo due to associated impairments of the proteasome (34;410;425;432). Alternatively, α-syn may exert its detrimental effects by inducing mitochondrial impairments (95;103;169;256;261;264;279;329;339;340;388;425;447;448;474).

An array of α-syn animal models has been developed for the purpose of understanding the physiological role of α-syn in vivo. α-Syn null mice were generated in

order to determine the effect of α-syn loss-of-function (1). However, although subtle alterations in DA neurotransmission were reported, α-syn null mice exhibited normal life spans, did not display nigrostriatal deficits, and appeared to be normal as it related to synaptic nerve terminal integrity (1). Alternatively, gain-of-function, transgenic mouse models expressing human α-syn protein have yielded more provocative findings. In brain tissues of transgenic mice expressing wild-type (WT) human α-syn protein, α-syn was phosphorylated and exhibited reduced biochemical extractability (315). This was interesting since both biochemical features are common to human LB diseases (11;117;375;463). Transgenic mice expressing pathogenic mutant A30P human α-syn developed phosphorylated, aggregated, proteinase K-resistant LB-like deposits of α-syn in various regions of the central nervous system (CNS) (199;315) and this was associated with the onset of fatal motor impairments in an age-dependent manner (315). Similarly, when expressed in mice, pathogenic mutant A53T human α-syn aggregated into Lewy-like inclusions that could be detected throughout the neuroaxis (131;247;444). This resulted in marked axonal degeneration (131;279;444) and the induction of progressive, severe motor abnormalities (131;444;247). These mouse studies suggest that the onset of disease phenotypes directly correlate to the propensity for α-syn to aggregate in vivo; however it remains to be determined what cellular mechanisms may act to modulate this, especially as it relates to how other gene products may be implicated. Identifying such factors would be insightful.

1.23 *PARK 2 (Parkin)*

Evidence of autosomal recessive types of juvenile parkinsonism (AR-JP) were first reported by Yamamura and colleagues in 1973 (481). AR-JP was described as an insidious disease with juvenile to early-onset (before 40 years of age) (481;184;420) that was clinically characterized by progressive typical parkinsonism, superb levodopa responsiveness, and a slow and protracted disease course (481). Neuropathological analyses of AR-JP cases showed highly selective degeneration of neurons in SNpc but without evidence of LB formation. Additionally, degeneration could be detected to a lesser degree in the locus coeruleus. Gliosis was also prominent in the affected brain regions (420). In 1997, Matsumine and colleagues identified a gene for AR-JP which mapped to chromosome 6q25.2-27 (284). This gene, which was designated as *PARK*2 (285), was later cloned by Kitada et al. and was discovered to encode a protein product that was called "Parkin" (208).

The parkin protein is 465 amino acids in length (208). It is expressed in many tissues with highest expression in skeletal muscle, heart, testis and brain (208). In general, parkin can be detected throughout the brain (84;226) and can be localized to neurons, astrocytes, and microglia (172;391;411). It is most abundant in cell soma (84;411) but can also localize to processes and presynaptic terminals (84;172;411).

Based on sequence homology studies, it was determined that parkin shows similarity to ubiquitin protein at the N-terminus (208). It was also originally thought that parkin had one Really Interesting New Gene (RING) finger motif at the C-terminus (208), but it was later determined that parkin actually contains two C-terminal RING

finger domains separated by an In-Between-Ring (IBR) finger domain (308). Many proteins with this RING1-IBR-RING2 signature are found in nature (445), and it was known that some RING finger proteins could act as E3 ligases in the UPS (194). Together, this knowledge provoked several studies which aimed to determine whether parkin could act as an E3 ligase. Subsequently, it was determined that parkin could interact with the E2 enzymes UbcH7, UbcH8, Ubc7, and Uev1/UbcH13 (100;178;283;325;392;490) and that this association could result in parkin autoubiquitination (283;490) as well as polyubiquitylation of unidentified cellular protein substrates (178;392). Thus, it was concluded that parkin can function as an E3 ligase; however, the physiological relevance for this function has yet to be fully established.

The *parkin* gene consists of 12 exons and large intron regions spanning a total of 1.38 Mega bases in size, making it one of the largest known genes (16). Genes of large size, such as *parkin,* may be particularly susceptible to mutations. To date, it is known that a variety of *parkin* exonic deletion, duplication, triplication, splice site, missense, and nonsense mutations result in juvenile to early-onset PD (26;155;270;282;359;416). In fact, parkin mutations are the leading cause of recessive juvenile PD (478). Thus, there has been much focus on understanding the role of parkin protein, especially as it relates to how parkin mutations may be causal of PD.

It is thought that parkin mutations cause disease by a loss-of-function. Supporting this idea, it has been reported that many pathogenic parkin missense mutants show reduced or impaired E3 ligase activities when analyzed in vitro (72;283;392;407;490). It is also known that several pathogenic parkin mutants have a tendency to form

intracellular aggregates when expressed in cultured cells (81;143;148;407;460) and that this may be due to improper folding of mutant protein (383). Based on these findings, one would expect for parkin-associated PD patients to exhibit an overabundance of parkin-positive pathologies in their brains; however such an observation is very uncommon. In fact, to the contrary, most parkin-associated PD patients seemingly resist inclusion formation since neither LBs nor other pathological inclusions are typically detected during postmortem analyses (4). However, it should be mentioned that α-syn and/or parkin positive pathologies have been observed in the brains of a few patients with parkin mutations (106;361;378;384).

The absence of Lewy inclusions in parkin-associated PD brains led some to speculate that functional parkin protein must be required for LB formation (72;384). In agreement with this notion, parkin has been shown in some studies to localize to LBs in sporadic and inherited forms of PD (22;384;391) and may act to ubiquitinate O-glycosylated forms of α-syn as a substrate in vivo (393). Additionally, parkin may ubiquitinate α-syn positive LB-like inclusions in cultured cells (72). Further, the α-syn interacting protein, synphilin-1 (104;317;202), was identified as a putative parkin substrate by Chung and colleagues in 2001 (72). This is interesting since synphilin-1 can localize to LBs in sporadic PD brains (458;312;22) and can promote the formation of cytosolic α-syn-positive inclusions in cultured cells (104;72). Though the physiological role for synphilin-1 is not clear, it is known to be polyubiquitylated in the presence of parkin and to co-immunoprecipitate with parkin in vivo (72). Additionally, although it is thought that parkin may facilitate polyubiquitylation of synphilin via Lys-63-linked chains and that this may regulate synphilin in a proteasome-independent manner, it is

known that parkin can mediate proteasome degradation of synphilin under certain experimental conditions (257).

It should also be mentioned that to date, a growing number of other putative parkin substrates has been identified. Among them are included the synaptic vesicle associated protein, CDCrel-1 (490); the parkin-associated endothelin receptor-like receptor, Pael-R (177); cytoskeletal proteins α/β-Tubulin (370); the synaptic vesicle protein, synaptotagmin XI (173); the aminoacyl-tRNA synthetase cofactor, p38/JTV-1 (83;217); the cell division control-related protein, SEPT5_v2/CDCrel-2 (68); the cell cycle protein, cyclin E (409); and the p38/JTV-interacting protein, far upstream element-binding protein 1 (FBP1; 216). Determining the authenticity of these proposed substrates remains to be confirmed *in vivo* since studies in parkin deficient animals and AR-JP brains have been somewhat limited. More work must be done to determine the effects of parkin on putative substrates especially as it relates to how these effects may contribute to PD pathogenesis.

Studies suggest that parkin acts to protect against a multiplicity of toxic insults. It is known that parkin actively decreases ROS formation (190) and can also mitigate the effects of harmful protein aggregation (311;262). When overexpressed in cultured cells, parkin can protect against noxious agents such as $ONOO^-$, H_2O_2, MPP^+, DA, 6-OHDA, and MG-132 (174;175;440;190;71;151). It can also assuage the deleterious effects following MPTP or 6-OHDA exposure *in vivo* (345;450). It is thought that parkin may prevent cell death by activating protective signaling pathways (156;386) and also by down-regulating classical apoptotic signaling molecules (85;151;190;56). Additionally,

parkin may have a specific role at protecting cells by maintaining mitochondrial homeostasis (373;314;126;230;229;75;342;485;358;93;341;268;141;35).

Parkin deficient animals are known to be particularly vulnerable to certain types of stressors and this is likely due to a loss of protective parkin function. For example, transgenic parkin null worms and mice exhibit selective vulnerability to rotenone exposure (447;55). Parkin deficient *Drosophila* are highly sensitive to paraquat (353). Systemic exposure of aged parkin deficient mice to the inflammatory stimulus, lipopolysaccharide (LPS), can result in selective nigral dopaminergic neurodegeneration (116). Taken together, this evidence supports the notion that loss of parkin function can have detrimental consequences within certain confines. However, in the absence of stressful stimuli, determining the *in vivo* effects of parkin loss-of-function has proven to be difficult, especially in mouse models. Parkin deficient mice appear to be phenotypically normal as it relates to lifespan, body weight, brain size, brain morphology, and nigrostriatal neuronal integrity (135;186;211;350;379;496). Some labs report mild motor or learning deficits in parkin null mice (135;186;350;454;496); however these observations are not confirmed in other studies (379). Parkin deficient mice also show slight alterations in nigrostriatal dopamine neurotransmission and/or turnover (186;496) (135;379), although this finding is inconsistent with other reports (116;349;350). Interestingly, von Coelln and colleagues observed a loss of locus coeruleus neurons in parkin null mice (454), but this finding was not reported by other groups. Additionally, some studies suggest that parkin deficient animals suffer from mitochondrial impairments, oxidative stress, and glial dysfunction (335;372;401) while others show that parkin null mice are resilient against stressors like MPTP and 6-OHDA (349;431), and

the latter findings seem contradictory to the former. Thus, the reported inconsistencies regarding the effects of parkin loss-of-function in mice make it very difficult to conclude what physiological role parkin may play in PD pathogenesis.

1.24 *PARK7(DJ-1)*

In 2001, a report was published by van Duijn and colleagues about 4 individuals in a Dutch family who presented with early-onset parkinsonism (446). The affected individuals developed symptoms prior to 40 years of age, were responsive to levodopa and dopamine agonist therapies, showed severe abnormalities consistent with nigrostriatal dopaminergic system dysfunction, and had slow disease progression (446). The affected patients did not harbor mutations in the other known PD-linked genes, and a novel locus at chromosome 1p36 was identified and linked to the disease phenotype with an autosomal recessive pattern of inheritance (446). The new locus was called *PARK7* (446). In later studies, Bonifati et al. sequenced the candidate genes at the *PARK7* locus and identified an exonic deletion in the affected Dutch family which mapped to the *DJ-1*gene (46). Interestingly, in the same report, Bonifati and colleagues also discovered a homozygous missense mutation in the *DJ-1* gene that was causal of early-onset PD in an Italian family (46). Together, these discoveries sparked new interest in *DJ-1* as a novel PD-linked gene.

To date, a variety of pathogenic *DJ-1* mutations have been reported (**Table 1-3**) and are thought to cause disease by a loss of DJ-1 function (46). While most affected

patients clinically exhibit the cardinal symptoms of PD, autopsy tissues are not yet available to determine the neuropathological features associated with causative *DJ-1* mutations (200). These mutations are rare (433;66;214), perhaps only contributing to 1-2% of all early-onset PD cases (154).

Table 1-3

Mutation	Inheritance	Average Age of disease onset	Ethnic group affected	Year reported (Reference)
L166P	Homozygous	30	Italian	2003(45;47)
M26I	Homozygous	39	Ashkenazi Jesish	2003 (2)
E64D	Homozygous	34	Turkish	2004 (157)
E163K	Homozygous	31.6	Italian	2005 (14)
L10P	Homozygous	18.5	Chinese	2008 (144)
P158DEL	Homozygous	33.8	Dutch	2009 (270)
14 kb deletion	Homozygous	32.6	Dutch	2003 (47;446)
R98Q	Heterozygous	< 50	European descent	2003 (146;263)
A104T	Heterozygous	35	Latino	2003(146)
c.253-322 deletion	Heterozygous	45	Serbian	2004 (98)
A179T	Heterozygous	47	Dutch	2009 (270)
Exon1-5 duplication	Heterozygous	46	Dutch	2009 (270)
c.C56DEL c.G57A c. intron6, G1C	Compound Heterozygous	24	Latino	2003 (146)
D149A G78G	Compound Heterozygous	36	Afro-Caribbean	2003(2)

The *DJ-1* gene is comprised of 7 exons and 8 introns that span 16-24 kilobases, and exons 2-6 encode DJ-1 protein (419). DJ-1 had originally been discovered in 1997 by

Nagakubo et al. in a yeast two-hybrid study to identify proteins that interacted with the known cancer gene, c-myc (313). In this study, the nucleotide and amino acid sequences determined for one of the isolated clones was designated as "DJ-1". DJ-1 was later found to be a false-positive clone that actually did not interact with c-myc directly. Nevertheless, Nagakubo and colleagues knew that DJ-1 was a novel protein and reported that it could function as an oncogene (313). Later studies to clarify the role for DJ-1 identified it as a protective protein component in rat sperm (457), a modulator for androgen-receptor mediated transcription (421), as well as a regulatory component of RNA-binding protein complexes (163).

It is known that DJ-1 is a 189 amino acid protein (313) that is ubiquitously expressed in the brain and peripheral tissues (47;228;489). It can be detected in neurons (309;476;218;371;316;324), astrocytes (21;218;324;316), reactive astrocytes (309;316), and microglia (181). It exhibits a diffuse cellular localization pattern (313;163) and can be redistributed to cell nuclei and mitochondria during stressful conditions (489;53;253;196), though neither nuclear nor mitochondrial localization signals have yet been identified for the protein.

Crystallization studies reveal that DJ-1 is composed of eight α-helices and 11 β-strands that are arranged into a helix-strand-helix sandwich (170). These structural features are common to the ThiJ/PfpI superfamily of enzyme proteins (167;170;469). Like other members of the ThiJ/PfpI superfamily, DJ-1 conserves a catalytic cysteine residue, Cys-106 (469); however, DJ-1 lacks the other coordinating residues required to form a catalytic active site, and this distinguishes DJ-1 from its structural homologues

(167;170;469). Further, it is known that DJ-1 exists as an obligate homodimer (469) (170) which may be able to associate into filaments (57).

Extensive analyses reveal that DJ-1 exhibits a diversity of protective functions. For instance, DJ-1 acts as a molecular chaperone *in vitro* (389;494). It has also been shown to protect against cell toxicity that is induced by proteasome inhibition and/or toxic protein aggregation (260;479;487;493). DJ-1 may also act to maintain mitochondrial homeostasis (43;196) since it can protect against mitochondrial toxins such as MPTP/MPP^+ and rotenone (204;8;418;53;253;43;345;310) and has specifically been shown to bind and maintain the activity of mitochondrial complex I (153). Several studies also support a role for DJ-1 in regulating the transcription of specific mRNA targets (163;395;421;479;491;443) such as pro-survival genes (43). DJ-1 can also protect against ischemia-induced insults (482) and inflammatory stimuli (456).

Following the discovery of oxidized forms of DJ-1 in human umbilical vein endothelial cells, it was proposed that DJ-1 may play a role in maintaining cell redox homeostasis (299). It is known that oxidative stress can upregulate the DJ-1 promoter (203). This may explain why DJ-1 protein is often increased both *in vitro* and *in vivo* following oxidative insult (251-253;294;418;185). DJ-1 protein levels are also elevated and/or oxidized in various human diseases (21;29;65;251;374;428).

The oxidation state of DJ-1 is thought to be regulated by a major oxidation site at amino acid residue Cys-106 (13;43;207;327;455;494). Oxidation of Cys-106 to cysteine sulfinic acid is thought to facilitate the protective functions of DJ-1 protein (53);

however, further oxidation of DJ-1 to cysteine sulfonic acid functionally inactivates the protein (301;494).

DJ-1 is known to protect against a variety of toxic oxidative agents such as DA (252), 6-OHDA (181;418;253;27), H_2O_2 (204;418;479;253;482;27;196) and paraquat (137). It is possible that DJ-1 may not directly quench ROS since it has been shown in many studies to mediate cell viability by modulating other protein targets. For instance, DJ-1 may exert its protection by upregulating chaperones such as Hsp70 (27;260;255) (493) or by modulating signaling proteins such as extracellular related kinases 1 and 2 (ERK1 and 2) (252;142), apoptosis signal-regulating kinase 1 (ASK1) (198;455), phosphatidylinositol 3-kinase (Akt) (8;129;484), homeodomain interacting protein kinase (HIPK1) (385), or c-Jun N-terminal Kinase (JNK1) (303;498). Alternatively, DJ-1 may ameliorate harmful oxidation by acting to upregulate other known antioxidant proteins (13;77;271;492). On account of these factors, it is reasonable to understand why the loss of DJ-1 function may have detrimental consequences *in vivo*.

Surprisingly, genetically altered DJ-1 null mice do not exhibit phenotypes that model disease. Ablation of DJ-1 in mice does not result in nigrostriatal degeneration or obvious neuropathology (13;60;63;136;211;274). However, subtle alterations have been detected in some animals. For example, in a study by Andres-Mateos et al., DJ-1 deficient mice exhibited reduced brain mitochondrial peroxidase enzyme activities and this resulted in increased mitochondrial H_2O_2 production (13). Chandran and colleagues detected abnormal gait, decreased grip strength, and hypokinesia in DJ-1 null animals but this was not due to any apparent nigrostriatal abnormalities (60). Some studies suggest

that DJ-1 may regulate DA neurotransmission since the loss of DJ-1 in mice results in subtle defects. For instance, age-dependent motor abnormalities, increased stimulated DA release, and higher striatal DA levels resulted from the lack of DJ-1 in one mouse model (63). Additionally, nigral neurons in DJ-1 deficient mice were less responsive to D2 autoreceptor stimulation (136). DJ-1 null mice also demonstrated increased levels of striatal cell surface DAT protein (274).

Although DJ-1 deficient mice do not display overt parkinsonian phenotypes, several studies suggest that they may be particularly vulnerable to stressful stimuli. Paraquat induces behavioral and biochemical deficits in DJ-1 deficient animals that are not observed in WT mice (483). Rotenone alters the firing pattern of nigral neurons in mice lacking DJ-1 but does not affect WT mice to the same extent (354). DJ-1 null animals are also hypersensitized to the MPTP neurotoxin (204), although this is thought to be due to enhanced DAT-mediated uptake (274). Future studies to assess for the effects of stress on DJ-1 deficient mice may give insights into the biochemical and cellular functions of DJ-1 protein.

Alternatively, approaches to investigate the effects of pathogenic DJ-1 mutations on protein function may also prove to be beneficial in understanding the role of DJ-1 in the etiology of PD.

1.25 Hypotheses and Organizational Overview

The focus of this thesis was to analyze the biochemical and cellular properties of mutant DJ-1, α-syn, and parkin proteins using cultured cell and mouse models.

Little is known about the effects of recently reported pathogenic DJ-1 mutations, E163K, L10P, or P158DEL, on protein function. Since it is thought that DJ-1 mutations cause disease by a loss of function, it was hypothesized that mutants would exhibit aberrant biochemical properties in comparison to WT DJ-1 protein and would also cause other secondary effects related to such functional deficits. In chapter two, it is shown that pathogenic E163K mutant DJ-1 is similar to WT DJ-1 protein when assessed for protein stability, solubility, and dimerization. However, E163K mutant DJ-1 renders stably expressing mouse Neuro-2A neuroblastoma cells to be selectively vulnerable to oxidative insults. Additionally, following oxidative stress, E163K mutant DJ-1 shows aberrant subcellular localization in comparison to WT protein. Interestingly, since both WT and E163K mutant DJ-1 proteins are protective against proteasomal and mitochondrial stressors, it suggests that the E163K DJ-1 mutation specifically abolishes the antioxidant properties of the protein and may implicate a role for DJ-1 in multiple biochemical pathways.

In chapter three, the pathogenic DJ-1 mutants, L10P, P158DEL and L166P, are characterized biochemically in comparison to WT protein. It is discovered that all 3 pathogenic DJ-1 mutants exhibit reduced protein stabilities. Additionally, all mutants can be partially stabilized in the presence of proteasome inhibitors, though the effects of this on L10P are most provocative. Further analyses reveal that unlike L166P DJ-1, the L10P and P158DEL DJ-1 mutants can form dimers. Interestingly however, all of the pathogenic DJ-1 mutants show aberrant folding patterns in comparison to WT protein. Further, under normal cellular conditions, P158DEL mutant DJ-1 demonstrates reduced solubility in comparison to all other DJ-1 variants. Insoluble pools of L10P and L166P

are also accumulated in response in proteasome inhibition. Immunocytochemistry analyses reveal that L10P and P158DEL mutant proteins can associate into inclusions under normal culturing conditions. Further, proteasome inhibition results in the formation of atypical intracellular protein inclusions in cells expressing L10P, L166P, or P158DEL DJ-1 while these inclusions are not detected in cells expressing WT DJ-1 under the same conditions. Together, these findings suggest that the aberrant folding patterns adopted by L10P, P158DEL and L166P DJ-1 protein mutants result in rapid degradation of the respective protein variants and that this could thereby have deleterious effects on downstream cellular targets.

It has been previously shown that transgenic mice expressing human pathogenic mutant A53T α-syn (M83 mice) develop an age-dependent severe motor impairment phenotype associated with the formation of cytoplasmic α-syn inclusions throughout the neuroaxis (131). While reports by other labs suggest that DJ-1can chaperone misfolded α-syn *in vitro* (389;494), it is not known whether DJ-1 regulates α-syn *in vivo*. Thus it is of interest to better understand the physiological role of DJ-1 especially as it relates to its effects on α-syn aggregation. Chapter four describes the generation of homozygous Ala-53-Thr α-syn transgenic mice on a DJ-1 null background (M83-DJnull mice). If DJ-1 normally acts to modulate α-syn *in vivo*, it is hypothesized that M83-DJnull mice should exhibit an exacerbated phenotype in comparison to M83 mice. M83-DJnull mice were analyzed and compared to M83 mice as it relates to survival rate, distribution of α-syn pathologies, nigrostriatal integrity, biochemical properties of the α-syn protein, and the secondary effects of expressing mutant α-syn. These analyses revealed that there were no significant differences between mouse genotypes, suggesting that DJ-1 may not directly

modulate α-syn, nor protect against the harmful effects that result from α-syn aggregation *in vivo*.

There are few studies to assess for the effects of pathogenic parkin mutations *in vivo.* Analyses of genetically altered parkin deficient mice demonstrate that these animals do not recapitulate the key features of PD. Studies using more suitable approaches to model parkin deficiency *in vivo* would be very useful. In chapter five, we describe the discovery of a novel homologous endogenous mutation in the C3H mouse strain which results in the E398Q parkin amino acid substitution. Characterization of E398Q parkin in cultured cells reveals that it may be functionally inactive in comparison to WT parkin protein as the mutant shows aberrant biochemical properties. Mutant parkin also exhibits reduced interactions with UbcH7 and UbcH8 E2 enzymes. Additionally, C3H mice display age-dependent alterations in the steady-state levels of synphilin-1. Together, these findings suggest that C3H (E398Q) parkin may be functionally inactive and that C3H mice may serve as natural parkin loss-of-function models, similar to PD patients harboring missense parkin mutations.

In chapter six, I conclude by discussing the implications of these findings in the realm of the field. Additionally, I propose outstanding questions and future directions for these studies.

CHAPTER TWO

THE E163K DJ-1 MUTANT SHOWS SPECIFIC ANTIOXIDANT DEFICIENCY

By

Chenere P. Ramsey[#] and Benoit I. Giasson [#]*

(published in *Brain Research*, November 6th, 2008. Volume 1239, pages 1-11.

From

[#]Department of Pharmacology, University of Pennsylvania School of Medicine, Philadelphia, Pennsylvania 19104.

Running title: Antioxidant Deficiency of E163K Mutant DJ-1

*** Address correspondence to:**

Dr. Benoit I. Giasson, Department of Pharmacology, University of Pennsylvania School of Medicine, 125 John Morgan Building, 3620 Hamilton Walk, Philadelphia, PA 19104-6084. Tel: 215-573-6012; Fax: 215-573-2236; E-mail: giassonb@mail.med.upenn.edu.

Specific contributions:

-Generation of pZeoEKhDJ, pc3.1WThDJ1, pc3.1EKhDJ1, pc3.1WThDJ1-Nflag, and pc3.1E163KhDJ1-NFlag constructs

-Generation of stable cell lines expressing WT and E163K DJ-1

-Performed biochemical fractionation experiments

-Conducted gel filtration chromatography experiments

-Performed pulse-chase protein turn-over analysis experiments

-Performed subcellular fractionation analyses

-Conducted cell viability assays using various inhibitors

-Conducted co-immunoprecipitation and heterodimer studies

-Performed immunofluorescence and confocal microscopy

-Wrote intitial draft of the manuscript and worked with Benoit Giasson to revise it.

2.1 Abstract

Recent discoveries of genetic mutations linked to familial forms of PD, including mutations in *DJ-1*, have provided insights into the pathogenesis of sporadic PD. Recently, a novel homozygous missense mutation in the gene encoding human DJ-1 protein resulting in the E163K amino acid substitution has been reported. This mutation is associated with early-onset and clinical presentations that include parkinsonism, cognitive decline, and amyotrophic lateral sclerosis. The specific effect of this mutation on the function of DJ-1 protein as it relates to disease pathogenesis is currently unknown. Herein we show that the E163K pathogenic mutant retains similar properties to WT DJ-1 protein as it relates to protein stability, solubility, and dimerization. However, we show that the E163K mutant loses the ability to protect against oxidative stress while demonstrating a reduced redistribution towards mitochondria, but retains the ability to mitigate toxicity due to mitochondrial stress and proteasomal impairment. These findings suggest that DJ-1 influences several neuroprotective pathways and that the E163K mutation impairs the mechanism that is more specific to oxidative stress.

2.2 Introduction

Although the majority of PD cases are idiopathic, a growing number of mutations have been found to be associated with familial forms of the disease (110;213;305). Mutations in genes at multiple loci, designated *PARK1* through *PARK 13*, result in parkinsonian phenotypes with distinct features (32;80;213). Various mutations in *PARK7* (DJ-1), including truncation, missense, splice-site, and large deletions have been discovered (2;47). Mutations in *DJ-1* cause autosomal recessive PD with early to mid age of onset, and these may contribute to 1-2% of early onset PD cases (154;263).

DJ-1 encodes a 189 amino acid protein which is a member of the ThiJ/PfPI superfamily based on its structure (170;248;313;469). It is expressed in both neurons and astrocytes in the brain (19;21;218;325;387), but it is also expressed in many other organs (121;170;248;324;324;469;489). A number of studies have shown that DJ-1 can have protective functions against oxidative, proteasomal and mitochondrial stresses (53;181;204;281;418;483;487;493).

Interestingly, a novel missense E163K *DJ-1* mutation was reported for a family in southern Italy which results in a severe phenotype as early as 24 years. Subjects homozygous for this E163K mutation develop symptoms that include parkinsonism, dementia, and amyotrophic lateral sclerosis (14). Characteristics include weakness and muscle atrophy in the upper and lower extremities, speech deficits, cognitive impairment, and parkinsonism. Because of the early onset and more extensive phenotype associated with this mutation, its analysis and an understanding of how it can lead to disease may provide new insights into the function of DJ-1. In this study, we explore the properties of

human E163K mutant DJ-1 protein as it relates to its solubility, dimerization, stability, subcellular localization, and effects on cell viability as compared to WT protein.

2.3 Results

Neuro-2A (N2A) mouse neuroblastoma cell lines (**Figure 2-1a**) and Chinese Hamster Ovary (CHO) cell lines (data not shown) stably expressing WT and E163K DJ-1 were generated as described in "Material and Methods". The studies on solubility, dimerization, and protein stability were reproduced in both types of cells, but toxicity studies were conducted exclusively on N2A cell lines (see below).

Figure 2-1

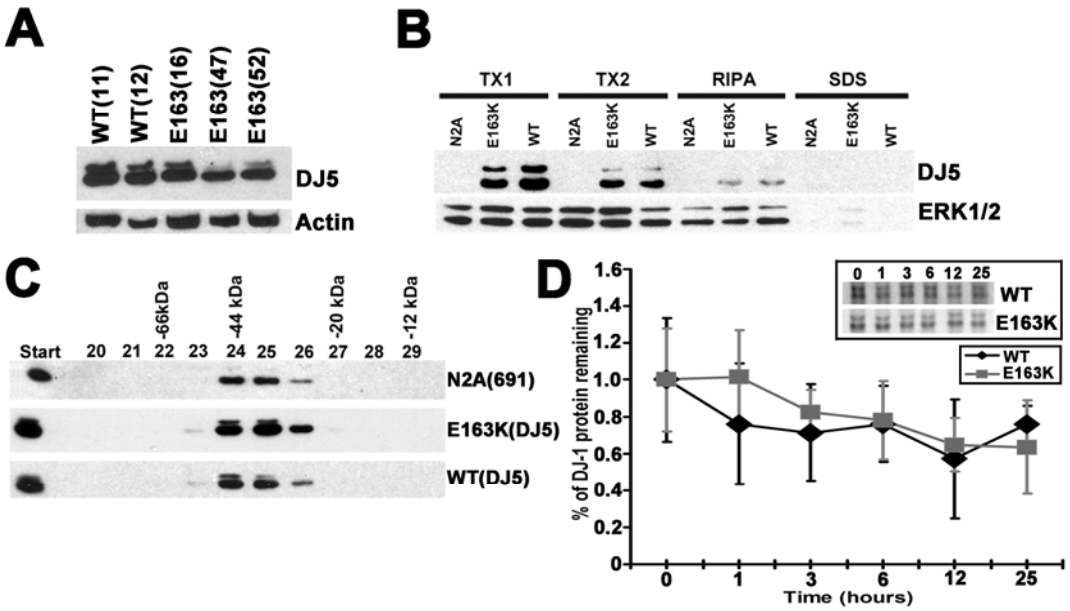

Assessment of the solubility, dimerization and stability of E163K human DJ-1 in N2A cells.
(A) Western blot analysis with DJ5 antibody, specific for human DJ-1, showing the expression of WT human DJ-1 in two stable N2A cell lines (clones 11 and 12) and E163K human DJ-1 in three stable N2A cell lines (clones 16, 47 and 52). An immunoblot with an anti-Actin antibody is shown as a loading control. **(B)** Biochemical fractionation was performed on N2A cells and stable cell clones of N2A cells expressing WT (clone 11) or E163K (clone 16) human DJ-1. Cellular proteins were extracted with buffers of increasing solubilization strengths as described in "Experimental Procedures". Each fraction was analyzed by western blotting with the anti-human DJ-1 antibody, DJ5, and an anti-ERK 1/2, ERK1, antibody to verify equal protein loading. **(C)** Size-exclusion chromatography was performed to analyze the native size

of E163K human DJ-1 compared to WT human DJ-1 and endogenous murine DJ-1. Soluble extracts from N2A cells and stable cell clones of N2A cells expressing WT (clone 11) or E163K (clone 16) human DJ-1 were loaded on a precalibrated Superose 6 column as described in "Experimental Procedures". The total cell lysates ("Start") and fractions were collected and analyzed by western blot analysis with DJ5 antibody to detect human DJ-1 or 691 antibody to detect endogenous murine DJ-1. Fractions 20-30 are shown. The elution profile of known molecular mass standards [BSA (66 kDa), ovalbumin (44 kDa), carbonic anhydrase (29kDa) and cytochrome C (12kDa)] are indicated above. **(D)** Pulse-chase turnover assay of E163K human DJ-1 compared to WT human DJ-1. N2A stable cell clones expressing WT (clone 11) or E163K (clone 16) human DJ-1 were pulsed with ^{35}S-methionine for 30 minutes and chased for 0, 3, 6, 12, or 25 hours. Experiments were conducted in quadruplicates. The results are plotted as percentage of protein over time standardized to the 0 hrs time point. The error bars show standard deviation.

The E163K mutation does not lead to changes in solubility.

Protein aggregation is known to be a key component in the disease pathogenesis of many neurodegenerative disorders (245) and reduced solubility of DJ-1 has been reported in some diseased brains (227;296;304;316;371). To assess whether the E163K mutation may lead to changes in solubility, N2A cells stably expressing WT and E163K DJ-1 were sequentially extracted with buffers of increasing solubilization strengths. The WT and the E163K mutant form of human DJ-1 both were extracted most abundantly in the soluble Triton X-100 fractions (TX1 and TX2) (**Figure 2-1b**) and to a lesser extent in the RIPA fractions. Additionally, neither E163K mutant nor WT DJ-1 were detected in the SDS fractions, and there were no differences between the distribution of WT and E163K DJ-1 across any of the biochemical fractions.

Biochemical fractionation experiments also were performed in CHO cells stably expressing the human WT or E163K mutant DJ-1 protein and no differences in protein solubility between the WT and E163K variants were observed in these cells (data not shown).

The E163K mutation does not alter the ability of DJ-1 to dimerize.

DJ-1 has been previously shown to form a homodimer in vitro which may be essential to its function (139;248;324). Some mutations like L166P have previously been shown to affect protein folding such as to prevent dimer formation, resulting in rapid degradation (28;42;139;158;171;298;324). Crystal structure analysis of DJ-1 protein shows that the L166P mutation occurs in helix 7, which is one of the helices in the dimer interface of DJ-1 (167;170;426;469). Since the E163K mutation also occurs in helix 7, it is possible that a similar effect could occur. To assess whether E163K DJ-1 dimerizes under native conditions, size exclusion chromatography was performed on soluble extracts from N2A cells expressing endogenous DJ-1 alone or expressing WT or E163K human DJ-1. The elution of purified proteins with known molecular masses was used to standardize this assay. Both the WT DJ-1 and the E163K mutant DJ-1 exclusively eluted in fractions 24 through 26 **(Figure 2-1c**), which corresponds to a molecular mass of ~42 kDa, the proposed molecular mass for the DJ-1 dimer. Endogenous DJ-1 protein expressed in N2A cells also eluted in the same fractions.

Size exclusion chromatography was also performed in CHO cells stably expressing either the WT or the E163K mutant form of DJ-1 protein in order to confirm the protein dimerization results. In the CHO cells, both the WT and the E163K mutant DJ-1 protein eluted in fractions 24 and 25 (data not shown), corresponding to the mass of a dimer.

The DJ-1 E163K mutant shows comparable stability to WT.

It has been previously shown that some pathogenic mutants of DJ-1 like M26I are structurally similar to WT DJ-1 in the ability to form a homodimer, but can demonstrate

reduced stability compared to the WT protein (42;324;422;479). Therefore, the effect of the E163K mutant on protein stability was assessed by pulse-chase experiments with ^{35} S-methionine and comparison to the WT protein. Both the E163K mutant and WT DJ-1 proteins showed similar turnover in N2A cells **(Figure 2-1d)**, indicating that the E163K mutation does not result in reduced stability. These experiments were also performed in CHO cells (data not shown) and both protein variants also showed similar turnover rates in this alternate cell type.

The E163K mutant DJ-1 does not show altered subcellular localization by western blot.

DJ-1 is normally diffusely expressed in cells (21), but WT DJ-1 as well as pathogenic mutants may localize to the mitochondria (489) and the latter localization may increase in response to mitochondrial stress (37;42). However, the subcellular localization of the E163K pathogenic mutant form of DJ-1 has not been previously investigated. To determine a possible effect of this mutation on altering the localization of DJ-1, subcellular fractionation was performed by differential centrifugation as previously used by others (298). Untransfected N2A cells and N2A cells stably expressing either human WT DJ-1 or human E163K DJ-1 were homogenized in triplicate in subfractionation buffer. Cytosolic and mitochondrial fractions were collected. Cell lysates were resolved by SDS-PAGE and analyzed by western blot analysis with DJ5 (human specific monoclonal DJ-1 antibody), 691 (polyclonal DJ-1 antibody that reacts with mouse and human protein), Tim23 (translocases of the inner mitochondrial membrane) as a mitochondrial marker, and ERK1/2 as a cytoplasmic marker.

Endogenous DJ-1 protein in N2A cells and both human WT and E163K DJ-1 expressed in these cells demonstrated similar predominant cytoplasmic distributions (**Figure 2-2**).

Figure 2-2

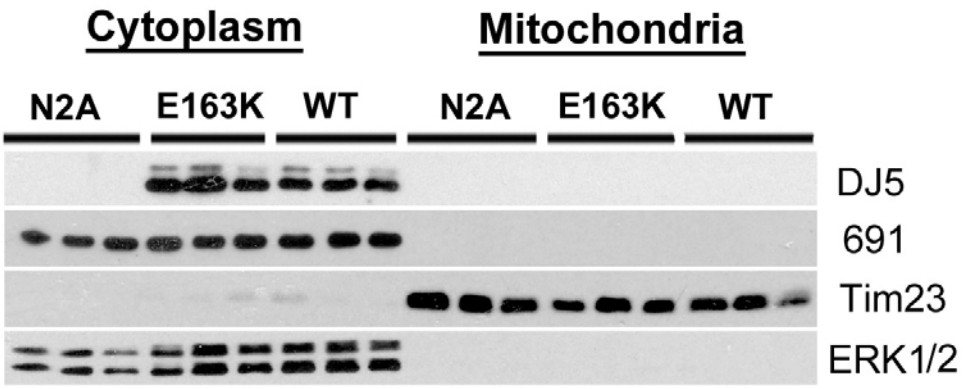

The E163K mutant does not show altered subcellular localization. N2A cells and stable cell clones of N2A cells expressing WT (clone 11) or E163K (clone 16) human DJ-1 were subjected to subcellular fractionation by differential centrifugation as described in "Experimental Procedures". Cellular fractions were analyzed by western blot with the monoclonal anti-human DJ-1 antibody, DJ5, the polyclonal anti-DJ-1 antibody, 691, anti-Tim 23 antibody (used as a mitochondrial marker), and anti-ERK1/2 antibody (used as a cytoplasmic marker). Experiments are shown in triplicates.

The E163K mutant protein fails to rescue under conditions of oxidative stress.

Many studies have reported that WT DJ-1 can serve in a protective capacity when overexpressed in various cells lines (53;389;447;487;493). To investigate the ability of human E163K DJ-1 to protect N2A mouse neuroblastoma cells from mitochondrial stress, proteasomal stress, and oxidative stress, cells expressing WT or E163K human DJ-1 were challenged with various specific stressors.

Native N2A cells or N2A cells stably expressing WT DJ-1 or E163K mutant DJ-1 were treated with either fresh DMEM/FBS or DMEM/FBS containing MG-132 (a proteasome inhibitor) or MPP dihydrochloride (a mitochondrial complex I inhibitor) at a range of concentrations. N2A cells demonstrated reduced cell viability to MG-132 treatment at all concentrations used (10-30 uM). Additionally, N2A cells were vulnerable to MPP dihydrochloride concentrations that exceeded 10 uM and WT DJ-1 protein was able to protect against both of these stressors at all toxic concentrations tested (**Figure 2-3A**). Expression of E163K DJ-1 was also able to protect against MG-132 and MPP dihydrochloride toxicity.

To further assess the specific effect of the E163K mutation, other specific mitochondrial complex inhibitors were analyzed (**Figure 2-3B**). Antimycin, an inhibitor of mitochondrial complex III, resulted in a ~40% decrease in viability in N2A cells at the 100 nM concentration and a ~60% decrease in viability at the 200 nM concentration while expression of either WT or E163K DJ-1 had a protective effect at these concentrations (**Figure 2-3B**). The irreversible inhibitor of mitochondrial complex II, 3-nitropropionic acid (3-NP), did not have a significant effect on the viability of any of the three cell lines at the 5 uM or 10 uM concentrations tested. However, N2A cells showed a slight vulnerability to 15 uM 3-NP and expression of either the E163K mutant DJ-1 or WT DJ-1 was protective.

Figure 2-3

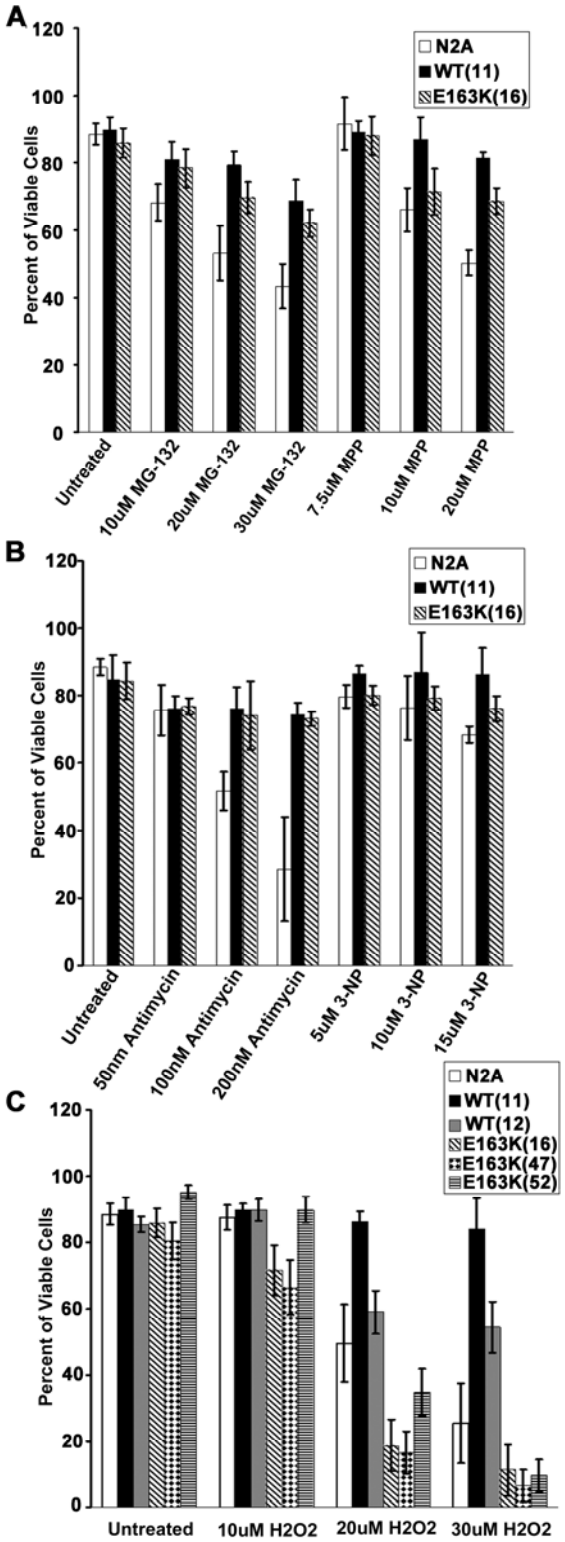

The E163K mutant fails to rescue under conditions of oxidative stress.

(**A**) N2A cells and stable cell clones of N2A cells expressing WT (clone 11) or E163K (clone 16) human DJ-1 were treated with various chemical stressors and the Trypan Blue Exclusion Assay was used to assess viability. Results were plotted as the percentage of viable cells over time of chemical treatment. The error bars show standard deviation. In **A**, cells were treated for 20 hrs with either fresh DMEM/FBS or DMEM/FBS containing 10-30 uM MG-132, or 7.5-20 uM MPP dihydrochloride. In **B**, cells were treated for 96 hours with either fresh DMEM/FBS or DMEM/FBS containing 50-200 nM Antimycin or 5-15 uM 3-nitropropionic acid. (**C**) Several N2A stable clones expressing either WT human (clones 11 and 12) or E163K human mutant DJ-1 (clones 16, 47 and 52) were treated for 20 hours with either fresh DMEM/FBS or DMEM/FBS containing 10-30uM H2O2.

Native N2A cells or stable clones expressing WT or E163K DJ-1 protein were challenged with H_2O_2 ranging from 10-30 uM in order to induce oxidative stress. We found that challenging the cell line expressing E163K mutant DJ-1 (E163K clone #16) that had been used in all of the aforementioned toxicity experiments not only demonstrated a lack of protection against H_2O_2 oxidative stress, but furthermore showed increased vulnerability to H_2O_2 exposure at all of the concentrations used (**Figure 2-3C**). To determine whether enhanced sensitivity to oxidative stress was due to expression of the E163K DJ-1 mutant, two additional N2A cell lines (clone #47 and clone #52) stably expressing the human E163K mutant DJ-1 were tested for H_2O_2 toxicity (**Figure 2-3C**). Both of these clones also revealed increased vulnerability to H_2O_2 oxidative stress when compared to native N2A cells. In contrast, two N2A cell lines stably expressing human WT DJ-1 (clones #11 and #12) demonstrated protection against H_2O_2 stress. These results indicate that the E163K mutation selectively compromises the protective role for DJ-1 on oxidative stress.

Human exogenous DJ-1 protein does not co-immunoprecipate with endogenous DJ-1 in N2A cells.

One plausible explanation for the selective vulnerability of N2A cell lines expressing E163K mutant DJ-1 to oxidative stress is that the mutant protein may behave as a dominant negative by forming a heterodimer with endogenous murine DJ-1 protein, inactivating the antioxidant capacity of the endogenous protein. Size exclusion chromatography analysis demonstrated that endogenous and human DJ-1 formed dimers, but these studies do not ascertain whether these proteins could form heterodimers **(Figure**

2-1). Coimmunoprecipitation experiments were performed to test the interaction between human WT and E163K DJ-1 with endogenous DJ-1. Since mouse and human DJ-1 migrate with the same mobility on SDS-PAGE, transfections with N-terminal flagged human DJ-1 constructs were used for these studies. Cell extracts from N2A cells or extracts from N2A cells transiently expressing either WT Flag-DJ-1 or E163K Flag-DJ-1 were immunoprecipitated with a mouse anti-flag monoclonal antibody. Immunoprecipitates were resolved by SDS-PAGE and analyzed by western blot with the polyclonal DJ-1 antibody, 691. Endogenous DJ-1 protein was not pulled downed by immunoprecipitation with either WT-flag tagged or E163K-flag tagged DJ-1 **(Figure 2-4)**, indicating that there is no detectable formation of heterodimers between the endogenous DJ-1 and exogenous human DJ-1 protein.

Figure 2-4

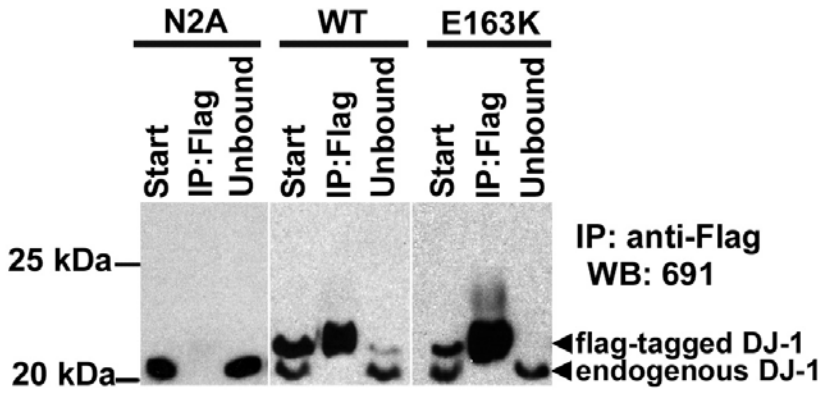

Human exogenous DJ-1 protein does not co-immunoprecipate with N2A endogenous DJ-1. N2A cells were mock transfected or transiently transfected with either flag-tagged human WT or E163K mutant DJ-1 constructs. Soluble protein extracts were immunoprecipitated with anti-flag antibody. Fractions were resolved by SDS-PAGE and immunoblotted with the polyclonal DJ-1 antibody, 691. The "Start" fraction represents the total soluble extracts before IP and the "Unbound" fraction represents the protein remaining in the protein lysates after the IP.

Immunofluorescence microscopy reveals an altered localization for E163K mutant DJ-1 protein in response to oxidative stress.

To further understand the effect of the E163K mutation, quantitative immunofluorescence studies were conducted comparing untreated cells and cells challenged with oxidative stress. Under normal conditions, DJ-1 exhibited a diffuse staining pattern throughout the cell and co-immunofluorescence experiments with the mitochondrial marker, MitoTracker ® Red CMXRos, revealed some overlap with both WT and E163K DJ-1 **(Figure 2-5a**). However, after treating with hydrogen peroxide, cells expressing WT DJ-1 showed a 5-fold increase in staining overlap of the human DJ-1 protein with the mitochondrial marker as compared to untreated cells. In striking contrast, under the same oxidative conditions, cells expressing the E163K mutant DJ-1 showed a 6-fold decrease in the overlap with mitochondrial marker (**Figure 2-5b**). To try to assess whether these alterations in DJ-1 distributions were due to changes in the presence of DJ-1 in the mitochondria, subcellular biochemical fractionation of cells treated with oxidative stress was performed. However, no biochemical mitochondrial localization was observed under harsh conditions of oxidative stress (**Figure 2-5c**). These results suggest that under oxidative stress, WT human DJ-1 in N2A cells can relocate in close proximity to the mitochondria, but does not enter these organelles, while E163K DJ-1 is impaired in this property, which may play a role in its inability to protect against oxidative stress.

Figure 2-5

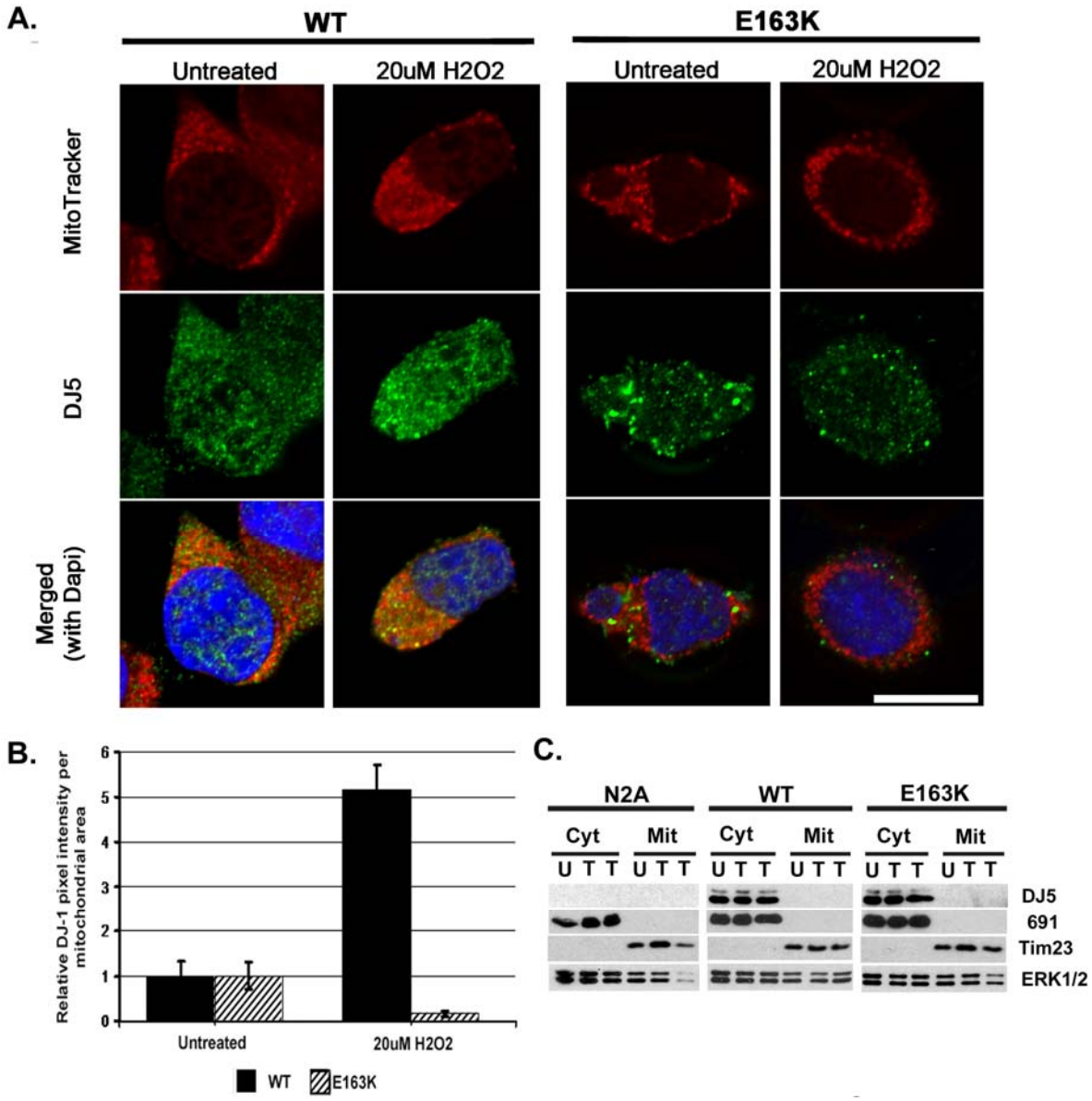

Immunofluorescence microscopy reveals an altered mitochondrial localization for E163K mutant DJ-1 protein in response to oxidative stress.

(**A**) N2A cells stably expressing WT (clone 11) or E163K (clone 52) human DJ-1 were treated either DMEM/FBS containing 20uM H_2O_2 or with DMEM/FBS. Cells were stained with Mitotracker (red), DJ5 (green), and DAPI (blue) and visualized by confocal microscopy. Representative images are shown. Bar = 13.5μm (**B**) The confocal microscopy images were quantified using MetaMorph 6.0. The graph represents the average of the relative pixel intensity for DJ-1 per mitochondrial area. The error bars show the standard deviation between replicate images. (**C**) N2A cells and N2A cells stably expressing WT (clone 11) or E163K (clone 52) human DJ-1 were either untreated (lanes labeled with "U") or treated with 350uM H_2O_2 (lanes labeled with "T") for 1.5 hrs and then fractions enriched for mitochondria were isolated by differential centrifugation as described in "Material and Methods". Cellular fractions were analyzed by western blot with the monoclonal anti- human DJ-1 antibody, DJ5, the polyclonal anti-DJ-1 antibody, 691, anti-Tim 23 antibody (used as a mitochondrial marker), and anti-ERK1/2 antibody. Experiments are shown in duplicates.

2.4 Discussion

DJ-1 mutations are associated with early-onset parkinsonism. The E163K mutation is also causal of early-onset disease, but clinical presentations are more extensive and diverse than for other DJ-1 disease-causing mutations (14). In this study, the properties and effects of this mutant were assessed in cultured cells. Under normal conditions, the E163K mutant had properties similar to WT DJ-1 in terms of subcellular localization, dimerization abilities, stability, and solubility. These findings are consistent with recent findings by Lakshminarasimhan and colleagues that showed that in vitro E163K DJ-1 was able to form stable dimers (233).

Many groups have shown that WT DJ-1 protein can act to mitigate the deleterious effects of various insults including oxidative stress both in cell culture and in animal models (181;242;281;297;418;487). While the E163K mutant retains the ability to protect N2A cells against proteasome inhibition as well as mitochondrial stress through mitochondrial complex I and III inhibition, this mutation compromises the ability of DJ-1 to protect against oxidative stress and even increases sensitivity to oxidative insult. A number of studies demonstrated that the DJ-1 pathogenic mutant, L166P, insufficiently protects against oxidative stress (139;181;198;281;418;493), but in contrast to the E163K mutation the L166P mutation impairs the ability of DJ-1 to form stable dimers resulting in a dramatic instability of the mutant protein and loss of expression that can explain the loss of protective function (138;269;298;324). The M26I mutant also displays reduced protection against oxidation stress (422) despite the ability to form stable dimers (42;304;422), but this mutation appears to reduce protein stability, albeit much less than

the L166P mutation (42;304;422;479). However, it is unclear if the reduced protection against oxidative stress by the M26I mutation is simply associated with reduced half-life or perhaps with an increased propensity for the M26I mutant protein to aggregate as recently reported (171).

In contrast to these other mutations in DJ-1, the effect of the E163K mutation on impairing DJ-1 function is specific to oxidative stress and it does not impair dimerization, protein stability or increase aggregation. E163 is in close proximity of L166, and both residues are located in α-helix G7 which is critical in forming stably folded protein (139;170). The E163K mutation clearly does not cause the dramatic structural changes of the L166P mutation which introduces a helix-breaking residue, but the fact that E163 is highly conserved in DJ-1 across species underscores the importance of this residue (139). The E163K mutation appears to result in subtle structural changes and recent biophysical studies by Lakshminarasimhan et al. demonstrated that E163 can form a salt bridge with R145 and that the disruption of this interaction by the E163K mutation results in increased mobility of R145 (233).

Our findings that oxidative stress promoted the redistribution of DJ-1 towards mitochondria but without evidence of mitochondrial import are consistent with the studies of Canet-Aviles and colleagues that reported that oxidative stress can increase the amount of DJ-1 on the cytoplasmic side of this organelle without resulting in import (53). It is shown in the present studies that under conditions of oxidative stress, the E163K mutant demonstrated a paucity of localization towards mitochondria. It is possible that simply the change from a negatively to positively charged residue and/or the subtle

structural effects discussed above may prevent the interaction of DJ-1 with other proteins that may be involved in the redistribution of DJ-1 under conditions of oxidative stress. Identifying such mechanisms may be important to further understand the function of DJ-1. The toxicity studies demonstrate that DJ-1 influences several neuroprotective pathways but that the E163K mutation specifically impairs the oxidative stress protective mechanism. The findings that this mutation appears to exacerbate the response to oxidation and diminish the redistribution of DJ-1 towards the mitochondria suggest that both processes may be related, but further studies will be needed to substantiate a direct association.

Our results reveal that the loss of DJ-1 protective function can occur without overt biochemical changes on the protein and demonstrate that alterations to specific residues in this protein can specifically affect individual functions indicating that DJ-1 is likely involved in multiple cellular pathways. A more detailed understanding of the mechanism by which DJ-1 can protect against stresses is still needed to better understand the activities of this protein and its role in neurodegenerative diseases.

2.5 Experimental Procedures

Antibodies

DJ-5 is a mouse monoclonal antibody specific for human DJ-1 protein (296). 691 is a rabbit polyclonal antibody raised against recombinant human DJ-1 protein but that reacts with DJ-1 from various species (296).

Anti-Tim23 is a purified mouse monoclonal antibody to Tim23 (BD Transduction Laboratories, San Jose, CA). Anti-extracellular signal related kinase-1 (ERK-1) (C-16) is an affinity purified rabbit polyclonal antibody (Santa Cruz Biotechnology, Santa Cruz, CA) that reacts with both ERK-1 and -2. Anti-Flag-tag mouse monoclonal antibody (GenScript Corporation, Piscataway, NJ) is a purified antibody that reacts with proteins with the amino acid sequence, DYKDDDDK . Anti-Actin is a purified mouse monoclonal antibody (Millipore Corporation, Billerica, MA 01821) that reacts with all six isoforms of vertebrate Actin.

Cloning of human DJ-1 constructs

Human full-length WT DJ-1 cDNA was cloned into the mammalian expression vector pZeoSV2 (Invitrogen, Carlsbad, CA) at the Not I and Hind III restriction sites to create the plasmid pZeoWThDJ. Using the pZeoWThDJ construct, the QuickChange® Site Directed Mutagenesis Kit (Stratagene, La Jolla, CA) was used in order to generate the E163K mutant form of human DJ-1 in the pZeoSV2 vector. The sequences of the oligonucleotides used for mutagenesis were as follows: Forward- 5'-GGG CCT GGG ACC AGC TTC AAG TTT GCG CTT GCA ATT GTT-3' and Reverse- 5'- AAC AAT TGC AAG CGC AAA CTT GAA GCT GGT CCC AGG CCC-3'. The sequence of the plasmid with E163K mutant DJ-1 was verified by DNA sequencing as a service offered by the DNA Sequencing Facility of the University of Pennsylvania, and the construct was named pZeoEKhDJ.

Sequential restriction digestions with Not I and Apa I were performed on both pZeoWThDJ and pZeoEKhDJ. The DNA fragments containing the full-length DJ-1

sequences were ligated into the pcDNA3.1 (Invitrogen, Carlsbad, CA) mammalian expression vector in order to generate the human WT and E163K mutant DJ-1 constructs named pc3.1WThDJ1 and pc3.1EKhDJ1, respectively.

An N-terminal flag-tagged WT DJ-1 construct was generated by PCR, using the pZeoWTDJ-1 construct as a template. The sequences for the oligonucleotides used were as follows: Forward-5'- GAT CGC GGC CGC CAC CAT GGA TTA CAA GGA TGA CGA CGA TAA GGC TTC CAA AAG AGC TCT GGT CAT CCT -3' and Reverse-5'- GAT CAA GCT TCT AGT CTT TAA GAA CAA GTG GAG CCT TC-3'. The tagged insert was cloned into the pCR 2.1 TOPO vector (Invitrogen, Carlsbad, CA) and subsequently cloned into the pcDNA3.1 (-) vector at the Hind III and Not I restriction sites. The construct was named pc3.1WThDJ1-Nflag. The sequence of the plasmid was verified by DNA sequencing as described above. The E163K N-terminal flag-tagged DJ-1 construct was generated by performing site directed mutagenesis using the pc3.1WThDJ1-Nflag construct as a template. The same oligonucleotides were used as described above for mutagenesis. The plasmid was named pc3.1E163KhDJ1-NFlag.

Cell culture

N2A and CHO cells were cultured in Dulbecco-modified Eagle medium (DMEM) (Invitrogen, Carlsbad, CA) supplemented with 10% fetal bovine serum (Sigma, St.Louis, MO), 100 U/mL penicillin and 100 μg/mL streptomycin (Invitrogen, Carlsbad, CA). Cells were incubated at 37ºC and 95% air/5% CO_2 atmosphere.

Generation of stable cell lines expressing WT and E163K DJ-1

The pc3.1WThDJ and pc3.1EKhDJ constructs were used to transfect N2A cells using FuGENE reagent following the manufacterer's protocol. Stably expressing clones were isolated and selected with G418 (Invitrogen, Carlsbad, CA) at 200-500 μg/mL and screened by Western blotting for the expression of DJ-1 using the antibody DJ5 that is specific for human DJ-1. Stably expressing clones expressing WT (clone #11 and clone #12) or E163K (clone #16, #47 and #52) human DJ-1 were used in the studies (See Figure 1A).

The pZeoWThDJ and pZeoEKhDJ constructs were used to transfect CHO cells using FuGENE (Roche, Basel, Switzerland) transfection reagent according to the manufacturer's protocol. Stably expressing clones were isolated following selection with Zeocin (Invitrogen, Carlsbad, CA) at 50 ug/mL.

Biochemical fractionation

Native N2A and CHO cells or stable clonal lines expressing WT or E163K human DJ-1 were cultured in 10 cm dishes as described above. Cells were grown to confluency, rinsed and scraped in PBS, and harvested by centrifugation at 13,000 x g. Cells were vortexed vigorously in 2 pellet volumes of PBS/0.1% Triton, sedimented, and the supernatant was collected as the TX1 fraction. This was repeated on the remaining pellet and the supernatant was collected as the TX2 fraction. The pellet was resuspended in 2 volumes of RIPA buffer, vortexed vigorously, sedimented, and the supernatant was collected as the RIPA fraction. The remaining pellet was solubilized in 2%SDS/17mM Tris, pH 8.0 and kept as the SDS fraction.

Gel filtration chromatography

Gel filtration chromatography was performed by calibrating a Superose 6 column (Amersham Biosciences) attached to a fast performance liquid chromatography (FPLC) system with standards of known molecular mass using 10 mM Tris, pH 7.5, 100 mM NaCl as the mobile phase. Molecular mass standards [BSA (66 kDa), ovalbumin (44 kDa), carbonic anhydrase (29 kDa) and cytochrome C (12 kDa)] were resolved separately to calibrate the column. The elution of the standards was monitored by protein absorbance at 280 nm. N2A or CHO cells and stable cell lines thereof were cultured in 10 cm dishes and grown to confluency. Cells were rinsed and scraped in phosphate buffered saline, pH 7.4. After recovery by centrifugation, cells were lysed in PBS/0.1% Triton and the cell debris was sedimented at 13,000 x g for 5 min. The extracts were filtered through a 0.45 μm filter and loaded onto the column. Fractions were analyzed by immunoblotting with anti-DJ-1 antibodies, DJ5 (1:1000) and 691 (1:1000).

Pulse-chase protein turnover experiments

N2A or CHO cells stably expressing WT or E163K DJ-1 were cultured in 6-well dishes. Cells were methionine-deprived for 15 minutes by incubation in methionine-free DMEM (Invitrogen, Carlsbad, CA)/ 10% dialyzed FBS before adding 100 μCi [^{35}S]-methionine (Invitrogen, Carlsbad, CA) per ml of methionine free DMEM/10% dialyzed FBS for 30 min. Chase experiments were conducted in quadruplicates with normal DMEM/FBS for 0, 3, 6, 12, and 25 hours. Cells were then rinsed with PBS and harvested in CSK buffer (100 mM NaCl, 50 mM Tris, pH 7.5, 2 mM EDTA, 1 % Triton X-100) containing 1 % SDS and boiled at 100 ºC for 5 minutes. CSK buffer was added to the

lysates in order to bring the final concentration of SDS to 0.25%. Lysates were frozen on dry ice and kept frozen at -20 ºC until the last time point was harvested. The radiolabelled protein extracts were pre-cleared with a rabbit serum pre-incubated with protein A-agarose (Santa Cruz Biotechnologies, Santa Cruz, CA) for 3 hours at 4ºC and radiolabelled extracts were then immunoprecipitated overnight at 4ºC with anti-DJ-1 polyclonal antibody 691 pre-incubated with protein A-agarose (Santa Cruz Biotechnologies, Santa Cruz, CA). The antibody-protein complexes were washed 3 times with 10 volumes of CSK buffer, resuspended in 2 volumes of 2X SDS sample buffer and boiled at 100 ºC for 5 minutes. The beads were removed by centrifugation and the samples were loaded on 12 % polyacrylamide gels. Following electrophoresis, gels were fixed with 50% methanol/5% glycerol, dried and exposed to a PhosphorImager plate and the signal was quantified using ImageQuant software (Molecular Dynamics, Inc., Sunnyvale, CA).

Subcellular fractionation

The subcellular fractionation procedures used were similar to those previously described (298) with some changes. Native N2A, or N2A cells stably expressing WT or E163K DJ-1 were cultured in 10 cm plates. Cells were rinsed and scraped in phosphate-buffered saline, pH 7.4 (Invitrogen, Carlsbad, CA) and pelleted at 13,000 x g. Cells were resuspended in 3 pellet volumes of subfractionation buffer (0.25 M sucrose, 10 mM HEPES/NaOH, pH 7.5, 1 mM DTT, and protease inhibitors). Cells were homogenized with 20 strokes of a Dounce homogenizer (Kontes Glass Co;Vineland, NJ). The nuclei and unlysed cells were pelleted by sedimentation at 489 x g for 10 minutes at room

temperature (RT). The supernatants were further cleared at 1585 x g for 10 minutes. The supernatants (S1) were removed to fresh tubes and sedimented for 10 minutes at 1585 x g at RT. The supernatants (S2) were removed to fresh tubes and pelleted for 17 minutes at 22000 x g at 4º C. The supernatants (S3) were removed as the crude cytoplasmic fraction and incubated on ice. In the mean time, the pellet (mitochondrial enriched fraction) was rinsed with 3 pellet volumes of subfractionation buffer and centrifuged again at 22000 x g for 17 minutes at 4ºC. The supernatant from this rinse was discarded and the mitochondrial pellet was solubilized in 3 pellet volumes of 2% SDS/17mM Tris and boiled at 100 ºC for 5 minutes. The tube containing the crude cytoplasmic supernatant (S3) was then sedimented at 103,000 x g for 25 minutes at 4 ºC in order to pellet small organelles and cell debris, and the resulting supernatant (S4) was collected as the cytosolic fraction. The protein concentrations were determined in each fraction using the bicinchoninic acid protein (BCA) Assay (Pierce, Rockford, IL) with and bovine serum albumin as a standard. Fractions were analyzed by immunobloting with antibodies DJ5 (1:1000), 691 (1:1000), Tim23 (0.5ug/mL), and ERK1 (0.2ug/mL).

For subcellular fractionation experiments that followed oxidative stress, N2A cells or cells stably expressing human WT or E163K mutant DJ-1 were cultured in 10 cm plates and were treated for 1.5 hours with DMEM/FBS or DMEM/FBS containing 350uM H_2O_2. Cells were treated with H_2O_2 in duplicate. Cells were rinsed and scraped in PBS. Subcellular fractionation by differential centrifugation was performed as described above.

Cell viability assay

Native N2A or N2A cell lines expressing WT or E163K DJ-1 were cultured separately into 48 well plates. Each cell type was treated for 20 hours in sextuplicates with DMEM/FBS containing either 10, 20 or 30 uM H_2O_2, 7.5, 10, or 20 uM MPP dihydrochloride (Sigma, St.Louis, MO), 10, 20, or 30 uM MG-132 (Sigma, St.Louis, MO), or fresh DMEM/FBS. In separate experiments, these cell lines were treated for 96 hours in sextuplicates with either 50, 100, or 200 nM Antimycin A (Sigma, St.Louis, MO) or 5, 10, or 15 uM 3-nitropropionic acid (Sigma, St.Louis, MO). After treatment, the media from each well was collected into separate 1.5 mL microfuge tubes. The cells remaining in the wells were trypsinized, and harvested in corresponding microfuge tubes. Cells were pelleted and resuspended in fresh DMEM/FBS, and then 3-fold volumes of Trypan Blue solution (Sigma, St.Louis, MO) was added. Live and dead cells were counted manually using a hemacytometer and an Olympus CKX41 microscope. The percentage of live cells relative to the total number in each well was calculated.

Co-immunoprecipitation and heterodimer studies

N2A cells were cultured in 10 cm plates. Cells were mock transfected or transiently transfected with pc3.1E163KhDJ1-NFlag, or pc3.1WThDJ1-NFlag constructs using Lipofectamine reagent (Invitrogen, Carlsbad, CA) according to the manufacturer's protocol. After 24 hours, cells were rinsed and scraped in PBS and lysed into 500 uL of 1X CSK buffer by vortexing. Cell debris was sedimented at 13,000 x g for 5 minutes and supernatants were removed to fresh tubes. 30 uL of each supernatant was saved as the "Start" fraction. The remainders of the supernatants were incubated at 4 ºC with a mouse anti-flag antibody preabsorbed to protein A/G PLUS Agarose beads (Santa Cruz

Biotechonogy, Inc., Santa Cruz, CA). The beads were sedimented, repeatedly rinsed with 1X CSK buffer, resuspended in sample buffer, heated to 100 ^{o}C and saved as the "IP" fractions. The supernatants remaining after the immunoprecipitation were saved as the "Unbound" fractions. Sample buffer was added to the "Start" and "Unbound" fractions and then they were heated to 100 ^{o}C for 5 minutes.

Immunofluorescence and confocal microscopy

Native N2A, or N2A cells stably expressing WT or E163K DJ-1 were treated with DMEM/FBS or DMEM/FBS containing 20 uM H_2O_2 for 3 hours. The media was removed and replaced with warmed DMEM/FBS containing 100 nM Mitotracker ® Red CMXRos (Invitrogen, Carlsbad, CA). The cells were allowed to respire for 20 minutes and then were fixed with neutral buffered formalin according to the manufacturer's protocol. The cells were rinsed with PBS for 5 minutes and then blocked for 30 minutes at room temperature in PBS/2% FBS/0.1% Triton. Cells were then incubated at 4ºC with DJ5 antibody diluted into PBS/2% FBS at a concentration of 1:500 overnight, washed 3 times with PBS at 10 minutes each, and then incubated at room temperature with a goat anti-mouse secondary antibody conjugated to Alexa Fluor ® 488 (Invitrogen) diluted into PBS/2% FBS at a concentration of 1:500 for 2 hours. Cells were rinsed for 10 minutes with PBS, incubated at room temperature with DAPI (Pierce, Rockford, IL) diluted into PBS at a concentration of 1ug/mL for 5 minutes, and then rinsed 3 times with PBS at 10 minutes each. Cells were coversliped with Cytoseal^{TM} 60 mounting media (Richard-Allen Scientific, Kalamazoo, MI). The images were visualized with a Zeiss LSM-510 Meta confocal microscope. For each sample, five 143 x 143 μm images were taken from a

single plane using the 63x /1.4 oil objective. The images were then quantified using MetaMorph 6.0 software (Molecular Devices, Sunnyvale, CA). The relative integrated staining for DJ-1 per mitochondrial area was calculated by measuring the integrated pixel intensity for DJ5 signal that overlapped with pixels positive for Mitotracker Red CMXRos divided by total mitochondrial area. Integrated pixel intensity is defined as pixel intensity times the area of pixels positive for the signal. The average values for the replicate images were calculated.

2.6 Acknowledgements

This work was funded by grant AG09215 from the National Institute on Aging. C.P.R. is supported by of a pre-doctoral NRSA fellowship (GM082026) from the National Institute on General Medicine Sciences.

CHAPTER THREE

L10P AND P158DEL DJ-1 MUTATIONS CAUSE PROTEIN INSTABILITY AND AGGREGATION WITHOUT IMPAIRING DIMERIZATION

By

Chenere P. Ramsey[#] and Benoit I. Giasson [#]*

(submitted for publication March 2010)

From

[#]Department of Pharmacology, University of Pennsylvania School of Medicine, Philadelphia, Pennsylvania 19104.

Running title: Destabilization of L10P and P158DEL Mutant DJ-1

*** Address correspondence to:**

Dr. Benoit I. Giasson, Department of Pharmacology, University of Pennsylvania School of Medicine, 125 John Morgan Building, 3620 Hamilton Walk, Philadelphia, PA 19104-6084. Tel: 215-573-6012; Fax: 215-573-2236; E-mail: giassonb@mail.med.upenn.edu.

Specific contributions:

-Cloning of untagged full-length WT, L10P, L166P, P158DEL, and HA-tagged WT pZeoSV2 DJ-1 constructs

-Conducted pulse-chase protein turn-over analyses

-Conducted all western blot analyses

-Performed size-exclusion chromatography experiments

-Conducted co-immunoprecipitation and heterodimer analyses

-Performed biochemical fractionation and cell compartment fractionation experiments

-Wrote the first draft of the manuscript and worked with Benoit Giasson to generate revised versions.

3.1 ABSTRACT

A variety of mutations in the gene encoding DJ-1 protein are causal of autosomal recessive early-onset parkinsonism. Recently, a novel pathogenic homozygous DJ-1 missense mutation resulting in the L10P amino acid substitution was reported. In a separate study, a novel homozygous mutation resulting in the deletion of DJ-1 residue P158 was also reported to be causative of disease. The specific effects of the novel L10P and P158DEL mutations on protein function have not been studied. Herein, L10P and P158DEL DJ-1 proteins were assessed for protein stability, dimerization, solubility, and subcellular localization in comparison to WT and the L166P DJ-1 pathogenic variant. It was discovered that in comparison to WT protein, L10P, L166P, and P158DEL DJ-1 variants exhibited dramatically reduced protein stabilities. Degradation of each of the respective pathogenic mutants appeared to be mediated in-part by the proteasome. Interestingly, unlike L166P DJ-1, the L10P and P158DEL DJ-1 variants retained the ability to dimerize and thus it was concluded that the observed decreases in protein stability were due to aberrations in protein folding. Supporting this idea, the L10P, L166P, and P158DEL DJ-1 variants exhibited altered profiles on size-exclusion chromatography and reduced solubilities in comparison to WT protein, and the latter aberration could be exacerbated in the presence of MG-132. Taken together, these findings suggest that DJ-1 mutations may cause disease by distinct mechanisms and indicate that the pathogenicity of the L10P and P158DEL variants are related to aberrations in protein stability and protein folding.

3.2 INTRODUCTION

Several genes, designated *PARK1-PARK13*, that can cause Parkinson disease (PD) have been indentified (124;250). A variety of mutations in *PARK7/DJ-1,* including large genetic deletions, splice-site alteration and missense mutations, are also known to be causal of autosomal recessive early-onset parkinsonism (200). Recently, two novel recessive mutations in the *PARK7/DJ-1* gene have been reported which result in early-onset parkinsonian phenotypes in the affected patients (144;270). A homozygous missense mutation resulting in the DJ-1 amino acid substitution L10P was identified in a consanguineous Chinese family (144). The affected patients presented with disease symptoms at 19 years of age which is the earliest age of onset reported for any PD case specifically linked to *DJ-1* mutations. Following this report, another *DJ-1* mutation carrier was identified in a genetic study conducted on early-onset PD patients from the Netherlands (270). The affected individual harbored a small homozygous deletion in *DJ-1* exon 7 which resulted in the deletion of the highly conserved DJ-1 residue, P158DEL (270).

Although the first causative *PARK7/DJ-1* mutations were reported nearly a decade ago (47) and DJ-1 has been implicated in many biological pathways (200 and the references therein;109), the specific role of DJ-1 in disease pathogenesis is still unclear. DJ-1 is a relatively small 189 amino acids protein that is evolutionarily conserved across many species (23;47;313). It is ubiquitously expressed in most tissues and is present in cell nuclei and cytoplasm (28;47;313). Crystallization studies reveal that DJ-1 is composed of eight α-helices and eleven β-strands that are arranged into a helix-strand-

helix sandwich (12;170). These structural features are common to members of the ThiJ/Pfp superfamily of proteins (167;170;469). Further, it is known that DJ-1 tightly associates into a homodimer and that the dimer interface is composed of α-helices 1, 7, and 8 and β-strands 3 and 4 (12;170;167;469). DJ-1 dimer formation may be required for the protein to function properly, though this hypothesis has never been proven. It is well known that the pathogenic DJ-1 mutant L166P fails to dimerize and that this deficit is likely caused by structural perturbations of the dimer interface (12;42;139;139;269;298;324;469). Such conformational abnormalities target L166P DJ-1 protein for rapid degradation by the proteasome, and the associated reductions in mutant protein abundance may be causative of disease phenotypes (139;263;298). Studies to assess for the effects of pathogenic DJ-1 mutations on protein function will give insights into the cellular mechanisms that may be implicated in the etiology of PD.

In the current study, the biochemical properties of the novel pathogenic DJ-1 mutants, L10P and P158DEL are explored. The novel mutants are assessed for protein stability, dimerization, solubility, and subcellular localization in comparison to WT and L166P DJ-1. These analyses reveal that L10P, L166P and P158DEL DJ-1 mutants are dramatically destabilized in comparison to WT protein. Interestingly, since L10P and P158DEL mutants retain the ability to dimerize, it suggests that enhanced turn-over of mutant proteins may be related to aberrant protein folding and not necessarily to dimerization. Taken together, the studies herein suggest that L10P, L166P, and P158DEL DJ-1 mutations may be causative of disease by distinct mechanisms.

3.3 RESULTS

Pathogenic DJ-1 mutants demonstrate reduced protein stabilities and are partially regulated by the proteasome.

It has been previously shown that L166P mutant DJ-1 demonstrates dramatically reduced protein stability in comparison to WT protein (42;138;139;269;298;307;324) and that this aberration is due in part to rapid degradation of mutant protein by the proteasome (138;139;298;307;324;422). To determine the effects of the recently reported L10P and P158DEL DJ-1 mutations on protein stability, protein turn-over pulse-chase experiments were performed with ^{35} S-methionine. The turn-over rates of WT, L10P, L166P, and P158DEL DJ-1 protein were compared. Following these analyses it was determined that the half-life of WT DJ-1 was ~8 hours (**Figure 3-1A**). As expected, the half-life of L166P mutant DJ-1 was ~1 hour, which is consistent with previous reports (307;324). L10P and P158DEL DJ-1 mutants exhibited half-lives of ~2.5 hours and ~4 hours respectively, demonstrating that both of these mutants also destabilize DJ-1.

To determine the effects of the proteasome complex on the turn-over rates of WT, L10P, L166P, and P158DEL DJ-1 protein variants, protein pulse-chase experiments were performed in the presence of 20μM MG-132. The ratio of DJ-1 protein remaining with the addition of MG-132 to that without the addition of MG-132 after 6 hours of chase was calculated and the results were compared for each DJ-1 variant. The turn-over rate for WT DJ-1 was not significantly affected by proteasome inhibition (**Figure 3-1B**). Conversely, treatment of cells with MG-132 partially stabilized all of the DJ-1 mutants analyzed, though the effect was most striking for the L10P DJ-1 mutant. Interestingly,

proteasome inhibition slowed the decay of L10P, L166P, P158DEL DJ-1 mutant proteins, but it did not completely block the degradation of these mutants. This observation has been previously reported for the L166P DJ-1 mutant (139;298;324), suggesting that in addition to proteasome-mediated degradation, turn-over of L10P, L166P, and P158DEL DJ-1 mutant proteins can also be regulated by proteasome-independent mechanisms.

Figure 3-1

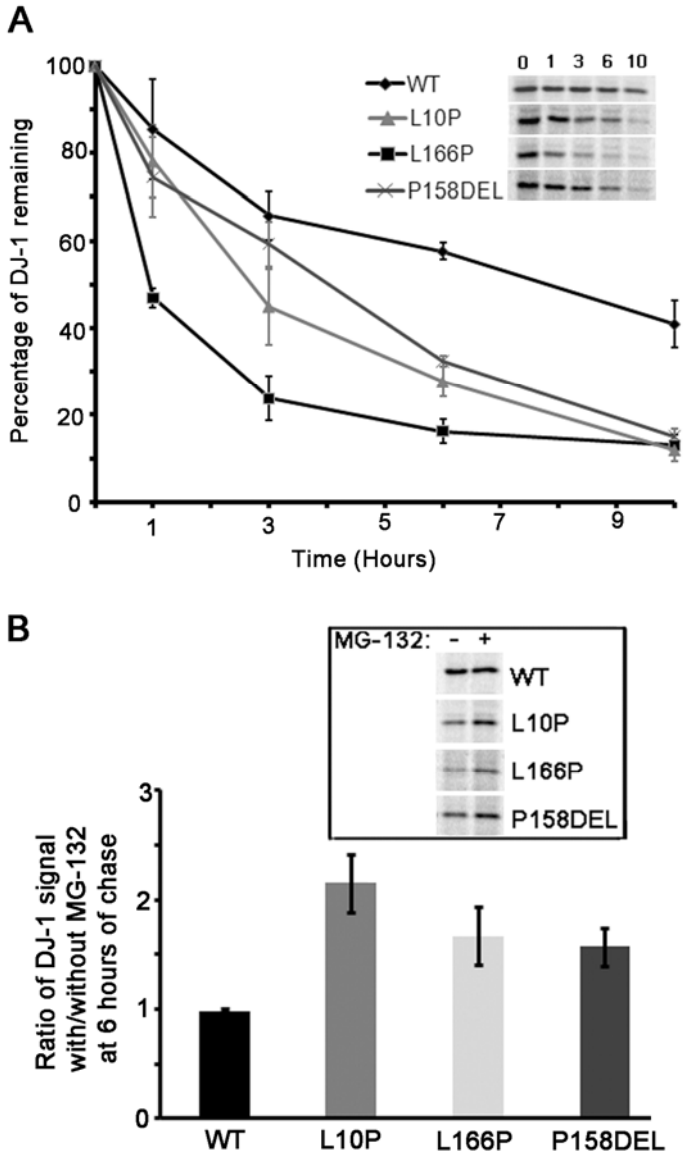

Pathogenic DJ-1 mutants demonstrate dramatically reduced protein stabilities that are partially due to proteasome degradation.

CHO cells were transfected with full-length WT, L10P, L166P, or P158DEL human DJ-1 pZeoSV2 "(+)" constructs. At 48 hours post transfection, cells were labeled with ^{35}S-methionine for 30 mins and chased for 0, 1, 3, 6, or 10 hours. **A)** The graph represents the protein turnover results for the respective DJ-1 variants. The results are plotted as percentage of protein remaining over time standardized to the 0 hrs time point. The error bars show standard deviation (n=6). The inset shows representative pulse-chase experiments. **B**) The ratio of DJ-1 decay in the presence of 20 μM MG-132 added at 0 hrs to that in the absence of MG-132 at 6 hours of chase was calculated for each sample. The graph depicts the average of the ratios between replicate samples for each DJ-1 variant. The error bars indicate standard deviation (n=3). The inset image represents the DJ-1 signal remaining after 6 hours of chase for each of the DJ-1 variants in the absence and presence of MG-132.

The L10P and P158DEL DJ-1 mutations do not disrupt dimer formation but may alter protein folding.

Previous studies reveal that in comparison to WT DJ-1 protein, L166P mutant DJ-1 displays aberrant folding (12;139;324;469) that impairs the dimerization of this mutant and that is associated with a dramatic instability of this mutant protein (12;42;139;269;298;307;324). Thus, it is possible that L10P and P158DEL DJ-1 mutants are destabilized due to disrupted dimerization and/or improper protein folding. To assess the ability of L10P and P158DEL DJ-1 variants to form dimers, co-transfection and co-immunoprecipitation experiments were conducted. Experiments with WT and L166P DJ-1 were also conducted for comparison. CHO cells were transiently co-transfected with human HA-tagged full-length WT DJ-1 and human untagged full-length WT, L10P, L166P, or P158DEL DJ-1. Cells extracts were immunoprecipitated with an anti-HA antibody followed by immunoblot with antibody DJ5. These analyses revealed that the untagged WT, L10P, and P158DEL DJ-1 variants were all co-immunoprecipitated with HA-tagged WT DJ-1 protein (**Figure 3-2A**). However, L166P DJ-1 was not co-immunoprecipitated with HA-tagged WT DJ-1. This indicates that L10P and P158DEL DJ-1 variants retain the ability to dimerize.

To further analyze the consequences of DJ-1 mutations on protein structure, size exclusion chromatography experiments were conducted. Soluble lysates were fractionated from CHO cells expressing WT, L10P, P158DEL, or L166P human DJ-1. The assay was standardized by elution of purified proteins of known molecular masses. Fractions were resolved by SDS-PAGE and analyzed by immunoblot with the anti-

Figure 3-2

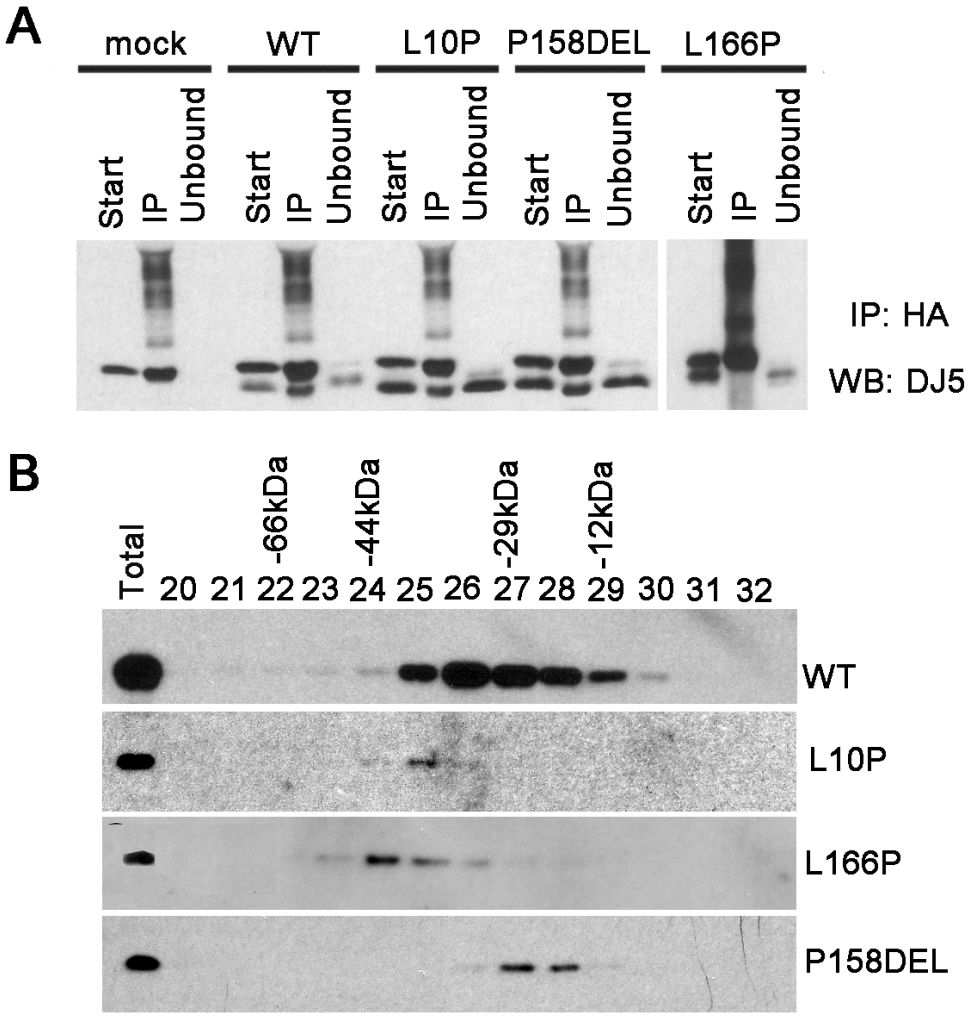

The L10P and P158DEL DJ-1 mutations do not disrupt dimer formation but appear to alter protein folding patterns. **A**) CHO cells were co-transfected with HA-tagged full-length WT DJ-1 and pZeoSV2 (+) mock vector ("mock") or with untagged full-length WT, L10P, P158DEL, or L166P human DJ-1 pZeoSV2 (+) constructs. At 24 hours post transfection, cells were harvested and soluble protein lysates were extracted ("Start"). The cell lysates were then immunoprecipitated using anti-HA polyclonal antibody ("IP"). Equal amounts of the start, IP, and unbound supernatant (Unbound) fractions were resolved by SDS-PAGE and analyzed by western blot ("WB") with the monoclonal DJ-1 antibody, DJ5. **B**) CHO cells were transiently transfected with full-length WT, L10P, L166P, or P158DEL human DJ-1 pZeoSV2 (+) constructs. Soluble extracts from CHO cells expressing the respective exogenous human DJ-1 proteins were loaded on a precalibrated Superose 6 column as described in the "Materials and Methods" section. The total cell lysates ("total") and fractions collected from the size-exclusion column were analyzed by western blot analysis with DJ5 antibody to detect human DJ-1. Fractions 20-32 are shown. The elution profile of known molecular mass standards [BSA (66 kDa), ovalbumin (44 kDa), carbonic anhydrase (29kDa) and cytochrome C (12kDa)] are indicated above.

human specific DJ-1 antibody DJ5. The peak elution fraction for WT human DJ-1 was fraction 26 (**Figure 3-2B**), consistent with dimer formation. It has been previously

reported that L166P DJ-1 forms high molecular weight complexes which increase its apparent molecular weight when analyzed by gel filtration analyses (269;324). In the studies herein, L166P DJ-1 eluted in peak fraction 24, suggesting that it also forms high-molecular weight complexes in CHO cells. Interestingly, L166P DJ-1 that would elute in fractions that would be consistent with monomeric forms of DJ-1 was not detected in these analyses. Surprisingly, the peak elution for L10P DJ-1 was fraction 25, indicating that the L10P mutant adopts an apparent larger conformation than WT DJ-1 protein. Conversely, P158DEL DJ-1 primarily eluted into fractions 27 and 28, suggesting that it adopts a smaller conformation than WT DJ-1 protein.

L10P, L166P and P158DEL DJ-1 mutants show reduced protein solubilities.

Protein misfolding and aggregation is a prominent feature of many neurodegenerative disorders (402) and reduced solubility of DJ-1 is correlated with human disease (227;296;304;316;371). L166P DJ-1 is known to be misfolded (12;139;324) and this may result in reduced solubility of the mutant in comparison to WT DJ-1 (394). Gel filtration analyses revealed that the L10P and P158DEL DJ-1 variants may adopt abnormal folding patterns (**Figure 3-2B**); however, it is unknown whether protein solubility is affected by these mutations. To assess for changes in solubility, CHO cells expressing full-length WT, L10P, L166P, or P158DEL human DJ-1 were harvested and cell lysates were extracted into buffers of increasing solubilization strengths. The lysates were then analyzed by western blot with antibody DJ5. WT, L10P, L166P, and P158DEL DJ-1 variants were all predominantly extracted in the soluble PBS/0.1% Triton

(TX) (**Figure 3-3A**). However, a significant fraction of P158DEL DJ-1 protein was extracted in the RIPA and SDS fractions.

Figure 3-3

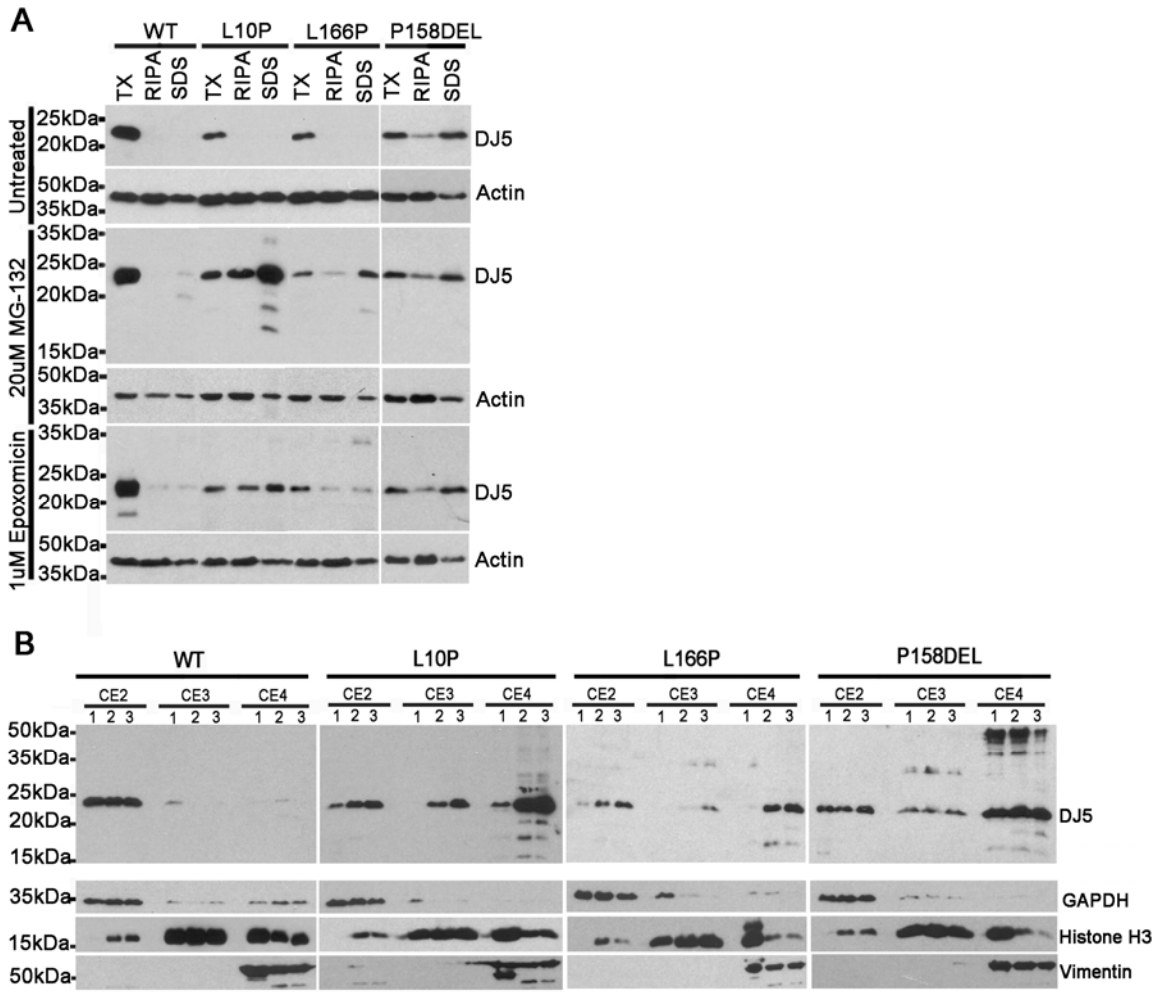

L10P, L166P and P158DEL DJ-1 mutants show reduced protein solubilities. CHO cells were transfected with full-length WT, L10P, L166P, or P158DEL human DJ-1 pZeoSV2 (+) constructs. At 24 hours post transfection, cells were cultured for an additional 18 hours in fresh DMEM with or without the addition of either 20μM MG-132 or 1μM Epoxomicin. **A**) Cells were harvested and sequentially extracted into PBS/0.1% Triton (TX) buffer, RIPA buffer, and 2% SDS/17mM Tris (SDS) buffer. Equal amounts (10ug) of each sample were loaded onto 13% polyacrylamide gels and analyzed by western blot for DJ-1 distribution with the DJ5 antibody. Blots were also probed with an actin antibody to assess equal protein loading. The mobility of molecular mass markers is indicated on the left. **B**) Cells were harvested and extracted using the Qproteome Cell Compartment Kit (Qiagen), following the manufacturer's instructions. Equal amounts (10ug) of each sample were loaded onto 13% polyacrylamide gels and analyzed by western blot with antibody DJ5 to assess the distribution of human DJ-1, GAPDH monoclonal antibody as a cytoplasmic marker, histone H3 polyclonal antibody as a nuclear marker, and vimentin polyclonal antibody as a cytoskeletal marker. "CE2" represents the cytoplasmic fractions, "CE3" represents the nuclear fractions and "CE4" represents the cytoskeletal/insoluble fractions. "1" lanes were loaded with extracts from cells treated with fresh DMEM only. "2" lanes were loaded with extracts from cells treated with fresh DMEM + epoxomicin. "3" lanes were loaded with extracts from cells treated with fresh DMEM +MG-132.

Proteasome inhibitors have been shown to stabilize insoluble forms of L166P DJ-1 protein when assessed in cell culture studies (307;325); however, it is not known whether L10P and P158DEL DJ-1 protein mutants display similar biochemical properties. To analyze the effects of proteasome inhibitors on DJ-1 solubility, CHO cells expressing WT, L10P, L166P, or P158DEL human DJ-1 were treated for 18 hours with 20μM MG-132 or 1μM epoxomicin followed by harvesting and extraction into buffers of increasing solubilization strengths. The extracts were then assessed by immunoblot with antibody DJ5. Treatments with either MG-132 or epoxomicin resulted in only trace amounts of WT DJ-1 detected in the RIPA or SDS-soluble fractions (**Figure 3-3A**). Both MG-132 and epoxomicin dramatically promoted the accumulation of RIPA and SDS-soluble forms of L10P DJ-1, though the effects were more provocative with MG-132. Similarly, MG-132 and epoxomicin resulted in the buildup of Triton-insoluble pools of L166P DJ-1. Interestingly, however, neither MG-132 nor epoxomicin treatments affected the amount of Triton-insoluble P158DEL DJ-1 protein.

To expand on these biochemical fractionation results and to assess for possible changes in cellular localization, protein fractionation experiments were performed using the Qproteome Cell Compartment Kit. CHO cells expressing WT, L10P, L166P, or P158DEL human DJ-1 were compared when untreated or challenged with 20μM MG-132 or 1μM Epoxomicin for 18 hours. Cytoplasmic (CE2), nuclear (CE3), and cytoskeletal/insoluble (CE4) protein fractions were generated. Cell extracts were analyzed by western blot with the antibodies to human DJ-1 (DJ-5), GAPDH, histone-H3, and vimentin. These analyses revealed that under normal conditions, WT DJ-1 protein primarily localized to cytoplasmic biochemical fractions and to a much lesser

extent into nuclear fractions (**Figure 3-3B**). WT DJ-1 protein was absent from cytoskeletal/insoluble protein fractions. As expected, MG-132 and epoxomicin treatments had little effect on WT DJ-1 protein. Under normal conditions, L10P DJ-1 was predominantly detected in both cytoplasmic and cytoskeletal/insoluble protein fractions. Following treatments with MG-132 or epoxomicin, L10P DJ-1 accumulated in the nucleus and cytoskeletal/insoluble fractions, suggesting that inhibition of the proteasome may act to stabilize insoluble forms of the L10P DJ-1. Under normal conditions, L166P DJ-1 was predominantly observed in the cytoplasmic fraction; however, following treatments with MG-132 or epoxomicin, L166P DJ-1 dramatically accumulated in cytoplasmic and cytoskeletal/insoluble protein fractions, and to a much lesser extent in nuclear fractions. In the absence of proteasome inhibitors, the P158DEL DJ-1 variant was extracted in all three fractions and treatments with either MG-132 or epoxomicin had no significant effect on the biochemical extractability of P158DEL DJ -1 protein as detected by this method (**Figure 3-3B**). This finding further implies that this mutant exhibits reduced solubility even in the absence of induced proteasome challenge.

L10P, L166P, and P158DEL DJ-1 form intracellular inclusions following proteasome inhibition.

Olzmann et al. showed that MG-132 induced the recruitment of L166P DJ-1 into aggresomes (325). To determine whether a similar effect would be observed for the L10P and P158DEL DJ-1 mutants, co-immunofluorescence studies were conducted comparing untreated and treated CHO cells expressing WT, L10P, L166P, or P158DEL human DJ-1 challenged for 12 hours with 20μM MG-132. Cells were co-labeled with DJ5 and

vimentin antibodies to assess for DJ-1 staining and inclusion formation, respectively. Under normal culturing conditions, WT and mutant DJ-1 proteins exhibited diffuse staining (**Figure 3-4A**). However, nuclear and cytoplasmic DJ-1 positive inclusions were detected in a small percentage of L10P and P158DEL DJ-1 expressing cells (**Figure 3-4A and C and data not shown**). MG-132 treatment induced the formation of intranuclear and cytoplasmic DJ-1 positive protein inclusions in cells expressing L10P, L166P, and P158DEL DJ-1 but had little effect on cells expressing WT DJ-1 (**Figure 3-4B and C**). Interestingly, co-immunofluorescence analyses with DJ5 and vimentin antibodies did not reveal any accumulation or redistribution of vimentin surrounding L10P or P158DEL DJ-1 protein inclusions, although vimentin was co-localized with these inclusions on rare occasions, suggesting that the observed DJ-1 positive inclusions are not classical aggresomes. MG-132 caused inclusion formation most provocatively in cells expressing L10P DJ-1 since ~74±15% of these cells had inclusions. P158DEL DJ-1 formed inclusions in 59±19% of cells, while L166P DJ-1 formed inclusions in 45±7% of cells.

3.4 DISCUSSSION

A short nucleotide deletion resulting in P158DEL DJ-1 and a missense mutation resulting in the L10P DJ-1 amino acid substitution are novel recently reported *PARK7/DJ-1* mutations causative of autosomal recessive early-onset parkinsonism (144;270). In the current study, the effects of these mutations on DJ-1 protein stability, dimerization, solubility, and localization were assessed in cultured cells. Additionally, the previously extensively characterized pathogenic L166P DJ-1 mutant was also analyzed in

Figure 3-4A

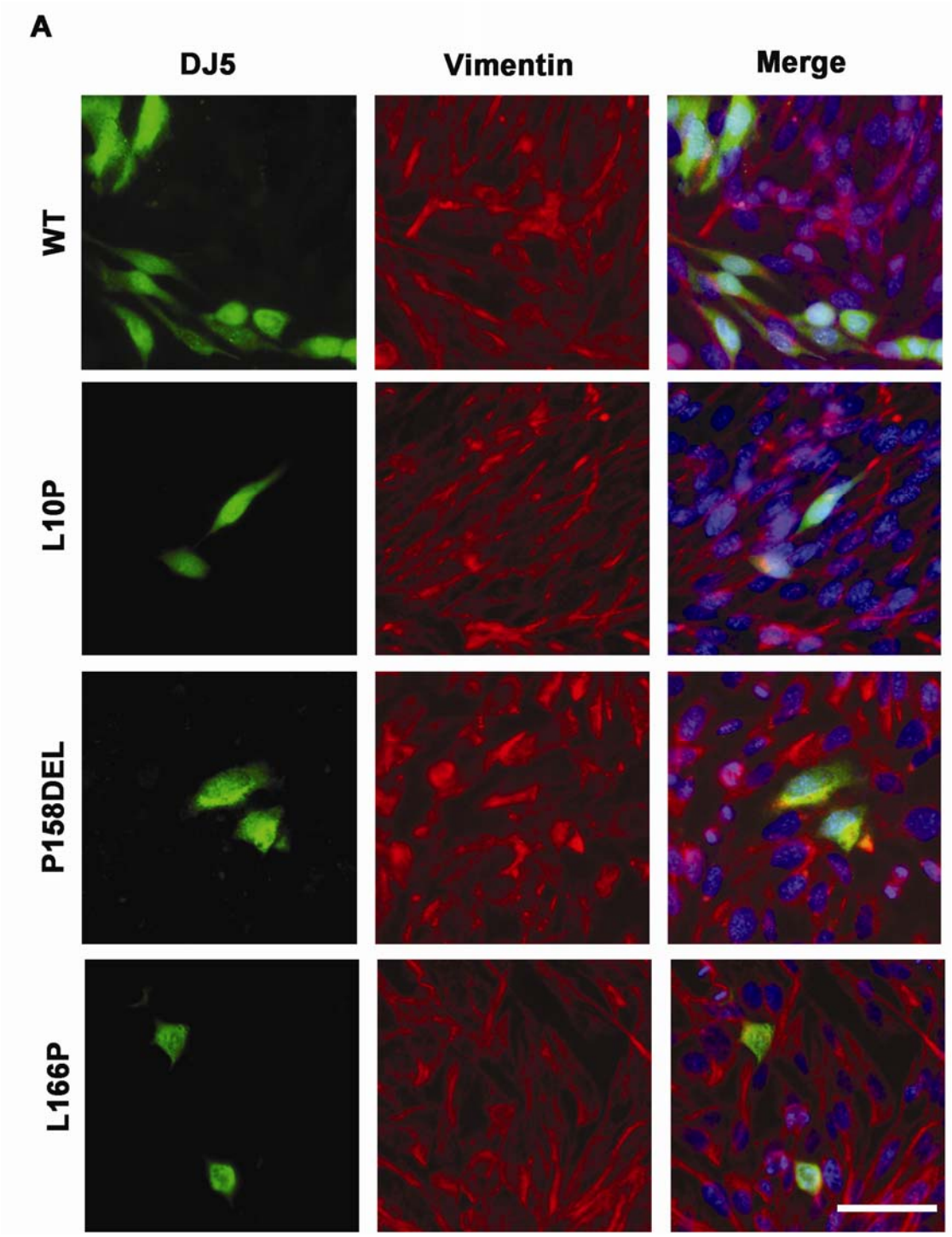

Figure 3-4B

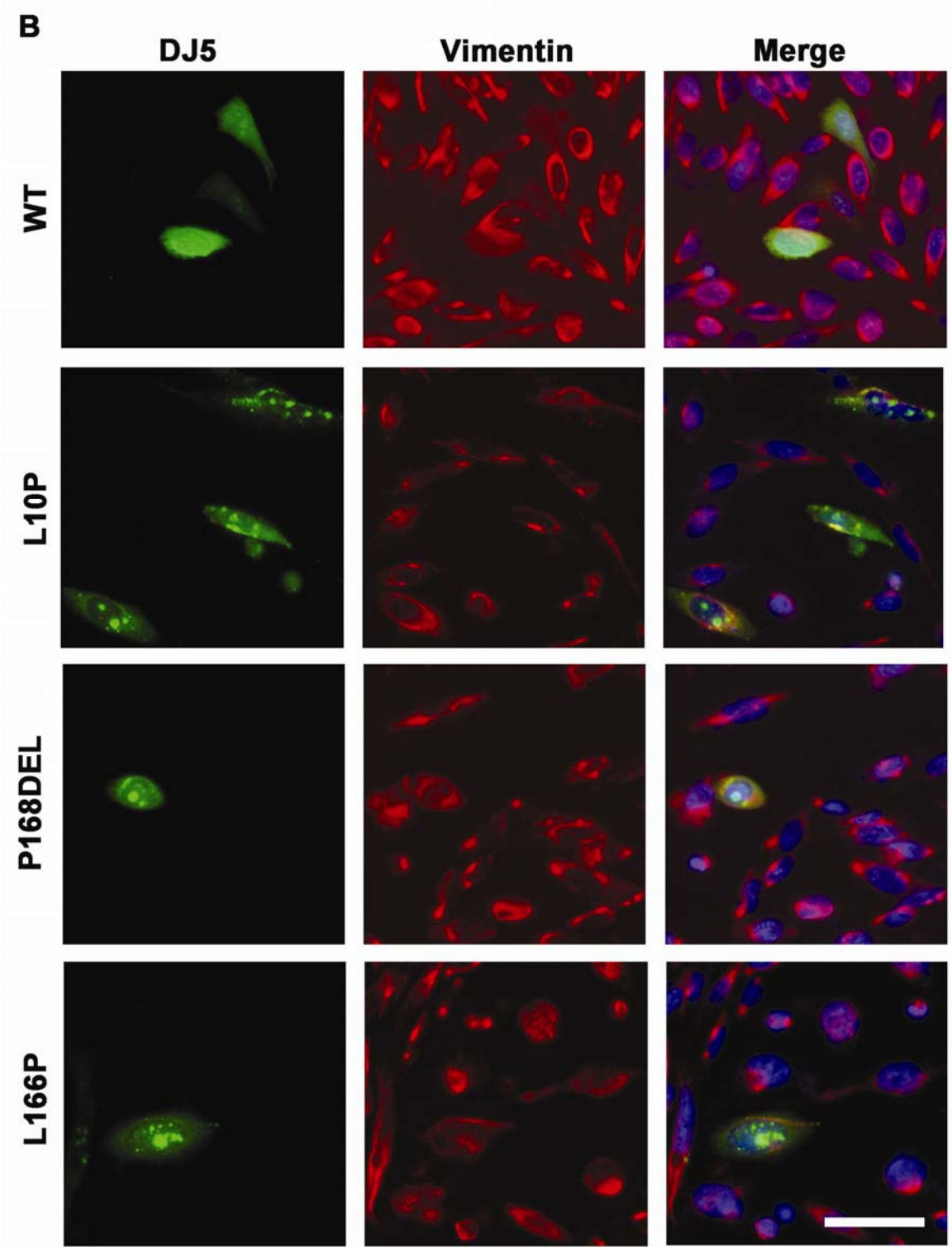

Figure 3-4C

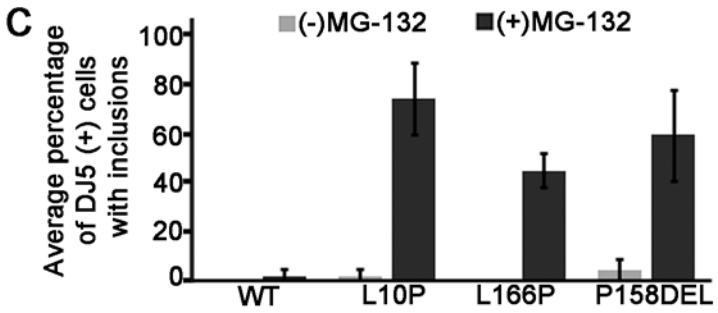

L10P, L166P, and P158DEL DJ-1 form intracellular inclusions following proteasome inhibition. CHO cells were transfected with full-length WT, L10P, L166P, or P158DEL human DJ-1 pZeoSV2 (+) constructs. At 48 hours post transfection, cells were cultured for an additional 12 hours in fresh DMEM with or without the addition of 20μM MG-132. Cells were stained with the mouse monoclonal anti-DJ-1 antibody DJ5 (green), a rabbit polyclonal anti-vimentin (red) and Hoechst 33342 (blue) and visualized by microscopy. Representative images are shown for cells that were not treated with MG-132 in **A**) and cells that were treated with MG-132 in **B**). Bar = 50μm (**C**) The proportion of cells depicting DJ-1 inclusions was quantified as the percentage of the total cells expressing full-length WT, L10P, L166P, or P158DEL human DJ-1 with or without MG-132 challenge. The graph represents the percentage of cells with inclusions averaged between replicate images. The error bars show standard deviation.

parallel. In comparison to WT DJ-1 protein, the L10P, L166P, and P158DEL DJ-1 mutants all exhibited reduced protein stabilities when assessed by pulse-chase protein turn-over analyses; however, the extent of the effects of the respective mutations on protein stability was variable. The L10P and P158DEL mutants were relatively less unstable than L166P. To begin to explain these findings, and because it was previously reported that the instability L166P DJ-1was at least partially mediated by the proteasome (138;139;298;307), pulse-chase analyses were conducted in the presence of the reversible proteasome inhibitor, MG-132. As previously shown by others (138;139), MG-132 only partially stabilized L166P DJ-1 protein in the studies herein. Similarly, MG-132 failed to completely block degradation of L10P and P158DEL DJ-1 mutants, though turn-over was dramatically slowed for both variants. Noteworthily, in comparison to the other mutants, MG-132 most effectively slowed the degradation of L10P DJ-1, suggesting that

this mutation renders DJ-1 to be more susceptible to degradation by the proteasome. Based on the findings herein, is it also likely that proteasome-independent mechanisms can act to degrade L10P, L166P, and P158DEL DJ-1 mutant proteins. It is worth mentioning that autophagy inhibitors did not impede the degradation of any of the DJ-1 protein variants analyzed in these studies (data not shown). This observation has also been reported by other groups (42;324). Though a recent paper by Giaime and colleagues supports a role for caspase-6 mediated cleavage of DJ-1, it is not clear what additional proteases may act to regulate DJ-1 protein (129). The current findings suggest that reduced DJ-1 protein stability resulting from the L10P and P158DEL mutations may at least be partially responsible for DJ-1 loss-of-function.

It has been previously shown that the L166P mutation causes DJ-1 to unfold and it is believed that this disconformity effectively disrupts dimer formation, which may be associated with rapid degradation (12;139;298;307;324). Interestingly, it was determined that unlike L166P DJ-1, L10P and P158DEL DJ-1 mutants were able to dimerize with WT DJ-1 protein. A similar finding has been reported for another pathogenic DJ-1 mutant, M26I, which also exhibits decreased stability without associated dimerization impairments (42). This indicates that the ability for DJ-1 to form dimers may not necessarily correlate to protein stability. However, improper protein folding may be causal of the decreased stability observed for some pathogenic DJ-1 mutants. Supporting this idea, the studies herein revealed that L10P and P158DEL DJ-1 variants adopted altered structural conformations in comparison to WT DJ-1 protein as determined by size exclusion chromatography. Though it is believed that L166P DJ-1 cannot dimerize, monomeric forms of L166P DJ-1 of the expected ~21 kDa size were not detected in the

current study. This may be due to the unstable nature of monomeric L166P DJ-1. Instead, the observed L166P DJ-1 eluted with an apparent molecule mass greater than that of WT DJ-1. This finding is consistent with a previous report showing that L166P DJ-1 forms higher-order protein complexes (269), and this suggests that L166P DJ-1 may also form such complexes in CHO cells. The elution of WT DJ-1 was primarily consistent with dimer formation, although the broad elution profile would also suggest equilibrium with a monomeric pool. Surprisingly, the L10P DJ-1 mutant exhibited an apparent elution profile that is consistent with a slightly larger conformation than WT protein. The L10P mutation is located in the first β-strand of DJ-1, which is not directly involved in the dimer interface (167;170;469). Therefore, this mutation is not predicted to affect dimerization, but would have a significant effect on disrupting the first β-strand. Conversely, P158DEL DJ-1 exhibited an elution profile that suggests that it is slightly smaller than WT protein. Residue P158 is also outside of the DJ-1 dimer interface; however it located right before the beginning of DJ-1 α-helix 7 which is required for dimer formation (167;170;469). Additionally, P158 is a highly conserved residue in the DJ-1 protein family (23). Thus, it is possible that deletion of residue P158 shifts the conformation of DJ-1 in such a way as to allow for tighter packing of the monomer or the dimer and this could in turn result in apparent decreased protein size.

Without proper regulation, misfolded proteins can accumulate and aggregate with each other, and this can eventually lead to impaired cellular processes (291;323). Since our data indicate that the L10P, L166P, and P158DEL mutations can alter protein folding, it was of interest to determine the effects of these mutations on protein solubility. The respective solubilities of WT, L10P, L166P, and P158DEL DJ-1 proteins were assessed

by two different biochemical fractionation methods. When expressed in CHO cells under normal culturing conditions, P158DEL DJ-1 and to a lesser extent L10P DJ-1 demonstrated reduced solubilities. Interestingly, when biochemical fractionation experiments were performed following treatments with MG-132 or epoxomicin, L10P and L166P DJ-1 proteins demonstrated dramatic accumulations of insoluble proteins while WT DJ-1 was unaffected by these treatments. This indicated that L10P and L166P DJ-1 protein variants, which are inclined to misfolding and being degraded, accumulate as aggregates when degradation is impaired. The finding that more L10P accumulates in the insoluble fractions compared to L166P in the presence of MG132 suggests that the ability of the former variant to still form dimers may also promote this process. Surprisingly, while P158DEL formed insoluble aggregates under native conditions, proteasome inhibition did not enhance the accumulation of insoluble species. These findings suggest that P158DEL DJ-1 can spontaneously accumulate as misfolded aggregates that are largely regulated by proteasome-independent mechanisms.

Aggregation of DJ-1 mutant proteins also was studied at the microscopic level. Under normal conditions, only a small percent of cells expressing L10P and P158DEL DJ-1 depicted DJ-1 inclusions. Such a finding has not been reported for other pathogenic DJ-1 mutants, suggesting that these mutants may be more prone to aggregation. MG-132 treatments induced the formation of L10P, L166P, and P158DEL DJ-1 intranuclear and intracytoplasmic protein inclusions that were not detected in cells expressing WT DJ-1 protein under the same conditions. Most of the observed inclusions did not co-localize with common aggresome markers, suggesting that they likely represent deposits of aggregated DJ-1. The formation of these inclusions did not correlate with formation of

insoluble DJ-1 observed biochemically. For example, biochemical analysis demonstrated that P158DEL DJ-1 forms an intrinsic insoluble pool of protein and this is not significantly altered by MG132 treatment. It is possible that MG132 treatment induced this pool of P158DEL DJ-1 to coalesce into inclusions. Remarkably, inclusions were most prominent in cells expressing L10P DJ-1 following MG132 challenge. Biochemical analysis demonstrated that MG132 resulted in a dramatic accumulation of insoluble L10P DJ-1 and it is possible that such a pool is required for inclusion formation. Similarly, MG132 treatment resulted in the accumulation of insoluble L166P DJ-1 and inclusion formation. Olzmann and colleagues showed that L166P DJ-1 formed perinuclear aggresomes in cultured cells following treatments with MG-132; however it was determined that this phenomenon only occurred in the presence of the E3 ubiquitin-protein ligase, parkin (325). Interestingly, no interactions between parkin and L10P or P158DEL DJ-1 variants were discovered in the studies herein (data not shown), thus it is likely that L10P and P158DEL DJ-1 inclusion formation is regulated by alternative mechanisms.

In conclusion, these studies demonstrate that the pathogenic L10P and P158DEL mutants result in the destabilization of DJ-1 and that proteasome degradation is at least partially involved in this process. Additionally, the L10P and P158DEL mutations do not prevent dimer formation, indicating that that the observed decreases in protein stability may be caused by limited and localized perturbations in protein folding. These alterations in protein structure are likely responsible for reduced protein solubilities and intracellular protein inclusion formation. These properties of L10P and P158DEL mutants may collectively contribute to DJ-1 loss-of-function by depleting the pool of functional

protein. In addition, these novel findings indicate that different pathogenic DJ-1 mutants can display diverse altered biochemical properties. Future studies to assess for specific effects of pathogenic DJ-1 mutations on biological pathways *in vivo* and studies in patients would give insights into the physiological role for DJ-1 protein especially as it relates to the etiology of PD.

3.5 MATERIALS AND METHODS

Antibodies

DJ-5 is a mouse monoclonal antibody that is specific for human DJ-1 protein (296). Affinity purified mouse anti-actin (clone C4) monoclonal antibody reacts with all forms of vertebrate actin (Millipore, Billerica, MA). The affinity purified polyclonal antibody, HA.11 (Covance, Emeryville, CA), reacts with proteins with the amino acid sequence, YPYCVPVYA. Vimentin (C-20) is an affinity purified polyclonal antibody that reacts with vimentin (Santa Cruz Biotechnology, Inc, Santa Cruz, CA). Anti-histone H3, CT, pan (Millipore, Temecula, CA) is a polyclonal antibody that recognizes histone H3 protein. Affinity purified glyceraldehyde-3-phosphate dehydrogeanase (GAPDH) (clone 6C5) monoclonal antibody reacts with GAPDH from various species (Advanced Immunochemical, Long Beach, CA).

Cloning of Human DJ-1 Constructs

Human full-length WT DJ-1 cDNA was cloned into the pZeoSV2 (Invitrogen, Carlsbad, CA) mammalian expression vector at the HindIII and Xho I restriction sites. Using the WT DJ-1 construct, the QuickChange® Site Directed Mutagenesis Kit

(Stratagene, La Jolla, CA) was used in order to generate L10P, L166P, and P158DEL mutant forms of DJ-1 in the pZeoSV2 vector. The sequences of the oligonucleotides used for mutagenesis are listed in Table 1. The respective DJ-1 plasmid sequences were verified by DNA sequencing as a service offered by the DNA Sequencing Facility of the University of Pennsylvania.

A human N-terminal HA-tagged WT DJ-1 construct was generated by PCR, using the human full-length WT pZeoSV2 construct as a template. The sequences for the oligonucleotides are listed in **Table 3-1**. The tagged insert was cloned into the pCR 2.1 TOPO vector (Invitrogen) and subsequently cloned into the pZeoSV2 vector at the Hind III and Xho I restriction sites. The sequence of the plasmid was verified by DNA sequencing as described above.

Cell Culture

Chinese Hamster Ovary (CHO) cells were cultured in Dulbecco-modified Eagle medium (DMEM) (Invitrogen) supplemented with 10% fetal bovine serum (Hyclone, Logan, UT), 100 U/mL penicillin and 100 μg/mL streptomycin (Invitrogen). Cells were incubated at 37ºC and 95% air/5% CO_2 atmosphere.

Pulse-chase Protein Turnover Analysis

CHO cells were cultured in 100 mm dishes. Cells were transfected with pZeoSV2 full-length WT, L10P, L166P, or P158DEL human DJ-1 constructs using Lipofectamine Reagent (Invitrogen), following the manufacturer's protocol. At 24 hours post transfection, cells were split into 35 mm dishes and cultured in complete DMEM for an

additional 24 hours. At 48 hours post transfection, cells were methionine-deprived for 15 minutes by incubation in pre-warmed methionine-free DMEM (Invitrogen)/10% dialyzed FBS (Hyclone) before adding 100μCi [^{35}S]-methionine (Perkin-Elmer, Waltham, MA) per ml of methionine free DMEM/10% dialyzed FBS for 30 min. Chase experiments were conducted in triplicates with normal DMEM/FBS with or without 20μM MG-132 for 0, 1, 3, 6, and 10 hours. Cells were then rinsed with PBS and harvested in cytoskeleton (CSK) buffer (100 mM NaCl, 50 mM Tris, pH 7.5, 2 mM EDTA, 1 % Triton X-100) containing 1 % SDS and boiled at 100 ºC for 5 minutes. CSK buffer was added to the lysates in order to bring the final concentration of SDS to 0.25%. Lysates were frozen on dry ice and kept frozen at -20 ºC until the last time point was harvested. The radiolabelled protein extracts were pre-cleared with a rabbit serum pre-incubated with protein A-agarose (Santa Cruz Biotechnology, Inc.) for 3 hours at 4ºC and radiolabelled extracts were then immunoprecipitated overnight at 4ºC with antibody DJ5 pre-incubated with protein A/G PLUS-agarose (Santa Cruz Biotechnology, Inc). The antibody-protein complexes were washed 3 times with 10 volumes of CSK buffer, resuspended in 2 volumes of 2X SDS sample buffer and boiled at 100 ºC for 5 minutes. The beads were removed by centrifugation and the samples were loaded onto 13 % polyacrylamide gels. Following electrophoresis, gels were fixed with 50% methanol/5% glycerol, dried and exposed to a PhosphorImager plate and the signal was quantified using ImageQuant software (Molecular Dynamics, Inc., Sunnyvale, CA).

Western Blot Analysis

Protein samples were resolved by SDS-PAGE followed by electrophoretic transfer onto nitrocellulose membranes. Membranes were blocked in Tris buffered saline (TBS) with 5% dry milk, and incubated overnight with primary antibodies diluted in TBS/ 5% dry milk. Each incubation was followed by goat anti-mouse conjugated horseradish peroxidase (HRP) (Amersham Biosciences, Piscataway, NJ) or goat anti-rabbit HRP (Santa Cruz Biotechnology, Inc, Santa Cruz, CA), and immunoreactivity was detected using chemiluminescent reagent (NEN, Boston, MA) followed by exposure onto X-ray film.

Size Exclusion Chromatography

Gel filtration chromatography was performed as previous described (366). CHO cells transiently expressing human full-length WT, L10P, L166P, or P158DEL DJ-1 were cultured in 100 mm dishes, grown to confluency, and harvested. To harvest cells, the cells were rinsed and scraped in PBS. After recovery by centrifugation, cells were lysed in PBS/0.1% Triton and the cell debris was sedimented at 13,000 x g for 5 min. The extracts were filtered through a 0.22 μm filter and loaded onto the column. Fractions were analyzed by immunoblotting with anti-human DJ-1 specific antibody DJ5. Experiments were repeated at least 3 times and similar results were obtained.

Co-Immunoprecipitation and Heterodimer Analysis

CHO cells were cultured in 100 mm plates. Cells were transfected with N-terminal HA-tagged full-length WT human DJ-1 construct (HA-WThDJ/pZeoSV2) or co-transfected with HA-WThDJ/pZeoSV2 and pZeoSV2 full-length untagged WT, L10P,

L166P, or P158DEL human DJ-1 constructs. After 24 hours, cells were rinsed and scraped in PBS and lysed by vortexing into 500 uL of ice-cold 1X CSK buffer with protease inhibitors. Cell debris was sedimented at 13,000 x g for 1 minute and supernatants were removed to fresh tubes. 50 uL of each supernatant was saved as the "Start" fraction. The remainders of the supernatants were incubated for 3 hours at 4 °C with anti-HA tag antibody, HA.11 (Covance) preabsorbed to protein A-Agarose beads (Santa Cruz Biotechonogy, Inc.). The beads were sedimented, repeatedly rinsed with ice-cold 1X CSK buffer, resuspended in 2X SDS sample buffer, heated to 100 ^{o}C and saved as the "IP" fractions. The supernatants remaining after immunoprecipitation were saved as the "Unbound" fractions. Sample buffer was added to the "Start" and "Unbound" fractions and then they were heated to 100 ^{o}C for 5 minutes. The Start, IP, and Unbound fractions were resolved by SDS-PAGE and immunoblotted with DJ5 antibody.

Biochemical Fractionation and Cell Compartment Fractionation

CHO cells were cultured in 100 mm dishes and transfected with pZeoSV2 full-length WT, L10P, L166P, or P158DEL DJ-1 constructs using Lipofectamine transfection reagent. At 24 hours post transfection, the cells were cultured for an additional 18 hours in fresh DMEM with or without the addition of either 20μM MG-132 or 1μM Epoxomicin. For biochemical fractionation, cells were scraped into PBS, sedimented, and lysed into buffers of increasing solubilization strengths using previously described methods (366). The respective biochemical fractions were analyzed by western blot with the monoclonal antibodies DJ5 and anti-actin.

For cell compartment fractionation, cells were scraped into ice-cold PBS and fractionated into cellular compartments using the Qproteome Cell Compartment Kit (Qiagen, Valencia, CA) following the manufacture's protocol. Cell lysates were quantified using the BCA assay and analyzed by western blot with the monoclonal antibodies DJ5 and GAPDH and the polyclonal antibodies anti-histone H3 and vimentin (C-20).

Double-immunofluorescence Analyses

CHO cells were cultured in 35 mm dishes and transfected with pZeoSV2 full-length WT, L10P, L166P, or P158DEL DJ-1 constructs using Lipofectamine transfection reagent. At 48 hours post transfection, the cells were cultured for an additional 12 hours in fresh DMEM with or without the addition of 20μM MG-132. Cells were rinsed in PBS and fixed by incubation in ice-cold acetic-methanol (1 part acetic acid to 20 parts methanol) at -20 °C for at least 30 minutes. Cells were rehydrated with water, rinsed with PBS, and blocked in PBS/1% FBS/1% skin fish gelatin (Sigma)/1% milk/0.1% Triton for 30 minutes. Primary antibodies were diluted into blocking solution and cells were labeled for 1-2 h at room temperature. Following PBS washed, coverslips were incubated with anti-mouse IgG antibody secondary conjugated to Alexa 488 and anti-rabbit IgG antibody conjugated to Alexa 594. Nuclei were counterstained with Hoechst trihydrochloride trihydrate 33342 (Invitrogen), and coverslips were mounted using Fluoromount-G (Southern Biotech, Birmingham, AL). Images were captured using an Olympus BX51 fluorescence microscope mounted with a DP71 digital camera (Olympus, Center Valley, PA). For quantification of cells with DJ-1 inclusions, images were captured with a 20x objective and all cells in the field were counted.

Table 3-1

Human DJ-1 Variant	Forward Oligonucleotide sequence	Reverse Oligonucleotide Sequence
L10P	5'-GCT CTG GTC ATC CCG GCT AAA GGA GCA GAG-3'	5'-CTC TGC TCC TTT AGC CGG GAT GAC CAG AGC-3'
L166P	5'-TTC GAG TTT GCG CCT GCA ATT GTT GAA-3'	5'-TTC AAC AAT TGC AGG CGC AAA CTC GAA-3'
P158DEL	5'-CTT ACA AGC CGG GGG GGG ACC AGC TTC GAG-3'	5'-CTC GAA GCT GGT CCC CCC CCG GCT TGT AAG-3'
HA-tagged WT	5'-AAG CTT GCC ACC ATG TAC CCA TAC GAT GTT CCA GAT TAC GCT ATG GCT TCC AAA AGA GCT CTG GTC ATC-3'	5'-CTC GAG CTA GTC TTT AAG AAC AAG-3'

3.6 ACKNOWLEDGEMENTS

This work was funded by grants from the National Institute on Aging (AG09215) and the National Institute of Neurological Disorders and Stroke (NS053488). C.P.R. is supported by a pre-doctoral NRSA fellowship (F31GM082026) from the National Institute on General Medicine Sciences. The content is solely the responsibility of the authors and does not necessarily represent the official views of the National Institutes of Health.

CHAPTER FOUR

DJ-1 DEFICIENT MICE DEMONSTRATE SIMILAR VULNERABILITY TO PATHOGENIC A53T HUMAN α-SYN TOXICITY

By

Chenere P. Ramsey[1], Elpida Tsika[2,4], Harry Ischiropoulos[1,2,3]

and Benoit I. Giasson [1]*

(published in *Human Molecular Genetics* in January of 2010)

From

[1]Department of Pharmacology, University of Pennsylvania School of Medicine, Philadelphia, Pennsylvania 19104. [2]The Children's Hospital of Philadelphia Research Institute and [3]Department of Pediatrics, The Children's Hospital of Philadelphia, Philadelphia, Pennsylvania 19104, and [4]Department of Molecular Biology and Genetics, Democritus University of Thrace, Alexandroupolis, Greece

*** Address correspondence to:**

Dr. Benoit I. Giasson, Department of Pharmacology, University of Pennsylvania School of Medicine, 125 John Morgan Building, 3620 Hamilton Walk, Philadelphia, PA 19104-6084. Tel: 215-573-6012; Fax: 215-573-2236; E-mail: giassonb@mail.med.upenn.edu.

Specific contributions:

-Performed immunohistochemical and double-labeling immunofluorescence analyses

- Performed Thioflavin-S staining

- Performed mouse protein analyses

- Conducted sequential biochemical fractionation experiments

-Assisted with mouse striatal tissue dissections for catechol quantification experiments

-Wrote the first draft of the manuscript and worked with Benoit Giasson to generate revised versions

4.1 ABSTRACT

PD is the most common neurodegenerative movement disorder. A pathological hallmark of PD is the presence of intraneuronal inclusions comprised of fibrillized α-syn in affected brain regions. Mutations in the gene, *PARK7*, which encodes DJ-1, can cause autosomal recessive early-onset PD. Although DJ-1 has been shown to be involved in diverse biological processes, several in vitro studies suggest that it can inhibit the formation and protect against the effects of α-syn aggregation. We previously established and characterized transgenic mice expressing pathogenic A53T human α-syn (M83 mice) that develop extensive α-syn pathologies in the neuroaxis resulting in severe motor impairments and eventual fatality. In the current study, we have crossbred M83 mice on a DJ-1 null background (M83-DJnull mice) in efforts to determine the effects of the lack of DJ-1 in these mice. Animals were assessed and compared for survival rate, distribution of α-syn inclusions, biochemical properties of α-syn protein, demise and function of nigral dopaminergic neurons, and extent of gliosis in the neuroaxis. M83 and M83-DJnull mice displayed a similar onset of disease and pathological changes, and none of the analyses to assess for changes in pathogenesis revealed any significant differences between M83 and M83-DJnull mice. These findings suggest that DJ-1 may not function to directly modulate α-syn nor does DJ-1 appear to play a role in protecting against the deleterious effects of expressing pathogenic A53T α-syn in vivo. It is possible that α-syn and DJ-1 mutations may lead to PD via independent mechanisms.

4.2 INTRODUCTION

In 1997, the seminal identification of a missense mutation (A53T) in α-syn in several kindred with PD (357) lead to subsequent studies showing that α-syn is a major component of several types of brain amyloidogenic pathological inclusions (133;320;405;464). For example, it is now established that Lewy bodies, characteristic neuronal inclusions of PD, are predominantly comprised of α-syn polymerized into 10-15 nm fibrils (133;320;464). The spectrum of neurodegenerative disorders with α-syn pathological inclusions are termed synucleinopathies (122;133;320;405;464). α-Syn is a 140 amino acid protein that is predominantly expressed in the brain and which localizes to presynaptic nerve terminals (76;133;320). The physiological role for α-syn is not fully understood, but several functions including the abilities to act as an auxiliary molecular chaperone and to play a role in maintaining synaptic nerve terminal integrity have been suggested (33;59;76;464). Although there is substantial evidence supporting the toxic nature of aberrant α-syn aggregation, mutations (missense or gene multiplication) in the *α-syn* gene *(SNCA)* provide the most direct evidence for a pathogenic role of α-syn (133;320;357;405;464).

PD is the most common neurodegenerative movement disorder (90;465). The clinical features of PD include bradykinesia, postural instability, resting tremor, and rigidity, which result from the progressive loss of dopaminergic neurons in the substantia nigra pars compacta (86;112;127;164;334), as well as a range of nonmotor symptoms (62;355). While for most patients the cause for PD is idiopathic, mutations in genes at multiple loci, designated *PARK1* through *PARK 13*, result in parkinsonian phenotypes with distinct features (32;80;124;213). DJ-1 was initially associated with PD

pathogenesis when homozygous recessive mutations in the *PARK7* gene encoding DJ-1 protein were identified in patients with early-onset PD (46). Since this initial report, various autosomal recessive mutations in DJ-1, including, missense, splice-site, frameshift and large deletions have been discovered (2;14;46;144;146;157;270) in 1-2% of PD patients with early to mid age of onset (144;154;263). DJ-1 mutations are thought to cause PD due to a loss of functional DJ-1 protein, though the natural role for DJ-1 as it relates to sporadic PD is not known (41;109;365;486). In addition, no autopsies have been performed on individuals with DJ-1 mutations; therefore, the exact neuropathological manifestations of disease in patients harboring DJ-1 mutations remains to be determined.

DJ-1 encodes a 189 amino acid protein which is a member of the ThiJ/PfPI superfamily based on its structure (170;248;313;469). It is expressed in both neurons and astrocytes in the brain (19;21;218;325;387), but it is also expressed in many other organs (121;324;489). DJ-1 has been shown to protect against a variety of insults including oxidation, inflammation, mitochondrial inhibition, and proteasome dysfunction (139;260;310;366;418;422;456;487;498). More specifically, in vitro studies have suggested that DJ-1 may act to directly prevent α-syn aggregation (389;494) and several groups have reported that DJ-1 can ameliorate the harmful effects of mutant α-syn *in vitro* and in cell culture studies (27;389;493). Interestingly, elevated levels of oxidized DJ-1 protein are present in the brains of patients with sporadic PD (65) and DJ-1 associates with inclusions in various other synucleinopathies (296;316). Thus, it is plausible to hypothesize that DJ-1 may physiologically act to protect against the formation or the harmful effects of aggregated α-syn.

We previously reported a transgenic mouse of synucleinopathies that was generated by expressing human A53T α-syn in the nervous system using the mouse prion protein (PrP) promoter (131). These mice developed an age-dependent severe movement disorder which is associated with abundant neuronal α-syn inclusions in the neuraxis and axonal degeneration (131). Since DJ-1 has been postulated to have several protective functions, including anti-α-syn aggregation properties, we sought to study the effects of the lack of DJ-1 in these mice. We hypothesize that the loss of DJ-1 may exacerbate the extent or promote the onset of disease in these mice, either by promoting α-syn aggregation or the consequences of α-syn inclusions. In the current study, transgenic mice homozygotically expressing human A53T α-syn ("M83 mice") were crossed with genetically altered null DJ-1 mice in order to generate homozygous A53T α-syn transgenic mice on a DJ-1 null background ("M83-DJnull mice"). M83-DJnull mice were analyzed and compared to M83 mice as it relates to survival rate, distribution of α-syn pathologies, biochemical properties of the α-syn protein, and extent of gliosis in the neuroaxis.

4.3 RESULTS

Generation of DJ-1 null mice

DJ-1 null mice were generated as described in detail in "Materials and Methods" in order to create a loss-of-function DJ-1 mouse model. The disruption of DJ-1 expression was demonstrated with several DJ-1 antibodies by western blot analysis of

total protein lysates that were extracted from the brain cortices of DJ-1 null, heterozygous (Het), and WT mice (**Fig. 4-1C**). The protein signal for DJ-1 in DJ-1 Het mice was ~0.6 fold the intensity compared to WT mice and was completely absent in samples from DJ-1 null mouse tissues. Similar results were obtained using other tissues including cerebellum, brainstem, spinal cord, liver and lung (data not shown). As reported by others for other DJ-1 null mice, extensive histological analyses did not demonstrate any evidence of degeneration in the nervous system (data not shown and see Fig. 3C) (13;60;63;136;274).

M83-DJnull mice display a similar motor phenotype and age of onset as M83 mice.

In attempts to understand the role for DJ-1 in modulating α-syn pathology in vivo, the previously established transgenic mouse line M83 expressing human A53T α-syn (131) was cross-bred with the DJ-1 deficient mouse line described above in order to generate mice homozygous for both the α-syn transgene and the DJ-1 null allele ("M83-DJnull" mice). The double homozygous transgenic genotype was confirmed as described in the "Materials and Methods" section. The lack of DJ-1 was confirmed by western blot analysis that also demonstrated that the deficiency of DJ-1 did not alter the expression levels of human α-syn (**Fig. 4-1D**). It is known that M83 mice exhibit a severe motor impairment with mid to late age of onset and which eventually results in fatality (131). To determine whether a DJ-1 deficiency would alter the disease motor phenotype and onset of disease, a cohort of M83-DJnull mice and M83 mice were housed in parallel. It was observed that the M83-DJnull mice presented symptoms of weight loss, neglect of

grooming, decreased mobility, paralysis, and eventual fatality, symptoms similar to those characterized for the M83 mice described

Figure 4-1

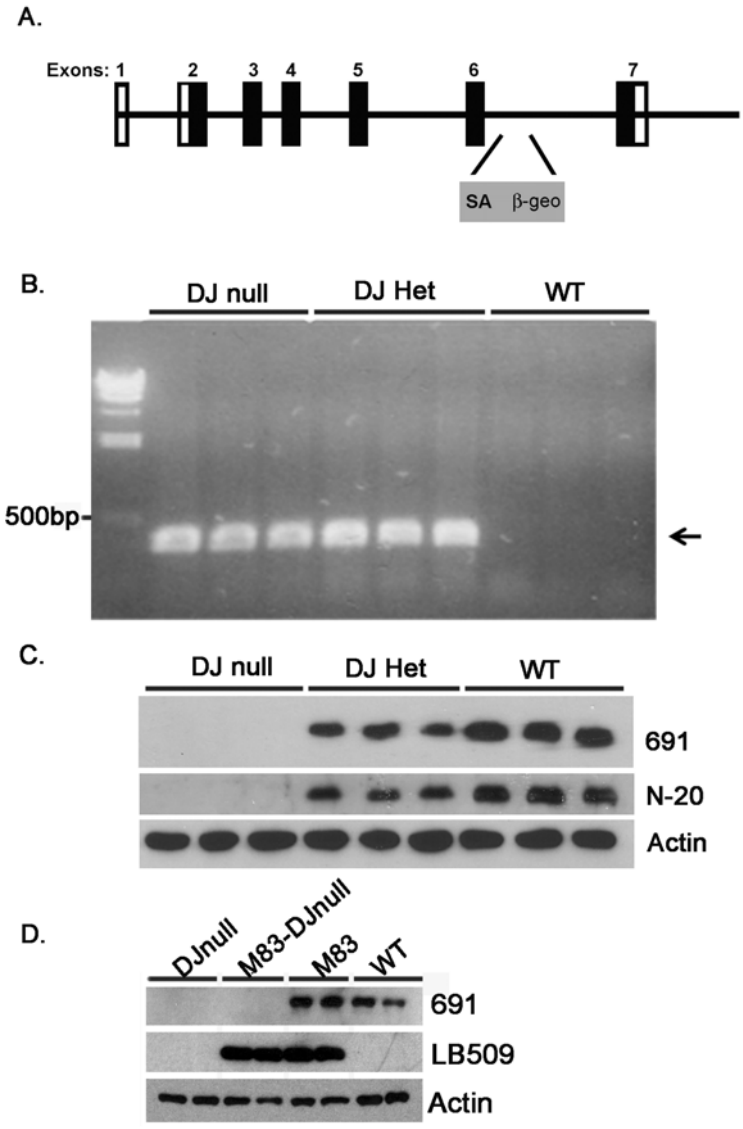

Generation of DJ-1 null mice. **A**) Schematic of the *DJ-1* gene (419) showing the inserting of the β-geo trap (gray box) in the intron between exon 6 and 7 resulting in disruption of the gene. The β-geo trap includes a splice acceptor (SA), a selectable marker β-Geo, which is a fusion of β-galactosidase and neomycin phosphotransferase II, followed by a stop codon and a polyadenylation signal. **B**) Image showing the analyses from 3 individual 6-month old DJ-1 null (DJ null), DJ-1 het (DJ het), and wild-type (WT) mice. Tail DNA was extracted and analyzed by PCR with primers specific for the neo gene. An agarose gel stained with ethidium bromide is shown. The arrow indicates the predicted PCR product for the neo cassette insert used to disrupt DJ-1 expression. **C**) Cerebral cortical tissues were harvested and total protein lysates were extracted. Equal amounts (12 ug) of protein extracts were loaded onto 13% polyacrylamide gels and analyzed by western blot analysis with the polyclonal anti-DJ-1 antibodies, 691 and N-20 as well as a monoclonal anti-actin antibody to confirm equal protein loading. Three samples were loaded, each from the same mice depicted in B. **D**) The brainstem and spinal cord tissues were harvested from 2 individual DJ-1 null (DJnull), M83-DJnull, M83, and WT mice and HS protein lysates were extracted. 4 ug of protein extracts were loaded onto 13% polyacrylamide gels and analyzed by immunoblot with antibody 691 to assess DJ-1 expression. Blots were also analyzed with the human specific monoclonal anti-α-syn antibody, LB509, as well as a monoclonal anti-actin antibody to assess protein loading.

previously (131). The severity of disease symptoms was comparable between M83-DJnull mice and M83 mice. Further, while the age range for the onset of disease in the M83-DJnull mice was 4-16 months of age (**Fig. 4-2**), this was not significantly different from the age of disease onset in M83 mice, which was 8-17 months of age. To confirm this observation, statistical analyses comparing the survival rates between mice revealed that the median age of disease onset for both mouse genotypes was 11 months of age.

Figure 4-2

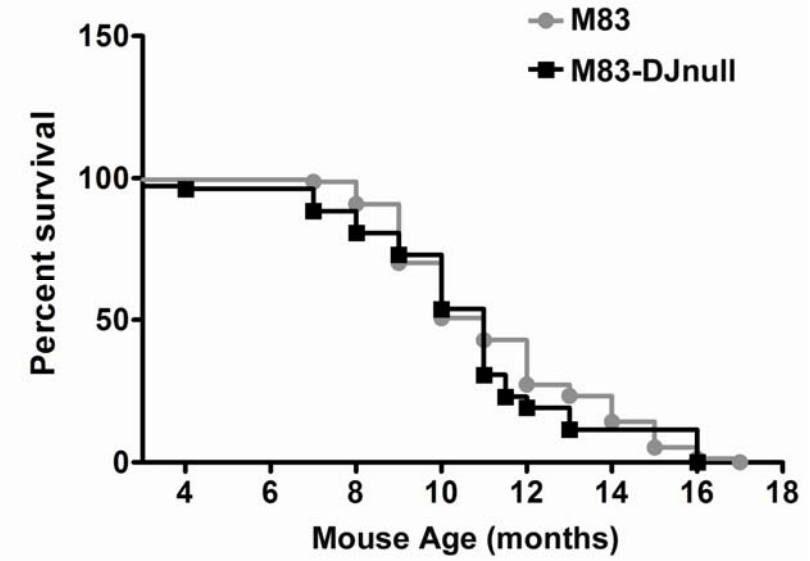

The lack DJ-1 does not affect the survival of M83-DJnull mice. The graph depicts the onset of motor phenotype in M83 mice (n=77) and M83-DJnull mice (n=26).

The distribution and extent of α-syn pathologies is similar between M83-DJnull and M83 mice.

Although M83-DJnull mice did not exhibit enhanced motor impairment or decreased survival rate in comparison to M83 mice, it is possible that DJ-1 deficient animals may display an altered distribution of α-syn inclusions, perhaps affecting areas of

the nervous system that were not previously observed in M83 mice. Certain neuronal populations, including the hippocampus, the olfactory bulb, dopaminergic neurons of the substantia nigra, and Purkinje cells of the cerebellum are completely devoid of α-syn inclusions in the M83 mouse (131). Thus, post mortem immunohistochemical and immunofluorescence analyses were conducted on brain and spinal cord tissues from sick M83-DJnull mice in order to assess the distribution of α-syn inclusions. These analyses revealed that affected M83-DJnull mice demonstrate the same distribution of somatodendritic α-syn neuronal inclusions and dystrophic α-syn neurites throughout the neuraxis as seen in M83 mice. A high density of inclusions was observed in the spinal cord, throughout the brainstem, the deep cerebellar nuclei, and some regions of the thalamus, such as the medioventral, ventromedial and paracentral nuclei (**Fig. 4-3A and data not shown**). In the cortex, α-syn inclusions were predominantly observed in the motor cortex. Conversely, regions that were devoid of pathology in M83 mice, such as the olfactory bulb, hippocampus, or Purkinje neurons were also spared of inclusions in M83-DJnull mice (**Fig. 4-3A and data not shown**). In representative images showing the similarities between the mouse genotypes, inclusions were immunoreactive with antibody Syn 514 which detects pathological α-syn (**Fig. 4-3A**). Ubiquitin, which is known to modify α-syn in the inclusions in M83 mice (131;376), also localized to most of the α-syn inclusions in M83-DJnull animals (**Fig. 4-3A**). It was previously shown that α-syn inclusions that are present in the diseased tissues of M83 mice are highly phosphorylated at Ser129 in α-syn (463). Similarly, the majority of the α-syn inclusions in M83-DJnull mice were immunoreactive for an antibody specific for this modification (**Fig. 4-3A**). Notably, while α-syn inclusions were present in a few of the tyrosine hydroxylase (TH)-

positive neurons of the locus coeruleus (**Fig. 4-3B**), none were present in the TH-positive neurons of the substantia nigra in M83-DJnull animals (**Fig. 4-3B**), a phenomenon which was also previously observed in M83 mice (131). Further, stereological analyses of the substantia nigra in WT, M83, DJ-1 null and M83-DJnull animals did not reveal any significant differences in the total number of dopaminergic neurons between mouse genotypes when animals were analyzed at 6 and 12 months of age (**Fig. 4-3C**). However, similar to M83 mice, a significant number of the α-syn inclusions in M83-DJnull mice were positive for the amyloid binding dye Thioflavin-S (**Fig. 4-3D**)(131).

Figure 4-3

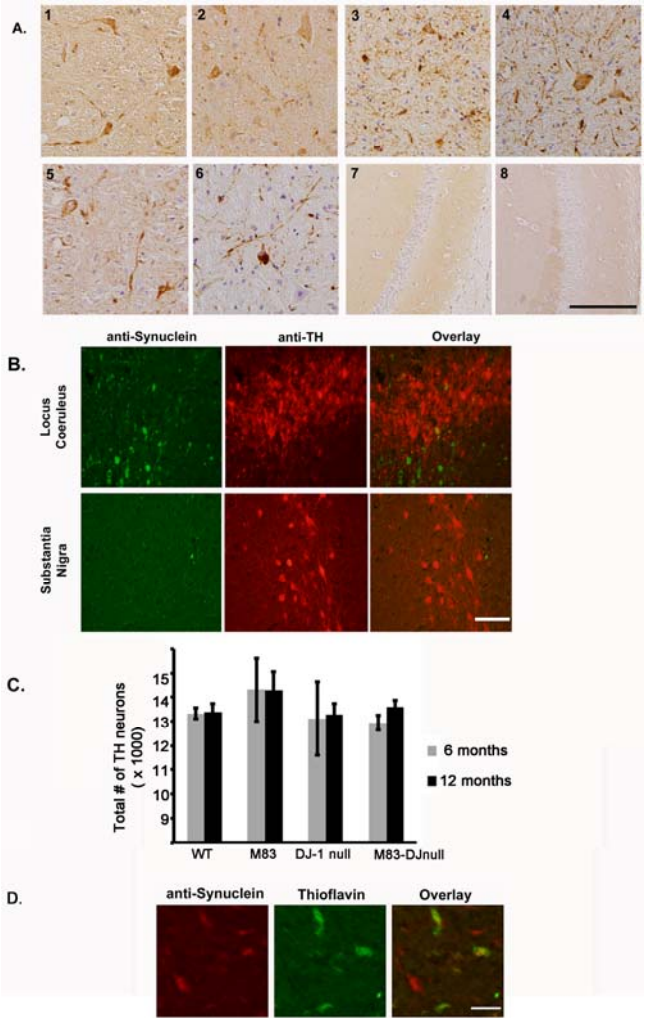

Neither the distribution of α-syn pathologies nor the numbers of TH positive neurons in substantia nigra are altered in M83-DJnull mice compared to M83 mice. **A**) Immunohistochemical analyses were performed as described in "Materials and Methods". M83 (1, 3, 5, and 7) and M83-DJnull tissues (2, 4, 6, and 8) were stained with the anti-ubiquitin antibody (1 and 2); anti-pSer129 antibody (3 and 4), or anti-α-syn antibody Syn 514 (5-8). The representative images depict the pons (1-6) and CA2 region of the hippocampus (7 and 8). **B**) Double immunofluorescence analysis of the locus coeruleus and substantia nigra from a 10 month old sick M83-DJnull mouse. Tissues were double labeled with anti-α-syn antibody Syn303 (green) and anti-TH (red). The overlay is shown on the right. **C**) Stereological analysis of TH positive neurons in substantia nigra of WT, M83, DJ-1 null, and M83-DJnull mice at ages 6 and 12 months. The graph represents the mean value of the total number of TH positive neurons for each mouse strains as indicated. The error bars indicate standard deviation (n=3). **D**) Spinal cord tissues were double labeled with antibody Syn303 (red) and Thioflavin S staining (green). The image shows amyloidogenic α-syn inclusions in a 12 month old diseased M83-DJnull mouse. The bar = 100μm in A and B and 10μm in C.

The α-syn in M83-DJnull mice does not display altered abundance or biochemical properties compared to M83 mice.

Previous studies of M83 mice revealed that the formation of α-syn inclusions is reflected by the accumulation of insoluble α-syn protein in the respective tissues analyzed (131). While M83-DJnull mice did not reveal histological differences in comparison to M83 mice, biochemical studies may reveal more subtle differences. Western blot analyses were performed using extracts from brain cortical, cerebellar, and brainstem/spinal cord (BS/SC) tissues which had been fractionated into buffers of increasing solubilization strengths. Analyses between age-matched sick M83-DJnull and M83 mice were compared. These analyses revealed that the abundance and biochemical distribution of human α-syn was similar between the M83-DJnull and M83 mice in all of the tissues analyzed. In the cerebral cortex, human α-syn was most abundantly extracted into the HS, HS-TX and RIPA fractions for both mouse genotypes (**Fig. 4-4A**). In the cerebellum of M83 and M83-DJnull mice, α-syn was distributed in a similar manner (**Fig.4-4B**). However, α-syn exhibited slightly reduced solubility into SDS fractions in cerebellar tissues of some of the mice analyzed (**Fig. 4-4B**). This observation was not due to a DJ-1 deficiency, however, since it was variable from mouse to mouse, irrespective of genotype (data not shown). In the BS/SC regions of affected M83 and M83-DJnull mice, biochemical analysis revealed a similar accumulation of RIPA-insoluble/SDS-soluble human α-syn (**Fig. 4-4C**). Additionally, while there were no differences in the abundance or extractability of the α-syn present in the BS/SC tissues of the predicted ~17 kDa size, when comparing between M83 and M83-DJnull mice, several insoluble, higher molecular weight α-syn species were detected on some immunoblots (**Fig. 4-4C**). These species

were previously shown to represent ubiquitinated forms of α-syn (376). However, this phenomenon was not due to a DJ-1 deficiency since it was variable and independent of DJ-1 expression (data not shown)(376).

M83-DJnull mice do not display increased levels of Ser 129 specific α-syn phosphorylation.

In a previous report, diseased M83 mice exhibited increased levels of insoluble α-syn protein which was highly phosphorylated specifically at amino acid residue Ser129 (463). To determine whether a DJ-1 deficiency could alter the levels of the Ser129-specific phosphorylation of α-syn in brain cortical, cerebellar, and BS/SC tissue extracts from age-matched diseased M83 and M83-DJnull mice were compared by western blot analysis with the antibody pSer129. α-Syn that was extracted from BS/SC tissues from M83-DJnull mice was highly phosphorylated in the SDS-soluble fraction but barely detectable in the HS, HS-TX, or RIPA fractions in all of the mice analyzed (**Fig. 4-4C**). However, there were no differences between M83 and M83-DJnull mice when the levels of phosphorylated α-syn were compared.

Figure 4-4

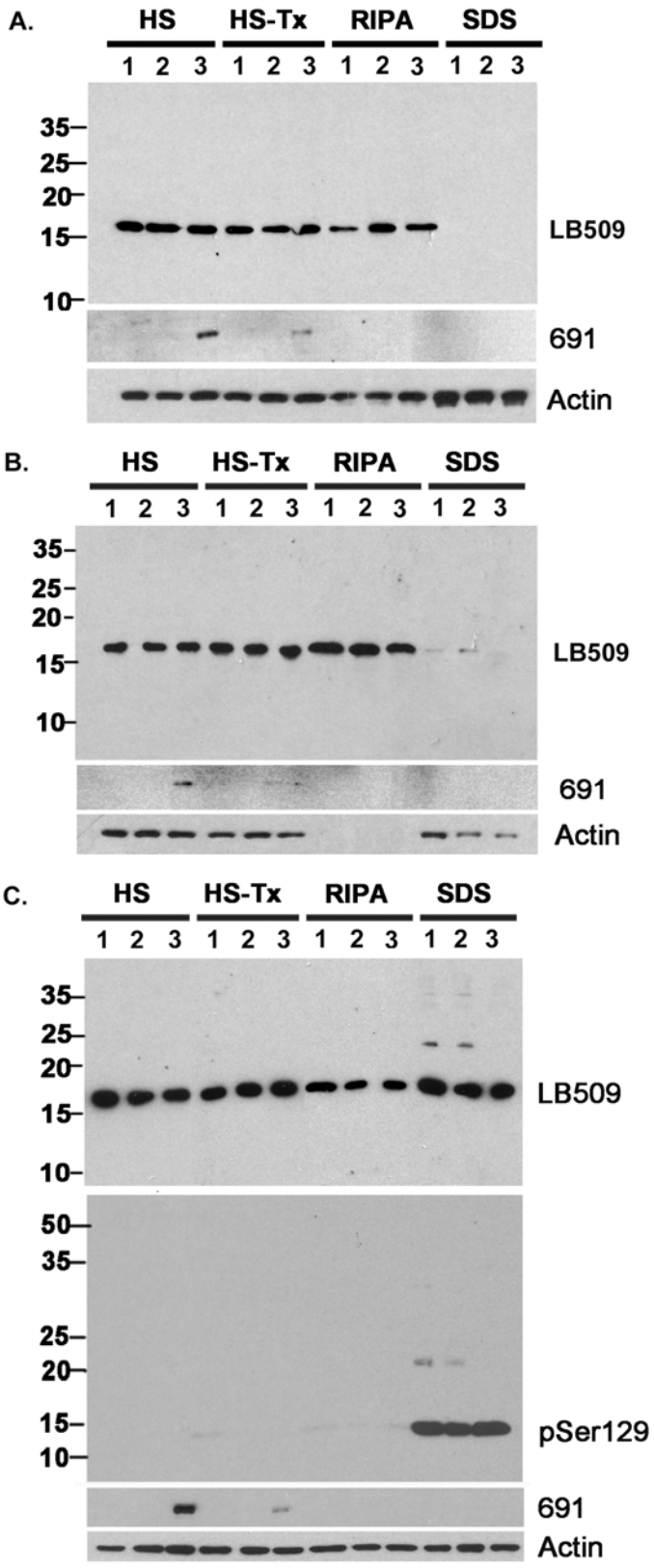

The paucity of DJ-1 does not affect the levels or biochemical distribution of α-syn nor does it affect Ser 129 specific α-syn phosphorylation. Age-matched (10 month old) diseased M83-DJnull ("1" and "2") and M83 ("3") mice were analyzed for the abundance and solubility of α-syn protein. The levels of Ser 129 specific α-syn phosphorylation were also compared between mice. The brain cortex (**A**), cerebellum (**B**) and BS/SC (**C**) were harvested and sequentially extracted into HS extraction solution, HS-Tx extraction solution, RIPA extraction solution, and 2% SDS/8M urea extraction solution (SDS). Equal amounts (5ug) of each sample were loaded onto 15% polyacrylamide gels and analyzed for α-syn distribution by western blot analysis with the monoclonal human specific α-syn antibody, LB509 (in **A**-**C**). Ser 129 specific α-syn phosphorylation in the BS/SC was assessed with the monoclonal antibody, pSer129 (in **C**). Additionally, blots were probed with antibody 691 to assess DJ-1 and an actin antibody to confirm equal protein loading. The mobility of molecular mass markers is indicated on the left.

M83-DJnull mice do not show increased gliosis.

It is well known that reactive gliosis can follow brain tissue damage and is typically accompanied by inflammation (123). A recent study by Waak et al. showed that the disruption of DJ-1 expression in astrocytes resulted in enhanced neurotoxcity which was due to an elevated neuroinflammatory response (456). Diseased M83 mice exhibit astrocytic gliosis in the brain regions where α-syn inclusions are the most abundant (131). It is possible that a DJ-1 deficiency in M83-DJnull mice would result in an aberrant inflammatory response in these animals. To test this hypothesis, M83 and M83-DJnull mouse brain tissues were evaluated by immunohistochemistry analysis with the reactive microglial antibody marker, IBA-1 as well as the astrocyte marker, GFAP. The distributions of the microglia and astrocytes present in the mouse tissues were compared. While these analyses revealed that reactive microglia were primarily localized to the brainstem and spinal cord tissue regions, the distribution and abundance of microglia was similar in M83 and M83-DJnull mouse tissues (**Fig. 4-5A and data not shown**). Astrogliosis also was observed in areas of the neuroaxis such as the brainstem and spinal cord where abundant α-syn pathological inclusions were present; however, the prevalence was similar in M83 and M83-DJnull mice (**Fig. 4-5A and data not shown**). This observation was further confirmed by biochemical fractionation/western blot analysis for IBA-1 (**Fig. 4-5B**) and GFAP (**Fig. 4-5C**).

Figure 4-5

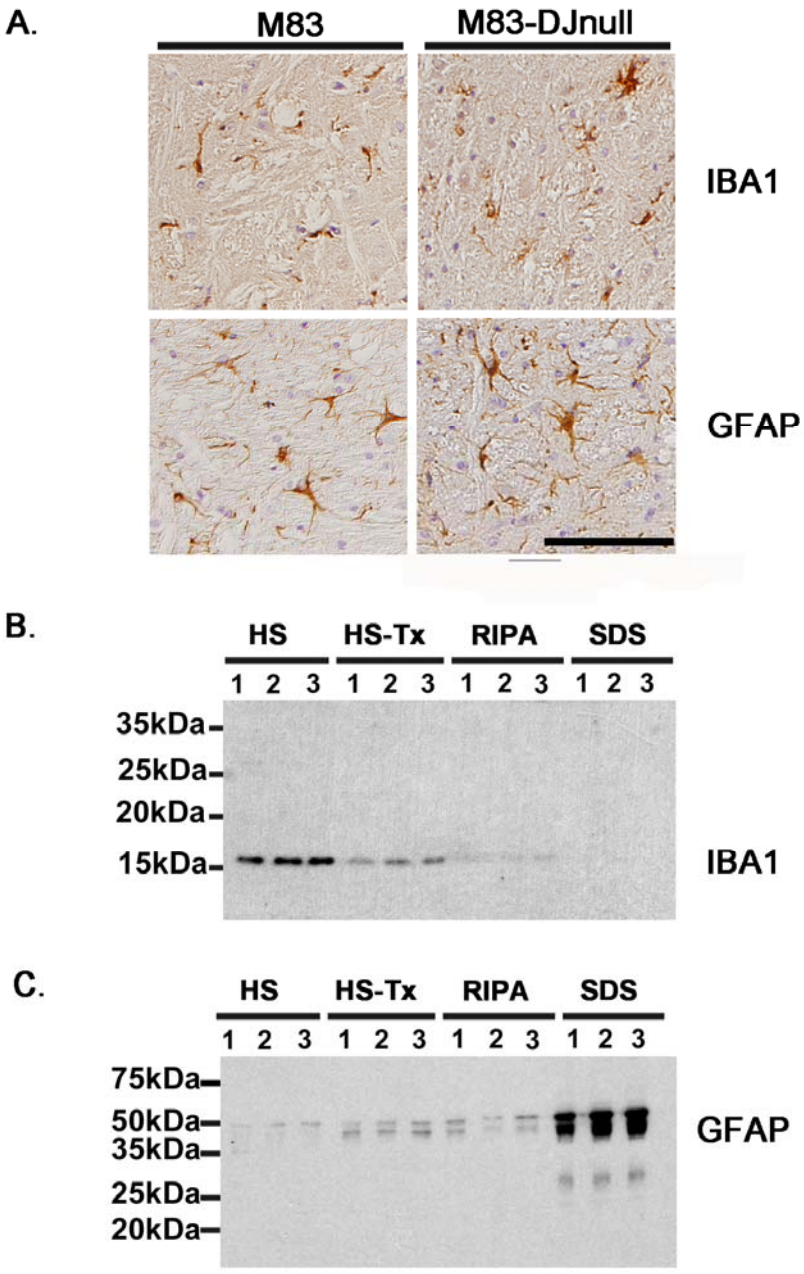

Gliosis in M83-DJnull mice does not differ from M83 mice.
A) Immunohistochemical analyses were performed using brain tissues harvested from diseased M83 and M83-DJnull mice. The distribution of microglia was assessed between mice using the polyclonal antibody, IBA1, which is specific for reactive microglia. Analyses to determine the presence of astrocytes were conducted using the polyclonal antibody, GFAP. The representative images show staining in the pons. The scale bar = 100µm. In **B**) and **C**), age-matched diseased M83-DJnull ("1" and "2") and M83 ("3") mice were analyzed biochemically for changes in gliosis. The representative images show the analyses from 10 month old mice. Brainstem and spinal cord tissues were harvested, pooled together and sequentially extracted as described in "Materials and Methods". Equal amounts (5ug) of each sample were loaded onto 13% polyacrylamide gels and analyzed by western blot analysis with antibody IBA1 in **B**) and antibody GFAP in **C**). In **B**) and **C**), the mobility of molecular mass markers is indicated on the left.

M83-DJnull mice do not have elevated levels of Peroxiredoxin 6.

During the course of previous proteomics analysis, we discovered that affected M83 mice display increased levels of peroxiredoxin (Prx) 6 that is substantiated by western blot analysis (**Fig. 4-6A**) and this may reflect an attempt to activate a protective mechanism. In addition, DJ-1 is thought to be able to act as an atypical Prx-like peroxidase (13) and to protect against oxidative insults (13;53;181;196;253;366;455;493). It is possible that the disruption of DJ-1 expression may induce further reactive stress in M83-DJnull mice. Therefore, the effect of the paucity of DJ-1 on the levels of Prx6 induced by α-syn pathology was assessed. However, no major differences between M83 and M83-DJnull mice were detected as it related to the extent of Prx6 expression or biochemical distribution.

M83-DJnull mice do not exhibit changes in the levels of dopamine or its metabolites.

Since some studies suggest that DJ-1 and α-syn may modulate TH and L-3,4-dihydroxyphenylalanine (L-DOPA) decarboxylase enzyme activities (185), it is possible that M83-DJnull mice could display altered levels of dopamine (DA) and its metabolites. To test this hypothesis, striatum tissues were dissected from WT, M83, DJ-1 null, and M83-DJnull mice at 6 and 12 months of age. Tissues were analyzed by high performance liquid chromatography-electrochemical detection (HPLC-ECD) to quantify and compare the total levels of L-DOPA, DA, and 3,4-dihydoxyphenylacetic acid (DOPAC) between mouse genotypes. However, there were no significant differences between animals for either of the age groups analyzed (**Fig. 4-7**), indicating normal dopamine-related biochemical activities in M83-DJnull mice.

Figure 4-6

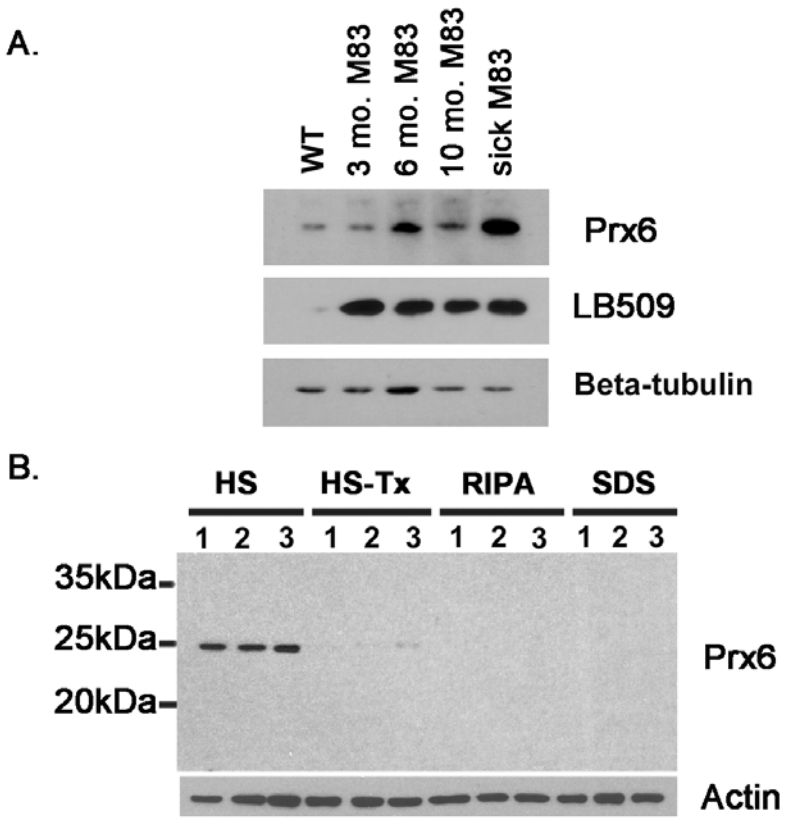

M83-DJnull mice do not have elevated levels of Prx 6 relative to M83 mice. **A)** The representative immunoblots were performed with HS-soluble extracts from brainstem and spinal tissues that were harvested from a WT non-transgenic mouse, M83 mice that were sacrificed before the manifestation of a motor phenotype at 3 months, 6 months, and 10 months of age, as well as a diseased M83 mouse. Equal amounts (10 ug) of protein extracts were loaded onto 15% polyacrylamide gels and analyzed by western blot analysis with antibody anti-Prx6 to assess the levels of Prx 6 in the mice. Blots were also probed with the human specific α-syn antibody, LB509 to verify the expression of human α-syn protein as well as a β-tubulin antibody to assess protein loading. **B)** Age-matched diseased M83-DJnull ("1" and "2") and M83 ("3") mice were analyzed for the levels of Prx 6. Brainstem and spinal cord tissues were harvested, pooled together and sequentially extracted as described in "Material and Methods". Equal amounts (5ug) of each sample were loaded onto 13% polyacrylamide gels and analyzed by western blot for Prx6 as well as actin. The representative images show the analyses from 10 month old mice. The mobility of molecular mass markers is indicated on the left.

4.4 DISCUSSION

Some in vitro studies and cell culture paradigms indicate that DJ-1 may be able to modulate the aggregation of α-syn and/or act to mitigate the toxicity of pathogenic forms of α-syn (27;389;493;494). However, these properties of DJ-1 have not been directly assessed in vivo. M83 transgenic mice are previously described animals that express human A53T α-syn and developed a severe age-dependent motor phenotype

Figure 4-7

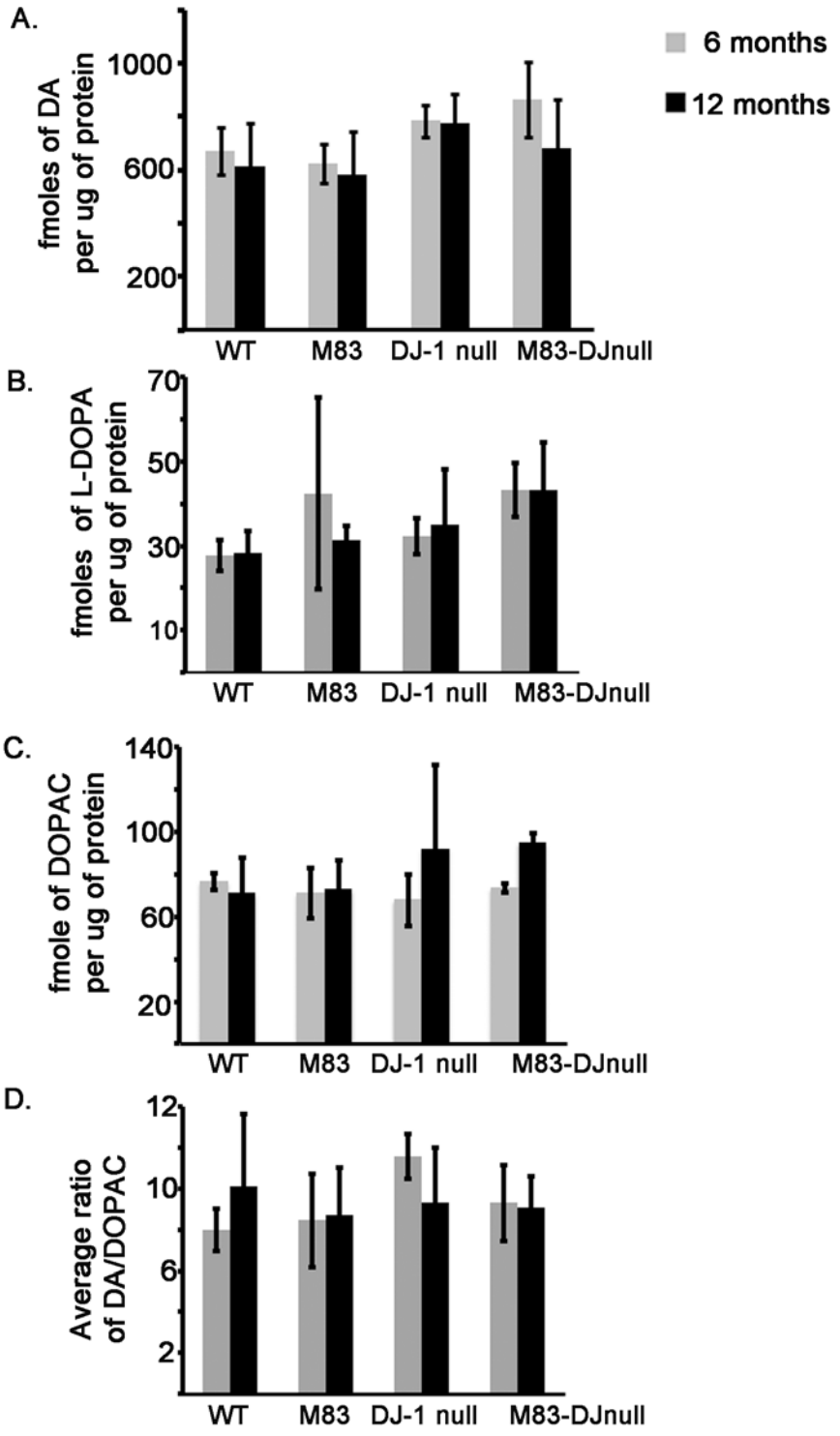

Unaltered levels of DA in the striatum of M83-DJnull animals. Striatal tissues were dissected from WT, M83, DJ-1 null, and M83-DJnull mice at ages 6 months and 12 months. Tissues were analyzed by HPLC to quantify DA in (**A**), L-DOPA in (**B**), and DOPAC in (**C**). The graphs in **A-C** depict the mean of the levels of the respective analytes for each of the indicated mouse strains at the respective ages. **D**) The ratio of DA/DOPAC was calculated. In **A-D**, errors bars indicate standard deviation (n=3 for 6 month animals and n=5 for 12 month animals).

associated with the formation of α-syn pathological inclusions in the neuroaxis (131). These inclusions were demonstrated to be composed of fibrillized aggregates of insoluble α-syn protein with a high abundance in the brainstem and spinal cord while inclusions were absent in some regions such as the olfactory bulb, hippocampus, and dopaminergic neurons of the substantia nigra (131). In the current study, in efforts to ascertain whether DJ-1 modulates α-syn aggregation and pathology in vivo, double homozygous M83-DJnull transgenic mice were generated which express human A53T α-syn on a DJ-1 null background. If DJ-1 normally acts to mitigate α-syn aggregation or has protective functions against the deleterious effects of α-syn aggregation, it was hypothesized that the DJ-1 deficient M83-DJnull mice would exhibit an exacerbated phenotype in comparison to that observed in M83 mice. Statistical analyses comparing the survival rates revealed that the disease onset was not earlier in M83-DJnull mice compared to M83 mice. The median age of survival for both groups of animals was 11 months of age. This suggested that DJ-1 may not play a major role in ameliorating the harmful effects of expressing A53T mutant α-syn in vivo. However, to further assess the differences between these mice, several analyses were conducted. Nevertheless, no major differences between M83 and M83-DJnull mice were observed in any of the analyses that were performed. Immunohistochemical analyses comparing the distributions of α-syn pathologies throughout the neuroaxis failed to detect any overt variations between M83 and M83-DJnull mice. Both mouse groups consistently exhibited abundant pathologies in the same tissue regions while the absence of inclusions in other areas was remarkably similar between mice. These analyses also revealed that most of the inclusions in diseased M83-DJnull animals were composed of ubiquitinated, fibrillized α-syn protein that was highly

phosphorylated at amino acid residue Ser129 similar to inclusions in diseased M83 mice (131;463) and in patients (117;150;232;404;463). The formation of inclusions in M83 and M83-DJnull mice was further validated by biochemical and western blot analyses to assess the soluble extractability. However, the studies herein did not reveal any changes relating to α-syn aggregation in M83-DJnull animals. In addition, these studies did not reveal any differences in the levels of the phosphorylation of Ser129. Thus, these findings suggest that DJ-1 does not directly alter α-syn in vivo as it relates to protein fibrillization, phosphorylation, or aggregation. Neither does DJ-1 appear to directly modulate the expression of mutant α-syn since similar levels of the mutant protein were observed between mice in the brain regions analyzed.

While the present study suggests that DJ-1 does not act to directly regulate A53T mutant α-syn in vivo, it is possible that DJ-1 can mitigate secondary deleterious effects of α-syn aggregation in mice such as inflammation and oxidative stress. It was previously established that M83 mice exhibited astrocytic gliosis associated with the formation of α-syn inclusions (131). Additionally, recent studies using a primary neuron and astrocyte co-cultured model reveal that a DJ-1 deficiency is causal of an enhanced neuroinflammatory response that results in increased neurotoxicity (456). To determine whether DJ-1 modulates the gliosis associated with α-syn aggregation in vivo, diseased M83 and M83-DJnull mice were analyzed by immunohistochemistry with astrocyte specific and reactive microglia specific markers. However, these analyses did not reveal any differences between mouse types relating to the distribution and/or extent of gliosis. Additionally, the biochemical and immunoblot assessments of protein extracts from M83

and M83-DJnull mouse tissues also did not identify any differences. Thus, since gliosis was independent of DJ-1 expression, DJ-1 may not act to regulate gliosis in M83 mice.

Since DJ-1 and α-syn may regulate TH promoter activation and have an effect on TH enzyme activity (189), it was relevant to assess for the levels of striatal DA in M83-DJnull mice in comparison to WT, DJ-1 null, and M83 animals. However, no differences were revealed for any of the genotypes when mice were analyzed for the levels of L-DOPA, DA, or DOPAC. This supports previous findings in the literature which report normal DA levels and its metabolites in DJ-1 null animals (136). Further, in the studies herein, stereological analyses revealed no change in the number of nigral dopaminergic neurons in both a young and old cohort of M83-DJnull mice. Our finding is also in agreement with other reports which do not detect degeneration of these neurons in DJ-1 null mice (136).

In a variety of model systems, the expression of mutant A53T α-syn has been shown to result in increased levels of oxidative stress (191;197;339).While DJ-1 has been shown to be involved in diverse biological processes, several studies demonstrate its ability to mitigate the toxic effects of aberrant oxidation (13;53;181;200;253;366;455;493). In addition, in some studies DJ-1 was reported to be able to act as an atypical Prx-like peroxidase (13). The current study demonstrated that when compared to WT mice and healthy M83 mice, sick M83 animals exhibited increased steady-state expression of Prx6. This phenomenon specifically occurred in the BS/SC tissues of M83 mice where α-syn pathologies were most abundant. Comparatively, no alterations in Prx6 were observed in the cortex in diseased M83

animals (data not shown). This suggests that the increased levels of Prx6 observed in sick M83 mouse BS/SC tissues may be a protective attempt against α-syn aggregation. It is known that Prx6 levels are increased in PD and that this increase is associated with the recruitment of Prx6 to Lewy body inclusions (360). Additionally, since Prx6 has been shown to be up-regulated in response to oxidation (69), it could imply that α-syn inclusion formation is accompanied by increased oxidative stress in sick M83 mice. To determine whether these observed alterations in Prx6 were modulated by DJ-1 in vivo, BS/SC tissues from sick M83 and M83-DJnull mice were analyzed by western blot analysis and compared for immunoreactivity with the Prx6 antibody. However, these analyses revealed that diseased M83 and M83-DJnull mice expressed Prx6 at similar levels.

Herein, a loss-of-function DJ-1 mouse model was employed in attempts to ascertain the role for DJ-1 in mitigating mutant α-syn in vivo. Many groups have utilized DJ-1 deficient animals in efforts to define a physiological role for DJ-1 protein in vivo as it relates to PD (13;60;136;204;274;354;480;483). However, while DJ-1 null animals have been shown to exhibit mild behavioral changes, these were not associated with any observed degeneration in the nervous system (13;60;63;136;480). Neither have DJ-1 null mice exhibited increased signs of oxidative stress (63;480). A few studies have shown that DJ-1 deficient animals are more vulnerable to paraquat (483), MPTP (204;274), and rotenone toxicity (354), suggesting a role for DJ-1 in protecting against oxidative stress and mitochondrial impairments.

In the present study, DJ-1 deficient animals were not more vulnerable to the toxic effects of mutant A53T α-syn. These studies suggest that DJ-1 may not have a significant role in mitigating the formation of α-syn inclusions and their deleterious effects in vivo. Alternatively, there may be compensatory mechanisms in the mouse which act to mimic the function of the lost DJ-1 protein. For example, recent studies by other groups suggest a possible genetic interaction between DJ-1 and other PD related genes, PINK1 and parkin (449;477). It is of interest to note that in the current study, no alterations in the steady-state levels of parkin protein were observed in the brains of M83 and M83-DJnull mice when they were analyzed by western blot (data not shown). Neither did PINK1 protein levels appear to be modulated by DJ-1 in the mice analyzed (data not shown). Further, triple knockout mice that are deficient for DJ-1, parkin, and PINK1 do not have decreased life spans nor do they exhibit phenotypes that are comparable to any of the symptoms of PD (211). It is possible that yet unidentified candidate genes may be acting to compensate for the loss of DJ-1 in vivo. Identifying such candidate genes would give new insights into plausible biochemical mechanisms that underlie the pathogenesis of PD.

4.5 MATERIALS AND METHODS

Antibodies

Anti-IBA1 is a rabbit polyclonal antibody raised against ionized calcium-binding adaptor molecule 1 (Iba1), a marker for activated microglial cells (Wako Chemicals USA, Inc., Richmond, VA). Anti-glial fibrillary acidic protein **(**GFAP) is a rabbit polyclonal antibody against glial fibrillary acidic protein, a specific marker for astrocytes (Promega

Corporation, Madison, WI). LB509 is a mouse monoclonal antibody that specifically reacts with human α-syn (18;132). Syn 303 and 514 are monoclonal antibodies raised against oxidized forms of human α-syn and that preferentially recognize pathological forms of the protein (130;462). pSer129 is a monoclonal antibody that specifically recognizes α-syn that is phosphorylated at the Ser129 (463). Anti-ubiquitin (clone 1510) is a mouse monoclonal antibody that reacts with conjugated and unconjugated forms of ubiquitin (Millipore, Billerica, MA). Anti-actin (clone C4) is an affinity purified monoclonal antibody that reacts with all vertebrate isoforms of actin (Millipore). Anti-TH antibody (Millipore) is an affinity purified rabbit polyclonal antibody. An affinity purified rabbit polyclonal antibody raised against a synthetic peptide corresponding to amino acid residues 196-210 of human Prx6 was obtained from Sigma-Aldrich (Saint Louis, MO). 691 is a rabbit polyclonal antibody raised against recombinant human DJ-1 protein but that reacts with DJ-1 from various species (296). DJ-1 (N-20) is an affinity purified goat polyclonal antibody raised against a peptide corresponding to the N-terminus of human DJ-1 (Santa Cruz Biotechnology, Inc., Santa Cruz, CA). Anti-β-tubulin (clone TUB2.1) is a monoclonal antibody raised against β-Tubulin (Sigma). Goat anti-mouse IgG Alexa Fluor 488 conjugated antibody and goat anti-rabbit or anti-mouse IgG Alexa Fluor 594 conjugated antibodies were purchased from Molecular Probes (Eugene, OR).

Generation of DJ-1 null mice

Murine embryonic stem (ES) cells (clone XE726) with a recombination resulting in the disruption of the *DJ-1* gene were obtained from BayGenomics (San Francisco, CA). This cell line was generated by random exon trapping and it was determined by DNA

sequencing that the recombination event occurred after exon 6 in the murine DJ-1 gene (see Fig. 1A). These ES cells were injected into C57BL/6J blastocysts as a service of the University of Pennsylvania Transgenic and Chimeric Mouse Facility and chimeric mice were generated. The germ line transmission of the null-gene was determined by breeding chimeras with C57BL/6J mice and PCR analyses of tail DNA with primers specific for the neomycin gene. Mice homozygous for the null-allele were generated by crossing F1 mice, and homozygous null mice were determined by PCR analyses of tail DNA and western blot analysis of mouse tail protein samples (dissolved in 4%SDS, 8M urea) using an antibody to DJ-1.

Generation of M83-DJnull mice

The previously established homozygous transgenic mice line M83 expressing A53T human α-syn (131), was bred with the homozygous DJ-1 null mouse line described in the previous section. The double heterozygous offspring were mated to generate double homozygous transgenic mice. Mouse genotypes were confirmed by Southern blot analysis of tail genomic DNA with a probe for human α-syn. Homozygous α-syn transgenic lineages were identified by quantitative Southern blot analysis and verified by backcrossing. Null DJ-1 homozygosity was determined by PCR against the neo gene and western blot analysis of mouse tail protein samples as described in the previous section. In some mice, immunoblotting of brain tissue extracts with 691 and LB509 antibodies were used to confirm the loss of DJ-1 protein and the expression of human pathogenic α-syn protein respectively. Mice were sacrificed by CO_2 euthanization as approved by the University of Pennsylvania Institutional Animal Care and Use Committee.

Immunohistochemical Analysis

Mice were sacrificed with CO_2 euthanization and perfused with PBS/heparin, followed by perfusion with either 70% ethanol/150mM NaCl or PBS buffered formalin. The brain and spinal cord were then removed and fixed for 24 hours in the respective fixatives used for perfusion. As previously described tissues were dehydrated at room temperature through a series of ethanol solutions, followed by xylene and then were infiltrated with paraffin at 60ºC (434). The tissues were then embedded into paraffin blocks which were then cut into 6μm sections. Immunostaining of the sections was then performed using previously described methods (102).

Double-Labeling Immunofluorescence Analysis

Paraffin-embedded tissue sections were deparaffinized and hydrated through a series of graded ethanol solutions followed by 0.1M Tris, pH 7.6. The sections were incubated simultaneously with the Syn 303 and anti-TH primary antibodies diluted in 5% dry milk/0.1M Tris, pH 7.6. After extensive washing, sections were incubated with goat anti-mouse secondary conjugated to Alexa 488 and goat anti-rabbit secondary conjugated to Alexa 594. After washing, the sections were coverslipped with VectaShield-DAPI mounting medium (Vector Laboratories, Burlingame, CA) and visualized using an Olympus BX51 microscope.

Unbiased Stereological Determination of Dopaminergic Neurons in the Substantia Nigra

The number of anti-TH immunoreactive neurons in the entire substantia nigra was assessed for WT, M83, DJ-1 null, and M83-DJnull mice at ages 6 months and 12 months using similar methods described by Kitada et al. (211) with a few exceptions. Brains were fixed in 70% ethanol/150mM NaCl and sectioned at 10μm thickness. Every fifth section was stained with anti-TH polyclonal antibody (Millipore). Three brains were analyzed for each of the indicated mouse strains at each of the respective ages.

Thioflavin-S Staining

Paraffin-embedded tissue sections were incubated with antibody Syn303 followed by anti-mouse conjugated Alexa Fluor 594 as described above. Sections were stained with thioflavin-S by immersing in freshly made 0.0125% thioflavin-S/40%EtOH/60% PBS and differentiated in 50% EtOH/50% PBS. The sections were coverslipped and visualized as described above.

Mouse Protein Analysis

Cerebral cortical tissues were harvested from 6 month old DJ-1 null, DJ-1 Het, and WT mice. Tissues were sonicated in 3 tissue volumes of 2% SDS/8M urea. Total protein extracts were then quantified using the bicinchoninic acid (BCA) assay (Pierce Biotechnology, Rockford, IL) and bovine serum albumin as the standard. Equal amounts of protein extracts were resolved by SDS-PAGE and analyzed by western blot.

Sequential Biochemical Fractionation

The cortex, cerebellum, brainstem and spinal cord were dissected from mice. For each mouse, the brainstem and spinal cord were pooled together and then all tissues were

weighed and homogenized with a pellet pestle motor in 3 tissue volumes of high-salt (HS) buffer (50 mM Tris [pH 7.5], 750 mM NaCl, 5 mM EDTA, with a protease inhibitor cocktail at 1:1000 and PMSF at 1:500, and the phosphatase inhibitors, 20 uM NaF, 1 uM $NaVO_4$, and 1 uM okadaic acid) followed by sedimentation at 100,000 x g for 20 minutes. Supernatants were saved as the HS fraction. Pellets were homogenized in 3 tissues volumes of high salt-triton (HS-TX) buffer (HS buffer with 1% Triton X-100) and sedimented at 100,000 x g for 20 minutes. The supernatants were saved as the HS-TX fraction. The pellets were subjected to a sucrose myelin float by homogenizing in 3 pellet volumes of sucrose buffer (HS buffer/1M sucrose) and after centrifugation, the myelin-rich supernatants were discarded. Pellets were then homogenized in 2 tissue volumes of radioimmunoprecipitation assay buffer (RIPA) buffer (50 mM Tris [pH 8.0], 150 mM NaCl, 5 mM EDTA, 1% NP40, 0.5% sodium deoxycholate, and 0.1% SDS with the protease and phosphatase inhibitors), sedimented at 100,000 x g for 20 minutes, and the supernatants were saved as the RIPA fraction. Pellets were then sonicated in 1 pellet volume of 2% SDS/8M urea and were designated to be the SDS fractions. The fractions were then quantified using the BCA assay, resolved by SDS-PAGE, and analyzed by immunoblot as previously described above.

Catechol Quantification by HPLC with Electrochemical Detection (ECD)

Striatal catecholamine content was assessed in WT, M83, DJ-1 null, and M83-DJnull mice. Mice were analyzed at 6 months and 12 months of age. In order to isolate the striatum, the brains were submerged into ice-cold phosphate buffer and dissected into 1 mm-thick coronal sections using a vibratome (Series 1000, R.L. Slaughter, Essex, UK).

Dissected tissues were weighed and homogenized by sonication in 10 volumes of 1 μM 3,4 dihydroxybenzylamine (DHBA) in 0.1M perchloric acid. Following centrifugation at 16,000 × g for 10min at 4^{o}C, 20μl of the supernatants were injected onto an 1100 series Agilent HPLC system controlled by Chemstation software (Agilent, Palo Alto, CA). The mobile phase consisted of 72 mM citric acid, 28.4 mM sodium phosphate, 2% methanol, pH 2.8. Catechols were resolved at a flow rate of 1 mL/min on a reverse-phase C18 Luna column (150 X 4.6 mm, 5um; Phenomenex, Torrance, CA) and detected with a Coularray detector (ESA Biosciences, Chemsford, MA) with the following working potentials (in mV): -200, +50, +300 and +400. Chemstation software (version 1.04, ESA Biosciences) was used for the quantification by comparing to the peak areas of known concentrations of standards. Acid-precipitated protein pellets were extracted in 2% SDS / 50mM Tris-Cl, pH 7.4 and the protein concentrations were determined using the microBCA kit (Peirce, Rockford, IL). Analyte levels were normalized to DHBA and protein concentration.

4.6 ACKNOWLEDGEMENTS

This work was supported by the National Institute on Aging [AG09215] and the National Institute of Neurological Disorders and Stroke [NS053488]. C.P. Ramsey is supported by a pre-doctoral NRSA fellowship from the National Institute on General Medicine Sciences [GM082026]. We would like to thank Dr. Thomas Chou for his help in the proteomics studies of α-syn transgenic mice.

CHAPTER FIVE

IDENTIFICATION AND CHARACTERIZATION OF A NOVEL ENDOGENOUS MURINE PARKIN MUTATION

BY

Chenere P. Ramsey[#] and Benoit I. Giasson [#]*

(published in the *Journal of Neurochemistry* in January of 2010)

From

Department of Pharmacology[#], University of Pennsylvania School of Medicine, Philadelphia, Pennsylvania 19104.

Address correspondence to: Dr. Benoit I. Giasson, Department of Pharmacology, University of Pennsylvania School of Medicine, 125 John Morgan Building, 3620 Hamilton Walk, Philadelphia, PA 19104-6084. Tel: 215-573-6012; Fax: 215-573-2236; E-mail: giassonb@mail.med.upenn.edu.

Running title: Characterization of a Novel Murine Parkin Mutation

Specific contributions:

-Generated pDEST15 [1-465, 1-420, 1-408, 1-399, 221-465, 381-465, and 399-465] parkin constructs for parkin antibodies epitope mapping

-Generated pDEST15 E399Q parkin construct for bacterial expression

-Generated pcDNA3.1 E399Q and T240R parkin constructs for mammalian expression

-Performed relative quantification of the mouse parkin and synphilin-1 mRNA transcripts

-Performed RT-PCR analysis and assisted in DNA sequencing experiments

-Conducted mouse protein analyses

-Conducted biochemical fractionation analyses of human parkin variants

-Performed Immunofluorescence and confocal analyses of Parkin

-Performed experiments to test the effects of parkin on synphilin-1 steady-state levels

-Conducted pulse-chase turnover analysis of synphilin-1

-Performed all co-immunoprecipitation/Western studies

5.1 ASTRACT

Various mutations in the *PARK2* gene which encodes the protein, parkin, are causal of a disease entity termed autosomal recessive juvenile parkinsonism. Parkin can function as an E3 ubiquitin protein ligase, mediating the ubiquitination of specific targeted proteins and resulting in proteasomal degradation. Parkin is thought to lead to parkinsonism as a consequence of a loss in its function. In this study, immunoblot analyses of brain extracts from Balb/c, C57BL/6, C3H, and 129S mouse strains demonstrated significant variations in immunoreactivity with anti-parkin monoclonal antibodies (PRK8, PRK28, and PRK109). This resulted partly from differences in the steady-state levels of parkin protein across mouse strains. There was also a complete loss of immunoreactivity for PRK8 and PRK28 antibodies in C3H mice which was due to a homologous nucleotide mutation resulting in an E398Q amino acid substitution. In cultured cells, parkin harboring this mutation had a greater tendency to aggregate, exhibited reduced interaction with the E2 ubiquitin conjugating enzymes, UbcH7 and UbcH8, and demonstrated loss of function in promoting the proteasomal degradation of a specific putative substrate, synphilin-1. *In situ*, C3H mice displayed age-dependent increased levels of brain cortical synphilin-1 compared to C57BL/6, suggesting that E398Q parkin in these mice is functionally impaired and that C3H mice may be a suitable model of parkin loss-of-function similar to patients with missense mutations.

5.2 INTRODUCTION

Parkinson disease (PD) is an insidious neurodegenerative disorder that is characterized by the selective demise of specific neuronal populations, including dopaminergic neurons of the substantia nigra, and is associated with an impairment of motor functions. Most cases of PD are sporadic, but several disease-causing genes have been identified (44). In 1998, it was shown that mutations in the *parkin* gene (also known as *PARK*2) were responsible for a disease entity termed autosomal recessive juvenile parkinsonism (AR-JP) (208). To date, a variety of nonsense, missense, exonic deletion, splice site, duplication, and triplication mutations in *PARK*2 have been identified in individuals with both early and late-onset PD (155;282;423;452). Since several community based reports suggest that parkin mutations may contribute to up to 15% of the inherited cases of PD and are the major cause of early-onset PD (44;144;266;352;475) , much work has been done to understand the role of parkin in the pathogenesis of PD.

The *parkin* gene is large, spanning over 1.4 Mega bases with 12 exons and large intronic regions (16;208;209). The gene encodes a ~52kDa protein that is 465 amino acids in length (208). The protein has an amino terminal ubiquitin-like (Ubl) domain as well as two RING finger domains which are separated by an IBR finger domain at the carboxyl terminus (208;308). These structural features are common to E3 ubiquitin-protein ligases (E3 ligases)(424) and parkin can function in this capacity (74;148;178;367;392;407). E3 ligases are a class of proteins that work in concert with ubiquitin-conjugating enzymes (E2s) to mediate the transfer of ubiquitin to specific

protein substrates. This ubiquitin transfer often targets substrates for proteolytic degradation by the 26S proteasome (74;194). It is known that parkin can interact with the E2 ubiquitin-conjugating enzymes, UbcH7 and UbcH8 (178;392;490). Additionally, many groups have shown that under certain experimental paradigms, parkin can facilitate the ubiquitination of a variety of substrates and can also aid in the subsequent degradation of a subset of these substrates (68;72;83;173;177;216;306;370;393;409;439;490). Thus, it is widely accepted that parkin functions as an E3 ligase; however, it is unclear how this function may be related to PD (99;109;254).

Several of the pathogenic mutations in parkin have been shown to impair its E3 ligase activity. Pathogenic mutations, such as the T240R mutation, have been shown to reduce the interactions between parkin and E2 ubiquitin-conjugating enzymes (143;178;392;490). Additionally, this disrupted association of parkin with E2 enzymes can result in reduced ubiquitination and degradation of parkin substrates (72;178;392;407;490). It is also known that parkin can ubiquitinate itself which then leads to its degradation by the proteasome (67;490). Pathogenic mutants which do not demonstrate the ability to autoubiquitinate often show altered protein solubility (407). This altered solubility may be related to decreased protein turnover that is specific to the proteasome pathway (490).

It is hypothesized that parkin mutations may lead to parkinsonism through a loss in parkin function since parkin has been shown to play a protective role in a number of studies (71;178;201;447). Parkin deficient mice have been generated by several labs in efforts to study the effects of parkin loss-of-function in vivo (135;186;212;350;379;454).

Several inconsistencies have been reported regarding the effects of abolishing parkin in mice. However, in general, parkin loss in mice is not associated with an increased morbidity or loss of dopaminergic neurons (135;186;350;379;454;496). Nor has parkin loss in mice been shown to have an effect on many of the putative parkin substrates (217).

In this report, the western blot analyses of endogenous brain parkin from four different mouse strains, C57BL/6, Balb/c, C3H, and 129S, are described. Dramatic variations in the protein levels of endogenous parkin were observed between mouse strains. Additionally, a novel endogenous homozygous missense mutation was discovered in C3H mice which resulted in the parkin amino acid substitution, E398Q. This mutation abolished the PRK8 and PRK28 parkin antibody epitopes in C3H mice while immunoreactivity with the PRK109 antibody was retained. Because C3H mice may potentially be used in future studies that involved parkin, the impact of the novel endogenous parkin mutation on protein function was examined. Characterization of this mutation indicates that C3H mouse parkin is functionally impaired, suggesting that the C3H mouse strain may be a suitable in vivo model for endogenous loss-of-function parkin studies.

5.3 RESULTS

Differential immunoreactivity for parkin protein in various mouse strains

During the course of analyzing parkin expression by immunoblotting in mice from various backgrounds, dramatic differences were observed for immunoreactivity

with 3 different monoclonal anti-parkin antibodies (**Fig. 5-1**). All three antibodies used here (PRK8, PRK28 and PRK109) were previously shown to specifically recognize human and mouse parkin and to recognize epitopes within the RING2 domain of parkin (amino acids residues 399-465 of human parkin) (347). In brain cortex, PRK109 showed the highest level of immunoreactivity in the 129S background, followed by the C3H background and lowest, and about equivalent, levels in the Balb/c and C57BL/6 (BL6) backgrounds. Immunoblotting with antibodies PRK8 and PRK28 also demonstrated equivalent higher immunoreactivity in a 129S background compared to the Balb/c and BL6 background. Surprisingly, the cortical brain extracts from C3H mice were devoid of reactivity with both PRK8 and PRK28 antibodies. However, this result was not due to a complete loss of parkin expression in C3H mice as the PRK109 antibody recognized parkin in C3H tissue extracts. These results suggest that PRK8, PRK28, and PRK109 antibodies recognize different epitopes and that somehow, in C3H mice, the epitope that is specifically recognized by the PRK8 and PRK28 antibodies is altered.

Figure 5-1

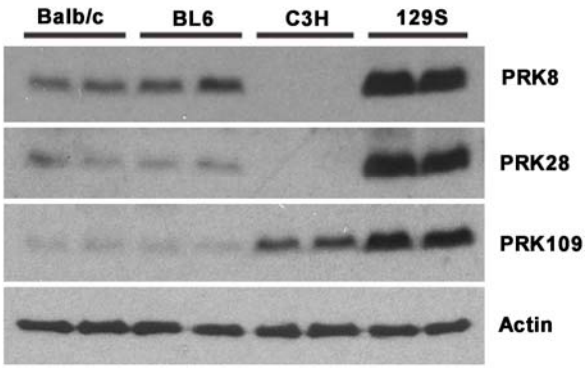

Western blot analysis showing differential levels of immunoreactivity with different parkin antibodies in various mouse strains. Cerebral cortical tissues were harvested from Balb/c, C57BL/6 (BL6), C3H, and 129S mice and total protein lysates were extracted. Equal amounts (18 ug) of total protein extracts were loaded on 13% polyacrylamide gels and analyzed by western blot analysis with the anti-parkin monoclonal antibodies, PRK8, PRK28, and PRK109 as well as an actin antibody to confirm equal protein loading. The representative blot above shows extracts from 10 week old mice. Two samples were loaded, each from separate mice of the indicated strains. All experiments were replicated and similar results were obtained for a total of n=4 mice from each strain.

Similar levels of the parkin mRNA transcript are observed in different mice backgrounds.

To begin to understand the reasons for the differences in immunoreactivity with parkin antibodies in the Balb/c, BL6, C3H, and 129S mice backgrounds, the levels of parkin mRNA in these mice was determined. Two-step quantitative real-time reverse-transcription polymerase chain reaction (qRT-PCR) analyses were performed using total RNA extracted from cortical tissues of Balb/c, BL6, C3H, and 129S mice. Analyses were performed in duplicate using 3 independent RNA samples for each of the different mouse strains. All mouse strains expressed comparable levels of the parkin mRNA transcript (**Fig. 5-2A and B**), indicating that the differences observed in parkin protein immunoreactivity levels are not due to differences in the amount of mRNA.

Figure 5-2

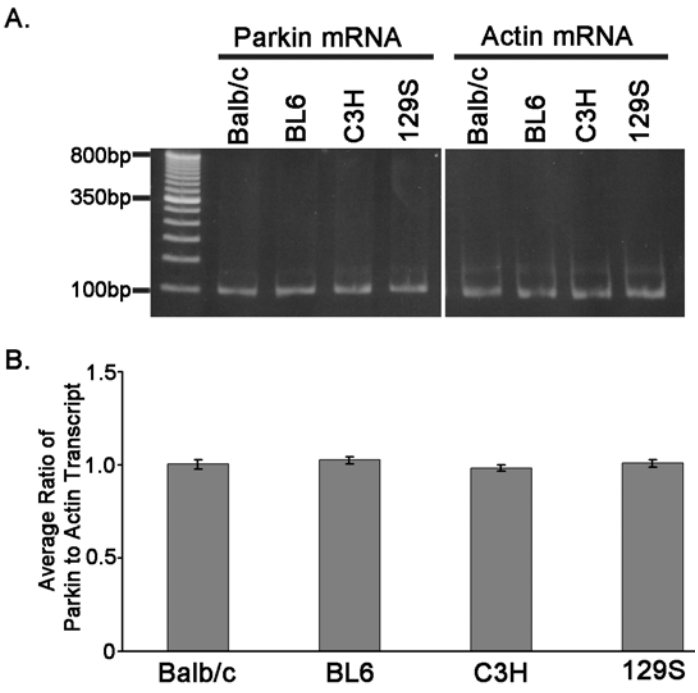

Similar levels of the parkin mRNA between different mice stains. Total RNA was extracted from cerebral cortical tissues that were harvested from Balb/c, BL6, C3H, and 129S mice. Parkin and actin mRNA transcripts were quantified using two-step qRT-PCR. Experiments were performed in duplicate and 3 separate samples were analyzed for each mouse strain. A) The parkin and actin qRT-PCR products are shown. The image represents the products from one of the mice analyzed for the indicated strain. B) The ratio of the Parkin to Actin C_T value was calculated for each sample. The graph depicts the average of the ratios between replicate samples for each mouse strain. The error bars indicate standard deviation (n=6).

Parkin antibody epitope mapping studies

To further explain the differences in immunoreactivity observed in various mouse strains with different parkin antibodies, the epitopes recognized by these antibodies were mapped in greater detail. For these epitope mapping studies, full-length and various N- and C-terminal truncated forms of human parkin were expressed in bacteria as N-terminally GST-tagged recombinant proteins (**Fig. 5-3**). Western blotting with an anti-GST antibody demonstrated similar expression for all proteins. The PRK8 antibody recognized GST-parkin(1-408), but not GST-parkin(1-399), indicating that the epitope for this antibody includes residues 400-408. PRK8 reacted with both GST-parkin(381-465) and GST-parkin(399-465), but reactivity for GST-parkin(399-465) was much weaker. These data indicate that the epitope of antibody PRK8 require residues 400-408, but extends further upstream of this sequence. Antibody PRK28 demonstrated similar immunoreactive properties to antibody PRK8, with an additional weak reactivity with GST-parkin(1-399). Therefore, the epitope for PRK28 also requires amino acid residues 400-408 and extends further upstream than PRK8. Antibody PRK109 reacted with GST-parkin(1-420), but not GST-parkin(1-408) indicating that the epitope for this antibody includes residues 409-420.

An endogenous mutation in the C3H parkin gene is responsible for the loss of PRK 8 and PRK 28 immunoreactivity.

Since genetic alterations can result in differences in the parkin protein that could be responsible for some of the differences in immunoreactivity observed in the different mouse strain backgrounds, we proceeded to determine the parkin cDNA sequence

Figure 5-3

Parkin antibodies epitope mapping studies. A. Schematic of parkin protein. The numbers indicate the amino acid residues that correspond to the respective protein domains. Ubl is the ubiquitin-like domain, Mid is the linker domain, R1 is the first RING finger domain, IBR is the in-between-ring-finger domain, and R2 is the second RING finger domain. B. Full-length human parkin cDNA corresponding to amino acids 1-465 and various truncated cDNA fragments of parkin were cloned in the bacterial expression vector pDEST15, that expresses N-terminal GST-tagged recombinant proteins. The recombinant proteins were expressed in BL21 E. coli cells. The cells were harvested and equal amounts of total protein lysates were analyzed by western blot with a GST antibody in order to confirm similar expression of the respective proteins. Additionally, equal amounts of the protein extracts were assessed for immunoreactivity with the PRK8, PRK28, and PRK109 antibodies. The experiments were performed in duplicate. Representative blots are shown for each construct. The identical blot for PRK28 is shown at different exposure times in order to reveal the faint immunoreactivity of the 1-399 construct that is not readily detectable at the shorter exposure time. The mobility of molecular mass markers is indicated on the left.

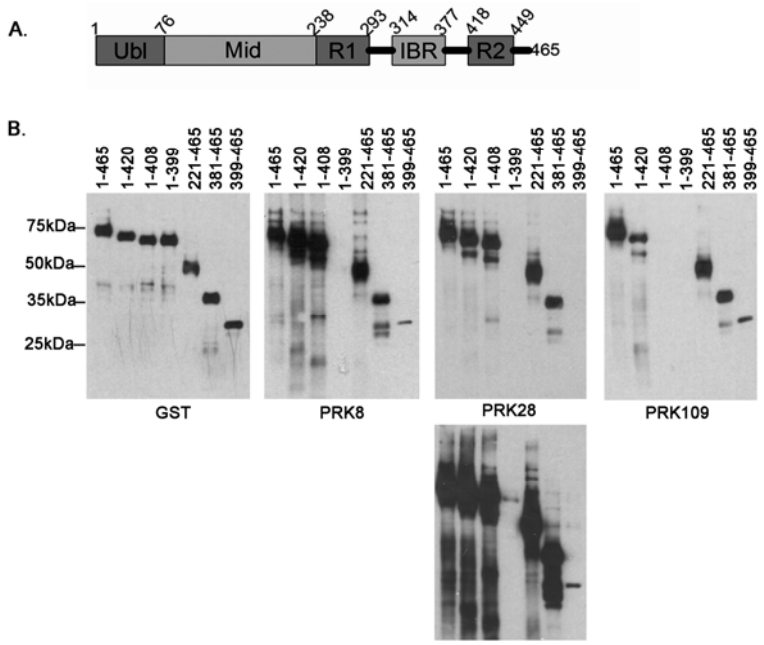

(nucleotides 963-1388) around the region comprising the antibody epitopes for each mouse strain. This analysis revealed that the cDNA sequences for Balb/c, BL6 and 129S mice was identical to the previously published sequence for Balb/c (210). However, the cDNA sequence for the C3H strain revealed 2 homologous nucleotide alterations (c. 1140 C>T and c. 1192G>C) (**Fig. 5-4 and data not shown**). The nucleotide change at position 1140 is a silent mutation that does not change the amino acid. The 1192G>C substitution results in the missense mutation E398Q. This mutation is equivalent to a E399Q mution in human parkin, since mouse parkin has one less residue (Gly 139) than human parkin (210). DNA sequencing of genomic tail DNA confirmed that the C3H

parkin mutation occurred at the DNA level and was not due to post-transcriptional events (**Figure 5-4S1**).

Figure 5-4

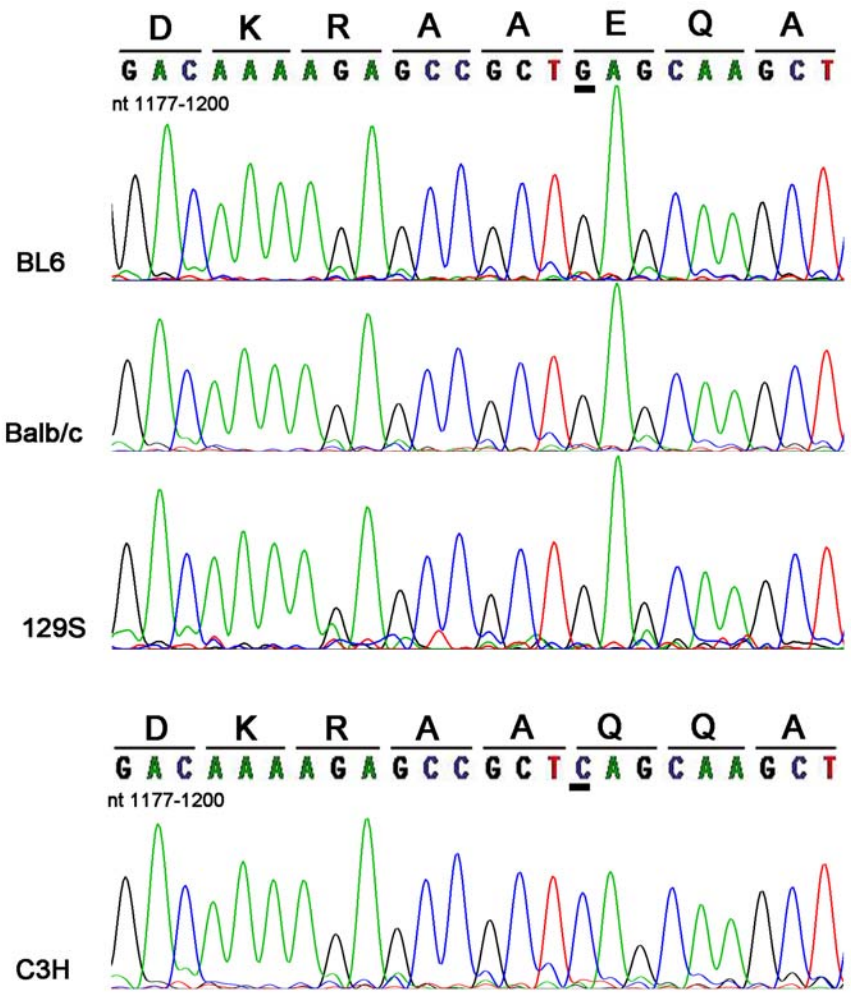

Discovery of a novel endogenous parkin mutation in C3H mice. RT-PCR was performed using total RNA that was extracted from cerebral cortical tissues of BL6, Balb/c, C3H, and 129S mice. The amplified PCR products spanned bases 895-1395 of the mouse parkin cDNA sequence. The PCR products were sequenced and analyzed for mutations. The image shows the respective portion (nucleotide bases 1177-1200) of sequencing electropherogram for the various mouse strains. The corresponding amino acid sequences are written above the respective DNA codons. A novel endogenous G1192C parkin cDNA mutation was identified in C3H mice. This mutation translates into a missense E398Q mutation. The 1192 cDNA residue is underlined in order to highlight the location of the novel G1192C mutation in the mouse parkin cDNA sequence.

Since the E399Q mutation is within the epitopes for both PRK8 and PRK28, the effects of this mutation on the reactivity of these antibodies was determined. The E399Q mutation was introduced into the bacterial vector expressing GST-parkin(380-465) and the protein was expressed concurrently with the similar WT protein. Immunoblotting

with an anti-GST antibody demonstrated equivalent expression of both proteins (**Fig. 5-5A)**. Immunoreactivity with PRK109 was not affected by the E399Q mutation, however this mutation abolished the reactivity with both PRK8 and PRK28 (**Fig 5-5A**).

To confirm these findings in mammalian cells, a construct expressing full-length untagged human WT parkin (parkin/pcDNA3.1) was used to overexpress human parkin in mouse neuroblastoma Neuro-2A (N2A) cells. In addition, similar vectors expressing T240R and E399Q mutant parkin were used. While antibody PRK109 recognized both WT and parkin mutants, antibodies, PRK8 and PRK28 did not react with E399Q parkin (**Fig. 5-5B**). These data indicate that the E399Q mutation disrupts the epitopes of the PRK8 and PRK28 antibodies and that the equivalent mutation (E398Q) in C3H mice explains the lack of immunoreactivity with these antibodies.

The E399Q human parkin mutant shows reduced solubility without associated inclusion formation.

Several of the reported PD-linked parkin mutations, some in close proximity to the E399Q mutation, lead to altered solubility when they are expressed in mammalian cells (148;407;460). To investigate whether the E399Q parkin amino acid substitution alters these biochemical properties of parkin, solubility assays were performed. HEK293T cells were transiently transfected with untagged full-length WT, E399Q, or T240R mutant human parkin constructs. Cell lysates were sequentially extracted in buffers of increasing solubilization strengths. Extracts were then analyzed by western blot with the PRK109 antibody. In comparison to the other fractions, WT Parkin protein was mostly extracted into the soluble TX fractions and to a lesser extent into the SDS

insoluble fractions (**Fig. 5-6A and B**). A significant fraction of both E399Q and pathogenic T240R human parkin mutants was extracted in the insoluble SDS-fractions (**Fig. 5-6A and B**).

Figure 5-4S1

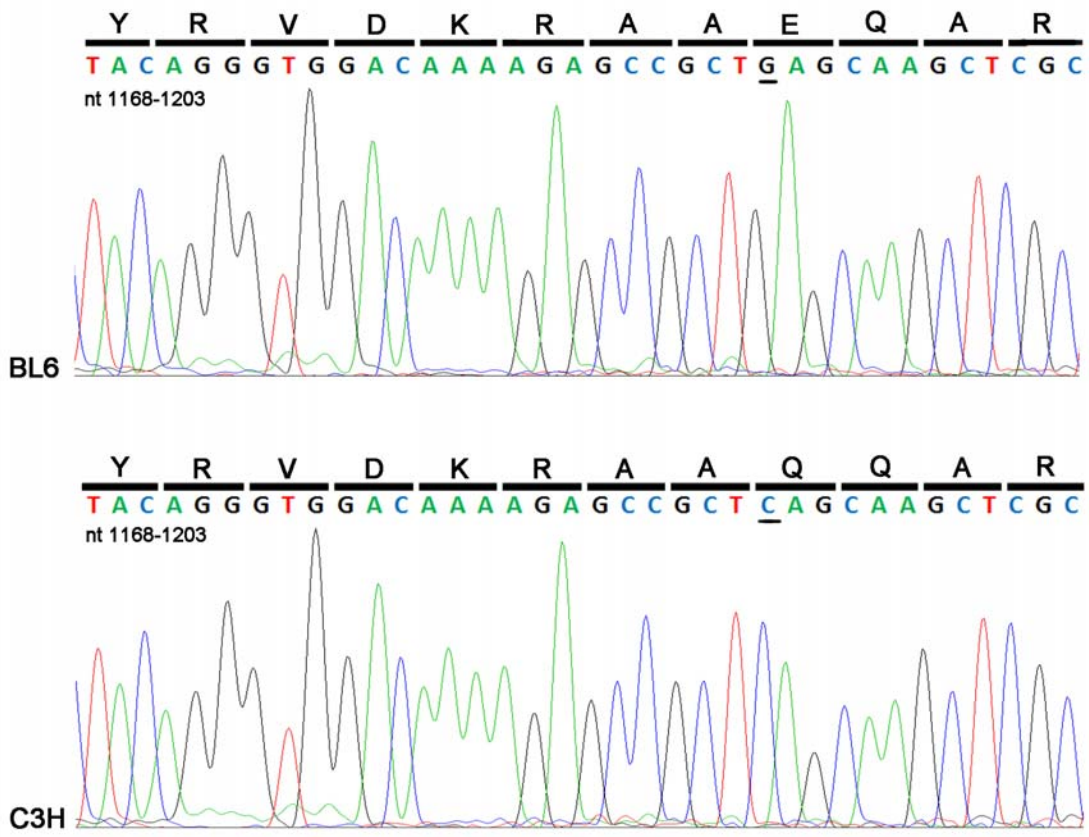

DNA sequencing of mouse parkin from genomic tail DNA. Genomic DNA was extracted from the tails of 10 week old BL6 and C3H mice using the Wizard SV Genomic DNA Purification System (Promega, Madison, WI) following the manufacture's protocol. Polymerase chain reactions were conducted on the purified DNA in order to amplify nucleotides 1167-1273 of the mouse parkin sequence. The primer sequences for the reaction were as follows. Forward: 5'-CTA CAG GGT GGA CAA AAG AGC CGC -3' and Reverse: 5'- CAA TTG GCA CGT TGC AGC GAG GAC-3'. The reaction products were confirmed by topoisomerase reaction into pCRTopo2.1 vector (Invitrogen Corporation) and DNA sequencing.

Figure 5-5

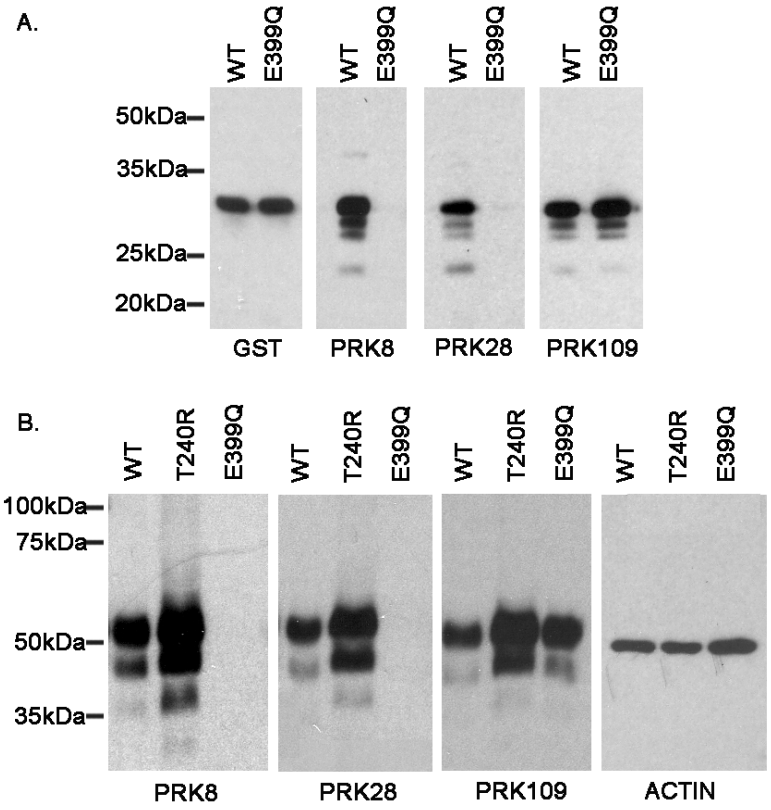

Abolishment of the PRK8 and PRK28 antibody epitopes due to the E399Q human parkin mutation. **A**) pDEST15/parkin 380-465 and pDEST15/parkin 380-465 E399Q constructs were used to express the respective proteins in BL21 E. coli. Total protein lysates were extracted and equal amounts of protein (600 ng) were resolved on 13% polyacrylamide gels and analyzed by western blot with GST, PRK8, PRK28, and PRK109 antibodies. **B**) Full-length untagged wild-type and mutant (T240R and E399Q) human parkin cDNA cloned in the mammalian expression vector pcDNA3.1 were used to express these proteins in mouse N2A neuroblastoma cells. Following transfection with the respective constructs, equal amounts (4 ug) of total protein lysates were resolved on 13% polyacrylamide gels and assessed by western blot for recognition of the indicated parkin antibodies. Additionally, the blots were probed with an actin antibody to confirm equal protein loading. The mobility of molecular mass markers is indicated on the left.

To determine whether this altered extractability of E399Q mutant parkin is associated with the formation of protein inclusions, immunofluorescence studies were conducted. HEK293T cells transiently expressing untagged full-length WT, E399Q, or T240R human parkin were assessed for parkin localization with the PRK109 antibody. Following these analyses, while parkin was found to exhibit similar homogeneous cytoplasmic staining for all of the parkin variants, inclusions were not detected in any of the cells analyzed (**Fig. 5-6C**).

Figure 5-6

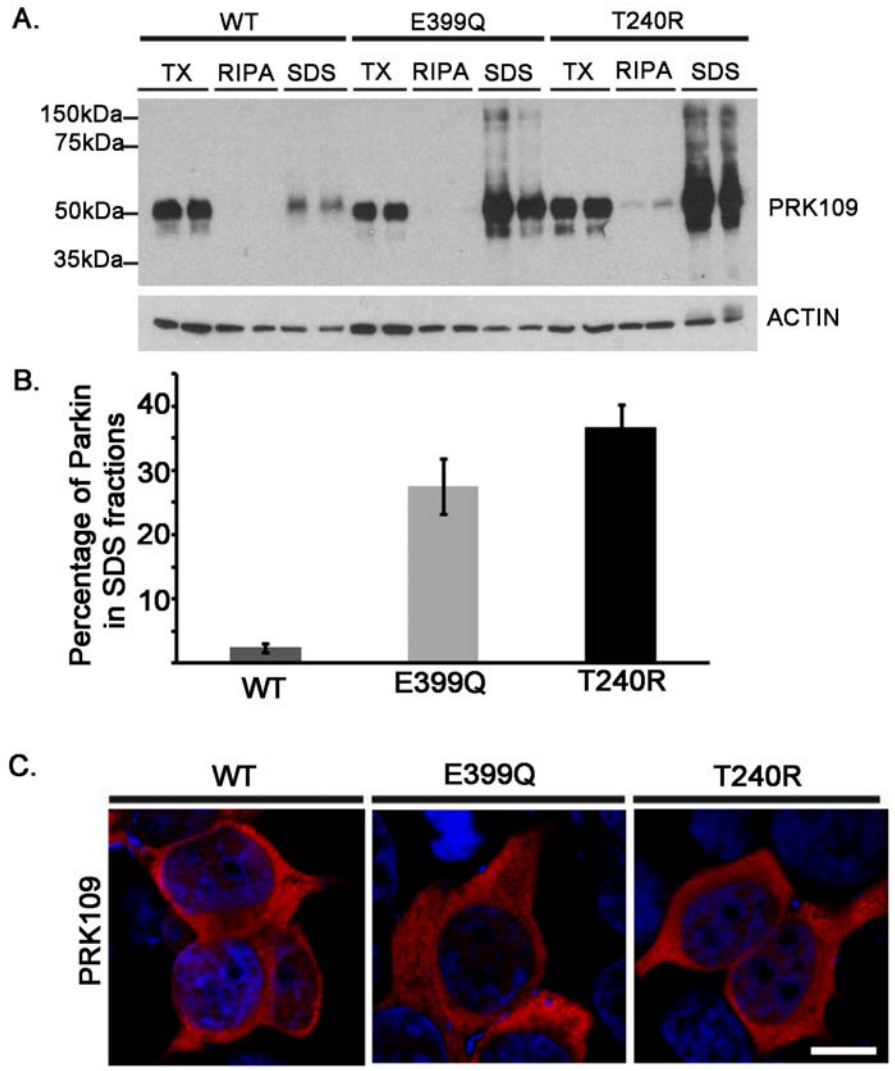

The E399Q human parkin mutant shows reduced solubility in mammalian cells without associated inclusion formation. HEK293T cells were transfected in duplicate with untagged full-length WT, E399Q, or T240R human parkin/pcDNA 3.1 constructs. **A**) and **B**) At 48 hours post transfection, cells were harvested and sequentially extracted into PBS/0.1% Triton (TX) buffer, RIPA buffer, and 2% SDS/17mM Tris (SDS) buffer. Equal amounts (16ug) of each sample were loaded onto 10% polyacrylamide gels and analyzed by western blot for parkin distribution with the PRK109 antibody. Blots were also probed with an actin antibody to assess equal protein loading. The mobility of molecular mass markers is indicated on the left. The western blot images were quantified as described in "Materials and Methods". The total percentage of parkin extracted into SDS fractions was calculated for each sample. Error bars indicate standard deviation (n=4). **C**) Immunofluorescence analysis of HEK293T cells expressing WT or mutant parkin immunostained with PRK109 (red) and counterstained with Hoerscht (blue). The merged images depict the absence of inclusions in cells expressing WT, E399Q, or T240R parkin. Scale bar =10um.

The E399Q parkin mutant is functionally impaired.

Parkin functions as an E3 ubiquitin-protein ligase, acting to promote the ubiquitination and subsequent degradation of its substrates (178;367;490). Synphilin-1

has been identified as one of the putative substrates for parkin (72;257). Several of the pathogenic mutations in parkin, including the T240R mutation, have been shown to impair the ability for parkin to promote the degradation of synphilin-1 (72;407). In order to ascertain whether the E399Q mutation hinders parkin function, steady-state levels of synphilin-1 were analyzed in the presence of WT, T240R, or E399Q parkin. The levels of synphilin-1 were compared between parkin variants. In addition, some transfected cells were treated with the proteasome inhibitor, clasto-lactacystin β-lactone (Omuralide), to assess that the degradation of synphilin-1 promoted by parkin was due to the proteasome. HEK293T cells were co-transfected with myc-tagged synphilin-1 and either pcDNA3.1 mock vector or the respective pcDNA3.1 untagged parkin constructs. Cells were transfected with a 4:1 cDNA ratio of parkin to synphilin-1 as under these conditions, it has been previously shown that parkin promotes the degradation of synphilin-1 (257). Total cell lysates were analyzed by immunoblot with anti-c-Myc and PRK109 antibodies. Expression of WT parkin led to a significant decrease in synphilin-1 steady-state levels in comparison to the levels for synphilin-1 when it had been co-expressed with mock vector (**Fig. 5-7A and B**). However, neither the T240R nor the E399Q parkin had any effect on the steady-state levels of synphilin-1. Additionally, as it has been previously shown, parkin-mediated degradation of synphilin-1 occurs via the proteasome pathway (257), since it was completely blocked in the presence of a specific proteasome inhibitor.

To further determine the effects of WT, T240R, and E399Q parkin on the stability of synphilin-1, HEK293T cells were co-transfected with myc-tagged synphilin-1 and either pcDNA3.1 mock vector or the respective pcDNA3.1 untagged human parkin constructs as described above. Synphilin-1 turnover was assessed by pulse-chase analyses

Figure 5-7

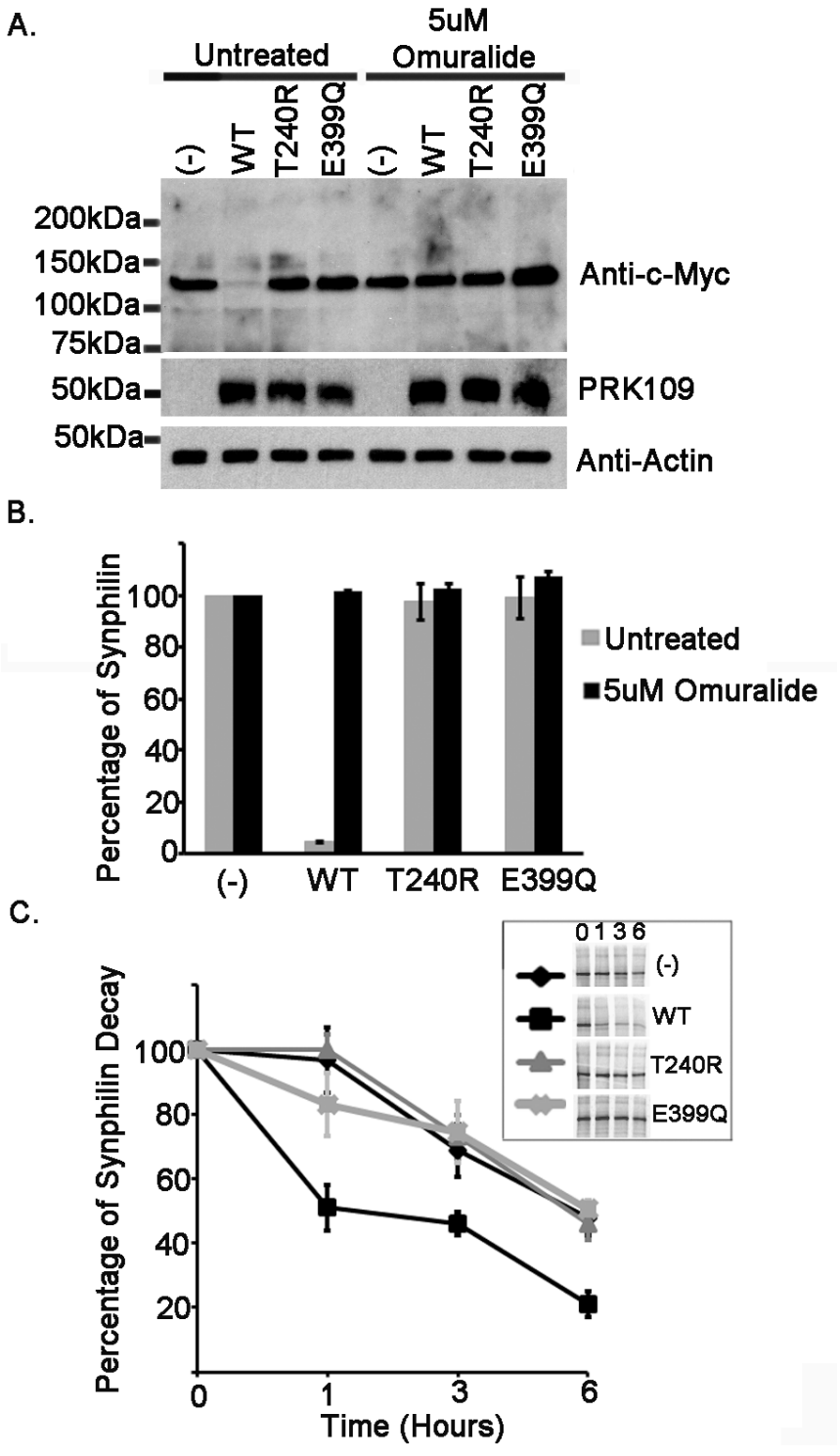

E399Q mutant parkin is functionally impaired. HEK293T cells were co-transfected either with mock pcDNA3.1 vector "(-)" or full length WT, T240R, or E399Q human parkin pcDNA 3.1 constructs as well as the pcDNA3.1 myc-tagged full-length synphilin-1 construct. The co-transfection experiments were performed using a parkin to synphilin-1 cDNA ratio of 4:1. At 24 hours post transfection, (**A** and **B**) cells were incubated for 16 hours with fresh DMEM or with DMEM containing 5uM Omuralide. Cells were then harvested and total protein lysates were extracted. Extracts were resolved by 10 % polyacrylamide gels and immunoblotted with the monoclonal antibodies anti-c-Myc clone 9E10 to assess synphilin-1 levels, PRK109 antibody to confirm parkin expression, and anti-actin antibody to ensure equal protein loading. All experiments were performed in triplicate and repeated at least 3 times. The mobility of molecular mass markers is indicated on the left. The levels of synphilin-1 were quantified as described in "Materials and Methods" and the graph in B depicts the percentage of synphilin-1 protein standardized to that in the mock vector samples. The error bars indicate standard deviation between replicate samples (n=4). **C**) Cells were pulsed with ^{35}S-methionine for 1 hour and chased for 0, 1, 3, or 6 hours. The inset shows representative pulse-chase experiments. Experiments were conducted in triplicates. The results are plotted as percentage of protein over time standardized to the 0 hrs time point. The error bars show standard deviation (n=3).

with ^{35} S-methionine and the effects of the respective parkin variants on synphilin-1 turnover were compared. Synphilin-1 exhibited a half-life of ~6 hours in the absence of parkin (**Fig. 5-7C**). WT parkin enhanced the turn-over of synphilin-1, reducing the half-life to ~1 hour. However, neither T240R nor E399Q parkin had an effect on synphilin-1 degradation, suggesting that both mutants are functionally inactive.

Synphilin-1 was initially identified as a substrate for parkin in studies investigating interacting proteins (72). It is possible that the E399Q mutation disrupts the direct interaction between mutant parkin and synphilin-1 that would prevent parkin-mediated degradation. To determine whether there is a loss in the direct interaction between E399Q mutant parkin and synphilin-1, co-transfection and co-immunoprecipitation experiments were conducted. HEK293T cells were co-transfected with myc-tagged synphilin-1 and untagged human WT, E399Q, or T240R mutant parkin constructs. At 48 hours post transfection, soluble cells lysates were immunoprecipated with an anti-c-Myc antibody followed by immunoblot with the PRK109 antibody. All parkin variants, including the E399Q mutant, were co-immunoprecipitated with synphilin-1 (**Fig. 5-8**). Thus, the E399Q Parkin mutation does not disrupt the interaction between parkin and synphilin-1.

It has been previously shown that parkin specifically interacts with the E2 ubiquitin conjugating enzymes, UbcH7 and UbcH8, in order to exert its function as an E3 ligase (178;392;490). One plausible explanation for the impaired function exhibited by the E399Q parkin mutant could be disrupted binding with E2 enzymes. To test this hypothesis, co-transfection and co-immunoprecipitation experiments were conducted.

Figure 5-8

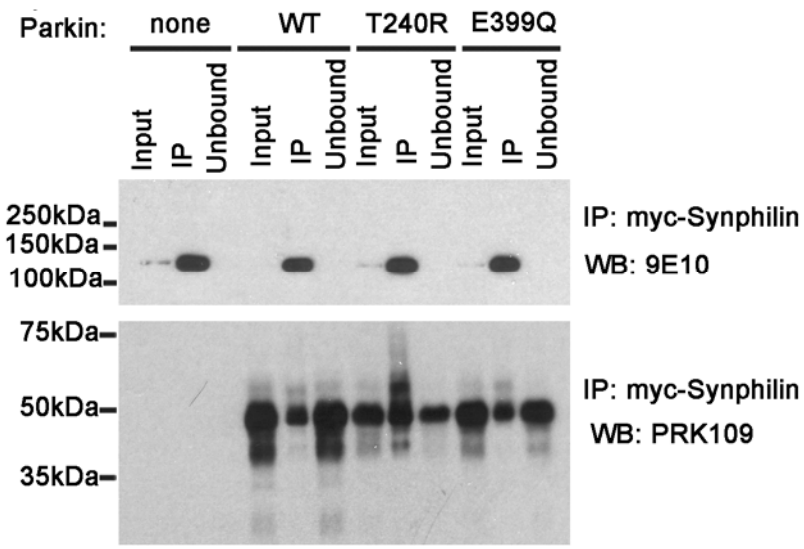

E399Q mutant parkin can directly interact with synphilin-1. HEK293T cells were transiently co-transfected with myc-tagged synphilin-1 and pcDNA3.1 mock vector ("none") or with untagged full-length WT, T240R, or E399Q human parkin pcDNA3.1 constructs. Cells were harvested and soluble protein lysates were extracted ("Input"). The cell lysat es were then immunoprecipitated using anti-c-Myc polyclonal antibody ("IP"). Equal amounts of the input, IP, and unbound supernatant (Unbound) fractions were resolved by SDS-PAGE and analyzed by western blot ("WB") with anti-c-Myc monoclonal antibody 9E10 or with anti-parkin antibody PRK109. Experiments were repeated at least 3 times. The mobility of molecular mass markers is indicated on the left.

HEK293T cells were co-transfected with HA-tagged UbcH7 or UbcH8 constructs and either mock pcDNA3.1 or untagged pcDNA3.1 full-length WT, T240R, or E399Q human parkin constructs. At 48 hours post transfection, cell lysates were immunoprecipitated with a polyclonal anti-HA antibody, HA.11, followed by immunoblot with the monoclonal antibodies PRK109 and anti-HA (clone 12CA5). These analyses revealed that while UbcH7 recruited similar levels of both WT and T240R parkin, the binding of E399Q parkin with UbcH7 was dramatically reduced (**Fig. 5-9**). Interestingly, in comparison to binding with UbcH7, parkin was recruited less effectively by UbcH8 and the levels of T240R and E399Q mutant parkin recruited by UbcH8 were modestly reduced in comparison to WT parkin. Together, these results indicate a loss of function of

the E399Q mutant may be due, at least in part, to reduced interactions with E2 ubiquitin conjugating enzymes.

Figure 5-9

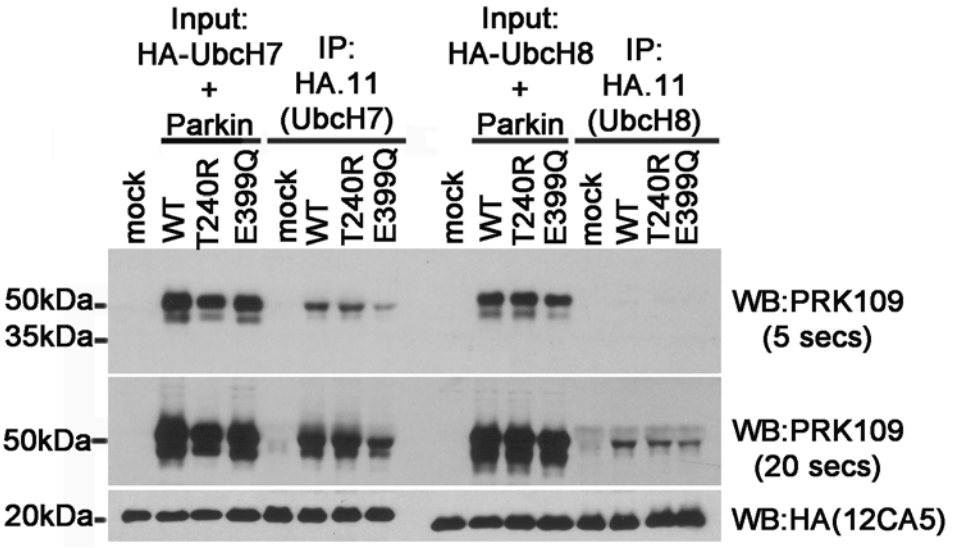

The E399Q parkin mutant shows reduced binding to UbcH7 and UbcH8. HEK293T cells were co-transfected with pRK5-HA-UbcH7 or pRK5-HA-UbcH8 and either pcDNA3.1 mock vector ("mock") or with untagged full-length WT, T240R, or E399Q human parkin pcDNA3.1 constructs. Cells were harvested and soluble protein lysates were extracted ("Input"). The cell lysates were then immunoprecipitated using the anti-HA polyclonal antibody, HA.11 ("IP"). Input and IP fractions were resolved by SDS-PAGE and analyzed by immunoblot with the monoclonal antibodies PRK109 and anti-HA (clone 12CA5). The PRK109 blots are shown at 5 second and 20 second exposure times to highlight the differences in signal intensity reflected by the binding of parkin with UbcH7 versus that with UbcH8.

Synphilin-1 levels are increased in C3H mice.

Since E399Q mutant parkin was incapable of down-regulating synphilin-1 expression in cultured cells (**Fig. 5-7**), it is plausible to hypothesize that the parkin in C3H mice, harboring the homologous E398Q mutation, may show increased levels of the synphilin-1 substrate in situ. To test this hypothesis, total protein extracts from cerebral cortical tissues of 10 week old BL6 and C3H mice were analyzed by western blot with the affinity purified synphilin-1 antibody, UPN79. No differences in synphilin-1 were

detected between mice at this age (**Fig. 5-10A and B**). However, it is possible that synphilin-1 may accumulate in C3H mice in an age dependent manner. To determine this, cerebral cortical protein extracts from 8 month old BL6 and C3H mice were immunoblotted with antibody UPN79. Remarkably, extracts from 8 month old C3H mice revealed 2.0 ± 0.18 fold higher synphilin-1 levels than BL6 mice of the same age (**Fig 5-10C and D**).

To confirm that these changes were not due to differences at the transcriptional level, qRT-PCR analyses were performed using total RNA extracted from cortical tissues of the 8 month old BL6 and C3H mice used for synphilin-1 protein analysis described above. Both mouse strains expressed comparable levels of the synphilin-1 mRNA transcript (**Fig. 5-10D and E**), indicating that the differences observed in synphilin-1 protein immunoreactivity are not due to differences in the amount of mRNA. These findings are consistent with the notion that the E398Q mutation impairs the ability of parkin to mediate the degradation of synphilin-1, leading to an age-dependent accumulation of synphilin-1 in C3H mice.

5.4 DISCUSSION

Western blot analyses of brain extracts from Balb/c, C57BL/6, C3H, and 129S mice revealed dramatic variations in immunoreactivity with 3 monoclonal parkin antibodies (PRK8, PRK28, and PRK109). Notably, immunoreactivity for PRK8 and PRK28 was absent in C3H mice. This was especially unexpected since it had been previously reported that the epitopes for the PRK8, PRK28, and PRK109 antibodies were similarly located around the second RING domain of parkin (347). In efforts to gain insights into

Figure 5-10

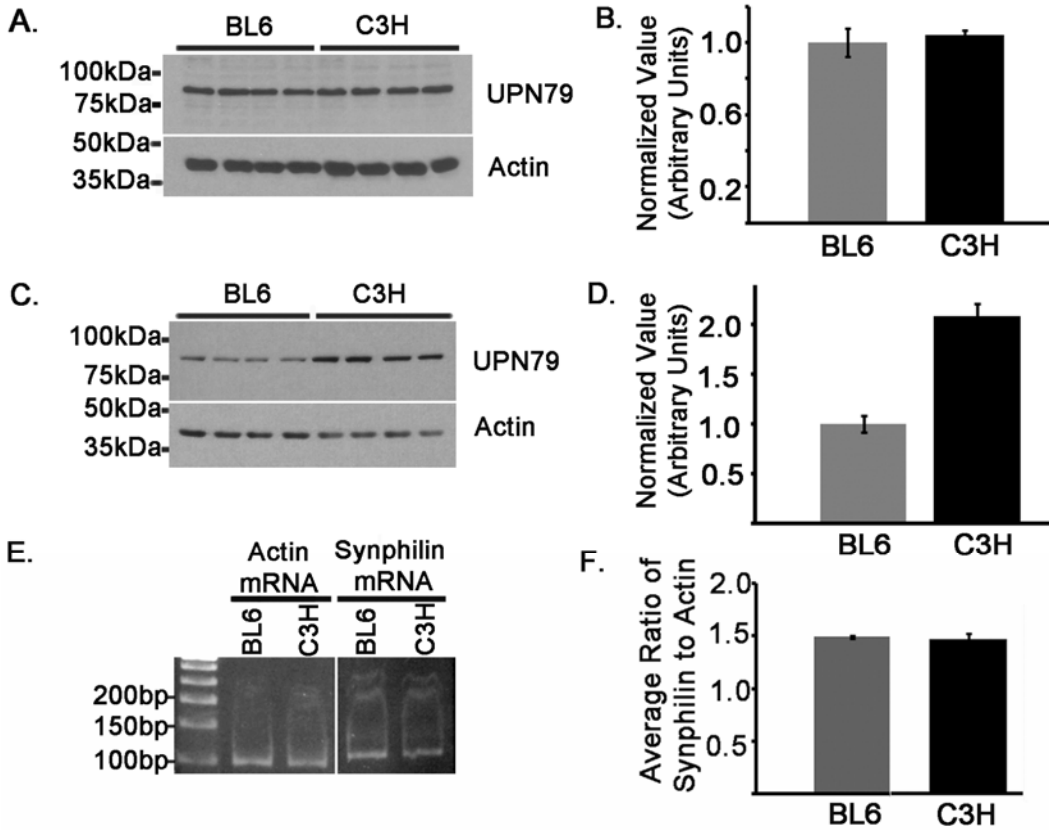

Synphilin-1 protein levels are increased in C3H mice. Cerebral cortical tissues were harvested from BL6 and C3H mice. Protein lysates were extracted from animals at ages 10 weeks (**A** and **B**) and 8 months (**C** and **D**). Equal amounts (18 ug) of high-salt protein extracts were loaded onto 10% polyacrylamide gels and analyzed by western blot analysis with the affinity purified polyclonal antibody, UPN79 to assess synphilin-1, as well as an actin antibody to confirm equal protein loading. Four samples were loaded, each from separate mice of the indicated strains. The graphs in **B** and **D** show the average ratios of the levels of UPN79 to actin normalized to the values in BL6 animals at the respective aforementioned ages. **E**) Total RNA was extracted from cerebral cortical tissues that were harvested from the same BL6 and C3H mice analyzed in **C**. Synphilin-1 and actin mRNA transcripts were quantified using two-step qRT-PCR. Experiments were performed in duplicate and 3 separate samples were analyzed for each mouse strain. The synphilin-1 and actin qRT-PCR products are shown. The image shows the products from one of the mice analyzed for the indicated strains. **F**) The ratio of the synphilin-1 to actin C_T value was calculated for each sample. The graph depicts the average of the ratios between replicate samples for each mouse strain. The error bars indicate standard deviation (n=6).

how epitope differences could account for some of these changes in mouse parkin immunoreactivity, thorough epitope mapping studies were conducted. The analyses of a variety of recombinant N-terminal and C-terminal truncated parkin proteins allowed for the PRK8, PRK28 and PRK109 antibody epitopes to be more discretely mapped. The

PRK8 antibody epitope requires residues 400-408 of human parkin but also extends upstream of these residues. The PRK28 epitope also requires residues 400-408 but extends slightly further upstream of the PRK8 epitope. Lastly, the PRK109 epitope is further downstream and includes residues 409-420 of human parkin protein.

Genetic analysis revealed a homologous nucleotide substitution (c. 1192G>C) in C3H mice that results in an E398Q missense amino acid change. This alteration is responsible for the disruption of the PRK8 and PRK28 epitopes in C3H mice. These findings and the epitope mapping are particularly important due to the prevalent use of these parkin antibodies in several studies (52;115;156;243;244;347).

Immunoblotting with antibody PRK109 demonstrated variations in the levels of parkin in different mouse strains with the highest level being observed in 129S mice followed by C3H and lowest, and about equivalent levels, in the Balb/c and BL6 mice. Similar results were obtained when comparing parkin levels in 129S, Balb/c and BL6 mice with antibodies PRK8 and PRK28. Genetic studies revealed no alterations that would affect the PRK109 epitope in 129S, C3H, Balb/c and BL6 mice. Nor were any genetic mutations identified that would affect the PRK8 or PRK28 epitopes in 129S, Balb/c and BL6 mice. Additionally, the levels of brain parkin mRNA were found to be similar between strains, indicating post-transcriptional effects. These findings are likely a reflection of differences in parkin protein levels that may result from differences in translation efficiencies or turnover rates in the different mouse strains. Interestingly, no differences in the steady-state levels of other PD relevant proteins including α-syn, DJ-1, or tau were observed between mouse strains (data not shown). Neither were there

differences in the levels of the E3 ligase, ARIH1 (data not shown), which shares close functional homology to parkin (275). Thus, the differences that were observed in parkin between mice strains appear to be specific and not due to the consequence of more generalized effects.

There has been no report of a naturally occurring human E399Q parkin polymorphism or pathogenic mutation, however there are several reported pathogenic mutations that are in close proximity to the this residue [R396G (475), A398T(282;452), R402C (26;270), R402H (416), R402W(359)], suggesting that it may affect protein structure or function. In addition, this glutamic acid residue at the 398 is conserved in other species including rat, pig, and macaque (208;210); NCBI protein database accession numbers NP_064478, NP_001038068, and ACL68652). Directly supporting this hypothesis, it was shown in this study that the E399Q mutant parkin exhibited reduced solubility when it was overexpressed in mammalian cells. However, this did not lead to the formation of aggregated protein that could be observed at the microscopic level. This suggests that the E399Q parkin mutation may result in protein misfolding without the accumulation into large aggregates. Changes in parkin solubility have been associated with a variety of stimuli including oxidative stress, heat shock, as well as a battery of other types of stress and may have a consequence on parkin function (243;459;470). For instance, changes which induce a shift in parkin solubility could thereby deplete soluble pools of parkin and may result in the impairment of parkin's function toward substrates.

It was further shown in this report that the E399Q mutant parkin is deficient in the ability to mediate the degradation of the parkin substrate, synphilin-1, similar to the T240R parkin pathological mutant. Neither the steady-state levels nor the turn-over rate of synphilin-1 were affected by co-expression of the E399Q or T240R parkin mutants in HEK293T cells, while expression of WT parkin dramatically reduced the levels of synphilin-1 in these studies. These data supported previous findings which showed a marked decrease in synphilin-1 steady-state levels with the co-expression of WT parkin at a parkin to synphilin-1 cDNA ratio of 4:1, findings which were not observed under the same conditions for the T240R parkin mutant (257). It is of interest to note that high molecular weight forms of polyubiquitylated synphilin were not detected in any of the parkin co-expression experiments performed in the studies herein (Fig. 7). This could be because typical ubiquitination "smears" are below detectable levels under the experimental conditions used and/or these observations may be related to the finding by Lim et al. which suggests that parkin can mediate different types of ubiquitin linkage (257). Nevertheless, the data herein demonstrates impaired function of E399Q and T240R parkin mutants towards down-regulating synphilin protein levels in comparison to WT parkin protein. This was not due to the inability for these mutants to interact with synphilin since WT, E399Q, and T240R parkin all showed similar interactions with synphilin by co-immunoprecipitation studies, consistent with previous findings (72).

It is interesting that the novel E399Q parkin mutation lies between the IBR and RING2 domains of the parkin protein. This feature is also common to the previously characterized T415N pathogenic parkin mutant. The T415N parkin mutation interfered with the proper recruitment of E2 enzymes to parkin (490) and resulted in impairments in

parkin-mediated degradation (407). However, this was not associated with a loss in substrate binding activity (72;407). Similarly, in the current study, in comparison to the other parkin variants analyzed, the E399Q parkin mutant showed dramatically reduced binding with the E2 enzyme, UbcH7. This aberration likely partially contributes to the deficiencies exhibited by the E399Q parkin mutant related to degradation of the synphilin-1 substrate.

The novel E399Q parkin mutant showed reduced solubility and functional impairments when it was analyzed in mammalian cells indicating that the homologous E398Q mutation in C3H mice may result in mice that are deficient or impaired in parkin activity. To support this hypothesis, there was a 2 fold increase in the cortical levels of synphilin-1 in 8 month old C3H mouse brains in comparison to BL6 mice. This difference was not observed in mice at 10 weeks of age which suggests that other E3 ligases or other modes of degradation play a more prominent role in the turnover of synphilin-1 at this age. While C3H mice do not show any overt behavioral characteristics that may be attributed to a functional parkin deficiency, the attempts to identify in vivo effects of parkin's loss-of-function in mice have proven to be very difficult. Genetically generated parkin null mice fail to display any major differences in most of the behavioral, morphological, and biochemical analyses that have been previously conducted (349;350;431;453). Subtle differences in parkin null mice have been identified in a few studies, but many inconsistencies have also been reported (116;135;186;335;379;496). Interestingly, no differences in synphilin-1 levels were detected in brain tissues of parkin null animals in comparison to WT animals in previous studies (217). However, this does not discredit the finding of the increased steady-state levels of synphilin-1 observed in

C3H mice in the current study. It is possible that this discrepancy could be due to a number of factors including antibody specificity, tissue extraction method, or tissue-specific differences in parkin regulation of synphilin-1. Further, since it is likely that synphilin-1 may also be regulated by parkin independent mechanisms, it is unknown how this may be affected in a model system that is completely devoid of parkin versus a system where parkin is available, albeit impaired. Analysis of other putative parkin substrates such as Pael-R or p38/JTV-1 (217) could also indirectly help to confirm a loss of parkin function in C3H mice. However, while specific antibodies are not readily available, future studies to assess for alterations in these putative substrates would be informative.

In summary, these studies demonstrate that parkin protein levels differ in various mouse background strains. Additionally, the C3H mouse harbors a previously unreported mutation (E398Q) in parkin that abolishes immunoreactivity with antibodies PRK8 and PRK28. Characterization of this novel mutation revealed that it promotes the misfolding of parkin, impairs its ability to interact with E2 conjugating enzymes, and disrupts its function towards the synphilin-1 substrate. These findings indicate that C3H mice are carriers of a missense parkin mutation and that they may be a suitable model of parkin loss-of-function similar to human patients that have missense mutations. In addition, the difference in the level of parkin expression demonstrated here in various widely-used mouse strains is an important confound that should be taken into account in mouse studies.

5.5 EXPERIMENTAL PROCEDURES

Mouse strains

C57BL/6, C3H, BALB/c, and 129S mice at 10-12 weeks and 8 months of age were used for studies. All mice were purchased from Charles River Laboratories Inc (Wilmington, MA). Mice were sacrificed by CO_2 euthanization as approved by the University of Pennsylvania Institutional Animal Care and Use Committee.

Antibodies

PRK8, PRK28, and PRK109 are mouse monoclonal antibodies raised against human parkin but that react with parkin from various species, including murine (347). Mouse anti-(GST) monoclonal antibody clone A00865.01 was obtained from GenScript (Piscataway, NJ). Affinity purified mouse anti-actin (clone C4) monoclonal antibody reacts with all forms of vertebrate actin (Millipore, Billerica, MA). Two c-Myc antibodies were used in these studies: purified anti-c-Myc monoclonal antibody clone 9E10 (M4439, Sigma-Aldrich, Saint Louis, MO) and an affinity purified anti-c-Myc polyclonal antibody (Sigma-Aldrich, Saint Louis, MO). Two HA antibodies were used in these studies: anti-HA monoclonal antibody clone 12CA5 (Roche Diagnostics, Indianapolis, IN) and affinity purified polyclonal antibody, HA.11 (Covance, Emeryville, CA). UPN79 is an affinity purified polyclonal antibody raised against human full-length recombinant synphilin-1 (312).

Relative quantification of the mouse parkin mRNA transcript

Cerebral cortical tissues were harvested from 10 week old Balb/c, BL6, C3H, and 129S mice and divided in half. Half of the tissue was frozen on dry ice for subsequent protein analysis and total RNA was extracted from the remaining half using TRIzol reagent (Invitrogen Corporation, Carlsbad, CA) according to the manufacturer's protocol. Three tissue samples were prepared for each mouse strain. The RNA products were reverse transcribed to cDNA using Taqman RT-PCR reagents (Applied Biosystems Inc, Foster City, CA) with oligo dT primers that were supplied in the kit. The RT reactions were conducted according to the manufacturer's protocol. Real-time PCR analyses were performed on the cDNA products using 2X SYBR Green Master Mix reagent (Applied Biosystems) and Applied Biosystems 7000 Real-Time PCR System (Applied Biosystems). Reactions were performed in duplicate for each cDNA sample in a 96 well plate. Primers were designed to amplify a 98 base pair product of mouse parkin cDNA that corresponds to nucleotides 396-494. The sequences for the parkin primers were as follows. Forward: 5'-AGCAGCCAGAGGTCCAGTTA-3' and Reverse: 5'-CACTGAACTCGGAGCTTTCC-3'. Additionally, a mouse β-actin loading control was amplified. Mouse β-actin primers were designed to amplify a 99 base pair product corresponding to cDNA nucleotides 698-797. The sequences of the β-actin primers were as follows. Forward: 5'-CTTCCTCCCTGGAGAAGAGC-3' and Reverse: 5'-AAGGAAGGCTGGAAAAGAGC-3'. The thermo cycling conditions for the amplification were as follows: 1 cycle for 2 minutes at 50ºC, 1 cycle for 10 minutes at 95ºC, followed by 40 cycles of 15 seconds at 95ºC and 1 minute at 60ºC, followed by 1 cycle for 15 seconds at 95ºC, 1 cycle for 20 seconds at 60ºC, and 1 cycle for 15 seconds at 95ºC. The C_T values for each sample were obtained. Parkin values were normalized to

β-actin by taking the ratio of parkin to β-actin for each sample. The normalized results were averaged for replicate samples and graphed. Error bars represent standard deviation where n=6. After the reaction, equal volumes of the PCR products, one for each sample type, were loaded onto 7-8% non-denaturing polyacrylamide/Tris Borate EDTA (TBE) gels and were resolved by electrophoresis. The gels were then stained with ethidium bromide at 1ug/mL for 20 minutes and the DNA bands were visualized with a UV light and photographed. Additionally, the reaction products were confirmed by DNA sequencing.

RT-PCR analysis and DNA sequencing of the mouse parkin cDNAs

Mouse total RNA was extracted and reverse transcribed from cortical tissue as described above. Polymerase chain reactions were conducted on the cDNA products using AccuPrime™ SuperMix II (Invitrogen) in order to amplify nucleotides 895-1395 of the mouse Parkin cDNA sequence. The primer sequences for the reaction were as follows. Forward: 5'-GAGCTCCATCACTTCAGGATCCTTGGA-3' and Reverse: 5'-CTACACGTCAAACCAGTG ATC TCC CAT-3'. The PCR products were digested with ExoSAP-IT ® reagent (USB Corporation, Cleveland, OH) and sequenced by the DNA sequencing facility of the University of Pennsylvania.

Mouse protein analysis

Cerebral cortical tissues were harvested from mice as described above. The tissue was sonicated in 3 tissue volumes of either high salt (HS) buffer (50mM Tris [pH 7.5], 750 mM NaCl, 5mM EDTA, with a protease inhibitor cocktail at 1:1000 and PMSF at 1:500)

or 2% SDS/8M urea. Tissue extracts were then quantified using the bicinchoninic acid (BCA) assay (Pierce Biotechnology, Rockford, IL) and bovine serum albumin as the standard. Equal amounts of protein extracts were resolved by SDS-PAGE. The samples were analyzed by western blot with PRK8, PRK28, PRK109 and UPN79 antibodies. Additionally, membranes were blotted with anti-actin antibody to assess equal loading. At least 4 independent tissue samples were analyzed for each mouse strain at each respective age.

Parkin antibodies epitope mapping

Using full length human parkin cDNA as a template, primers were designed to generate various truncated parkin constructs by PCR. See **Table 5-1** for the oligonucleotide sequences used for PCRs. AccuPrime SuperMix II (Invitrogen) was used for the reactions. PCR products were cloned by topoisomerase reaction into the shuttling vector pCR8/GW/TOPO (Invitrogen) and confirmed by DNA sequencing. These cDNA fragments were introduced into the Gateway pDEST15 vector by recombinase reaction using LR Clonase II enzyme (Invitrogen). BL21 cells were then transformed with positive pDEST15 clones. Transformed cultures were subsequently induced with 500uM Isopropyl Beta-D-1-thiogalatopyranoside (IPTG) for 2 hours at 37ºC in a shaking incubator. After induction of protein expression, the cells were lysed by sonication in 3 pellet volumes of 2% SDS/8M urea. Protein extracts were then quantified using the BCA assay and analyzed by immunoblot with anti-GST, PRK8, PRK28, and PRK109 antibodies.

Table 5-1 Oligonucleotide sequences used to generate N-and C- terminal truncated human parkin mutants for PRK8, PRK28 and PRK109 epitope mapping studies.

Nucleotides amplified in PCR	Corresponding Amino Acid Sequence	Forward Oligonucleotide sequence	Reverse Oligonucleotide sequence
1-1398	1-465	5'-ATG ATA GTG TTT GTC AGG TTC AAC TCC-3'	5'- CTA CAC GTC GAA CCA GTG GTC CCC CAT -3'
1-1260	1-420	5'-ATG ATA GTG TTT GTC AGG TTC AAC TCC-3'	5'-CTA GCG GGG ACA GGG CTT GGT GGT TTT CTT-3'
1-1224	1-408	5'-ATG ATA GTG TTT GTC AGG TTC AAC TCC-3'	5'-CTA TTT GGA GGC TGC TTC CCA ACG AGC CTG-3'
1-1197	1-399	5'-ATG ATA GTG TTT GTC AGG TTC AAC TCC-3'	5'-CTA CTC GGC GGC TCT TTC ATC GAC TCT GT-3'
661-1398	221-465	5'-GAA ACA CCA GTA GCT TTG CAC CTG AT-3'	5'- CTA CAC GTC GAA CCA GTG GTC CCC CAT -3'
1141-1398	381-465	5'-TTT GAA GCC TCA GGA ACA ACT ACT CAG-3'	5'- CTA CAC GTC GAA CCA GTG GTC CCC CAT -3'
1195-1398	399-465	5'-GAG CAG GCT CGT TGG GAA GCA GCC-3'	5'- CTA CAC GTC GAA CCA GTG GTC CCC CAT -3'

Generation of E399Q human parkin construct for bacterial expression

For expression in bacteria, using the Gateway pDEST15 human parkin 381-465 construct as a template (described above), the QuickChange Site Directed Mutagenesis Kit (Stratagene, La Jolla, CA) was used in order to generate the E399Q mutant form of human parkin protein. The oligonucleotide sequence for the mutagenesis reaction was as follows: forward-5'- GAAAGAGCCGCCCAGCAGGCTCGTTGG-3' and reverse-5'-CCAACGAGCCTGCTG GGCGGCTCT TTC-3'. The sequence of the construct was confirmed by DNA sequencing. The plasmid was subsequently expressed in BL21 cells, harvested, and analyzed as described in the previous section.

Generation of human parkin constructs for expression in mammalian cells

The full-length untagged WT human parkin cDNA was cloned into the XhoI and Apa I restriction sites on the pcDNA3.1(+) mammalian expression vector (Invitrogen). This WT parkin construct was used as a template to perform site directed mutagenesis in order to generate the full-length E399Q mutant. The same oligonucleotides were used as in the E399Q mutagenesis reaction as described in the previous section. Additionally, the WT parkin/pcDNA 3.1 construct was used as a template in a site directed mutagenesis reaction to generate the human parkin T240R pathogenic mutant. The oligonucleotide sequences for the T240R mutagenesis reaction were as follows: forward-5'-ATCACTTGC ATTAGGTGCACAGACGTC-3' and reverse-5'-GACGTCTGTGCACCTAATGCAAGTGAT-3'. The sequence for both the E399Q and T240R parkin mutants were verified by DNA sequencing.

Cell culture

Neuro-2A mouse neuroblastoma (N2A) cells and human embryonic kidney (HEK)-293T cells were cultured in Dulbecco-modified Eagle medium (DMEM) (Invitrogen, Carlsbad, CA) supplemented with 10% fetal bovine serum (FBS) (Sigma, St.Louis, MO), 100 U/mL penicillin and 100 μg/mL streptomycin (Invitrogen, Carlsbad, CA). Cells were incubated at 37ºC and 95% air/5% CO_2 atmosphere.

Biochemical fractionation of human parkin variants

HEK293T cells were cultured in 10 cm dishes. In duplicate, cells were transfected with either the pcDNA3.1 full-length WT, E399Q, or T240R human parkin constructs using

Lipofectamine Reagent (Invitrogen), following the manufacterer's protocol. At 48 hours post transfection, cells were rinsed and scraped in 1X PBS and sedimented at 13,000 g. Cells were vortexed vigorously in 2 pellets volumes of ice-cold PBS/0.1% Triton buffer containing protease inhibitors. The cell debris were sedimented at 13,000 g for 2 minutes and the supernatants were stored on ice. The PBS/0.1% Triton extraction was repeated and following sedimentation, the supernatants from both extractions were pooled together as the TX fraction. The remaining pellet was rinsed with the PBS/0.1% Triton buffer and the rinse was discarded. The cell pellet was then resuspended into 2 pellet volumes of ice-cold RIPA buffer with protease inhibitors, vortexed vigorously, stored on ice for 5-10 minutes, and then vortexed again. The cell debris were sedimented at 13,000 g for 2 min and the supernatant was collected as the RIPA fraction. The remaining pellet was rinsed with RIPA buffer and the rinse was discarded. Lastly, the pellet was solubilized in 1 pellet volume of 2% SDS/8M urea which was collected as the SDS fraction. All extracts were quantified by BCA assay and analyzed by western blot analysis with the PRK109 and actin antibodies. Western blot images were scanned using a CanoScan Lide30 scanner (Canon U.S.A., Inc., Lake Success, NY). The levels of PRK109 signal were quantified for each sample using ImageQuant 5.0 analysis software (GE Healthcare, Piscataway, NJ).

Immunofluorescence and Confocal Analyses of parkin

HEK293T cells were cultured in 35 mm dishes. Cells were transfected in duplicate either with the pcDNA3.1 full-length WT, E399Q, or T240R human parkin constructs using Lipofectamine Reagent (Invitrogen), following the manufacterer's protocol. At 24 hours

post transfection, cells were rinsed in PBS and fixed by incubation in ice-cold acetic-methanol (1:20) at -20 °C for 30 minutes. Cells were rehydrated with water, rinsed with PBS, and blocked in PBS/2% FBS/0.1% Triton. Cells were then incubated with PRK109 antibody diluted into PBS/2% FBS at a concentration of 1:2000 overnight at 4°C, washed 3 times with PBS at 10 minutes each, and then incubated at room temperature (~23 ºC) with a goat anti-mouse secondary antibody conjugated to Alexa Fluor ® 594 (Invitrogen) diluted into PBS/2% FBS for 1 hour. Cells were rinsed 3 times with PBS and then stained with Hoerscht 33342 trihydrochloride trihydrate (0.5ug/mL) (Invitrogen) for 5 minutes at room temperature (~23 ºC). Cells were rinsed with water and then coverslipped with Cytoseal^{TM} 60 mounting media (Richard-Allen Scientific, Kalamazoo, MI). The images were visualized with a Zeiss LSM-510 Meta confocal microscope (Carl Zeiss MicroImaging Inc, Thorwood, NY, USA).

Effects of parkin on synphilin-1 steady-state levels

A mammalian expression construct expressing C-terminal myc-tagged full-length human synphilin-1 (synphilin-c-myc/pcDNA 3.1) was kindly provided by Dr. Virginia Lee. In triplicate, HEK293T cells were co-transfected with synphilin-c-myc/pcDNA 3.1 and either pcDNA3.1 mock vector, or pcDNA3.1 human full-length WT parkin, E399Q mutant parkin, or T240R mutant parkin constructs. Cells were co-transfected with parkin to synphilin-1 cDNA ratio of 4:1 using the calcium phosphate transfection protocol described by Gallagher et al. (120). At 21 hours post transfection, fresh complete media was added to the cells that were cultured for an additional 16 hours with or without 5uM clasto-lactacystin-β-lactone (Omuralide)(EMD Chemicals Inc, Gibbstown, NJ). Cells

were then rinsed in PBS and lysed by sonication in 2% SDS/8M urea. Cell extracts were quantified by BCA assay and analyzed by western blot with monoclonal antibodies anti-c-myc clone 9E10, PRK109, and anti-actin. The 9E10 signal was quantified as described in previous sections.

Pulse-chase synphilin-1 turnover analysis

In triplicate, HEK293T cells were cultured in 35mm dishes. Cells were co-transfected with synphilin-c-myc/pcDNA 3.1 and either pcDNA3.1 mock vector, or pcDNA3.1 human WT parkin, E399Q mutant parkin, or T240R mutant parkin constructs. Cells were co-transfected with a parkin to synphilin-1 cDNA ratio of 4:1 using the calcium phosphate transfection protocol described above. At 24 hours post transection, cells were methionine-deprived for 20 minutes by incubation in pre-warmed methionine-free DMEM (Invitrogen, Carlsbad, CA)/10% dialyzed FBS before adding 100μCi [^{35}S]-methionine (Invitrogen, Carlsbad, CA) per ml of methionine free DMEM/10% dialyzed FBS for 1 hour. Chase experiments were conducted with normal DMEM/FBS for 0, 1, 3, and 6 hours. Cells were then rinsed with PBS and harvested in ice-cold cytoskeleton (CSK) buffer (100 mM NaCl, 50 mM Tris, pH 7.5, 2 mM EDTA, 1 % Triton X-100, protease inhibitors). The radiolabelled protein extracts were pre-cleared with a rabbit serum pre-incubated with protein A-agarose (Santa Cruz Biotechnologies, Santa Cruz, CA) for 3 hours at 4ºC and radiolabelled extracts were then immunoprecipitated overnight at 4ºC with anti c-Myc polyclonal antibody (Sigma) pre-incubated with protein A-agarose (Santa Cruz Biotechnology, Inc). The antibody-protein complexes were washed 3 times with 10 volumes of CSK buffer, resuspended in 2 volumes of 2X SDS

sample buffer and boiled at 100 ºC for 5 minutes. The beads were removed by centrifugation and the samples were loaded onto 13 % polyacrylamide gels. Following electrophoresis, gels were fixed with 50% methanol/5% glycerol, dried and exposed to a PhosphorImager plate and the signal was quantified using ImageQuant 5.0 analysis software.

Co-immunoprecipitation/Western studies of parkin and synphilin-1

In triplicate, using the calcium phosphate transfection method, HEK293T cells were transfected in 35mm dishes with either synphilin-c-myc/pcDNA 3.1 alone or co-transfected with synphilin-c-myc/pcDNA 3.1 as well as either the pcDNA3.1 untagged full-length human WT, E399Q, or T240R parkin constructs. At 21 hours post transfection, fresh complete media was added to the cells that were cultured for an additional 24 hours. Cells were then rinsed, scraped, and harvested in PBS by centrifugation at 13,000 g for 2 minutes. The cell pellets were lysed in 500 uL of ice-cold CSK buffer (100 mM NaCl, 50 mM Tris, pH 7.5, 2 mM EDTA, 1 % Triton X-100) and cell debris was sedimented at 13,000 x g for 2 minutes. 30 uL of the supernatant was incubated at 100ºC for 5 minutes with SDS sample buffer as the "Input" fraction. The remaining supernatant was incubated overnight at 4ºC with anti-c-Myc polyclonal antibody (Sigma-Aldrich) that had been pre-incubated with protein A-agarose beads (Santa Cruz Biotechnologies, Santa Cruz, CA). The antibody-protein complexes were then washed 3 times with 10 volumes of CSK buffer, resuspended in 20uL of 2X SDS sample buffer, and incubated at 100ºC for 5 minutes as the immunoprecipitate ("IP") fractions. 30uL of the unbound supernatants were also incubated at 100ºC for 5 minutes

with SDS sample buffer as the "Unbound" fractions. The Start, IP, and Unbound fractions were resolved by SDS-PAGE and immunoblotted with PRK109 antibody.

Co-immunoprecipitation/Western studies of parkin with UbcH7 and UbcH8-

The mammalian expression vectors expressing N-terminal HA-tagged full-length human UbcH7 or UbcH8 (pRK5-HA-UbcH7 and pRK5-HA-UbcH8, respectively) were kindly donated by Dr. Ted Dawson. In triplicate, using the calcium phosphate transfection method, HEK293T cells were co-transfected in 35mm dishes with either pRK5-HA-UbcH7 or pRK5-HA-UbcH8 and pcDNA 3.1 mock vector or pcDNA3.1 untagged full-length WT, E399Q, or T240R human parkin constructs. Cells were cultured, harvested, and lysed as described in the previous section. 50uL of the lysate was incubated at 100°C for 5 minutes with SDS sample buffer as the "Input" fraction. The remaining lysate was incubated for 3 hours at 4°C with HA.11 polyclonal antibody (Covance) that had been preabsorbed to protein A-agarose beads (Santa Cruz Biotechnologies). The antibody-protein complexes were then washed 3 times with 10 volumes of CSK buffer, resuspended in 20uL of 2X SDS sample buffer, and incubated at 100ºC for 5 minutes as the "IP" fractions. The Input and IP fractions were resolved by SDS-PAGE and immunoblotted with the monoclonal antibodies PRK109 and anti-HA (Roche).

Quantification of mouse synphilin-1 protein

Western blot images were obtained (described above) and scanned using a CanoScan Lide30 scanner. The levels of UPN79 and actin were quantified for each mouse using ImageQuant 5.0 analysis software. The levels of UPN79 were normalized between mice

by calculating the ratio between the UPN79 value to that for actin. The normalized results for the mice of the same genetic background were averaged together and graphed.

Relative quantification of the mouse synphilin-1 mRNA transcript

Cerebral cortical tissues were harvested from 8 month old BL6 and C3H mice. Half of the tissue was frozen on dry ice for protein analysis and total RNA was extracted from the remaining half using TRIzol reagent (Invitrogen) as described in detail in previous sections. Three tissue samples were prepared for each mouse strain. Reverse transcription reactions and real-time PCR analyses were performed as described above. Primers were designed to amplify a 107 base pair product of mouse synphilin-1 cDNA that corresponds to nucleotides 988-1095. The sequences for the synphilin-1 primers were as follows. Forward: 5'-ATATCGCTCTTGCCACACCTA-3' and Reverse: 5'-CAGGCATTCTGCATGGCCCTT-3'. Additionally, a mouse β-actin loading control was amplified as described above. The C_T values for each sample were obtained. Synphilin-1 values were normalized to β-actin by taking the ratio of synphilin-1 to β-actin for each sample.

5.6 ACKNOWLEDGEMENTS

This work was supported by the National Institute on Aging [AG09215] and the National Institute of Neurological Disorders and Stroke [NS053488]. C.P. Ramsey is supported by a pre-doctoral NRSA fellowship from the National Institute on General Medicine Sciences [GM082026].

CHAPTER SIX

Discussion

In efforts to gain insights into the biochemical pathways involved in idiopathic PD, much attention has been devoted towards understanding the roles for a number of the gene products implicated in familial forms of the disease. This thesis aimed to investigate the biochemical and cellular properties of mutant DJ-1, α-syn and parkin proteins using cell culture and mouse models. Based on the findings described herein (chapters 2-5), several conclusions can be drawn regarding the relevance of these studies as it relates to the field at large.

6.1 DJ-1 acts to mitigate oxidative stress but can also protect against a variety of other toxic insults.

In chapter 2, stable overexpression of WT and E163K human DJ-1variants in N2A cells revealed that in response to noxious stimuli, DJ-1 is generally a protective protein. DJ-1 acted to protect against proteolytic stress induced by inhibitors of the 26S proteasome. It also protected against toxicity caused by mitochondrial complex I and III inhibitors. Remarkably, while WT DJ-1 efficiently ameliorated the harmful effects of oxidation, E163K DJ-1 failed to protect against oxidative stress and rendered cells to be selectively vulnerable to oxidative insults. This suggests that the E163K DJ-1 mutation acts as a dominant-negative, specifically during conditions of oxidative stress. It also implies that specific DJ-1 residues affect individual functions of the protein and may implicate DJ-1 in a variety of biochemical pathways.

It remains to be elucidated how DJ-1 mechanistically protects against cell toxicity and thus it is unknown why E163K DJ-1 renders cells to be selectively vulnerable to oxidative insults. It is thought that oxidation of DJ-1 residue C106 to cysteine sulfinic acid acts to regulate the protective properties of DJ-1 protein (43;53;185;301;328;455;494). Blackinton and colleagues discovered that hydrogen bonding of C106 with DJ-1 residue E18 modulates C106 oxidation propensity (43). Based on knowledge gained from crystallization studies, residue E163 is not thought to be in close proximity to C106 (233;471). It is worth mentioning that additional DJ-1 residues other than C106 can be modified by oxidation both *in vitro* and *in vivo* (65;207;389). Perhaps the E163K substitution creates electrostatic abnormalities that could account for the oxidative deficiencies exhibited by mutant protein in the studies herein. It is known that the E163K DJ-1 substitution disrupts a salt bridge that normally occurs between residues E163 and R145 in DJ-1 and that this alteration thereby weakens a network of hydrogen bonds that span the DJ-1 dimer interface (233). Future studies to assess for changes that occur to specific residues of E163K DJ-1 protein under oxidative conditions would be insightful.

It was somewhat surprising to find that E163K DJ-1 behaved as a dominant-negative when expressed in mouse N2A cells during oxidative stress. One plausible explanation for this finding is that E163K DJ-1 dimerizes with and inactivates endogenous murine DJ-1 protein, thereby rendering cells expressing E163K DJ-1 to be selectively vulnerable to oxidative insults. In the studies herein, we were unable to co-immunoprecipitate E163K human DJ-1 together with endogenous murine DJ-1, suggesting that co-dimerization of the two DJ-1 isoforms does not occur. However, our

co-immunoprecipitation studies were not completely exhaustive since alternative approaches utilizing additional types of tagged DJ-1 constructs and/or additional antibodies may have yielded different results. Thus, it would be premature to definitively conclude that E163K human DJ-1 does not somehow inactivate endogenous murine DJ-1 under oxidative conditions.

There can also be other explanations for the dominant-negative effect exhibited by E163K DJ-1 in N2A cells. It is thought that while oxidation of DJ-1 residue C106 to sulfinic acid activates the protective function of DJ-1 protein, further oxidation of C106 to sulfonic acid under extreme oxidizing condition inactivates the protein (43;53;301;494). Though it has never been investigated, one would expect that inactivated or damaged forms of DJ-1 would need to be cleared from the cell by one of the cardinal protein degradation pathways. Perhaps E163K DJ-1 is particularly vulnerable to inactivation following oxidation and thus in a model system in which the inactivated E163K DJ-1 mutant is overexpressed during oxidative insult, this could result in a combinatorial strain on cellular antioxidant mechanisms as well as protein degradation machineries. The proposed combination of events could be the cause for the dominant-negative effect exhibited by E163K DJ-1 during oxidative stress. It would be interesting to determine the effects of oxidative stress on the turn-over rate of E163K mutant DJ-1 in efforts to address the question of whether oxidation plays a role in modulating degradation of the E163K mutant. Additionally, studies to assess for the pathogenicity of inactivated DJ-1 protein on cells during stress would be enlightening.

Since we showed that E163K DJ-1 can effectively protect against mitochondrial stress in N2A cells, it was unexpected to find that in response to oxidative stress, E163K DJ-1 demonstrated reduced redistribution towards mitochondria. Mitochondrial localization sequences have not yet been identified for DJ-1 neither is it fully understood what mechanistic role DJ-1 plays to maintain mitochondrial homeostasis. However, since E163K DJ-1 retained protective properties in the presence of mitochondrial toxins but failed to redistribute to mitochondria in response to oxidative stress specifically, it suggests that DJ-1 may have a variety of mitochondrial functions and that these functions may be regulated by different mechanisms. Canet-Aviles and colleagues argued that mitochondrial localization of DJ-1 is driven by C106 oxidation (53). If this is true, it is possible that residue C106 in E163K DJ-1 has aberrant redox properties. Thus, it would be interesting to determine the role of C106 in the regulation of E163K DJ-1 mitochondrial localization.

Though we and others have shown that DJ-1 protects against oxidative stress (27;137;181;196;204;252;253;418;479;482), Gorner and colleagues argue that DJ-1 is not a direct antioxidant but instead indirectly influences cell viability by modulating redox signaling pathways (139). Since we showed that the cytoprotective properties of the E163K DJ-1 mutant were impaired during oxidative stress, it would be interesting to determine the impact of this on signaling pathways. It is worth noting that we were unable to detect differences in any of the signaling molecules analyzed in the studies herein including phosphorylated and nonphosphorylated Akt and phosphorylated and nonphosphorylated ERK1 and 2 (data not shown). However, the discrepancies between our findings and those reported in literature (129;142;252;484), may be due to differences

between cell-types used for studies. Thus, it would be interesting to assess for the effects of E163K DJ-1 on signaling pathways during oxidative stress by conducting studies using cell lines better fitted for protein signaling analyses.

6.2 Misfolded DJ-1 mutants can be degraded by the proteasome pathway but alternative catabolic mechanisms are likely.

In chapter 3, it was shown that in comparison to WT DJ-1 protein, pathogenic DJ-1 mutants, L10P, L166P, and P158DEL, were dramatically destabilized when expressed in CHO cells. Interestingly, the analyzed mutant proteins were only partially stabilized by MG-132, albeit to variable degrees. It was also discovered that all of the DJ-1 mutants exhibited aberrant folding patterns. Additionally, insoluble forms of mutant L10P and L166P DJ-1 proteins could be stabilized following treatments with either MG-132 or epoxomicin, and P158DEL DJ-1 demonstrated reduced solubility even in the absence of these treatments. Further, L10P, L166P, and P158DEL DJ-1 proteins were associated into atypical intranuclear and cytoplasmic protein inclusions in CHO cells following exposure to MG-132. Conversely, the biochemical properties of WT DJ-1 protein were completely unaffected by proteasome inhibition in the analyses herein. Taken together, these findings suggest that L10P, L166P, and P158DEL DJ-1 mutations contribute to disease as a function of decreased protein stability and indicate that the 26S proteasome can regulate specific variants of DJ-1 protein.

It is interesting to note that turnover of WT DJ-1 protein was unaltered by inhibition of the proteasome. Additionally, the highly unstable pathogenic DJ-1 mutants analyzed could only be stabilized in part by MG-132. While neither L10P nor P158DEL DJ-1

proteins have been characterized prior to the studies herein, L166P DJ-1 has been shown by others to be stabilized in cells treated with various proteasome inhibitors (138;139;298;307;324). Interestingly, however, among all of these studies, it was only Gorner and colleagues who chose to report that MG-132 and epoxomicin were not sufficient to completely stabilize L166P DJ-1 in mammalians cells (138;139). Perhaps others chose to overlook this observation, though it is also possible that proteasome regulation of mutant DJ-1 proteins could be cell-type specific. Notwithstanding, our findings support a role for degradation of both WT and mutants forms of DJ-1 by proteasome-independent mechanisms.

To date, it is not fully elucidated what alternative proteolytic pathways may act to regulate DJ-1 protein. A recent study by Giaime and colleagues revealed that DJ-1 could be cleaved by caspase-6 enzyme (129). It was also determined in the study by Giaime et al. that the L166P mutation enhanced DJ-1 susceptibility to caspase-6 cleavage. Further, since DJ-1 cleavage by other caspases was not discovered in the study, it was implied that proteolysis of DJ-1 by caspase-6 is specific. Ironically however, though it was demonstrated that caspase-6 cleavage of DJ-1 could occur *in vitro*, the proteasome inhibitor, lactacystin, and the calpain inhibitor, ALLN, acted to stabilize L166P DJ-1 much more potently than caspase-6 inhibitors (129). Thus, this suggests that regulation of DJ-1 likely occurs via diverse catabolic pathways and it will be interesting to determine what factors act to target DJ-1 for degradation by these distinct mechanisms.

Since pathogenic DJ-1 mutants are partially destabilized by the proteasome, it is of interest to ascertain which E3 ligases may act to mediate this effect. Interestingly, Moore

et al. showed that WT DJ-1 associated with the E3 ligase, parkin, during oxidative conditions (304). Additionally, when co-expressed together in mammalian cells, various pathogenic DJ-1 mutants, including L166P, were able to interact with parkin (304). However, in the study by Moore et al., parkin failed to enhance the degradation of DJ-1 but instead acted to stabilize WT and L166P DJ-1 variants (304). Olzmann and colleagues also reported that parkin failed to mediate the degradation of L166P DJ-1, though interaction between the two proteins was also detected in that study (325). We were unable to detect any interactions between parkin and WT, L10P or P158DEL DJ-1 variants in the studies herein (data not shown) and thus, it is unlikely that these DJ-1 variants are regulated by parkin-mediated mechanisms.

Novel DJ-1 interacting proteins including TNF receptor-associated protein (TTRAP) and Bcl-2-associated athanogene 1 (BAG1) may be involved in modulating DJ-1 (91;498). TTRAP selectively interacted with L166P DJ-1 in mammalian cells and this association was potently enhanced in the presence of MG-132 (498). BAG1 was also discovered to interact with both WT and L166P DJ-1 proteins and was reported to increase the dimer/monomer ratio for both variants (91), although the latter finding may be somewhat controversial since L166P DJ-1 fails to dimerize in our studies or in other reports. It remains to be determined whether TTRAP or BAG1 proteins can modulate the turn-over rates of WT DJ-1 or pathogenic DJ-1 mutants. Thus, studies to investigate the effects of TTRAP and BAG1 on DJ-1 turnover would clarify the regulatory effects of these proteins on DJ-1.

It is possible that BAG1 and/or TTRAP may act to regulate the solubility of pathogenic DJ-1 mutants. Deeg and colleagues reported that L166P DJ-1 accumulated abnormally in cell nuclei under normal culturing conditions and that this aberration could be down-regulated by BAG1 protein (91). Interestingly, Zucchelli et al. showed that upon treating neuroblastoma cells with MG-132, TTRAP protein formed large juxtanuclear aggresomes, though it wasn't reported whether DJ-1 localized to these inclusions (498). In the studies herein, L10P, L166P, and P158DEL DJ-1 variants formed intranuclear and cytoplasmic inclusions following treatments with MG-132. The majority of these inclusions were not classical aggresomes and this finding was somewhat surprising. To date, there have been no other reports describing the type of atypical DJ-1 positive inclusions that were observed in the studies herein. Previously, Olzmann and colleagues had reported that L166P and parkin colocalized into perinuclear aggresomes following proteasome impairments (325); however, the observations described in this thesis do not fit that profile. Thus, more thorough investigations into the mechanisms of DJ-1 inclusion formation are needed.

It has been shown that L166P DJ-1 can exhibit a gain-of-function toxicity effect when expressed in mammalian cells (91;389;418;487;498). Zucchelli and colleagues showed that while TTRAP protected against MG-132-induced apoptosis in neuroblastoma cells, L166P DJ-1 significantly inhibited the protective activity of TTRAP by modulating signaling of pro-apoptotic mediators (498). Expression of L166P DJ-1 rendered transiently expressing mammalian cells to be selectively vulnerable to endoplasmic reticulum stress (487) and H_2O_2 induced cell death (389;418). L166P DJ-1 was also shown to reduce cell viability when expressed in cells under normal culturing conditions

(91), although this finding has never been reported by others. Since L10P, L166P, and P158DEL DJ-1 variants form atypical protein inclusions following proteasome impairments, it is hypothesized that all three DJ-1 mutants may be toxic to cells, though this question has never been addressed. Further, autopsy tissues are currently unavailable for PD patients harboring L10P, L166P or P158DEL DJ-1 mutations. Thus, it will be interesting to determine whether any of the three mutant DJ-1 proteins can act to enhance protein aggregation *in vivo*.

6.3 Genetically altered mice may not fully recapitulate the molecule pathways affected by genes associated with PD.

Pathogenic DJ-1 mutations are thought to cause PD as a consequence of the loss of DJ-1 protective function (47). In efforts to model a DJ-1 loss-of-function *in vivo*, DJ-1 deficient mice were generated as described in chapter four. However, mice lacking DJ-1 did not demonstrate any of the cardinal signs of parkinsonism, neither were there any signs of nervous system degeneration in these animals. This was not completely surprising since similar findings have been reported by other groups (13;60;63;136;274). Nevertheless, many have shown DJ-1 null mice to be susceptible to a variety of toxic insults (204;354;483) and this suggests that DJ-1 acts in a protective capacity *in vivo*.

It was reported that DJ-1 could modulate the aggregation of α-syn and/or act to alleviate the toxic effects of pathogenic forms of α-syn *in vitro* (27;389;493;494); however, prior to the findings described herein, it had never been reported whether similar functions for DJ-1 could be recapitulated *in vivo*. As detailed in chapter four, generation of homozygous double-transgenic M83-DJnull mice enabled us to address this

question for the first time. M83-DJnull mice were analyzed and compared to previously characterized M83 mice (131) as it related to survival rate, distribution of α-syn pathologies, biochemical properties of the α-syn protein, and the secondary effects of expressing mutant α-syn. Since no significant differences were discovered between mouse genotypes, it was concluded that DJ-1 may not directly modulate α-syn, nor protect against the harmful effects that result from α-syn aggregation *in vivo*.

The findings reported in this thesis suggest that attempting to gain insights into familial forms of PD using mouse models may prove to be difficult. While in humans, DJ-1 deficiency may result in early-onset PD (47;152;200), we and others have shown that mice lacking DJ-1 are relatively normal (13;60;63;136;211;274). Similarly, although patients harboring the A53T α-syn mutation develop PD marked by nigrostriatal dopamine neurodegeneration and associated nigral LB pathologies (134), it is clear that transgenic mice expressing human A53T α-syn exhibit a phenotype that is distinct from human disease (51;131;247;279;444). Further, in chapter 5, we describe our discovery of a novel endogenous E398Q parkin mutation in C3H mice which appears to inactivate parkin in these animals. A variety of parkin mutations are causative of juvenile to early-onset forms of PD which are thought to result from parkin loss-of-function (26;154;155;270;282;359;416;478). Our analyses in chapter 5 reveal that C3H mice may be suitable parkin loss-of-function models; however, unlike patients harboring parkin missense mutations, C3H mice do not demonstrate any of the classical symptoms of PD. Future thorough anatomical, biochemical, and behavioral characterizations of the nigrostriatal dopaminergic system in C3H animals may be insightful.

Stories told from the studies of genetically altered mice suggest that it may be presumptuous to assume that any single genetic mutation alone can be causative of PD. Instead, one could argue that patients harboring PD-linked mutations may just be more susceptible to environmental stimuli and/or other noxious insults that may synergistically lead to nigral neurodegeneration and the onset of behavioral impairments. If this is true, it is possible that if insulted with the proper stimuli, genetically altered mice may be able reproduce some of the classical symptoms of PD. To support this idea, it has been shown that parkin deficient mice are particularly susceptible to nigral degeneration caused by neuroinflammatory stimuli (116). Similarly, in comparison to normal mice, DJ-1 deficient animals are more vulnerable to paraquat exposure (483) as well as exposure to mitochondrial inhibitors (204;354). Paraquat exposure also exacerbates disease in transgenic mice expressing human A53T α-syn (321). Nonetheless, it is not fully elucidated what mechanisms contribute to the vulnerabilities displayed by the genetically altered animals used in these studies. Future studies to identify factors that can enhance the effects of modulating parkin, DJ-1, or α-syn *in vivo* will give insights into the roles of these proteins in the pathogenesis of both inherited and sporadic forms of PD.

6.4 Oxidative stress, mitochondrial dysfunction and protein degradation impairments may all impinge on PD pathogenesis.

This thesis presented a range of studies involving the effects of mutations on DJ-1, parkin, and α-syn proteins in efforts to gain insights into the molecular mechanisms that may be causal of PD. Based on the findings presented herein, it is fair to conclude that PD is a complex disorder that may develop subsequent to a combination of events that

synergistically result in the disease. Our findings from the studies of the E163K DJ-1 mutant suggest that oxidative stress may be a pathogenic factor in PD and also support a role for DJ-1 in acting to mitigate this insult. It is known that oxidative damage of DJ-1 is linked to sporadic PD (65;374). Further, we have shown that DJ-1 can effectively protect against oxidative toxicity. Thus it is proposed that development of therapeutic strategies that would act to upregulate DJ-1 and thereby ameliorate any harmful oxidation that may occur *in vivo* would likely serve to protect against the development of PD in humans.

It is also suggested from our studies that interactions of DJ-1 with mitochondria may be required for the protective effects of DJ-1 against oxidative insults. Though there is much to be learned regarding this idea, it is possible that impairments in DJ-1 activity may somehow link oxidative stress to mitochondrial dysfunction in PD. It's known that mitochondrial complex I is vulnerable to oxidative damage (64;435). We have shown that DJ-1 can assuage H_2O_2 toxicity and can also protect against inhibitors of mitochondrial complexes. Whether these protective mechanisms exhibited by DJ-1 are somehow related remains to be determined. Future studies to assess for the mitochondrial role of DJ-1 especially as it relates to how oxidation may modulate this would be beneficial in determining how mitochondrial impairments may contribute to the onset of PD.

It is also apparent from our studies of DJ-1, parkin, and α-syn mutations that protein degradation impairments may be involved in PD pathogenesis. We showed that L10P, L166P and P158DEL DJ-1 mutants were capable of promoting the formation of intracellular inclusion bodies in a proteasome dependent manner. Though it remains to be elucidated, if similar effects occur in patients, it is possible that certain DJ-1 mutations

may contribute to disease as a consequence of proteasome impairments and/or impairments in other protein degradation machineries. Our studies also revealed that parkin mutations, such as T240R and E399Q, may disrupt parkin E3 ligase function. In patients harboring parkin mutations, accumulation of parkin substrates such as synphilin-1 may work to induce proteolytic stress and this may act to instigate subsequent disease. The latter idea is supported in the literature (212;265;461). Further, in agreement with previous studies (131;247;444), we showed that pathogenic mutant A53T α-syn protein tended to aggregate in mice, forming intracellular inclusions that were reminiscent of LB pathologies, similar to those observed in patients with disease. We did not investigate the effects of α-syn inclusion formation on activities of the proteasome or other known cellular proteases. Studies by other groups have attempted to address this question; however many of the reported findings are in disagreement (280;319;410). We showed that many of the α-syn inclusions in mice were positive for ubiquitin, and this finding may support a role for the ubiquitin-proteasome pathway in clearing misfolded forms of pathogenic α-syn protein *in vivo*. Taken together, we provide evidence to suggest that therapeutic strategies that aim to directly modulate and/or mitigate the effects of impaired protein degradation in humans may help to prevent neurodegeneration observed in PD.

BIBLIOGRAPHY

1. Abeliovich, A., Schmitz, Y., Farinas, I., Choi-Lundberg, D., Ho, W. H., Castillo, P. E., Shinsky, N., Verdugo, J. M., Armanini, M., Ryan, A., Hynes, M., Phillips, H., Sulzer, D., and Rosenthal, A. (2000) *Neuron* **25,** 239-252

2. Abou-Sleiman, P. M., Healy, D. G., Quinn, N., Lees, A. J., and Wood, N. W. (2003) *Ann.Neurol.* **54,** 283-286

3. Abramova, E. B., Sharova, N. P., and Karpov, V. L. (2002) *Mol.Biol.(Mosk)* **36,** 761-776

4. Ahlskog, J. E. (2009) *Parkinsonism.Relat Disord.* **15,** 721-727

5. Ahn, M., Kim, S., Kang, M., Ryu, Y., and Kim, T. D. (2006) *Biochem.Biophys.Res.Commun.* **346,** 1142-1149

6. Alberts, B., Bray, D., Lewis, J., Raff, M., Roberts, K., and Watson, J. D. (1989) Small Molecules, Energy, and Biosynthesis. In Adams, R., editor. *Molecular Biology of the Cell: Second Edition*, Garland Publishing Inc, New York

7. Alerte, T. N., Akinfolarin, A. A., Friedrich, E. E., Mader, S. A., Hong, C. S., and Perez, R. G. (2008) *Neurosci.Lett.* **435,** 24-29

8. Aleyasin, H., Rousseaux, M. W., Marcogliese, P. C., Hewitt, S. J., Irrcher, I., Joselin, A. P., Parsanejad, M., Kim, R. H., Rizzu, P., Callaghan, S. M., Slack, R. S., Mak, T. W., and Park, D. S. (2010) *Proc.Natl.Acad.Sci.U.S.A* **107,** 3186-3191

9. Andersen, J. K. (2004) *Nat.Med.* **10 Suppl,** S18-S25

10. Anderson, J. J., Bravi, D., Ferrari, R., Davis, T. L., Baronti, F., Chase, T. N., and Dagani, F. (1993) *J.Neurol.Neurosurg.Psychiatry* **56,** 477-480

11. Anderson, J. P., Walker, D. E., Goldstein, J. M., de Laat, R., Banducci, K., Caccavello, R. J., Barbour, R., Huang, J., Kling, K., Lee, M., Diep, L., Keim, P. S., Shen, X., Chataway, T., Schlossmacher, M. G., Seubert, P., Schenk, D., Sinha, S., Gai, W. P., and Chilcote, T. J. (2006) *J.Biol.Chem.* **281,** 29739-29752

12. Anderson, P. C. and Daggett, V. (2008) *Biochemistry* **47,** 9380-9393

13. Andres-Mateos, E., Perier, C., Zhang, L., Blanchard-Fillion, B., Greco, T. M., Thomas, B., Ko, H. S., Sasaki, M., Ischiropoulos, H., Przedborski, S., Dawson, T. M., and Dawson, V. L. (2007) *Proc.Natl.Acad.Sci.U.S.A* **104,** 14807-14812

14. Annesi, G., Savettieri, G., Pugliese, P., D'Amelio, M., Tarantino, P., Ragonese, P., La, B., V, Piccoli, T., Civitelli, D., Annesi, F., Fierro, B., Piccoli, F., Arabia, G., Caracciolo, M., Ciro, C., I, and Quattrone, A. (2005) *Ann.Neurol.* **58,** 803-807

15. Apel, K. and Hirt, H. (2004) *Annu.Rev.Plant Biol.* **55,** 373-399

16. Asakawa, S., Tsunematsu, K., Takayanagi, A., Sasaki, T., Shimizu, A., Shintani, A., Kawasaki, K., Mungall, A. J., Beck, S., Minoshima, S., and Shimizu, N. (2001) *Biochem.Biophys.Res.Commun.* **286,** 863-868

17. Athanassiadou, A., Voutsinas, G., Psiouri, L., Leroy, E., Polymeropoulos, M. H., Ilias, A., Maniatis, G. M., and Papapetropoulos, T. (1999) *Am.J.Hum.Genet.* **65,** 555-558

18. Baba, M., Nakajo, S., Tu, P. H., Tomita, T., Nakaya, K., Lee, V. M. Y., Trojanowski, J. Q., and Iwatsubo, T. (1998) *Am.J.Pathol.* **152,** 879-884

19. Bader, V., Ran, Z., X, Lubbert, H., and Stichel, C. C. (2005) *Brain Res.* **1041,** 102-111

20. Ballard, P. A., Tetrud, J. W., and Langston, J. W. (1985) *Neurology* **35,** 949-956

21. Bandopadhyay, R., Kingsbury, A. E., Cookson, M. R., Reid, A. R., Evans, I. M., Hope, A. D., Pittman, A. M., Lashley, T., Canet-Aviles, R., Miller, D. W., McLendon, C., Strand, C., Leonard, A. J., Abou-Sleiman, P. M., Healy, D. G., Ariga, H., Wood, N. W., de Silva, R., Revesz, T., Hardy, J. A., and Lees, A. J. (2004) *Brain* **127,** 420-430

22. Bandopadhyay, R., Kingsbury, A. E., Muqit, M. M., Harvey, K., Reid, A. R., Kilford, L., Engelender, S., Schlossmacher, M. G., Wood, N. W., Latchman, D. S., Harvey, R. J., and Lees, A. J. (2005) *Neurobiol.Dis.* **20,** 401-411

23. Bandyopadhyay, S. and Cookson, M. R. (2004) *BMC.Evol.Biol.* **4,** 6

24. Bansal, B. and Goyal, V. (2008) Role of Levodopa in Late Stage of Parkinson's Disease. In Mehrotra, T. and Bhattacharya, K., editors. *Parkinson's Disease and Movement Disorders*, McGraw-Hill, New York

25. Bansal, B. and Tripathi, M. (2008) Basic Principles in the Pharmacotherapy of Parkinson's Disease. In Mehta, N. D. and Bhattacharyya, K. B., editors. *Parkinson's Disease and Movement Disorders*, McGraw-Hill, New York

26. Bardien, S., Keyser, R., Yako, Y., Lombard, D., and Carr, J. (2009) *Parkinsonism.Relat Disord.* **15,** 116-121

27. Batelli, S., Albani, D., Rametta, R., Polito, L., Prato, F., Pesaresi, M., Negro, A., and Forloni, G. (2008) *PLoS.ONE.* **3,** e1884

28. Baulac, S., LaVoie, M. J., Strahle, J., Schlossmacher, M. G., and Xia, W. (2004) *Mol.Cell Neurosci.* **27,** 236-246

29. Baulac, S., Lu, H., Strahle, J., Yang, T., Goldberg, M. S., Shen, J., Schlossmacher, M. G., Lemere, C. A., Lu, Q., and Xia, W. (2009) *Mol.Neurodegener.* **4,** 12

30. Bear, M. F., Connors, B. W., and Paradiso, M. A. (2007) An Illustrated Guide to Human Neuroanatomy. *Neuroscience: Exploring the Brain*, Lippincott Williams & Wilkins, Philadelphia

31. Bedford, L., Hay, D., Paine, S., Rezvani, N., Mee, M., Lowe, J., and Mayer, R. J. (2008) *Biochim.Biophys.Acta* **1782,** 683-690

32. Belin, A. C. and Westerlund, M. (2008) *FEBS J.* **275,** 1377-1383

33. Bennett, M. C. (2005) *Pharmacol.Ther.* **105,** 311-331

34. Bennett, M. C., Bishop, J. F., Leng, Y., Chock, P. B., Chase, T. N., and Mouradian, M. M. (1999) *J.Biol.Chem.* **274,** 33855-33858

35. Berger, A. K., Cortese, G. P., Amodeo, K. D., Weihofen, A., Letai, A., and LaVoie, M. J. (2009) *Hum.Mol.Genet.* **18,** 4317-4328

36. Berry, C., La Vecchia, C., and Nicotera, P. (2010) *Cell Death.Differ.,* **in press [online]**

37. Betarbet, R., Canet-Aviles, R. M., Sherer, T. B., Mastroberardino, P. G., McLendon, C., Kim, J. H., Lund, S., Na, H. M., Taylor, G., Bence, N. F., Kopito, R., Seo, B. B., Yagi, T., Yagi, A., Klinefelter, G., Cookson, M. R., and Greenamyre, J. T. (2006) *Neurobiol.Dis.* **22,** 404-420

38. Betarbet, R., Sherer, T. B., MacKenzie, G., Garcia-Osuna, M., Panov, A. V., and Greenamyre, J. T. (2000) *Nat.Neurosci.* **3,** 1301-1306

39. Bhattacharyya, K. B. (2008) The Life and Works of James Parkinson. *Parkinson's Disease and Movement Disorders*, McGraw-Hill, New York

40. Bindoff, L. A., Birch-Machin, M. A., Cartlidge, N. E., Parker, W. D., Jr., and Turnbull, D. M. (1991) *J.Neurol.Sci.* **104,** 203-208

41. Biskup, S., Gerlach, M., Kupsch, A., Reichmann, H., Riederer, P., Vieregge, P., Wullner, U., and Gasser, T. (2008) *J.Neurol.* **255 Suppl 5,** 8-17

42. Blackinton, J., Ahmad, R., Miller, D. W., van der Brug, M. P., Canet-Aviles, R. M., Hague, S. M., Kaleem, M., and Cookson, M. R. (2005) *Brain Res.Mol.Brain Res.* **134,** 76-83

43. Blackinton, J., Lakshminarasimhan, M., Thomas, K. J., Ahmad, R., Greggio, E., Raza, A. S., Cookson, M. R., and Wilson, M. A. (2009) *J.Biol.Chem.* **284,** 6476-6485

44. Bonifati, V. (2007) *Parkinsonism.Relat Disord.* **13 Suppl 3,** S233-S241

45. Bonifati, V., Breedveld, G. J., Squitieri, F., Vanacore, N., Brustenghi, P., Harhangi, B. S., Montagna, P., Cannella, M., Fabbrini, G., Rizzu, P., van Duijn, C. M., Oostra, B. A., Meco, G., and Heutink, P. (2002) *Ann.Neurol.* **51,** 253-256

46. Bonifati, V., Rizzu, P., Squitieri, F., Krieger, E., Vanacore, N., van Swieten, J. C., Brice, A., van Duijn, C. M., Oostra, B., Meco, G., and Heutink, P. (2003) *Neurol.Sci.* **24,** 159-160

47. Bonifati, V., Rizzu, P., van Baren, M. J., Schaap, O., Breedveld, G. J., Krieger, E., Dekker, M. C., Squitieri, F., Ibanez, P., Joosse, M., van Dongen, J. W., Vanacore, N., van Swieten, J. C., Brice, A., Meco, G., van Duijn, C. M., Oostra, B. A., and Heutink, P. (2003) *Science* **299,** 256-259

48. Bove, J., Prou, D., Perier, C., and Przedborski, S. (2005) *NeuroRx* **2,** 484-494

49. Brooks, A. I., Chadwick, C. A., Gelbard, H. A., Cory-Slechta, D. A., and Federoff, H. J. (1999) *Brain Res.* **823,** 1-10

50. Burns, R. S., Markey, S. P., Phillips, J. M., and Chiueh, C. C. (1984) *Can.J.Neurol.Sci.* **11,** 166-168

51. Cabin, D. E., Gispert-Sanchez, S., Murphy, D., Auburger, G., Myers, R. R., and Nussbaum, R. L. (2005) *Neurobiol.Aging* **26,** 25-35

52. Cairns, N. J., Uryu, K., Bigio, E. H., Mackenzie, I. R., Gearing, M., Duyckaerts, C., Yokoo, H., Nakazato, Y., Jaros, E., Perry, R. H., Arnold, S. E., Lee, V. M., and Trojanowski, J. Q. (2004) *Acta Neuropathol.* **108,** 213-223

53. Canet-Aviles, R. M., Wilson, M. A., Miller, D. W., Ahmad, R., McLendon, C., Bandyopadhyay, S., Baptista, M. J., Ringe, D., Petsko, G. A., and Cookson, M. R. (2004) *Proc.Natl.Acad.Sci.U.S.A* **101,** 9103-9108

54. Cannon, J. R., Tapias, V., Na, H. M., Honick, A. S., Drolet, R. E., and Greenamyre, J. T. (2009) *Neurobiol.Dis.* **34,** 279-290

55. Casarejos, M. J., Menendez, J., Solano, R. M., Rodriguez-Navarro, J. A., Garcia, d. Y., and Mena, M. A. (2006) *J.Neurochem.* **97,** 934-946

56. Cha, G. H., Kim, S., Park, J., Lee, E., Kim, M., Lee, S. B., Kim, J. M., Chung, J., and Cho, K. S. (2005) *Proc.Natl.Acad.Sci.U.S.A* **102,** 10345-10350

57. Cha, S. S., Jung, H. I., Jeon, H., An, Y. J., Kim, I. K., Yun, S., Ahn, H. J., Chung, K. C., Lee, S. H., Suh, P. G., and Kang, S. O. (2008) *J.Biol.Chem.* **283,** 34069-34075

58. Chade, A., Kasten, M., and Tanner, C. M. (2007) Epidemiology of Parkinson's Disease. In Dawson, T. M., editor. *Parkinson's Disease: Genetics and Pathogenesis*, Informa Healthcare USA, Inc., New York

59. Chandra, S., Gallardo, G., Fernández-Chacón, R., Schlüter, O. M., and Südhof, T. C. (2005) *Cell* **123,** 383-396

60. Chandran, J. S., Lin, X., Zapata, A., Hoke, A., Shimoji, M., Moore, S. O., Galloway, M. P., Laird, F. M., Wong, P. C., Price, D. L., Bailey, K. R., Crawley, J. N., Shippenberg, T., and Cai, H. (2008) *Neurobiol.Dis.* **29,** 505-514

61. Chartier-Harlin, M. C., Kachergus, J., Roumier, C., Mouroux, V., Douay, X., Lincoln, S., Levecque, C., Larvor, L., Andrieux, J., Hulihan, M., Waucquier, N., Defebvre, L., Amouyel, P., Farrer, M., and Destee, A. (2004) *Lancet* **364,** 1167-1169

62. Chaudhuri, K. R., Healy, D. G., and Schapira, A. H. (2006) *Lancet Neurol.* **5,** 235-245

63. Chen, L., Cagniard, B., Mathews, T., Jones, S., Koh, H. C., Ding, Y., Carvey, P. M., Ling, Z., Kang, U. J., and Zhuang, X. (2005) *J.Biol.Chem.* **280,** 21418-21426

64. Chinta, S. J. and Andersen, J. K. (2008) *Biochim.Biophys.Acta* **1780,** 1362-1367

65. Choi, J., Sullards, M. C., Olzmann, J. A., Rees, H. D., Weintraub, S. T., Bostwick, D. E., Gearing, M., Levey, A. I., Chin, L. S., and Li, L. (2006) *J.Biol.Chem.* **281,** 10816-10824

66. Choi, J. M., Woo, M. S., Ma, H. I., Kang, S. Y., Sung, Y. H., Yong, S. W., Chung, S. J., Kim, J. S., Shin, H. W., Lyoo, C. H., Lee, P. H., Baik, J. S., Kim, S. J., Park, M. Y., Sohn, Y. H., Kim, J. H., Kim, J. W., Lee, M. S., Lee, M. C., Kim, D. H., and Kim, Y. J. (2008) *Neurogenetics.* **9,** 263-269

67. Choi, P., Ostrerova-Golts, N., Sparkman, D., Cochran, E., Lee, J. M., and Wolozin, B. (2000) *Neuroreport* **11,** 2635-2638

68. Choi, P., Snyder, H., Petrucelli, L., Theisler, C., Chong, M., Zhang, Y., Lim, K., Chung, K. K., Kehoe, K., D'Adamio, L., Lee, J. M., Cochran, E., Bowser, R., Dawson, T. M., and Wolozin, B. (2003) *Brain Res.Mol.Brain Res.* **117,** 179-189

69. Chowdhury, I., Mo, Y., Gao, L., Kazi, A., Fisher, A. B., and Feinstein, S. I. (2009) *Free Radic.Biol.Med.* **46,** 146-153

70. Chu, Y. and Kordower, J. H. (2007) *Neurobiol.Dis.* **25,** 134-149

71. Chung, K. K., Thomas, B., Li, X., Pletnikova, O., Troncoso, J. C., Marsh, L., Dawson, V. L., and Dawson, T. M. (2004) *Science* **304,** 1328-1331

72. Chung, K. K., Zhang, Y., Lim, K. L., Tanaka, Y., Huang, H., Gao, J., Ross, C. A., Dawson, V. L., and Dawson, T. M. (2001) *Nat.Med.* **7,** 1144-1150

73. Ciechanover, A. (1994) *Cell* **79,** 13-21

74. Ciechanover, A. (2001) *Nat.Med.* **7,** 1108-1109

75. Clark, I. E., Dodson, M. W., Jiang, C., Cao, J. H., Huh, J. R., Seol, J. H., Yoo, S. J., Hay, B. A., and Guo, M. (2006) *Nature* **441,** 1162-1166

76. Clayton, D. F. and George, J. M. (1999) *J.Neurosci.Res.* **58,** 120-129

77. Clements, C. M., McNally, R. S., Conti, B. J., Mak, T. W., and Ting, J. P. (2006) *Proc.Natl.Acad.Sci.U.S.A* **103,** 15091-15096

78. Cohen, G. and Heikkila, R. E. (1974) *J.Biol.Chem.* **249,** 2447-2452

79. Cook, C. and Petrucelli, L. (2009) *Biochim.Biophys.Acta* **1792,** 664-675

80. Cookson, M. R. (2005) *Annu.Rev.Biochem.* **74,** 29-52

81. Cookson, M. R., Lockhart, P. J., McLendon, C., O'Farrell, C., Schlossmacher, M., and Farrer, M. J. (2003) *Hum.Mol.Genet.* **12,** 2957-2965

82. Corti, O., Hampe, C., Darios, F., Ibanez, P., Ruberg, M., and Brice, A. (2005) *C.R.Biol.* **328,** 131-142

83. Corti, O., Hampe, C., Koutnikova, H., Darios, F., Jacquier, S., Prigent, A., Robinson, J. C., Pradier, L., Ruberg, M., Mirande, M., Hirsch, E., Rooney, T., Fournier, A., and Brice, A. (2003) *Hum.Mol.Genet.* **12,** 1427-1437

84. D'Agata, V., Zhao, W., Pascale, A., Zohar, O., Scapagnini, G., and Cavallaro, S. (2002) *Prog.Neuropsychopharmacol.Biol.Psychiatry* **26,** 519-527

85. da Costa, C. A., Sunyach, C., Giaime, E., West, A., Corti, O., Brice, A., Safe, S., Abou-Sleiman, P. M., Wood, N. W., Takahashi, H., Goldberg, M. S., Shen, J., and Checler, F. (2009) *Nat.Cell Biol.* **11,** 1370-1375

86. Damier, P., Hirsch, E. C., Agid, Y., and Graybiel, A. M. (1999) *Brain* **122 (Pt 8),** 1437-1448

87. Davis, G. C., Williams, A. C., Markey, S. P., Ebert, M. H., Caine, E. D., Reichert, C. M., and Kopin, I. J. (1979) *Psychiatry Res.* **1,** 249-254

88. Dawson, T. M. and Dawson, V. L. (2003) *Science* **302,** 819-822

89. Day, B. J., Patel, M., Calavetta, L., Chang, L. Y., and Stamler, J. S. (1999) *Proc.Natl.Acad.Sci.U.S.A* **96,** 12760-12765

90. de Rijk, M. C., Tzourio, C., Breteler, M. M., Dartigues, J. F., Amaducci, L., Lopez-Pousa, S., Manubens-Bertran, J. M., Alperovitch, A., and Rocca, W. A. (1997) *J.Neurol.Neurosurg.Psychiatry* **62,** 10-15

91. Deeg, S., Gralle, M., Sroka, K., Bahr, M., Wouters, F. S., and Kermer, P. (2010) *J.Cell Biol.* **188,** 505-513

92. Delong, M. R. (2000) Basal Ganglia. In Kandel, E. R., Schwartz, J. H., and Jessell, T. M., editors. *Principles of Neural Science*, McGraw-Hill, New York

93. Deng, H., Dodson, M. W., Huang, H., and Guo, M. (2008) *Proc.Natl.Acad.Sci.U.S.A* **105,** 14503-14508

94. Deutch, A. Y. and Winder, D. G. (2006) *Nat.Med.* **12,** 17-18

95. Devi, L., Raghavendran, V., Prabhu, B. M., Avadhani, N. G., and Anandatheerthavarada, H. K. (2008) *J.Biol.Chem.* **283,** 9089-9100

96. Di Fonzo, A., Dekker, M. C., Montagna, P., Baruzzi, A., Yonova, E. H., Correia, G. L., Szczerbinska, A., Zhao, T., Dubbel-Hulsman, L. O., Wouters, C. H., de Graaff, E., Oyen, W. J., Simons, E. J., Breedveld, G. J., Oostra, B. A., Horstink, M. W., and Bonifati, V. (2009) *Neurology* **72,** 240-245

97. Dick, L. R., Cruikshank, A. A., Grenier, L., Melandri, F. D., Nunes, S. L., and Stein, R. L. (1996) *J.Biol.Chem.* **271,** 7273-7276

98. Djarmati, A., Hedrich, K., Svetel, M., Schafer, N., Juric, V., Vukosavic, S., Hering, R., Riess, O., Romac, S., Klein, C., and Kostic, V. (2004) *Hum.Mutat.* **23,** 525

99. Dodson, M. W. and Guo, M. (2007) *Curr.Opin.Neurobiol.* **17,** 331-337

100. Doss-Pepe, E. W., Chen, L., and Madura, K. (2005) *J.Biol.Chem.* **280,** 16619-16624

101. Droge, W. (2002) *Physiol Rev.* **82,** 47-95

102. Duda, J. E., Giasson, B. I., Gur, T. L., Montine, T. J., Robertson, D., Biaggioni, I., Hurtig, H. I., Stern, M. B., Gollomp, S. M., Grossman, M., Lee, V. M., and Trojanowski, J. Q. (2000) *J.Neuropathol.Exp.Neurol.* **59,** 830-841

103. Elkon, H., Don, J., Melamed, E., Ziv, I., Shirvan, A., and Offen, D. (2002) *J.Mol.Neurosci.* **18,** 229-238

104. Engelender, S., Kaminsky, Z., Guo, X., Sharp, A. H., Amaravi, R. K., Kleiderlein, J. J., Margolis, R. L., Troncoso, J. C., Lanahan, A. A., Worley, P. F., Dawson, V. L., Dawson, T. M., and Ross, C. A. (1999) *Nat.Genet.* **22,** 110-114

105. Fahn, S. (2007) Treatment of Parkinson's Disease. In Dawson, T. M., editor. *Parkinson's Disease: Genetics and Pathogenesis*, Informa Healthcare USA, Inc., New York

106. Farrer, M., Chan, P., Chen, R., Tan, L., Lincoln, S., Hernandez, D., Forno, L., Gwinn-Hardy, K., Petrucelli, L., Hussey, J., Singleton, A., Tanner, C., Hardy, J., and Langston, J. W. (2001) *Ann.Neurol.* **50,** 293-300

107. Farrer, M., Kachergus, J., Forno, L., Lincoln, S., Wang, D. S., Hulihan, M., Maraganore, D., Gwinn-Hardy, K., Wszolek, Z., Dickson, D., and Langston, J. W. (2004) *Ann.Neurol.* **55,** 174-179

108. Fenteany, G., Standaert, R. F., Lane, W. S., Choi, S., Corey, E. J., and Schreiber, S. L. (1995) *Science* **268,** 726-731

109. Fitzgerald, J. C. and Plun-Favreau, H. (2008) *FEBS J.* **275,** 5758-5766

110. Forman, M. S., Lee, V. M., and Trojanowski, J. Q. (2005) *Neuron* **47,** 479-482

111. Fornai, F., Schluter, O. M., Lenzi, P., Gesi, M., Ruffoli, R., Ferrucci, M., Lazzeri, G., Busceti, C. L., Pontarelli, F., Battaglia, G., Pellegrini, A., Nicoletti, F., Ruggieri, S., Paparelli, A., and Sudhof, T. C. (2005) *Proc.Natl.Acad.Sci.U.S.A* **102,** 3413-3418

112. Forno, L. S. (1996) *J.Neuropathol.Exp.Neurol.* **55,** 259-272

113. Forno, L. S., Langston, J. W., DeLanney, L. E., and Irwin, I. (1988) *Brain Res.* **448,** 150-157

114. Forno, L. S., Langston, J. W., DeLanney, L. E., Irwin, I., and Ricaurte, G. A. (1986) *Ann.Neurol.* **20,** 449-455

115. Fournier, M., Vitte, J., Garrigue, J., Langui, D., Dullin, J. P., Saurini, F., Hanoun, N., Perez-Diaz, F., Cornilleau, F., Joubert, C., Ardila-Osorio, H., Traver, S., Duchateau, R., Goujet-Zalc, C., Paleologou, K., Lashuel, H. A., Haass, C., Duyckaerts, C., Cohen-Salmon, C., Kahle, P. J., Hamon, M., Brice, A., and Corti, O. (2009) *PLoS.ONE.* **4,** e6629

116. Frank-Cannon, T. C., Tran, T., Ruhn, K. A., Martinez, T. N., Hong, J., Marvin, M., Hartley, M., Trevino, I., O'Brien, D. E., Casey, B., Goldberg, M. S., and Tansey, M. G. (2008) *J.Neurosci.* **28,** 10825-10834

117. Fujiwara, H., Hasegawa, M., Dohmae, N., Kawashima, A., Masliah, E., Goldberg, M. S., Shen, J., Takio, K., and Iwatsubo, T. (2002). *Nat.Cell Biol*. **4**, 160-164. 2002.

118. Funayama, M., Hasegawa, K., Kowa, H., Saito, M., Tsuji, S., and Obata, F. (2002) *Ann.Neurol.* **51,** 296-301

119. Gai, W. P., Yuan, H. X., Li, X. Q., Power, J. T., Blumbergs, P. C., and Jensen, P. H. (2000) *Exp.Neurol.* **166,** 324-333

120. Gallagher, M. J., Huang, H., Grant, E. R., and Lynch, D. R. (1997) *J.Biol.Chem.* **272,** 24971-24979

121. Galter, D., Westerlund, M., Belin, A. C., and Olson, L. (2007) *Physiol Behav.* **92,** 46-53

122. Galvin, J. E., Lee, V. M., and Trojanowski, J. Q. (2001) *Arch.Neurol.* **58,** 186-190

123. Gao, H. M. and Hong, J. S. (2008) *Trends Immunol.* **29,** 357-365

124. Gasser, T. (2009) *Biochim.Biophys.Acta* **1792,** 587-596

125. Gasser, T., Muller-Myhsok, B., Wszolek, Z. K., Oehlmann, R., Calne, D. B., Bonifati, V., Bereznai, B., Fabrizio, E., Vieregge, P., and Horstmann, R. D. (1998) *Nat.Genet.* **18,** 262-265

126. Geisler, S., Holmstrom, K., Skujat, D., Fiesel, F., Rothfuss, O., Kahle, P., and Springer, W. (2010) *Nat.Cell Biol.* **12,** 119-131

127. Gelb, D. J., Oliver, E., and Gilman, S. (1999) *Arch.Neurol.* **56,** 33-39

128. Ghosh, B. and Kumar Das, S. (2008) Epidemiology of Movement Disorders in India and Other Countries. In Mehrotra, T. and Bhattacharyya, K. B., editors. *Parkinson's Disease and Movement Disorders*, McGraw-Hill, New York

129. Giaime, E., Sunyach, C., Druon, C., Scarzello, S., Robert, G., Grosso, S., Auberger, P., Goldberg, M. S., Shen, J., Heutink, P., Pouyssegur, J., Pages, G., Checler, F., and Alves, d. C. (2010) *Cell Death.Differ.* **17,** 158-169

130. Giasson, B. I., Duda, J. E., Murray, I. V., Chen, Q., Souza, J. M., Hurtig, H. I., Ischiropoulos, H., Trojanowski, J. Q., and Lee, V. M. (2000) *Science* **290,** 985-989

131. Giasson, B. I., Duda, J. E., Quinn, S. M., Zhang, B., Trojanowski, J. Q., and Lee, V. M. (2002) *Neuron* **34,** 521-533

132. Giasson, B. I., Jakes, R., Goedert, M., Duda, J. E., Leight, S., Trojanowski, J. Q., and Lee, V. M. (2000) *J.Neurosci.Res.* **59,** 528-533

133. Goedert, M. (2001) *Nat.Rev.Neurosci.* **2**, 492-501.

134. Golbe, L. I., Di Iorio, G., Bonavita, V., Miller, D. C., and Duvoisin, R. C. (1990) *Ann.Neurol.* **27,** 276-282

135. Goldberg, M. S., Fleming, S. M., Palacino, J. J., Cepeda, C., Lam, H. A., Bhatnagar, A., Meloni, E. G., Wu, N., Ackerson, L. C., Klapstein, G. J., Gajendiran, M., Roth, B. L., Chesselet, M. F., Maidment, N. T., Levine, M. S., and Shen, J. (2003) *J.Biol.Chem.* **278,** 43628-43635

136. Goldberg, M. S., Pisani, A., Haburcak, M., Vortherms, T. A., Kitada, T., Costa, C., Tong, Y., Martella, G., Tscherter, A., Martins, A., Bernardi, G., Roth, B. L., Pothos, E. N., Calabresi, P., and Shen, J. (2005) *Neuron* **45,** 489-496

137. Gonzalez-Polo, R., Niso-Santano, M., Moran, J. M., Ortiz-Ortiz, M. A., Bravo-San Pedro, J. M., Soler, G., and Fuentes, J. M. (2009) *J.Neurochem.* **109,** 889-898

138. Gorner, K., Holtorf, E., Odoy, S., Nuscher, B., Yamamoto, A., Regula, J. T., Beyer, K., Haass, C., and Kahle, P. J. (2004) *J.Biol.Chem.* **279,** 6943-6951

139. Gorner, K., Holtorf, E., Waak, J., Pham, T. T., Vogt-Weisenhorn, D. M., Wurst, W., Haass, C., and Kahle, P. J. (2007) *J.Biol.Chem.* **282,** 13680-13691

140. Graham, D. G. (1978) *Mol.Pharmacol.* **14,** 633-643

141. Greene, J. C., Whitworth, A. J., Kuo, I., Andrews, L. A., Feany, M. B., and Pallanck, L. J. (2003) *Proc.Natl.Acad.Sci.U.S.A* **100,** 4078-4083

142. Gu, L., Cui, T., Fan, C., Zhao, H., Zhao, C., Lu, L., and Yang, H. (2009) *Biochem.Biophys.Res.Commun.* **383,** 469-474

143. Gu, W. J., Corti, O., Araujo, F., Hampe, C., Jacquier, S., Lucking, C. B., Abbas, N., Duyckaerts, C., Rooney, T., Pradier, L., Ruberg, M., and Brice, A. (2003) *Neurobiol.Dis.* **14,** 357-364

144. Guo, J. F., Xiao, B., Liao, B., Zhang, X. W., Nie, L. L., Zhang, Y. H., Shen, L., Jiang, H., Xia, K., Pan, Q., Yan, X. X., and Tang, B. S. (2008) *Mov Disord.* **23,** 2074-2079

145. Haas, R. H., Nasirian, F., Nakano, K., Ward, D., Pay, M., Hill, R., and Shults, C. W. (1995) *Ann.Neurol.* **37,** 714-722

146. Hague, S., Rogaeva, E., Hernandez, D., Gulick, C., Singleton, A., Hanson, M., Johnson, J., Weiser, R., Gallardo, M., Ravina, B., Gwinn-Hardy, K., Crawley, A., George-Hyslop, P. H., Lang, A. E., Heutink, P., Bonifati, V., Hardy, J., and Singleton, A. (2003) *Ann.Neurol.* **54,** 271-274

147. Hall, A., Karplus, P. A., and Poole, L. B. (2009) *FEBS J.* **276,** 2469-2477

148. Hampe, C., Ardila-Osorio, H., Fournier, M., Brice, A., and Corti, O. (2006) *Hum.Mol.Genet.***15***,* 2059-2075

149. Hanada, M., Suguwara, K., Kaneta, K., Toda, S., Nishiyama, Y., Tomita, K., Yamaoto, H., and Konishi, M. (1992) *J.Antibiot.(Tokyo)* **45,** 1746-1752

150. Hasegawa, M., Fujiwara, H., Nonaka, T., Wakabayashi, K., Takahashi, H., Lee, V. M., Trojanowski, J. Q., Mann, D., and Iwatsubo, T. (2002) *J.Biol.Chem.* **277,** 49071-49076

151. Hasegawa, T., Treis, A., Patenge, N., Fiesel, F., Springer, W., and Kahle, P. (2008) *J.Neurochem.* **105,** 1700-1715

152. Hatano, T., Kubo, S., Sato, S., and Hattori, N. (2009) *J.Neurochem.* **111,** 1075-1093

153. Hayashi, T., Ishimori, C., Takahashi-Niki, K., Taira, T., Kim, Y. C., Maita, H., Maita, C., Ariga, H., and Iguchi-Ariga, S. M. (2009) *Biochem.Biophys.Res.Commun.* **390,** 667-672

154. Hedrich, K., Djarmati, A., Schafer, N., Hering, R., Wellenbrock, C., Weiss, P. H., Hilker, R., Vieregge, P., Ozelius, L. J., Heutink, P., Bonifati, V., Schwinger, E., Lang, A. E., Noth, J., Bressman, S. B., Pramstaller, P. P., Riess, O., and Klein, C. (2004) *Neurology* **62,** 389-394

155. Hedrich, K., Eskelson, C., Wilmot, B., Marder, K., Harris, J., Garrels, J., Meija-Santana, H., Vieregge, P., Jacobs, H., Bressman, S. B., Lang, A. E., Kann, M., Abbruzzese, G., Martinelli, P., Schwinger, E., Ozelius, L. J., Pramstaller, P. P., Klein, C., and Kramer, P. (2004) *Mov Disord.* **19,** 1146-1157

156. Henn, I. H., Bouman, L., Schlehe, J. S., Schlierf, A., Schramm, J. E., Wegener, E., Nakaso, K., Culmsee, C., Berninger, B., Krappmann, D., Tatzelt, J., and Winklhofer, K. F. (2007) *J.Neurosci.* **27,** 1868-1878

157. Hering, R., Strauss, K. M., Tao, X., Bauer, A., Woitalla, D., Mietz, E. M., Petrovic, S., Bauer, P., Schaible, W., Muller, T., Schols, L., Klein, C., Berg, D., Meyer, P. T., Schulz, J. B., Wollnik, B., Tong, L., Kruger, R., and Riess, O. (2004) *Hum.Mutat.* **24,** 321-329

158. Herrera, F. E., Zucchelli, S., Jezierska, A., Lavina, Z. S., Gustincich, S., and Carloni, P. (2007) *J.Biol.Chem.* **282,** 24905-24914

159. Hershko, A. (1996) *Trends Biochem.Sci.* **21,** 445-449

160. Hershko, A. and Ciechanover, A. (1998) *Annu.Rev.Biochem.* **67,** 425-479

161. Hicks, A. A., Petursson, H., Jonsson, T., Stefansson, H., Johannsdottir, H. S., Sainz, J., Frigge, M. L., Kong, A., Gulcher, J. R., Stefansson, K., and Sveinbjornsdottir, S. (2002) *Ann.Neurol.* **52,** 549-555

162. Hirsch, E., Graybiel, A. M., and Agid, Y. A. (1988) *Nature* **334,** 345-348

163. Hod, Y., Pentyala, S. N., Whyard, T. C., and El Maghrabi, M. R. (1999) *J.Cell Biochem.* **72,** 435-444

164. Hoehn, M. M. and Yahr, M. D. (1967) *Neurology* **17,** 427-442

165. Hoglinger, G. U., Feger, J., Prigent, A., Michel, P. P., Parain, K., Champy, P., Ruberg, M., Oertel, W. H., and Hirsch, E. C. (2003) *J.Neurochem.* **84,** 491-502

166. Holdorff, B. (2006) *J.Neurol.* **253,** 677-678

167. Honbou, K., Suzuki, N. N., Horiuchi, M., Taira, T., Niki, T., Ariga, H., and Inagaki, F. (2003) *Acta Crystallogr.D.Biol.Crystallogr.* **59,** 1502-1503

168. Horgan, D. J. and Singer, T. P. (1967) *Biochem.Biophys.Res.Commun.* **27,** 356-360

169. Hsu, L. J., Sagara, Y., Arroyo, A., Rockenstein, E., Sisk, A., Mallory, M., Wong, J., Takenouchi, T., Hashimoto, M., and Masliah, E. (2000) *Am.J.Pathol.* **157,** 401-410

170. Huai, Q., Sun, Y., Wang, H., Chin, L. S., Li, L., Robinson, H., and Ke, H. (2003) *FEBS Lett.* **549,** 171-175

171. Hulleman, J. D., Mirzaei, H., Guigard, E., Taylor, K. L., Ray, S. S., Kay, C. M., Regnier, F. E., and Rochet, J. C. (2007) *Biochemistry* **46,** 5776-5789

172. Huynh, D. P., Dy, M., Nguyen, D., Kiehl, T. R., and Pulst, S. M. (2001) *Brain Res.Dev.Brain Res.* **130,** 173-181

173. Huynh, D. P., Scoles, D. R., Nguyen, D., and Pulst, S. M. (2003) *Hum.Mol.Genet.* **12,** 2587-2597

174. Hyun, D. H., Lee, M., Halliwell, B., and Jenner, P. (2005) *J.Neurosci.Res.* **82,** 232-244

175. Hyun, D. H., Lee, M., Hattori, N., Kubo, S., Mizuno, Y., Halliwell, B., and Jenner, P. (2002) *J.Biol.Chem.* **277,** 28572-28577

176. Ibanez, P., Bonnet, A. M., Debarges, B., Lohmann, E., Tison, F., Pollak, P., Agid, Y., Durr, A., and Brice, A. (2004) *Lancet* **364,** 1169-1171

177. Imai, Y., Soda, M., Inoue, H., Hattori, N., Mizuno, Y., and Takahashi, R. (2001) *Cell* **105,** 891-902

178. Imai, Y., Soda, M., and Takahashi, R. (2000) *J.Biol.Chem.* **275,** 35661-35664

179. Inden, M., Kitamura, Y., Takeuchi, H., Yanagida, T., Takata, K., Kobayashi, Y., Taniguchi, T., Yoshimoto, K., Kaneko, M., Okuma, Y., Taira, T., Ariga, H., and Shimohama, S. (2007) *J.Neurochem.* **101,** 1491-1504

180. Inden, M., Kitamura, Y., Tamaki, A., Yanagida, T., Shibaike, T., Yamamoto, A., Takata, K., Yasui, H., Taira, T., Ariga, H., and Taniguchi, T. (2009) *Neurochem.Int.* **55,** 760-767

181. Inden, M., Taira, T., Kitamura, Y., Yanagida, T., Tsuchiya, D., Takata, K., Yanagisawa, D., Nishimura, K., Taniguchi, T., Kiso, Y., Yoshimoto, K., Agatsuma, T., Koide-Yoshida, S., Iguchi-Ariga, S. M., Shimohama, S., and Ariga, H. (2006) *Neurobiol.Dis.* **24,** 144-158

182. Irizarry, M. C., Growdon, W., Gomez-Isla, T., Newell, K., George, J. M., Clayton, D. F., and Hyman, B. T. (1998) *J.Neuropathol.Exp.Neurol.* **57,** 334-337

183. Ischiropoulos, H. and Beckman, J. S. (2003) *J.Clin.Invest* **111,** 163-169

184. Ishikawa, A. and Tsuji, S. (1996) *Neurology* **47,** 160-166

185. Ishikawa, S., Taira, T., Niki, T., Takahashi-Niki, K., Maita, C., Maita, H., Ariga, H., and Iguchi-Ariga, S. M. (2009) *J.Biol.Chem.* **284,** 28832-28844

186. Itier, J. M., Ibanez, P., Mena, M. A., Abbas, N., Cohen-Salmon, C., Bohme, G. A., Laville, M., Pratt, J., Corti, O., Pradier, L., Ret, G., Joubert, C., Periquet, M., Araujo, F., Negroni, J., Casarejos, M. J., Canals, S., Solano, R., Serrano, A., Gallego, E., Sanchez, M., Denefle, P., Benavides, J., Tremp, G., Rooney, T. A., Brice, A., and Garcia, d. Y. (2003) *Hum.Mol.Genet.* **12,** 2277-2291

187. Iwai, A., Masliah, E., Yoshimoto, M., Ge, N., Flanagan, L., de Silva, H. A., Kittel, A., and Saitoh, T. (1995) *Neuron* **14,** 467-475

188. Jakes, R., Spillantini, M. G., and Goedert, M. (1994) *FEBS Lett.* **345,** 27-32

189. Jeong, H., Kim, M. S., Kwon, J., Kim, K. S., and Seol, W. (2006) *Neurosci.Lett.* **396,** 57-61

190. Jiang, H., Ren, Y., Zhao, J., and Feng, J. (2004) *Hum.Mol.Genet.* **13,** 1745-1754

191. Jiang, H., Wu, Y. C., Nakamura, M., Liang, Y., Tanaka, Y., Holmes, S., Dawson, V. L., Dawson, T. M., Ross, C. A., and Smith, W. W. (2007) *Neurobiol.Aging* **28,** 1709-1717

192. Jin, J., Meredith, G. E., Chen, L., Zhou, Y., Xu, J., Shie, F. S., Lockhart, P., and Zhang, J. (2005) *Brain Res.Mol.Brain Res.* **134,** 119-138

193. Jin, M. H., Lee, Y. H., Kim, J. M., Sun, H. N., Moon, E. Y., Shong, M. H., Kim, S. U., Lee, S. H., Lee, T. H., Yu, D. Y., and Lee, D. S. (2005) *Neurosci.Lett.* **381,** 252-257

194. Joazeiro, C. A. and Weissman, A. M. (2000) *Cell* **102,** 549-552

195. Jog, M. S. and Almeida, Q. J. (2008) Basal Ganglia: Structure and Function. *Parkinson's Disease and Movement Disorders*, McGraw-Hill, NewYork

196. Junn, E., Jang, W. H., Zhao, X., Jeong, B. S., and Mouradian, M. M. (2009) *J.Neurosci.Res.* **87,** 123-129

197. Junn, E. and Mouradian, M. M. (2002) *Neurosci.Lett.* **320,** 146-150

198. Junn, E., Taniguchi, H., Jeong, B. S., Zhao, X., Ichijo, H., and Mouradian, M. M. (2005) *Proc.Natl.Acad.Sci.U.S.A* **102,** 9691-9696

199. Kahle, P. J., Neumann, M., Ozmen, L., Muller, V., Jacobsen, H., Schindzielorz, A., Okochi, M., Leimer, U., van der, P. H., Probst, A., Kremmer, E., Kretzschmar, H. A., and Haass, C. (2000) *J.Neurosci.* **20,** 6365-6373

200. Kahle, P. J., Waak, J., and Gasser, T. (2009) *Free Radic.Biol.Med.* **47,** 1354-1361

201. Kao, S. Y. (2009) *Biochem.Biophys.Res.Commun.* **382,** 321-325

202. Kawamata, H., McLean, P. J., Sharma, N., and Hyman, B. T. (2001) *J.Neurochem.* **77,** 929-934

203. Keyser, R. J., van der, M. L., Venter, M., Kinnear, C., Warnich, L., Carr, J., and Bardien, S. (2009) *BMC.Med.Genet.* **10,** 105

204. Kim, R. H., Smith, P. D., Aleyasin, H., Hayley, S., Mount, M. P., Pownall, S., Wakeham, A., You, T., Kalia, S. K., Horne, P., Westaway, D., Lozano, A. M., Anisman, H., Park, D. S., and Mak, T. W. (2005) *Proc.Natl.Acad.Sci.U.S.A* **102,** 5215-5220

205. Kim, T. D., Paik, S. R., and Yang, C. H. (2002) *Biochemistry* **41,** 13782-13790

206. Kim, T. D., Paik, S. R., Yang, C. H., and Kim, J. (2000) *Protein Sci.* **9,** 2489-2496

207. Kinumi, T., Kimata, J., Taira, T., Ariga, H., and Niki, E. (2004) *Biochem.Biophys.Res.Commun.* **317,** 722-728

208. Kitada, T., Asakawa, S., Hattori, N., Matsumine, H., Yamamura, Y., Minoshima, S., Yokochi, M., Mizuno, Y., and Shimizu, N. (1998) *Nature* **392,** 605-608

209. Kitada, T., Asakawa, S., Matsumine, H., Hattori, N., Minoshima, S., Shimizu, N., and Mizuno, Y. (1999) *Parkinsonism.Relat Disord.* **5,** 163-168

210. Kitada, T., Asakawa, S., Minoshima, S., Mizuno, Y., and Shimizu, N. (2000) *Mamm.Genome* **11,** 417-421

211. Kitada, T., Tong, Y., Gautier, C. A., and Shen, J. (2009) *J.Neurochem.* **111,** 696-702

212. Kitao, Y., Imai, Y., Ozawa, K., Kataoka, A., Ikeda, T., Soda, M., Nakimawa, K., Kiyama, H., Stern, D. M., Hori, O., Wakamatsu, K., Ito, S., Itohara, S., Takahashi, R., and Ogawa, S. (2007) *Hum.Mol.Genet.* **16,** 50-60

213. Klein, C. (2006) *Arch.Neurol.* **63,** 328-334

214. Klein, C., Djarmati, A., Hedrich, K., Schafer, N., Scaglione, C., Marchese, R., Kock, N., Schule, B., Hiller, A., Lohnau, T., Winkler, S., Wiegers, K., Hering, R., Bauer, P., Riess, O., Abbruzzese, G., Martinelli, P., and Pramstaller, P. P. (2005) *Eur.J.Hum.Genet.* **13,** 1086-1093

215. Klein, J. A. and Ackerman, S. L. (2003) *J.Clin.Invest* **111,** 785-793

216. Ko, H. S., Kim, S. W., Sriram, S. R., Dawson, V. L., and Dawson, T. M. (2006) *J.Biol.Chem.* **281***,* 16193-16196

217. Ko, H. S., von Coelln, R., Sriram, S. R., Kim, S. W., Chung, K. K., Pletnikova, O., Troncoso, J., Johnson, B., Saffary, R., Goh, E. L., Song, H., Park, B. J., Kim, M. J., Kim, S., Dawson, V. L., and Dawson, T. M. (2005) *J.Neurosci.* **25,** 7968-7978

218. Kotaria, N., Hinz, U., Zechel, S., and Bohlen Und, H. O. (2005) *Cell Tissue Res.* **322,** 503-507

219. Kovari, E., Horvath, J., and Bouras, C. (2009) *Brain Res.Bull.* **80,** 203-210

220. Kowall, N. W., Hantraye, P., Brouillet, E., Beal, M. F., McKee, A. C., and Ferrante, R. J. (2000) *Neuroreport* **11,** 211-213

221. Kowaltowski, A. J., Souza-Pinto, N. C., Castilho, R. F., and Vercesi, A. E. (2009) *Free Radic.Biol.Med.* **47,** 333-343

222. Krapfenbauer, K., Engidawork, E., Cairns, N., Fountoulakis, M., and Lubec, G. (2003) *Brain Res.* **967,** 152-160

223. Krige, D., Carroll, M. T., Cooper, J. M., Marsden, C. D., and Schapira, A. H. (1992) *Ann.Neurol.* **32,** 782-788

224. Kruger, R., Kuhn, W., Muller, T., Woitalla, D., Graeber, M., Kosel, S., Przuntek, H., Epplen, J. T., Schols, L., and Riess, O. (1998) *Nat.Genet.* **18,** 106-108

225. Krukoff, B. and Smith, A. (1937) *Am. J. Bot.* **24,** 573-587

226. Kuhn, K., Zhu, X. R., Lubbert, H., and Stichel, C. C. (2004) *Brain Res.Dev.Brain Res.* **149,** 131-142

227. Kumaran, R., Kingsbury, A., Coulter, I., Lashley, T., Williams, D., de Silva, R., Mann, D., Revesz, T., Lees, A., and Bandopadhyay, R. (2007) *Neurobiol.Dis.* **28,** 122-132

228. Kumaran, R., Vandrovcova, J., Luk, C., Sharma, S., Renton, A., Wood, N. W., Hardy, J. A., Lees, A. J., and Bandopadhyay, R. (2009) *Neurobiol.Dis.* **36,** 393-400

229. Kuroda, Y., Mitsui, T., Kunishige, M., and Matsumoto, T. (2006) *Biochem.Biophys.Res.Commun.* **348,** 787-793

230. Kuroda, Y., Mitsui, T., Kunishige, M., Shono, M., Akaike, M., Azuma, H., and Matsumoto, T. (2006) *Hum.Mol.Genet.* **15,** 883-895

231. Kuter, K., Smialowska, M., Wieronska, J., Zieba, B., Wardas, J., Pietraszek, M., Nowak, P., Biedka, I., Roczniak, W., Konieczny, J., Wolfarth, S., and Ossowska, K. (2007) *Brain Res.* **1155,** 196-207

232. Kuzuhara, S., Mori, H., Izumiyama, N., Yoshimura, M., and Ihara, Y. (1988) *Acta Neuropathol.(Berl)* **75,** 345-353

233. Lakshminarasimhan, M., Maldonado, M. T., Zhou, W., Fink, A. L., and Wilson, M. A. (2008) *Biochemistry* **47,** 1381-1392

234. Lang, A. E. and Lozano, A. M. (1998) *N.Engl.J.Med.* **339,** 1044-1053

235. Lang, A. E. and Lozano, A. M. (1998) *N.Engl.J.Med.* **339,** 1130-1143

236. Langston, J. W. and Ballard, P. (1984) *Can.J.Neurol.Sci.* **11,** 160-165

237. Langston, J. W., Ballard, P., Tetrud, J. W., and Irwin, I. (1983) *Science* **219,** 979-980

238. Langston, J. W., Forno, L. S., Rebert, C. S., and Irwin, I. (1984) *Brain Res.* **292,** 390-394

239. Langston, J. W., Forno, L. S., Tetrud, J., Reeves, A. G., Kaplan, J. A., and Karluk, D. (1999) *Ann.Neurol.* **46,** 598-605

240. Lapointe, N., St Hilaire, M., Martinoli, M. G., Blanchet, J., Gould, P., Rouillard, C., and Cicchetti, F. (2004) *FASEB J.* **18,** 717-719

241. Lautier, C., Goldwurm, S., Durr, A., Giovannone, B., Tsiaras, W. G., Pezzoli, G., Brice, A., and Smith, R. J. (2008) *Am.J.Hum.Genet.* **82,** 822-833

242. Lavara-Culebras, E. and Paricio, N. (2007) *Gene* **400,** 158-165

243. LaVoie, M. J., Cortese, G. P., Ostaszewski, B. L., and Schlossmacher, M. G. (2007) *J.Neurochem.* **103,** 2354-2368

244. LaVoie, M. J., Ostaszewski, B. L., Weihofen, A., Schlossmacher, M. G., and Selkoe, D. J. (2005) *Nat.Med.* **11,** 1214-1221

245. Layfield, R., Lowe, J., and Bedford, L. (2005) *Essays Biochem.* **41,** 157-171

246. Lee, D. H. and Goldberg, A. L. (1998) *Trends Cell Biol.* **8,** 397-403

247. Lee, M. K., Stirling, W., Xu, Y., Xu, X., Qui, D., Mandir, A. S., Dawson, T. M., Copeland, N. G., Jenkins, N. A., and Price, D. L. (2002) *Proc.Natl.Acad.Sci.U.S.A* **99,** 8968-8973

248. Lee, S. J., Kim, S. J., Kim, I. K., Ko, J., Jeong, C. S., Kim, G. H., Park, C., Kang, S. O., Suh, P. G., Lee, H. S., and Cha, S. S. (2003) *J.Biol.Chem.* **278,** 44552-44559

249. Leroy, E., Boyer, R., Auburger, G., Leube, B., Ulm, G., Mezey, E., Harta, G., Brownstein, M. J., Jonnalagada, S., Chernova, T., Dehejia, A., Lavedan, C., Gasser, T.,

Steinbach, P. J., Wilkinson, K. D., and Polymeropoulos, M. H. (1998) *Nature* **395,** 451-452

250. Lesage, S. and Brice, A. (2009) *Hum.Mol.Genet.* **18,** R48-R59

251. Lev, N., Ickowicz, D., Barhum, Y., Blondheim, N., Melamed, E., and Offen, D. (2006) *Antioxid.Redox.Signal.* **8,** 1987-1995

252. Lev, N., Ickowicz, D., Barhum, Y., Lev, S., Melamed, E., and Offen, D. (2009) *J.Neural Transm.* **116,** 151-160

253. Lev, N., Ickowicz, D., Melamed, E., and Offen, D. (2008) *Neurotoxicology* **29,** 397-405

254. Li, H. and Guo, M. (2009) *J.Clin.Invest* **119,** 442-445

255. Li, H. M., Niki, T., Taira, T., Iguchi-Ariga, S. M., and Ariga, H. (2005) *Free Radic.Res.* **39,** 1091-1099

256. Li, W. W., Yang, R., Guo, J. C., Ren, H. M., Zha, X. L., Cheng, J. S., and Cai, D. F. (2007) *Neuroreport* **18,** 1543-1546

257. Lim, K. L., Chew, K. C., Tan, J. M., Wang, C., Chung, K. K., Zhang, Y., Tanaka, Y., Smith, W., Engelender, S., Ross, C. A., Dawson, V. L., and Dawson, T. M. (2005) *J.Neurosci.* **25,** 2002-2009

258. Lindahl, P. E. and Oberg, K. E. (1960) *Nature* **187,** 784

259. Lindahl, P. E. and Oberg, K. E. (1961) *Exp.Cell Res.* **23,** 228-237

260. Liu, F., Nguyen, J. L., Hulleman, J. D., Li, L., and Rochet, J. C. (2008) *J.Neurochem.* **105**, 2435-2453

261. Liu, G., Zhang, C., Yin, J., Li, X., Cheng, F., Li, Y., Yang, H., Ueda, K., Chan, P., and Yu, S. (2009) *Neurosci.Lett.* **454,** 187-192

262. Lo, B. C., Schneider, B. L., Bauer, M., Sajadi, A., Brice, A., Iwatsubo, T., and Aebischer, P. (2004) *Proc.Natl.Acad.Sci.U.S.A* **101,** 17510-17515

263. Lockhart, P. J., Lincoln, S., Hulihan, M., Kachergus, J., Wilkes, K., Bisceglio, G., Mash, D. C., and Farrer, M. J. (2004) *J.Med.Genet.* **41,** e22

264. Loeb, V., Yakunin, E., Saada, A., and Sharon, R. (2010) *J.Biol.Chem.* **285,** 7334-7343

265. Lu, X. H., Fleming, S. M., Meurers, B., Ackerson, L. C., Mortazavi, F., Lo, V., Hernandez, D., Sulzer, D., Jackson, G. R., Maidment, N. T., Chesselet, M. F., and Yang, X. W. (2009) *J.Neurosci.* **29,** 1962-1976

266. Lucking, C. B., Durr, A., Bonifati, V., Vaughan, J., De Michele, G., Gasser, T., Harhangi, B. S., Meco, G., Denefle, P., Wood, N. W., Agid, Y., and Brice, A. (2000) *N.Engl.J.Med.* **342,** 1560-1567

267. Luo, Y. and Roth, G. S. (2000) *Antioxid.Redox.Signal.* **2,** 449-460

268. Lutz, A. K., Exner, N., Fett, M. E., Schlehe, J. S., Kloos, K., Lammermann, K., Brunner, B., Kurz-Drexler, A., Vogel, F., Reichert, A. S., Bouman, L., Vogt-Weisenhorn, D., Wurst, W., Tatzelt, J., Haass, C., and Winklhofer, K. F. (2009) *J.Biol.Chem.* **284,** 22938-22951

269. Macedo, M. G., Anar, B., Bronner, I. F., Cannella, M., Squitieri, F., Bonifati, V., Hoogeveen, A., Heutink, P., and Rizzu, P. (2003) *Hum.Mol.Genet.* **12,** 2807-2816

270. Macedo, M. G., Verbaan, D., Fang, Y., van Rooden, S. M., Visser, M., Anar, B., Uras, A., Groen, J. L., Rizzu, P., van Hilten, J. J., and Heutink, P. (2009) *Mov Disord.* **24,** 196-203

271. Malhotra, D., Thimmulappa, R., Navas-Acien, A., Sandford, A., Elliott, M., Singh, A., Chen, L., Zhuang, X., Hogg, J., Pare, P., Tuder, R. M., and Biswal, S. (2008) *Am.J.Respir.Crit Care Med.* **178,** 592-604

272. Manevich, Y. and Fisher, A. B. (2005) *Free Radic.Biol.Med.* **38,** 1422-1432

273. Mann, V., Cooper, J., Krige, D., Daniel, S., Schapira, A., and Marsden, C. (1992) *Brain* **115,** 333-342

274. Manning-Bog, A. B., Caudle, W. M., Perez, X. A., Reaney, S. H., Paletzki, R., Isla, M. Z., Chou, V. P., McCormack, A. L., Miller, G. W., Langston, J. W., Gerfen, C. R., and Dimonte, D. A. (2007) *Neurobiol.Dis.* **27,** 141-150

275. Marin, I., Lucas, J. I., Gradilla, A. C., and Ferrus, A. (2004) *Physiol Genomics* **17,** 253-263

276. Markopoulou, K., Wszolek, Z. K., Pfeiffer, R. F., and Chase, B. A. (1999) *Ann.Neurol.* **46,** 374-381

277. Maroteaux, L., Campanelli, J. T., and Scheller, R. H. (1988) *J.Neurosci.* **8,** 2804-2815

278. Martin, H. L. and Teismann, P. (2009) *FASEB J.* **23,** 3263-3272

279. Martin, L. J., Pan, Y., Price, A. C., Sterling, W., Copeland, N. G., Jenkins, N. A., Price, D. L., and Lee, M. K. (2006) *J.Neurosci.* **26,** 41-50

280. Martin-Clemente, B., Alvarez-Castelao, B., Mayo, I., Sierra, A. B., Diaz, V., Milan, M., Farinas, I., Gomez-Isla, T., Ferrer, I., and Castano, J. G. (2004) *J.Biol.Chem.* **279,** 52984-52990

281. Martinat, C., Shendelman, S., Jonason, A., Leete, T., Beal, M. F., Yang, L., Floss, T., and Abeliovich, A. (2004) *PLoS.Biol.* **2,** e327

282. Mata, I. F., Lockhart, P. J., and Farrer, M. J. (2004) *Hum.Mol.Genet.* **13 Spec No 1,** R127-R133

283. Matsuda, N., Kitami, T., Suzuki, T., Mizuno, Y., Hattori, N., and Tanaka, K. (2006) *J.Biol.Chem.* **281,** 3204-3209

284. Matsumine, H., Saito, M., Shimoda-Matsubayashi, S., Tanaka, H., Ishikawa, A., Nakagawa-Hattori, Y., Yokochi, M., Kobayashi, T., Igarashi, S., Takano, H., Sanpei, K., Koike, R., Mori, H., Kondo, T., Mizutani, Y., Schaffer, A. A., Yamamura, Y., Nakamura, S., Kuzuhara, S., Tsuji, S., and Mizuno, Y. (1997) *Am.J.Hum.Genet.* **60,** 588-596

285. Matsumine, H., Yamamura, Y., Hattori, N., Kobayashi, T., Kitada, T., Yoritaka, A., and Mizuno, Y. (1998) *Genomics* **49,** 143-146

286. McCormack, A. L., Thiruchelvam, M., Manning-Bog, A. B., Thiffault, C., Langston, J. W., Cory-Slechta, D. A., and Di Monte, D. A. (2002) *Neurobiol.Dis.* **10,** 119-127

287. McNaught, K. S., Belizaire, R., Isacson, O., Jenner, P., and Olanow, C. W. (2003) *Exp.Neurol.* **179,** 38-46

288. McNaught, K. S., Belizaire, R., Jenner, P., Olanow, C. W., and Isacson, O. (2002) *Neurosci.Lett.* **326,** 155-158

289. McNaught, K. S., Bjorklund, L. M., Belizaire, R., Isacson, O., Jenner, P., and Olanow, C. W. (2002) *Neuroreport* **13,** 1437-1441

290. McNaught, K. S. and Jenner, P. (2001) *Neurosci.Lett.* **297,** 191-194

291. McNaught, K. S. and Olanow, C. W. (2006) *Neurobiol.Aging* **27,** 530-545

292. McNaught, K. S., Perl, D. P., Brownell, A. L., and Olanow, C. W. (2004) *Ann.Neurol.* **56,** 149-162

293. Meng, L., Mohan, R., Kwok, B. H., Elofsson, M., Sin, N., and Crews, C. M. (1999) *Proc.Natl.Acad.Sci.U.S.A* **96,** 10403-10408

294. Menzies, F. M., Yenisetti, S. C., and Min, K. T. (2005) *Curr.Biol.* **15,** 1578-1582

295. Meredith, G. E., Totterdell, S., Petroske, E., Santa, C. K., Callison, R. C., Jr., and Lau, Y. S. (2002) *Brain Res.* **956,** 156-165

296. Meulener, M. C., Graves, C. L., Sampathu, D. M., Armstrong-Gold, C. E., Bonini, N. M., and Giasson, B. I. (2005) *J.Neurochem.* **93,** 1524-1532

297. Meulener, M. C., Xu, K., Thomson, L., Ischiropoulos, H., and Bonini, N. M. (2006) *Proc.Natl.Acad.Sci.U.S.A* **103,** 12517-12522

298. Miller, D. W., Ahmad, R., Hague, S., Baptista, M. J., Canet-Aviles, R., McLendon, C., Carter, D. M., Zhu, P. P., Stadler, J., Chandran, J., Klinefelter, G. R., Blackstone, C., and Cookson, M. R. (2003) *J.Biol.Chem.* **278,** 36588-36595

299. Mitsumoto, A., Nakagawa, Y., Takeuchi, A., Okawa, K., Iwamatsu, A., and Takanezawa, Y. (2001) *Free Radic.Res.* **35,** 301-310

300. Miwa, H., Kubo, T., Suzuki, A., Nishi, K., and Kondo, T. (2005) *Neurosci.Lett.* **380,** 93-98

301. Miyazaki, S., Yanagida, T., Nunome, K., Ishikawa, S., Inden, M., Kitamura, Y., Nakagawa, S., Taira, T., Hirota, K., Niwa, M., Iguchi-Ariga, S. M., and Ariga, H. (2008) *J.Neurochem.* **105,** 2418-2434

302. Mizuno, Y., Ohta, S., Tanaka, M., Takamiya, S., Suzuki, K., Sato, T., Oya, H., Ozawa, T., and Kagawa, Y. (1989) *Biochem.Biophys.Res.Commun.* **163,** 1450-1455

303. Mo, J. S., Kim, M. Y., Ann, E. J., Hong, J. A., and Park, H. S. (2008) *Cell Death.Differ.* **15,** 1030-1041

304. Moore, D. J., Zhang, L., Troncoso, J., Lee, M. K., Hattori, N., Mizuno, Y., Dawson, T. M., and Dawson, V. L. (2005) *Hum. Mol. Gen.* **14,** 71-84

305. Moore, D. J., West, A. B., Dawson, V. L., and Dawson, T. M. (2005) *Annu.Rev.Neurosci.* **28,** 57-87

306. Moore, D. J., West, A. B., Dikeman, D. A., Dawson, V. L., and Dawson, T. M. (2008) *J.Neurochem.* **105,** 1806-1819

307. Moore, D. J., Zhang, L., Dawson, T. M., and Dawson, V. L. (2003) *J.Neurochem.* **87,** 1558-1567

308. Morett, E. and Bork, P. (1999) *Trends Biochem.Sci.* **24,** 229-231

309. Mullett, S. J., Hamilton, R. L., and Hinkle, D. A. (2009) *Neuropathology.* **29,** 125-131

310. Mullett, S. J. and Hinkle, D. A. (2009) *Neurobiol.Dis.* **33,** 28-36

311. Muqit, M. M., Davidson, S. M., Payne Smith, M. D., MacCormac, L. P., Kahns, S., Jensen, P. H., Wood, N. W., and Latchman, D. S. (2004) *Hum.Mol.Genet.* **13,** 117-135

312. Murray, I. J., Medford, M. A., Guan, H. P., Rueter, S. M., Trojanowski, J. Q., and Lee, V. M. (2003) *Acta Neuropathol.(Berl)* **105,** 177-184

313. Nagakubo, D., Taira, T., Kitaura, H., Ikeda, M., Tamai, K., Iguchi-Ariga, S. M., and Ariga, H. (1997) *Biochem.Biophys.Res.Commun.* **231,** 509-513

314. Narendra, D., Tanaka, A., Suen, D., and Youle, R. (2008) *J.Cell Biol.* **183,** 795-803

315. Neumann, M., Kahle, P. J., Giasson, B. I., Ozmen, L., Borroni, E., Spooren, W., Muller, V., Odoy, S., Fujiwara, H., Hasegawa, M., Iwatsubo, T., Trojanowski, J. Q., Kretzschmar, H. A., and Haass, C. (2002) *J.Clin.Invest* **110,** 1429-1439

316. Neumann, M., Muller, V., Gorner, K., Kretzschmar, H. A., Haass, C., and Kahle, P. J. (2004) *Acta Neuropathol.(Berl)* **107,** 489-496

317. Neystat, M., Rzhetskaya, M., Kholodilov, N., and Burke, R. E. (2002) *Neurosci.Lett.* **325,** 119-123

318. Niu, C., Mei, J., Pan, Q., and Fu, X. (2009) *Stereotact.Funct.Neurosurg.* **87,** 69-81

319. Nonaka, T. and Hasegawa, M. (2009) *Biochemistry* **48,** 8014-8022

320. Norris, E. H., Giasson, B. I., and Lee, V. M. (2004) *Curr.Top.Dev.Biol.* **60,** 17-54

321. Norris, E. H., Uryu, K., Leight, S., Giasson, B. I., Trojanowski, J. Q., and Lee, V. M. (2007) *Am.J.Pathol.* **170,** 658-666

322. Oberg, K. E. (1961) *Exp.Cell Res.* **24,** 163-164

323. Olanow, C. W. and McNaught, K. S. (2006) *Mov Disord.* **21,** 1806-1823

324. Olzmann, J. A., Brown, K., Wilkinson, K. D., Rees, H. D., Huai, Q., Ke, H., Levey, A. I., Li, L., and Chin, L. S. (2004) *J.Biol.Chem.* **279,** 8506-8515

325. Olzmann, J. A., Li, L., Chudaev, M. V., Chen, J., Perez, F. A., Palmiter, R. D., and Chin, L. S. (2007) *J.Cell Biol.* **178,** 1025-1038

326. Omura, S., Fujimoto, T., Otoguro, K., Matsuzaki, K., Moriguchi, R., Tanaka, H., and Sasaki, Y. (1991) *J.Antibiot.(Tokyo)* **44,** 113-116

327. Ooe, H., Iguchi-Ariga, S. M., and Ariga, H. (2006) *Neurosci.Lett.* **404,** 166-169

328. Ooe, H., Maita, C., Maita, H., Iguchi-Ariga, S. M., and Ariga, H. (2006) *Neurosci.Lett.* **406,** 165-168

329. Orth, M., Tabrizi, S. J., Schapira, A. H., and Cooper, J. M. (2003) *Neurosci.Lett.* **351,** 29-32

330. Ortiz-Ortiz, M. A., Moran, J. M., Gonzalez-Polo, R. A., Niso-Santano, M., Soler, G., Bravo-San Pedro, J. M., and Fuentes, J. M. (2009) *Neurotox.Res.* **16,** 160-173

331. Ossowska, K., Wardas, J., Smialowska, M., Kuter, K., Lenda, T., Wieronska, J. M., Zieba, B., Nowak, P., Dabrowska, J., Bortel, A., Kwiecinski, A., and Wolfarth, S. (2005) *Eur.J.Neurosci.* **22,** 1294-1304

332. Paisan-Ruiz, C., Bhatia, K. P., Li, A., Hernandez, D., Davis, M., Wood, N. W., Hardy, J., Houlden, H., Singleton, A., and Schneider, S. A. (2009) *Ann.Neurol.* **65,** 19-23

333. Paisan-Ruiz, C., Jain, S., Evans, E. W., Gilks, W. P., Simon, J., van der, B. M., de Munain, A. L., Aparicio, S., Gil, A. M., Khan, N., Johnson, J., Martinez, J. R., Nicholl, D., Carrera, I. M., Pena, A. S., de Silva, R., Lees, A., Marti-Masso, J. F., Perez-Tur, J., Wood, N. W., and Singleton, A. B. (2004) *Neuron* **44,** 595-600

334. Pakkenberg, B., Moller, A., Gundersen, H. J., Mouritzen, D. A., and Pakkenberg, H. (1991) *J.Neurol.Neurosurg.Psychiatry* **54,** 30-33

335. Palacino, J. J., Sagi, D., Goldberg, M. S., Krauss, S., Motz, C., Wacker, M., Klose, J., and Shen, J. (2004) *J.Biol.Chem.* **279,** 18614-18622

336. Pan-Montojo, F., Anichtchik, O., Dening, Y., Knels, L., Pursche, S., Jung, R., Jackson, S., Gille, G., Spillantini, M. G., Reichmann, H., and Funk, R. H. (2010) *PLoS.ONE.* **5,** e8762

337. Pankratz, N., Nichols, W. C., Uniacke, S. K., Halter, C., Rudolph, A., Shults, C., Conneally, P. M., and Foroud, T. (2002) *Am.J.Hum.Genet.* **71,** 124-135

338. Papadimitriou, A., Veletza, V., Hadjigeorgiou, G. M., Patrikiou, A., Hirano, M., and Anastasopoulos, I. (1999) *Neurology* **52,** 651-654

339. Parihar, M. S., Parihar, A., Fujita, M., Hashimoto, M., and Ghafourifar, P. (2008) *Cell Mol.Life Sci.* **65,** 1272-1284

340. Parihar, M. S., Parihar, A., Fujita, M., Hashimoto, M., and Ghafourifar, P. (2009) *Int.J.Biochem.Cell Biol.* **41**, 2015-2024

341. Park, H. M., Kim, G. Y., Nam, M. K., Seong, G. H., Han, C., Chung, K. C., Kang, S., and Rhim, H. (2009) *Biochem.Biophys.Res.Commun.* **387,** 537-542

342. Park, J., Lee, S. B., Lee, S., Kim, Y., Song, S., Kim, S., Bae, E., Kim, J., Shong, M., Kim, J. M., and Chung, J. (2006) *Nature* **441,** 1157-1161

343. Park, S. M., Jung, H. Y., Kim, T. D., Park, J. H., Yang, C. H., and Kim, J. (2002) *J.Biol.Chem.* **277,** 28512-28520

344. Parkinson, J. (2002) *J.Neuropsychiatry Clin.Neurosci.* **14,** 223-236

345. Paterna, J. C., Leng, A., Weber, E., Feldon, J., and Bueler, H. (2007) *Mol.Ther.* **15,** 698-704

346. Pavlovic, S., Schulze, G., Wernicke, C., Bonnet, R., Gille, G., Badiali, L., Kaminska, A., Lorenc-Koci, E., Ossowska, K., and Rommelspacher, H. (2006) *Neuroscience* **139,** 1525-1537

347. Pawlyk, A. C., Giasson, B. I., Sampathu, D. M., Perez, F. A., Lim, K. L., Dawson, V. L., Dawson, T. M., Palmiter, R. D., Trojanowski, J. Q., and Lee, V. M. (2003) *J.Biol.Chem.* **278,** 48120-48128

348. Peng, X., Tehranian, R., Dietrich, P., Stefanis, L., and Perez, R. G. (2005) *J.Cell Sci.* **118,** 3523-3530

349. Perez, F. A., Curtis, W. R., and Palmiter, R. D. (2005) *BMC.Neurosci.* **6,** 71

350. Perez, F. A. and Palmiter, R. D. (2005) *Proc.Natl.Acad.Sci.U.S.A* **102,** 2174-2179

351. Perez, R. G., Waymire, J. C., Lin, E., Liu, J. J., Guo, F., and Zigmond, M. J. (2002) *J.Neurosci.* **22,** 3090-3099

352. Periquet, M., Latouche, M., Lohmann, E., Rawal, N., De Michele, G., Ricard, S., Teive, H., Fraix, V., Vidailhet, M., Nicholl, D., Barone, P., Wood, N. W., Raskin, S., Deleuze, J. F., Agid, Y., Durr, A., and Brice, A. (2003) *Brain* **126,** 1271-1278

353. Pesah, Y., Pham, T., Burgess, H., Middleton, B., Verstreken, P., Zhou, Y., Harding, M., Bellen, H., and Mardon, G. (2004) *Development* **131,** 2183-2194

354. Pisani, A., Martella, G., Tscherter, A., Costa, C., Mercuri, N. B., Bernardi, G., Shen, J., and Calabresi, P. (2006) *Neurobiol.Dis.* **23,** 54-60

355. Poewe, W. (2008) *Eur.J.Neurol.* **15 Suppl 1,** 14-20

356. Pollanen, M. S., Dickson, D. W., and Bergeron, C. (1993) *J.Neuropathol.Exp.Neurol.* **52,** 183-191

357. Polymeropoulos, M. H., Lavedan, C., Leroy, E., Ide, S. E., Dehejia, A., Dutra, A., Pike, B., Root, H., Rubenstein, J., Boyer, R., Stenroos, E. S., Chandrasekharappa, S., Athanassiadou, A., Papapetropoulos, T., Johnson, W. G., Lazzarini, A. M., Duvoisin, R. C., Di Iorio, G., Golbe, L. I., and Nussbaum, R. L. (1997) *Science* **276,** 2045-2047

358. Poole, A. C., Thomas, R. E., Andrews, L. A., McBride, H. M., Whitworth, A. J., and Pallanck, L. J. (2008) *Proc.Natl.Acad.Sci.U.S.A* **105,** 1638-1643

359. Poorkaj, P., Nutt, J. G., James, D., Gancher, S., Bird, T. D., Steinbart, E., Schellenberg, G. D., and Payami, H. (2004) *Am.J.Med.Genet.A* **129A,** 44-50

360. Power, J. H., Shannon, J. M., Blumbergs, P. C., and Gai, W. P. (2002) *Am.J.Pathol.* **161,** 885-894

361. Pramstaller, P. P., Schlossmacher, M. G., Jacques, T. S., Scaravilli, F., Eskelson, C., Pepivani, I., Hedrich, K., Adel, S., Gonzales-McNeal, M., Hilker, R., Kramer, P. L., and Klein, C. (2005) *Ann.Neurol.* **58,** 411-422

362. Przedborski, S. and Ischiropoulos, H. (2005) *Antioxid.Redox.Signal.* **7,** 685-693

363. Przedborski, S., Tieu, K., Perier, C., and Vila, M. (2004) *J.Bioenerg.Biomembr.* **36,** 375-379

364. Ramirez, A., Heimbach, A., Grundemann, J., Stiller, B., Hampshire, D., Cid, L. P., Goebel, I., Mubaidin, A. F., Wriekat, A. L., Roeper, J., Al Din, A., Hillmer, A. M., Karsak, M., Liss, B., Woods, C. G., Behrens, M. I., and Kubisch, C. (2006) *Nat.Genet.* **38,** 1184-1191

365. Ramsey, C. P. and Giasson, B. I. (2007) *Drugs Aging* **24,** 95-105

366. Ramsey, C. P. and Giasson, B. I. (2008) *Brain Res.* **1279,** 1-11

367. Rankin, C. A., Joazeiro, C. A., Floor, E., and Hunter, T. (2001) *J.Biomed.Sci.* **8,** 421-429

368. Recchia, A., Debetto, P., Negro, A., Guidolin, D., Skaper, S. D., and Giusti, P. (2004) *FASEB J.* **18,** 617-626

369. Rechsteiner, M., Hoffman, L., and Dubiel, W. (1993) *J.Biol.Chem.* **268,** 6065-6068

370. Ren, Y., Zhao, J., and Feng, J. (2003) *J.Neurosci.* **23,** 3316-3324

371. Rizzu, P., Hinkle, D. A., Zhukareva, V., Bonifati, V., Severijnen, L. A., Martinez, D., Ravid, R., Kamphorst, W., Eberwine, J. H., Lee, V. M., Trojanowski, J. Q., and Heutink, P. (2004) *Ann.Neurol.* **55,** 113-118

372. Rodriguez-Novarro, J., Casarejos, M., Menendez, J., Solano, R., Rodal, I., Gomez, A., de Yebenes, J., and Mena, M. (2007) *J.Neurochem.* **103,** 98-114

373. Rothfuss, O., Fischer, H., Hasegawa, T., Maisel, M., Leitner, P., Miesel, F., Sharma, M., Bornemann, A., Berg, D., Gasser, T., and Patenge, N. (2009) *Hum.Mol.Genet.* **18,** 3832-3850

374. Saito, Y., Hamakubo, T., Yoshida, Y., Ogawa, Y., Hara, Y., Fujimura, H., Imai, Y., Iwanari, H., Mochizuki, Y., Shichiri, M., Nishio, K., Kinumi, T., Noguchi, N., Kodama, T., and Niki, E. (2009) *Neurosci.Lett.* **465,** 1-5

375. Saito, Y., Kawashima, A., Ruberu, N. N., Fujiwara, H., Koyama, S., Sawabe, M., Arai, T., Nagura, H., Yamanouchi, H., Hasegawa, M., Iwatsubo, T., and Murayama, S. (2003) *J.Neuropathol.Exp.Neurol.* **62,** 644-654

376. Sampathu, D. M., Giasson, B. I., Pawlyk, A. C., Trojanowski, J. Q., and Lee, V. M. (2003) *Am.J.Pathol.* **163,** 91-100

377. Sanchetee, P. (2008) Major Symptoms and Signs of Parkinson's Disease. In Mehrotra, T. and Bhattacharyya, K. B., editors. *Parkinson's Disease and Movement Disorders*, McGraw-Hill, New York

378. Sasaki, S., Shirata, A., Yamane, K., and Iwata, M. (2004) *Neurology* **63,** 678-682

379. Sato, S., Chiba, T., Nishiyama, S., Kakiuchi, T., Tsukada, H., Hatano, T., Fukuda, T., Yasoshima, Y., Kai, N., Kobayashi, K., Mizuno, Y., Tanaka, K., and Hattori, N. (2006) *J.Neurosci.Res.* **84,** 1350-1357

380. Schapira, A. H., Cooper, J. M., Dexter, D., Clark, J. B., Jenner, P., and Marsden, C. D. (1990) *J.Neurochem.* **54,** 823-827

381. Schapira, A. H., Mann, V. M., Cooper, J. M., Dexter, D., Daniel, S. E., Jenner, P., Clark, J. B., and Marsden, C. D. (1990) *J.Neurochem.* **55,** 2142-2145

382. Schiller, F. (2000) *J Hist Neurosci* **9,** 148-151

383. Schlehe, J. S., Lutz, A. K., Pilsl, A., Lammermann, K., Grgur, K., Henn, I. H., Tatzelt, J., and Winklhofer, K. F. (2008) *J.Biol.Chem.* **283,** 13771-13779

384. Schlossmacher, M. G., Frosch, M. P., Gai, W. P., Medina, M., Sharma, N., Forno, L., Ochiishi, T., Shimura, H., Sharon, R., Hattori, N., Langston, J. W., Mizuno, Y., Hyman, B. T., Selkoe, D. J., and Kosik, K. S. (2002) *Am.J.Pathol.* **160,** 1655-1667

385. Sekito, A., Koide-Yoshida, S., Niki, T., Taira, T., Iguchi-Ariga, S. M., and Ariga, H. (2006) *Free Radic.Res.* **40,** 155-165

386. Sha, D., Chin, L. S., and Li, L. (2010) *Hum.Mol.Genet.* **19,** 352-363

387. Shang, H., Lang, D., Jean-Marc, B., and Kaelin-Lang, A. (2004) *Neurosci.Lett.* **367,** 273-277

388. Shavali, S., Brown-Borg, H. M., Ebadi, M., and Porter, J. (2008) *Neurosci.Lett.* **439,** 125-128

389. Shendelman, S., Jonason, A., Martinat, C., Leete, T., and Abeliovich, A. (2004) *PLoS.Biol.* **2,** e362

390. Sherer, T. B., Kim, J. H., Betarbet, R., and Greenamyre, J. T. (2003) *Exp.Neurol.* **179,** 9-16

391. Shimura, H., Hattori, N., Kubo, S., Yoshikawa, M., Kitada, T., Matsumine, H., Asakawa, S., Minoshima, S., Yamamura, Y., Shimizu, N., and Mizuno, Y. (1999) *Ann.Neurol.* **45,** 668-672

392. Shimura, H., Hattori, N., Kubo, S., Mizuno, Y., Asakawa, S., Minoshima, S., Shimizu, N., Iwai, K., Chiba, T., Tanaka, K., and Suzuki, T. (2000) *Nat.Genet.* **25,** 302-305

393. Shimura, H., Schlossmacher, M. G., Hattori, N., Frosch, M. P., Trockenbacher, A., Schneider, R., Mizuno, Y., Kosik, K. S., and Selkoe, D. J. (2001) *Science* **293,** 263-269

394. Shinbo, Y., Niki, T., Taira, T., Ooe, H., Takahashi-Niki, K., Maita, C., Seino, C., Iguchi-Ariga, S. M., and Ariga, H. (2006) *Cell Death.Differ.* **13,** 96-108

395. Shinbo, Y., Taira, T., Niki, T., Iguchi-Ariga, S. M., and Ariga, H. (2005) *Int.J.Oncol.* **26,** 641-648

396. Shults, C. W. (2006) *Proc.Natl.Acad.Sci.U.S.A* **103,** 1661-1668

397. Simola, N., Morelli, M., and Carta, A. R. (2007) *Neurotox.Res.* **11,** 151-167

398. Singer, T. P., Castagnoli, N., Jr., Ramsay, R. R., and Trevor, A. J. (1987) *J.Neurochem.* **49,** 1-8

399. Singh, M., ., and Raju, U. (2008) Diagnosis of Parkinsonism. In Mehrotra, T. and Bhattacharyya, K. B., editors. *Parkinson's Disease and Movement Disorders*, McGraw-Hill, New York

400. Singleton, A. B., Farrer, M., Johnson, J., Singleton, A., Hague, S., Kachergus, J., Hulihan, M., Peuralinna, T., Dutra, A., Nussbaum, R., Lincoln, S., Crawley, A., Hanson, M., Maraganore, D., Adler, C., Cookson, M. R., Muenter, M., Baptista, M., Miller, D., Blancato, J., Hardy, J., and Gwinn-Hardy, K. (2003) *Science* **302,** 841

401. Solano, R. M., Casarejos, M. J., Menendez-Cuervo, J., Rodriguez-Navarro, J. A., Garcia, d. Y., and Mena, M. A. (2008) *J.Neurosci.* **28,** 598-611

402. Soto, C. and Estrada, L. D. (2008) *Arch.Neurol.* **65,** 184-189

403. Souza, J. M., Giasson, B. I., Lee, V. M., and Ischiropoulos, H. (2000) *FEBS Lett.* **474,** 116-119

404. Spillantini, M. G., Crowther, R. A., Jakes, R., Hasegawa, M., and Goedert, M. (1998) *Proc.Natl.Acad.Sci.U.S.A* **95,** 6469-6473

405. Spillantini, M. G., Schmidt, M. L., Lee, V. M. Y., Trojanowski, J. Q., Jakes, R., and Goedert, M. (1997) *Nature* **388,** 839-840

406. Spira, P. J., Sharpe, D. M., Halliday, G., Cavanagh, J., and Nicholson, G. A. (2001) *Ann.Neurol.* **49,** 313-319

407. Sriram, S. R., Li, X., Ko, H. S., Chung, K. K., Wong, E., Lim, K. L., Dawson, V. L., and Dawson, T. M. (2005) *Hum.Mol.Genet.* **14,** 2571-2586

408. Starkov, A. A. (2008) *Ann.N.Y.Acad.Sci.* **1147,** 37-52

409. Staropoli, J. F., McDermott, C., Martinat, C., Schulman, B., Demireva, E., and Abeliovich, A. (2003) *Neuron* **37,** 735-749

410. Stefanis, L., Larsen, K. E., Rideout, H. J., Sulzer, D., and Greene, L. A. (2001) *J.Neurosci.* **21,** 9549-9560

411. Stichel, C. C., Augustin, M., Kuhn, K., Zhu, X. R., Engels, P., Ullmer, C., and Lubbert, H. (2000) *Eur.J.Neurosci.* **12,** 4181-4194

412. Strauss, K. M., Martins, L. M., Plun-Favreau, H., Marx, F. P., Kautzmann, S., Berg, D., Gasser, T., Wszolek, Z., Muller, T., Bornemann, A., Wolburg, H., Downward, J., Riess, O., Schulz, J. B., and Kruger, R. (2005) *Hum.Mol.Genet.* **14,** 2099-2111

413. Su, X., Federoff, H. J., and Maguire-Zeiss, K. A. (2009) *Neurotox.Res.* **16,** 238-254

414. Summers, L. (1980) Plant Physiology and Mode of Herbicidal Action. *The Bipyridinium Herbicides*, Academic Press Inc, London, England

415. Sun, F., Anantharam, V., Zhang, D., Latchoumycandane, C., Kanthasamy, A., and Kanthasamy, A. G. (2006) *Neurotoxicology* **27,** 807-815

416. Sun, M., Latourelle, J. C., Wooten, G. F., Lew, M. F., Klein, C., Shill, H. A., Golbe, L. I., Mark, M. H., Racette, B. A., Perlmutter, J. S., Parsian, A., Guttman, M., Nicholson, G., Xu, G., Wilk, J. B., Saint-Hilaire, M. H., DeStefano, A. L., Prakash, R., Williamson, S., Suchowersky, O., Labelle, N., Growdon, J. H., Singer, C., Watts, R. L., Goldwurm, S., Pezzoli, G., Baker, K. B., Pramstaller, P. P., Burn, D. J., Chinnery, P. F., Sherman, S., Vieregge, P., Litvan, I., Gillis, T., MacDonald, M. E., Myers, R. H., and Gusella, J. F. (2006) *Arch.Neurol.* **63,** 826-832

417. Szabo, C., Ischiropoulos, H., and Radi, R. (2007) *Nat.Rev.Drug Discov.* **6,** 662-680

418. Taira, T., Saito, Y., Niki, T., Iguchi-Ariga, S. M., Takahashi, K., and Ariga, H. (2004) *EMBO Rep.* **5,** 213-218

419. Taira, T., Takahashi, K., Kitagawa, R., Iguchi-Ariga, S. M., and Ariga, H. (2001) *Gene* **263,** 285-292

420. Takahashi, H., Ohama, E., Suzuki, S., Horikawa, Y., Ishikawa, A., Morita, T., Tsuji, S., and Ikuta, F. (1994) *Neurology* **44**, 437-441.

421. Takahashi, K., Taira, T., Niki, T., Seino, C., Iguchi-Ariga, S. M., and Ariga, H. (2001) *J.Biol.Chem.* **276,** 37556-37563

422. Takahashi-Niki, K., Niki, T., Taira, T., Iguchi-Ariga, S. M., and Ariga, H. (2004) *Biochem.Biophys.Res.Commun.* **320,** 389-397

423. Tan, E. K. and Skipper, L. M. (2007) *Hum.Mutat.* **28,** 641-653

424. Tanaka, K., Suzuki, T., Hattori, N., and Mizuno, Y. (2004) *Biochim.Biophys.Acta* **1695,** 235-247

425. Tanaka, Y., Engelender, S., Igarashi, S., Rao, R. K., Wanner, T., Tanzi, R. E., Sawa, A., Dawson, L., Dawson, T. M., and Ross, C. A. (2001) *Hum.Mol.Genet.* **10,** 919-926

426. Tao, X. and Tong, L. (2003) *J.Biol.Chem.* **278,** 31372-31379

427. Tehranian, R., Montoya, S. E., Van Laar, A. D., Hastings, T. G., and Perez, R. G. (2006) *J.Neurochem.* **99,** 1188-1196

428. Terracciano, C., Nogalska, A., Engel, W. K., Wojcik, S., and Askanas, V. (2008) *Free Radic.Biol.Med.* **45,** 773-779

429. Testa, C. M., Sherer, T. B., and Greenamyre, J. T. (2005) *Brain Res.Mol.Brain Res.* **134,** 109-118

430. Thiruchelvam, M., McCormack, A., Richfield, E. K., Baggs, R. B., Tank, A. W., Di Monte, D. A., and Cory-Slechta, D. A. (2003) *Eur.J.Neurosci.* **18,** 589-600

431. Thomas, B., von Coelln, R., Mandir, A. S., Trinkaus, D. B., Farah, M. H., Leong, L. K., Calingasan, N. Y., Flint, B. M., Dawson, V. L., and Dawson, T. M. (2007) *Neurobiol.Dis.* **26,** 312-322

432. Tofaris, G. K., Layfield, R., and Spillantini, M. G. (2001) *FEBS Lett.* **509,** 22-26

433. Tomiyama, H., Li, Y., Yoshino, H., Mizuno, Y., Kubo, S., Toda, T., and Hattori, N. (2009) *Neurosci.Lett.* **455,** 159-161

434. Trojanowski, J. Q., Schuck, T., Schmidt, M. L., and Lee, V. M. Y. (1989) *J.Histochem.Cytochem.* **37,** 209-215

435. Tsang, A. H. and Chung, K. K. (2009) *Biochim.Biophys.Acta* **1792,** 643-650

436. Tsubuki, S., Kawasaki, H., Saito, Y., Miyashita, N., Inomata, M., and Kawashima, S. (1993) *Biochem.Biophys.Res.Commun.* **196,** 1195-1201

437. Tsubuki, S., Saito, Y., Tomioka, M., Ito, H., and Kawashima, S. (1996) *J.Biochem.* **119,** 572-576

438. Ueda, K., Fukushima, H., Masliah, E., Xia, Y., Iwai, A., Yoshimoto, M., Otero, D. A., Kondo, J., Ihara, Y., and Saitoh, T. (1993) *Proc.Natl.Acad.Sci.U.S.A* **90,** 11282-11286

439. Um, J. W., Min, D. S., Rhim, H., Kim, J., Paik, S. R., and Chung, K. C. (2006) *J.Biol.Chem.* **281,** 3595-3603

440. Unschuld, P. G., Dachsel, J., Darios, F., Kohlmann, A., Casademunt, E., Lehmann-Horn, K., Dichgans, M., Ruberg, M., Brice, A., Gasser, T., and Lucking, C. B. (2006) *Mol.Biol.Rep.* **33,** 13-32

441. Valente, E. M., Abou-Sleiman, P. M., Caputo, V., Muqit, M. M., Harvey, K., Gispert, S., Ali, Z., Del Turco, D., Bentivoglio, A. R., Healy, D. G., Albanese, A., Nussbaum, R., Gonzalez-Maldonado, R., Deller, T., Salvi, S., Cortelli, P., Gilks, W. P., Latchman, D. S., Harvey, R. J., Dallapiccola, B., Auburger, G., and Wood, N. W. (2004) *Science* **304,** 1158-1160

442. Valente, E. M., Bentivoglio, A. R., Dixon, P. H., Ferraris, A., Ialongo, T., Frontali, M., Albanese, A., and Wood, N. W. (2001) *Am.J.Hum.Genet.* **68,** 895-900

443. van der Brug, M. P., Blackinton, J., Chandran, J., Hao, L. Y., Lal, A., Mazan-Mamczarz, K., Martindale, J., Xie, C., Ahmad, R., Thomas, K. J., Beilina, A., Gibbs, J. R., Ding, J., Myers, A. J., Zhan, M., Cai, H., Bonini, N. M., Gorospe, M., and Cookson, M. R. (2008) *Proc.Natl.Acad.Sci.U.S.A* **105,** 10244-10249

444. van der Putten, H., Wiederhold, K. H., Probst, A., Barbieri, S., Mistl, C., Danner, S., Kauffmann, S., Hofele, K., Spooren, W. P., Ruegg, M. A., Lin, S., Caroni, P., Sommer, B., Tolnay, M., and Bilbe, G. (2000) *J.Neurosci.* **20,** 6021-6029

445. van der Reijden, B. A., Erpelinck-Verschueren, C. A., Lowenberg, B., and Jansen, J. H. (1999) *Protein Sci.* **8,** 1557-1561

446. van Duijn, C. M., Dekker, M. C., Bonifati, V., Galjaard, R. J., Houwing-Duistermaat, J. J., Snijders, P. J., Testers, L., Breedveld, G. J., Horstink, M., Sandkuijl, L. A., van Swieten, J. C., Oostra, B. A., and Heutink, P. (2001) *Am.J.Hum.Genet.* **69,** 629-634

447. Ved, R., Saha, S., Westlund, B., Perier, C., Burnam, L., Sluder, A., Hoener, M., Rodrigues, C. M., Alfonso, A., Steer, C., Liu, L., Przedborski, S., and Wolozin, B. (2005) *J.Biol.Chem.* **280,** 42655-42668

448. Vekrellis, K., Xilouri, M., Emmanouilidou, E., and Stefanis, L. (2009) *J.Neurochem.* **109,** 1348-1362

449. Venderova, K., Kabbach, G., Abdel-Messih, E., Zhang, Y., Parks, R. J., Imai, Y., Gehrke, S., Ngsee, J., LaVoie, M. J., Slack, R., Rao, Y., Zhang, Z., Lu, B., Haque, M. E., and Park, D. S. (2009) *Hum.Mol.Genet.*

450. Vercammen, L., Van der, P. A., Vaudano, E., Gijsbers, R., Debyser, Z., Van den, H. C., and Baekelandt, V. (2006) *Mol.Ther.* **14,** 716-723

451. Vernon, A. C., Johansson, S. M., and Modo, M. M. (2010) *BMC.Neurosci.* **11,** 1

452. von Coelln, R., Dawson, V. L., and Dawson, T. M. (2004) *Cell Tissue Res.* **318,** 175-184

453. von Coelln, R., Thomas, B., Andrabi, S. A., Lim, K. L., Savitt, J. M., Saffary, R., Stirling, W., Bruno, K., Hess, E. J., Lee, M. K., Dawson, V. L., and Dawson, T. M. (2006) *J.Neurosci.* **26,** 3685-3696

454. von Coelln, R., Thomas, B., Savitt, J. M., Lim, K. L., Sasaki, M., Hess, E. J., Dawson, V. L., and Dawson, T. M. (2004) *Proc.Natl.Acad.Sci.U.S.A* **101,** 10744-10749

455. Waak, J., Weber, S. S., Gorner, K., Schall, C., Ichijo, H., Stehle, T., and Kahle, P. J. (2009) *J.Biol.Chem.* **284,** 14245-14257

456. Waak, J., Weber, S. S., Waldenmaier, A., Gorner, K., Alunni-Fabbroni, M., Schell, H., Vogt-Weisenhorn, D., Pham, T. T., Reumers, V., Baekelandt, V., Wurst, W., and Kahle, P. J. (2009) *FASEB J.* **23,** 2478-2489

457. Wagenfeld, A., Yeung, C. H., Strupat, K., and Cooper, T. G. (1998) *Biol.Reprod.* **58,** 1257-1265

458. Wakabayashi, K., Engelender, S., Yoshimoto, M., Tsuji, S., Ross, C. A., and Takahashi, H. (2000) *Ann.Neurol.* **47,** 521-523

459. Wang, C., Ko, H. S., Thomas, B., Tsang, F., Chew, K. C., Tay, S. P., Ho, M. W., Lim, T. M., Soong, T. W., Pletnikova, O., Troncoso, J., Dawson, V. L., Dawson, T. M., and Lim, K. L. (2005) *Hum.Mol.Genet.* **14,** 3885-3897

460. Wang, C., Tan, J. M., Ho, M. W., Zaiden, N., Wong, S. H., Chew, C. L., Eng, P. W., Lim, T. M., Dawson, T. M., and Lim, K. L. (2005) *J.Neurochem.* **93,** 422-431

461. Wang, H. Q., Imai, Y., Inoue, H., Kataoka, A., Iita, S., Nukina, N., and Takahashi, R. (2008) *J.Neurochem.* **107,** 171-185

462. Waxman, E. A., Duda, J. E., and Giasson, B. I. (2008) *Acta Neuropathol.* **116,** 37-46

463. Waxman, E. A. and Giasson, B. I. (2008) *J.Neuropathol.Exp.Neurol.* **67,** 402-416

464. Waxman, E. A. and Giasson, B. I. (2009) *Biochim.Biophys.Acta* **1792,** 616-624

465. Weintraub, D., Comella, C. L., and Horn, S. (2008) *Am.J.Manag.Care* **14,** S40-S48

466. Westlund, K. N., Denney, R. M., Kochersperger, L. M., Rose, R. M., and Abell, C. W. (1985) *Science* **230,** 181-183

467. Westlund, K. N., Denney, R. M., Rose, R. M., and Abell, C. W. (1988) *Neuroscience* **25,** 439-456

468. Williams, D. R., Hadeed, A., al Din, A. S., Wreikat, A. L., and Lees, A. J. (2005) *Mov Disord.* **20,** 1264-1271

469. Wilson, M. A., Collins, J. L., Hod, Y., Ringe, D., and Petsko, G. A. (2003) *Proc.Natl.Acad.Sci.U.S.A* **100,** 9256-9261

470. Winklhofer, K. F., Henn, I. H., Kay-Jackson, P. C., Heller, U., and Tatzelt, J. (2003) *J.Biol.Chem.* **278,** 47199-47208

471. Witt, A. C., Lakshminarasimhan, M., Remington, B. C., Hasim, S., Pozharski, E., and Wilson, M. A. (2008) *Biochemistry* **47,** 7430-7440

472. Wood, Z. A., Schroder, E., Robin, H. J., and Poole, L. B. (2003) *Trends Biochem.Sci.* **28,** 32-40

473. Wright, J. M., Wall, R. A., Perry, T. L., and Paty, D. W. (1984) *N.Engl.J.Med.* **310,** 325

474. Wu, F., Poon, W. S., Lu, G., Wang, A., Meng, H., Feng, L., Li, Z., and Liu, S. (2009) *Brain Res.* **1292,** 173-179

475. Wu, R. M., Bounds, R., Lincoln, S., Hulihan, M., Lin, C. H., Hwu, W. L., Chen, J., Gwinn-Hardy, K., and Farrer, M. (2005) *Arch.Neurol.* **62,** 82-87

476. Xie, Z., Zhuang, X., and Chen, L. (2009) *Neurosci.Lett.* **465,** 214-219

477. Xiong, H., Wang, D., Chen, L., Choo, Y. S., Ma, H., Tang, C., Xia, K., Jiang, W., Ronai, Z., Zhuang, X., and Zhang, Z. (2009) *J.Clin.Invest* **119,** 650-660

478. Xiromerisiou, G., Dardiotis, E., Tsimourtou, V., Kountra, P. M., Paterakis, K. N., Kapsalaki, E. Z., Fountas, K. N., and Hadjigeorgiou, G. M. (2010) *Neurosurg.Focus.* **28,** E7

479. Xu, J., Zhong, N., Wang, H., Elias, J. E., Kim, C. Y., Woldman, I., Pifl, C., Gygi, S. P., Geula, C., and Yankner, B. A. (2005) *Hum.Mol.Genet.* **14,** 1231-1241

480. Yamaguchi, H. and Shen, J. (2007) *Mol.Neurodegener.* **2,** 10

481. Yamamura, Y., Sobue, I., Ando, K., Iida, M., and Yanagi, T. (1973) *Neurology* **23,** 239-244

482. Yanagisawa, D., Kitamura, Y., Inden, M., Takata, K., Taniguchi, T., Morikawa, S., Morita, M., Inubushi, T., Tooyama, I., Taira, T., Iguchi-Ariga, S. M., Akaike, A., and Ariga, H. (2008) *J.Cereb.Blood Flow Metab* **28,** 563-578

483. Yang, W., Chen, L., Ding, Y., Zhuang, X., and Kang, U. J. (2007) *Hum.Mol.Genet.* **16,** 2900-2910

484. Yang, Y., Gehrke, S., Haque, M. E., Imai, Y., Kosek, J., Yang, L., Beal, M. F., Nishimura, I., Wakamatsu, K., Ito, S., Takahashi, R., and Lu, B. (2005) *Proc.Natl.Acad.Sci.U.S.A* **102,** 13670-13675

485. Yang, Y., Gehrke, S., Imai, Y., Huang, Z., Ouyang, Y., Wang, J. W., Yang, L., Beal, M. F., Vogel, H., and Lu, B. (2006) *Proc.Natl.Acad.Sci.U.S.A* **103,** 10793-10798

486. Yang, Y. X., Wood, N. W., and Latchman, D. S. (2009) *Neuroreport* **20,** 150-156

487. Yokota, T., Sugawara, K., Ito, K., Takahashi, R., Ariga, H., and Mizusawa, H. (2003) *Biochem.Biophys.Res.Commun.* **312,** 1342-1348

488. Zarranz, J. J., Alegre, J., Gomez-Esteban, J. C., Lezcano, E., Ros, R., Ampuero, I., Vidal, L., Hoenicka, J., Rodriguez, O., Atares, B., Llorens, V., Gomez, T. E., del Ser, T., Munoz, D. G., and de Yebenes, J. G. (2004) *Ann.Neurol.* **55,** 164-173

489. Zhang, L., Shimoji, M., Thomas, B., Moore, D. J., Yu, S. W., Marupudi, N. I., Torp, R., Torgner, I. A., Ottersen, O. P., Dawson, T. M., and Dawson, V. L. (2005) *Hum.Mol.Genet.* **14,** 2063-2073

490. Zhang, Y., Gao, J., Chung, K. K., Huang, H., Dawson, V. L., and Dawson, T. M. (2000) *Proc.Natl.Acad.Sci.U.S.A* **97,** 13354-13359

491. Zhong, N., Kim, C. Y., Rizzu, P., Geula, C., Porter, D. R., Pothos, E. N., Squitieri, F., Heutink, P., and Xu, J. (2006) *J.Biol.Chem.* **281,** 20940-20948

492. Zhong, N. and Xu, J. (2008) *Hum.Mol.Genet.* **17,** 3357-3367

493. Zhou, W. and Freed, C. R. (2005) *J.Biol.Chem.* **280,** 43150-43158

494. Zhou, W., Zhu, M., Wilson, M. A., Petsko, G. A., and Fink, A. L. (2006) *J.Mol.Biol.* **356,** 1036-1048

495. Zhou, Z. D. and Lim, T. M. (2009) *Free Radic.Res.* **43,** 417-430

496. Zhu, X. R., Maskri, L., Herold, C., Bader, V., Stichel, C. C., Gunturkun, O., and Lubbert, H. (2007) *Eur.J.Neurosci.* **26,** 1902-1911

497. Zimprich, A., Biskup, S., Leitner, P., Lichtner, P., Farrer, M., Lincoln, S., Kachergus, J., Hulihan, M., Uitti, R. J., Calne, D. B., Stoessl, A. J., Pfeiffer, R. F., Patenge, N., Carbajal, I. C., Vieregge, P., Asmus, F., Muller-Myhsok, B., Dickson, D. W., Meitinger, T., Strom, T. M., Wszolek, Z. K., and Gasser, T. (2004) *Neuron* **44,** 601-607

498. Zucchelli, S., Vilotti, S., Calligaris, R., Lavina, Z. S., Biagioli, M., Foti, R., De Maso, L., Pinto, M., Gorza, M., Speretta, E., Casseler, C., Tell, G., Del Sal, G., and Gustincich, S. (2009) *Cell Death.Differ.* **16,** 428-438